UNIVERSITE DE LILLE

ECOLE DOCTORALE BIOLOGIE - SANTE

THESE DE DOCTORAT

DISCIPLINE : Biochimie et Biologie Moléculaire

DETERMINISME MOLECULAIRE DES ANOMALIES RADIALES

Par Clémence VANLERBERGHE

Dirigée par le Professeur Florence PETIT

ULR7364 RADEME

Soutenue publiquement le 8 octobre 2024 à 14h
au Pôle Formation de la Faculté de Médecine de Lille

JURY :

Sous la présidence du Professeur Gaël NICOLAS

Pr Franck FITOUSSI, PU-PH	Université Paris 6	**Rapporteur**
Pr Gaël NICOLAS, PU-PH	Université Rouen Normandie	**Rapporteur**
Dr Muriel HOLDER-ESPINASSE, MCU	Guy's Hospital, Londres	**Examinatrice**
Pr Sylvie MANOUVRIER-HANU, PU-PH	Université Lille	**Examinatrice**
Pr Florence PETIT, PU-PH	Université Lille	**Directrice de thèse**

ENCADREMENT

ULR7364 RADEME

Maladies Rares du Développement : génétique, régulation et protéomique

Directrice de thèse : Pr Florence PETIT, PU-PH

Directeur d'unité : Pr Jamal GHOUMID

Faculté de Médecine - Pôle recherche

3ème étage EST
1 place Verdun
F-59000 LILLE

REMERCIEMENTS

Je remercie ici l'ensemble des personnes ayant contribué à la réalisation et à l'évaluation de ces travaux, tant sur le plan scientifique qu'humain. Cette liste non exhaustive témoigne du caractère collaboratif de ces travaux et de l'apport indispensable de chacune de ces expertises dans l'aboutissement de ces projets.

Florence, ce travail n'aurait pas pu aboutir sans toi. Ton soutien sans faille, ton implication scientifique mais aussi personnelle et amicale m'ont été d'une grande aide. Mille mercis pour ta confiance et pour ta disponibilité, à toutes épreuves, du début à la fin, de Londres à Dresde, en passant (ou pas !) par Francfort. Cette aventure de la thèse s'achève mais l'avenir nous en réserve de nouvelles. J'aurai beaucoup de plaisir à les partager avec toi !

Jamal, je te remercie pour ton soutien et ta confiance. Ton esprit de chercheur et ta curiosité scientifique sont d'une grande richesse pour RADEME. Nos échanges m'ont permis d'évoluer sereinement au sein de cette équipe ;

Je remercie **le Professeur Franck FITOUSSI** et le **Professeur Gaël NICOLAS** d'avoir accepté d'être rapporteurs de cette thèse. Veuillez trouver ici l'expression de mon profond respect ainsi que le témoignage de ma reconnaissance pour avoir consacré du temps à juger ce travail ;

Muriel, je te remercie beaucoup d'avoir accepté d'être examinatrice de ce travail. En tant qu'interne, ta pratique m'avait inspiré à la fois au contact des patients et en recherche. Nous sommes très heureux de te revoir à Lille pour cette occasion ;

Mme Manouvrier, votre présence au sein de ce jury et de mon Comité de Suivi de Thèse était indispensable. Je vous remercie d'avoir construit les bases nécessaires à la réalisation de ce travail : de l'expertise lilloise sur les malformations des membres à la création de RADEME, en passant par l'encadrement de ma thèse de médecine et votre publication du phénotype de la famille pour laquelle le séquençage du génome aura permis de résoudre l'errance diagnostique ;

Je remercie les membres de mon Comité de Suivi de Thèse, pour leur accompagnement, leur bienveillance et leur renforcement positif au cours de ces 6 années :

Pierre Olivier, pour votre disponibilité et les échanges toujours riches autour de ce travail, ainsi que pour votre collaboration pour les projets encore en cours ;

Emilie, et Fabrice, pour votre implication dans ce travail et pour vos nombreux enseignements en bio-informatique alors que je partais de loin, qui ont finalement permis d'identifier le variant de *RPL17* ! Pour votre confiance dans mon rôle de β-testeuse !

Malcolm, for your insights on limb developmental biology and your expertise on our favorite gene "Tea Box" 5

Anne Sophie, je te remercie tout particulièrement pour ta précieuse implication dans ces projets, notamment pour la réalisation des tests minigènes, mais aussi plus globalement pour tes conseils et ton expérience dans les tests *in vitro*.

Frederic, je te remercie tout particulièrement pour ton implication et ta ténacité dans ces projets, notamment pour les Western Blots et l'Immunohistochimie, mais aussi tes compétences de biochimiste pour la prédiction protéique.

Je remercie les membres de l'équipe EA7364 RADEME et de l'université de Lille :

Thomas, pour ta contribution dans ces projets, pour tes tutos en bio-info et tri de variants et ta confraternité/sororité de thésards ;

Fabienne, pour ton expertise dans les gènes du développement des membres et ton soutien dans ces projets ;

Perrine, pour ton aide dans la maîtrise des critères ACMG ! A nos futurs projets communs autour de nos gènes préférés ;

Simon, ton projet de thèse figure parmi les perspectives de cette thèse. A toi de jouer ! Merci encore pour ton relais à Valenciennes pendant mon absence dans le service ;

Fiona, merci pour ta contribution et cette année passée à RADEME ensemble.

Jade, merci ton dynamisme et ta disponibilité. Je me suis permise un teasing de CAR-SV dans les perspectives. Hâte d'avoir le fin mot de l'histoire de feu la « DUP-TRIP-DUP » ;

William, pour ton aide pour les RT-PCR au cours de ton Master 2 ;

Au plateau d'imagerie cellulaire, pour l'assistance au microscope confocal pour les nombreuses immunohistochimies

Je remercie mes collègues de la clinique de génétique « Guy Fontaine » pour leur soutien dans ce projet,

Luisa, pour nos échanges scientifiques (ou pas !), pour ton soutien quotidien en tant que colocataire et pour ton relais pour mes patients « Marfan » pendant mon absence et au-delà ;

Catherine, Sara, pour votre relais pour mes patients « Surdité » pendant mon absence ;

Geneviève, Carinne, Fabienne, pour votre gestion des multiples changements de planning liés à cette thèse et votre soutien ;

Je remercie les différents co-auteurs des articles de cette thèse :

Au Professeur Lydie DA COSTA, pour votre expertise dans le syndrome de Blackfan-Diamond et les tests fonctionnels des gènes *RPL* ;

Elise, pour ton intérêt dans les malformations des membres et nos futurs projets communs ;

Je remercie les membres du CRMR Anomalies des membres du CHU de Lille :

Laurence, pour tes conseils avisés sur l'encadrement de la recherche clinique et ton aide en tant qu'ARC ou chargée de mission ;

Aurélie, pour ta contribution à cette expertise locale ;

Marianne, pour nos échanges qui aboutiront aux futurs projets en recherche clinique ;

Je remercie les patients et leur famille pour avoir accepté de participer à la recherche ;

Je remercie **l'Université de Lille et le CHU de Lille** pour le financement Health PhD, qui m'a permis de prendre une disponibilité d'un an pour travailler à temps plein sur ces travaux, et le **GIRCI Nord-Ouest** pour le financement des génomes et tests fonctionnels dans le cadre du projet HOS-REG ;

Je remercie mes amis et ma famille,

Papa, Maman, pour m'avoir donné les moyens d'arriver à ce but et m'avoir encouragée à suivre la voie de la médecine pour faire de la recherche. Merci de votre soutien et de votre amour ;

Raphaël et Valentin, pour avoir parfois laissé Maman « écrire son livre » ;

Romain, pour ton soutien au quotidien, malgré les épreuves et les imprévus. L'année 2025 se profile sous des horizons plus doux, que je suis heureuse de vivre avec toi.

RESUME

TITRE : Déterminisme moléculaire des anomalies radiales

L'identification d'une cause moléculaire est cruciale pour la prise en charge des patients présentant une anomalie radiale, notamment du fait des possibles atteintes associées. Ici, nous présentons, pour contextualiser, une revue de la littérature sur les étiologies des anomalies radiales et les interactions entre la biologie fondamentale et la pathologie humaine dans ce domaine. Puis, nous développons l'une des étiologies monogéniques les plus fréquentes d'anomalies radiales, le syndrome de Holt-Oram, lié aux altérations du gène *TBX5*, afin d'en préciser les critères diagnostiques, à partir d'une large cohorte de patients. Plusieurs variants faux-sens et d'épissage de *TBX5* identifiés à partir de cette étude, puis de l'étude de la littérature, étaient de signification incertaine. Nous présentons les résultats de tests fonctionnels de ces variants, comprenant notamment un variant gain-de fonction responsable d'un phénotype atypique et un variant intronique profond responsable de l'incorporation d'un pseudo-exon décalant le cadre de lecture. Enfin, pour les patients présentant une anomalie radiale bilatérale isolée, en errance diagnostique après étude des gènes impliqués dans les malformations des membres, nous présentons les résultats d'étude de génome entier. Nous avons identifié, chez 5 patients d'une famille française, un variant causal, situé dans une région non-codante du gène *RPL26*, impliqué dans le syndrome de Blackfan-Diamond, décrit dans une seule famille jusqu'à présent. Grâce à un appel à collaboration, nous présentons les phénotypes associés aux variants de *RPL26* dans 3 autres familles. Par ailleurs, nous discutons un variant homozygote de *RPL17* identifié chez une patiente issue d'une union consanguine, pour lequel des études fonctionnelles sont envisagées. Nos travaux illustrent la place du séquençage de génome dans le diagnostic étiologique des malformations des membres et l'importance des collaborations interdisciplinaires et internationales dans ce domaine.

MOTS-CLES : Dysplasie radiale, syndrome de Holt-Oram, syndrome de Blackfan-Diamond, *TBX5, RPL26, RPL17*, développement des membres, caractérisation fonctionnelle

ABSTRACT

TITLE: Molecular determinism of radial defects

Molecular determinism is crucial for the management of patients presenting with a radial defect, in particular because of the possible associated features. Here, we introduce the topic presenting a literature review of the etiology of radial defects and the relationship between fundamental biology and human disease in this field. Then, we report a large cohort of patients with Holt-Oram syndrome, one of the most common monogenic cause of radial defect, caused by *TBX5* gene variants, in order to establish the diagnostic criteria for this rare disease. Some of the identified *TBX5* missense or splice variants in this series, and in the literature, were of uncertain significance. We present the results of functional assays for these variants, including a gain-of-function variant responsible for an atypical phenotype and a deep intronic variant responsible for the incorporation of a pseudo-exon leading to frame-shifting. Finally, we present the results of whole genome sequencing in patients presenting with isolated and bilateral radial defects, and without a molecular diagnosis after targeted high-throughput sequencing of genes involved in limb development. A non-coding causal variant in *RPL26* gene, that had been previously reported in only one family with Diamond-Blackfan syndrome, was identified in 5 related patients of one family of our cohort. Thanks to a call of collaboration, we present the phenotype associated to *RPL26* variants in 3 additional families. Finally, we discuss a homozygous *RPL17* missense variant identified in a girl born from consanguineous parents, for which functional assays are planned. Our work illustrates the role of genome sequencing as etiological diagnostic tool for limb malformations and the importance of interdisciplinary and international collaborations in this field.

KEY-WORDS: Radial Defect, Holt-Oram syndrome, Diamond-Blackfan syndrome, *TBX5, RPL26, RPL17*, limb development, functional characterization

TABLE DES MATIÈRES

TABLE DES ILLUSTRATIONS

ABREVIATIONS

ACPA	Analyse Chromosomique sur Puce à ADN
AER	Apical Ectodermal Ridge
BNDMR	Banque Nationale de Données Maladies Rares
CEREFAM	Centre de Référence des Anomalies des Membres
CHU	Centre Hospitalier Universitaire
ENCODE	Encyclopedia of DNA elements
ERN	European Reference Network
HCSP	Haut Conseil de la Santé Publique
HCERES	Haut Conseil de l'Evaluation de la Recherche et de l'Enseignement Supérieur
ILIAD	International Library of Intellectual disability and Anomalies of Development
ITHACA	Intellectual disability, TeleHealth, Autism and Congenital Anomalies
NMD	Nonsense-mediated mRNA decay
pb	Paires de bases
PFMG	Plan France Médecine Génomique
PNMR	Plan National Maladies Rares
RPL17	Ribosomal Protein L17
RPL26	Ribosomal Protein L26
SV	Variants structuraux
TBX5	T-box gene 5
VSI	Variant de signification incertaine
ZPA	Zone d'Activité Polarisante
ZRS	ZPA Regulatory Sequence

AVANT-PROPOS

Cette thèse d'articles présente 4 travaux originaux en langue anglaise :

- Une revue en cours de finalisation « *Radial ray: from developmental biology to human disease* ». Ce travail va être complété par une collaboration avec une équipe spécialisée dans l'évolution du développement des membres pour l'enrichir d'une partie « évo-dévo » : Dr Karen Sears (Departments of Ecology and Evolutionary Biology and Molecular, Cell, and Developmental Biology at UCLA, Los Angeles, USA) et Dr Aidan Couzens (College of Science & Engineering, Flinders University, Adelaide, Australia). Nous projetons de suggérer cette revue au journal *Human Genetics*.

- Un article publié en 2019 dans la revue *European Journal of Human Genetics* : « *Holt-Oram syndrome: clinical and molecular description of 78 patients with TBX5 variants* » . Ce travail a fait l'objet d'une communication orale au congrès international « International conference on limb development » à Edimbourg en 2017, et d'une communication affichée à l'European Society of Human Genetics conference à Copenhague en 2017.

- Un article publié en 2024 dans la revue *Genetics in Medecine* : « *Functional characterization vs in silico prediction for TBX5 missense and splice variants in Holt-Oram syndrome* ». Ce travail a fait l'objet d'une communication affichée aux Assises de Génétique Humaine à Paris en 2024 et d'une communication affichée au congrès international « International conference on limb development » à Dresde en 2024.

- Un article publié en 2024 dans la revue *Genetics in Medecine* : « *RPL26 variants: a rare cause of Diamond-Blackfan Anemia Syndrome with multiple congenital anomalies at the forefront* ». Ce travail a fait l'objet d'une communication affichée aux Assises de Génétique Humaine à Paris en 2024 et d'un e-poster à l'European Society of Human Genetics conference à Berlin en 2024.

INTRODUCTION

Les malformations congénitales, concernant 3 à 5 % des naissances, peuvent être d'origine génétique et s'intégrer alors dans plus de 10000 entités cliniques différentes. En Juillet 2024, la base OMIM répertoriait 6869 phénotypes dont les bases moléculaires sont connues et 3237 phénotypes dont les bases moléculaires sont, à ce jour, non élucidées. Depuis 2010, le nombre de gènes décrits comme associés à un phénotype a doublé, portant à environ 5000 les gènes impliqués en pathologie humaine (1).

Le diagnostic étiologique des syndromes malformatifs est indispensable, d'une part pour adapter la prise en charge et la surveillance de ces patients et, d'autre part, pour lever d'éventuels fantasmes ou sentiments de culpabilité des familles. Les analyses moléculaires ont pour but de confirmer le diagnostic mais aussi de préciser le conseil génétique en termes de risque de récurrence et de possibilité éventuelle de diagnostic prénatal ou préimplantatoire, si la gravité de la pathologie le justifie.

En 2016, seule une personne atteinte de maladie rare sur deux disposait d'un diagnostic précis et la recherche du diagnostic dépassait 5 ans pour plus d'un quart des personnes (2). Cette errance diagnostique est responsable d'une aggravation possible de l'état des malades, d'un retard sur les possibilités de conseil génétique et d'une multiplication des consultations diagnostiques. L'impasse diagnostique résulte de l'échec à définir la cause précise de la maladie après avoir mis en œuvre l'ensemble des investigations disponibles en l'état de l'art. Cette situation rend la prise en charge plus difficile et le caractère indéfini de la maladie est une source de souffrances supplémentaires (3).

L'arrivée du séquençage à haut débit a permis l'étude de panels de gènes, par enrichissement ciblé de gènes impliqués dans un même phénotype, puis le séquençage de l'exome couvrant les parties codantes des gènes connus (1 à 2% du génome), et enfin le séquençage de génome entier, permettant l'étude des parties codantes et non codantes des gènes mais aussi des régions régulatrices et des régions intergéniques (4). Du fait de la baisse du coût du séquençage, ces techniques

de pointe ont pu être rendues accessibles aux laboratoires de biologie moléculaire de routine, permettant le recours à ces analyses en pratique courante.

Les taux diagnostiques observés en étude de génome varient entre 16 et 45 % selon les études, avec des taux sensiblement plus élevés pour les indications neuro-pédiatriques (5). Les rares études comparatives d'analyse d'exome *vs* génome montrent que la probabilité de poser un diagnostic est 1,2 fois plus élevée avec l'analyse du génome. Cette même méta-analyse a étudié l'utilité clinique de ces analyses, définie par le pourcentage de patients ayant bénéficié d'une adaptation de leur prise en charge (surveillance, recours à un spécialiste, hospitalisation, indication ou contre-indication à une thérapeutique) au décours des résultats d'exome ou de génome, sans prendre en compte le conseil génétique. Elle a montré une utilité clinique supérieure pour l'étude du génome (0.61, 95% CI 0.50-0.73, 16 études, n = 3686) comparée à l'étude de l'exome (0.48, 95% CI 0.40-0.56, 47 études, n = 8869).

Alors que l'étude de l'exome a permis l'identification de variations dans les parties codantes des gènes, l'étude du génome a une meilleure sensibilité pour la détection des variants de structure, des anomalies en nombre de copie, des expansions de répétitions et permet la détection de variants non-codants, notamment des régions régulatrices et des régions introniques. Néanmoins, la quantité et la complexité des informations génétiques générées induisent une augmentation du nombre de variants de signification incertaine identifiés et donc la possibilité de situations d'incertitude, ne permettant pas de conclure quant au diagnostic étiologique (6).

L'interprétation de l'analyse de génome peut être variable en fonction des filtres utilisés et, bien sûr, du moment de l'interprétation, du fait de l'évolution des connaissances en génétique humaine et des outils d'interprétation. De récentes recommandations ont été publiées pour l'utilisation de l'analyse du génome en pratique courante pour le diagnostic des maladies rares, du contrôle qualité à la validation des procédures de laboratoire, aux pipelines informatiques, à l'interprétation des variants et aux considérations éthiques du rapport des résultats de l'analyse (7).

Sous l'impulsion du Plan National Maladies Rares 3 (PNMR3) et du Plan France Médecine Génomique (PFMG) 2025, la mise en place des plateformes de séquençage

à très haut débit, SeqOIA et AURAGEN, a permis l'accès au séquençage de génome entier pour ces patients, dans le but de réduire l'errance et l'impasse diagnostique en France. Néanmoins, le rapport conjoint du Haut Conseil de la Santé Publique (HCSP) et du Haut Conseil de l'Evaluation de la Recherche et de l'Enseignement Supérieur (HCERES) souligne l'enjeu majeur du développement des analyses fonctionnelles des variants de signification incertaine, non réalisées sur les plateformes SeqOIA et AURAGEN, et le besoin de simplification des règles européennes en matière de partage de données, dans le but de poursuivre cet effort commun de réduction des situations d'impasse diagnostique (8).

Au sein de la Filière Maladies Rares « AnDDI-rares » et du réseau CEREFAM, le Centre de Référence Maladies Rares « Anomalies des Membres » du CHU de Lille, récemment labellisé, bénéficie d'une expertise clinique et moléculaire dans les malformations des membres acquise grâce à la constitution de cohortes de patients précisément phénotypés ayant bénéficié de l'étude des gènes impliqués dans le développement des membres, et une étroite collaboration clinico-biologique entre le service de génétique clinique « Guy Fontaine » et l'équipe de biologie moléculaire du Centre de Biologie et Pathologie du CHU de Lille, depuis 2002.

La création de l'équipe de recherche ULR7364 RADEME (Maladies Rares du Développement : génétique, régulation et protéomique) en 2015 s'inscrit dans la continuité de cette volonté de mise en commun d'expertises complémentaires. L'équipe s'intéresse à la régulation génique, avec un axe dédié aux malformations des membres : caractérisation fonctionnelle de régions régulatrices (enhancers, 5'UTR, 3'UTR), régulation transcriptionnelle et traductionnelle, interactions enhancer-promoteur, étude de la méthylation dans les malformations sporadiques notamment. Plusieurs techniques de biologie moléculaire y sont donc utilisées (4C-seq, HiC-seq, ChIP-seq,…) et des modèles organoïdes y sont développés.

La création des Fédérations Hospitalo-Universitaires (FHU) vise également à renforcer les relations hôpitaux-universités-unités de recherche afin d'améliorer la qualité des soins, par une diffusion plus rapide des innovations. La FHU-G4 Génomique (Développement de la génomique médicale à l'ère post-exome) regroupe des équipes du CHU de Rouen, du CHU de Lille, du CHU d'Amiens, du CHU de Caen et du CRLCC

François Baclesse. Ses objectifs sont de (i) développer de nouveaux outils facilitant l'interprétation des variations génétiques détectées dans l'exome et (ii) détecter et interpréter des altérations situées dans les régions non codantes du génome.

Cette thèse s'inscrit dans cet effort collectif d'identification du déterminisme moléculaire d'anomalies congénitales que sont les atteintes du rayon radial, par différentes approches, notamment le séquençage de génome entier, l'utilisation de tests fonctionnels pour caractériser les variants d'intérêt mais de signification incertaine et l'utilisation des données de biologie fondamentale du développement des membres.

a. Le développement des membres

La diversité morphologique des membres entre les espèces en fait un sujet majeur d'étude, dans le champ de la biologie du développement et de l'évolution des espèces et a permis de décrire des processus biologiques fondamentaux de la morphogénèse et de l'organogénèse. Chez les mammifères, du fait de leurs habitats très variés (aérien, aquatique, terrestre …), l'adaptation de la forme et de la fonction de leurs membres leur a permis d'explorer de nouveaux environnements. Leurs membres peuvent être divisés en 3 parties : stylopode (humérus / fémur), zeugopode (radius, ulna / tibia, fibula) et autopode (carpe, métacarpe, doigts / tarse, métatarse, orteils) (Figure 1).

Figure 1 : Diversité de la morphologie des membres au cours de l'évolution des espèces

Adapté de "Integrating "Evo" and "Devo": The Limb as Model Structure", by Nathan M. Young (9). A. Description du membre des mammifères en 3 parties : stylopode, zeugopode, autopode. B. Diversité morphologique des membres des mammifères.

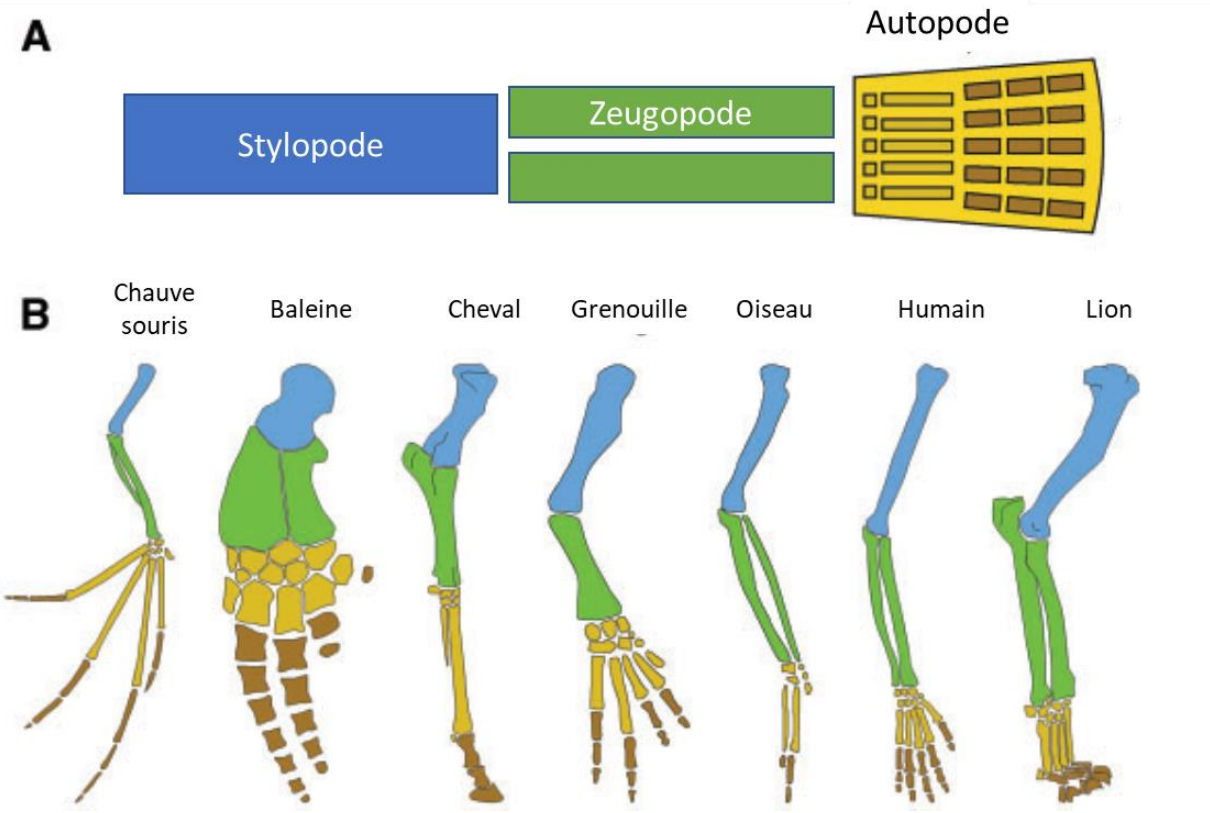

Les travaux sur le développement des membres chez l'animal sont facilités par leur accessibilité, permettant à la fois une intervention facile mais aussi une observation macroscopique de certaines malformations. Les expérimentations chez l'embryon de poulet (*knock-in* par électroporation dans le bourgeon de membre), les modèles murins transgéniques (*knock-out* ou délétion conditionnelle) ou, plus récemment, l'édition du génome par CRISPR-Cas9 chez le poisson-zèbre ont permis de décrire les profils d'expression et les fonctions des gènes majeurs du développement des membres. L'arrivée des technologies de nouvelle génération a permis le développement d'approches multi-omics avec, par exemple, l'analyse de l'architecture chromatinienne, des interactions entre enhancers et promoteurs ou encore les

approches basées sur l'intelligence artificielle pour simuler des modèles de réseaux de gènes.

Ces travaux ont permis de décrire les réseaux de gènes impliqués dans les 3 axes de développement du bourgeon de membre : proximo-distal (de l'épaule vers les doigts), antéro-postérieur (du pouce vers le 5ème doigt) et dorso-ventral (du dos vers la paume de la main), ainsi que 3 centres de signalisation contrôlant la morphogénèse du membre : la crête ectodermique apicale (AER) à l'extrémité distale, la zone d'activité polarisante (ZPA) au bord postérieur (post-axial) et l'ectoderme dorsal situé sur la face dorsale du bourgeon de membre (Figure 2).

Figure 2 : Développement des membres.

Axes de développement du bourgeon de membre : proximo-distal sous la dépendance de la crête ectodermique apicale (AER) (en bleu) ; pré-post-axial (antéropostérieur) dont le centre de signalisation est la zone d'activité polarisante (ZPA), au bord post-axial du bourgeon de membre (en rouge) ; dorso-ventral dépendant de l'ectoderme ventral (en vert) (de Classification des malformations congénitales des membres, S. Manouvrier-Hanu, F. Petit, A. Mezel, Elsevier Masson 2023)(10).

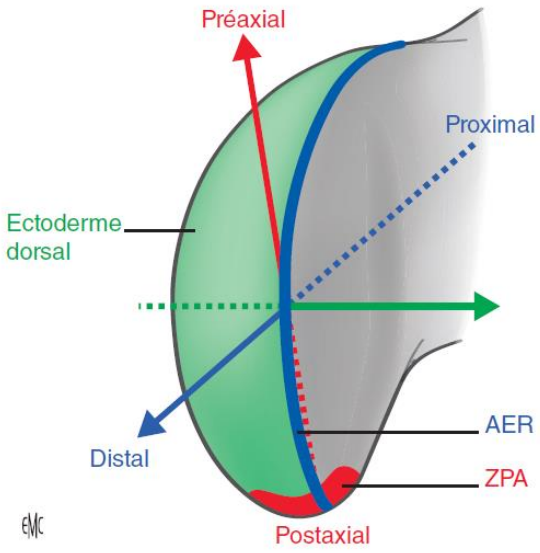

Néanmoins, il existe de grandes différences entre ces espèces et l'humain du fait de la transition des nageoires vers les membres, du bipédisme et de la fonction d'opposition du pouce propre à l'Homme. Les bourgeons de membre se développent à partir du mésoderme latéral, au 26ème jour de développement au cours de l'embryogénèse humaine (11). Les travaux sur le développement des membres chez l'humain sont plus récents et sont limités par les considérations éthiques qu'impliquent les études portant sur l'embryon humain.

b. Les malformations des membres supérieurs

Les malformations congénitales des membres touchent entre 5,6 et 21,1 naissances vivantes sur 10000, selon différentes études épidémiologiques (12,13). Leur prévalence est estimée à 3 ‰ chez les fœtus (12,14). Entre 10 et 20% des nouveaux nés atteints de malformations congénitales présentent une anomalie des membres supérieurs (17). Elles peuvent être observées au cours de la grossesse lors du suivi échographique, à la naissance ou, pour certaines atteintes mineures, au cours de l'enfance.

La classification des anomalies congénitales des membres supérieurs se base sur les connaissances en biologie du développement : malformations, déformations, dysplasies et syndromes (15,16). Au sein des malformations, les atteintes sont séparées selon qu'elles concernent le membre supérieur entier (atteinte précoce) ou qu'elles concernent la main (atteinte plus tardive au cours du développement), puis au sein de ces 2 groupes, selon l'axe de développement concerné : proximo-distal, antero-postérieur, dorso-ventral ou non spécifique. Sur le plan morphologique, ces atteintes sont de sévérité variable, et peuvent être transversales ou longitudinales, pré ou post-axiales (respectivement, du côté du radius ou de l'ulna), réductionnelles ou additionnelles (oligodactylie ou polydactylie par exemple). La diversité de ces présentations cliniques est illustrée par la Figure 3 et la Figure 4. La classification de Blauth pour les hypoplasies du pouce est détaillée par la Figure 5 (17).

Figure 3 : Malformations réductionnelles des membres.

A : Schématisation des membres avec leurs segments rhizomélique (proximal), mésomélique (moyen) et acromélique (distal) ; B : Absence totale de membre : amélie ; C : Anomalie déficitaire transverse : hémimélie transversale ; D : Anomalies déficitaires longitudinales : hémimélie longitudinale (pré- ou postaxiale) ; E : Phocomélie ; F : Mains et pieds fendus : ectrodactylie.

(de Classification des malformations congénitales des membres, S. Manouvrier-Hanu, F. Petit, A. Mezel, Elsevier Masson 2023)(10).

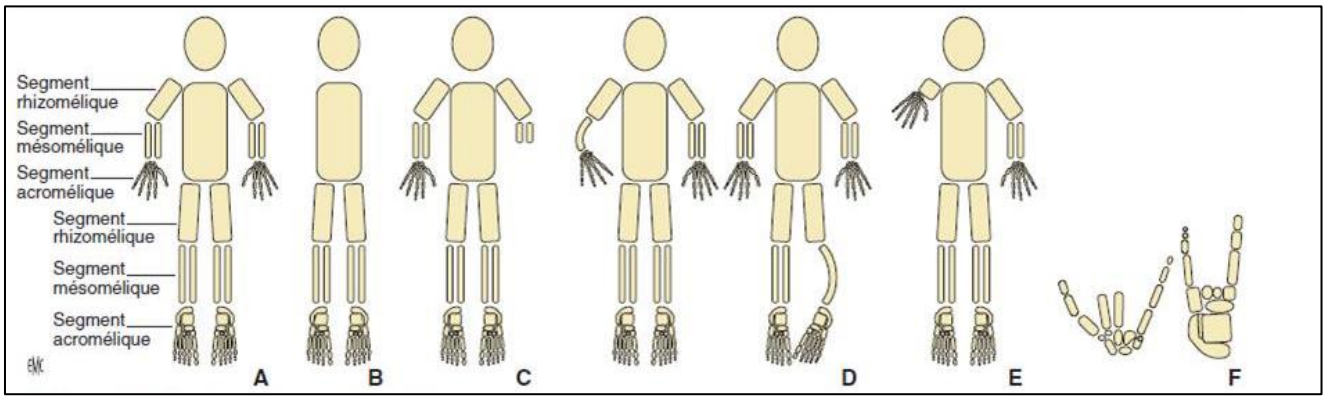

Figure 4 : Polydactylies.

A : Polydactylies préaxiales de type I ; B : Polydactylies préaxiales de type 2 ; C : Polydactylies préaxiales de type 3 ; D : Polydactylies postaxiales de type 1 (classification de Stelling et Turek) ou B (classification de Temtamy) ; E : Polydactylies postaxiales de type 2 (classification de Stelling et Turek) ou A (classification de Temtamy) ; F : Polydactylies postaxiales de type 3 (classification de Stelling et Turek) ou A (classification de Temtamy) ; G : Polydactylies croisées de type 1 : postaxiale aux membres supérieurs et préaxiale aux membres inférieurs, souvent associée à des syndactylies ; F : Polydactylies croisées de type 2 : préaxiale aux membres supérieurs et postaxiale aux membres inférieurs, souvent associée à des syndactylies ; I : Polydactylies mesoaxiales ; J : Polydactylies en miroir (exemples).

(de Classification des malformations congénitales des membres, S. Manouvrier-Hanu, F. Petit, A. Mezel, Elsevier Masson 2023)(10).

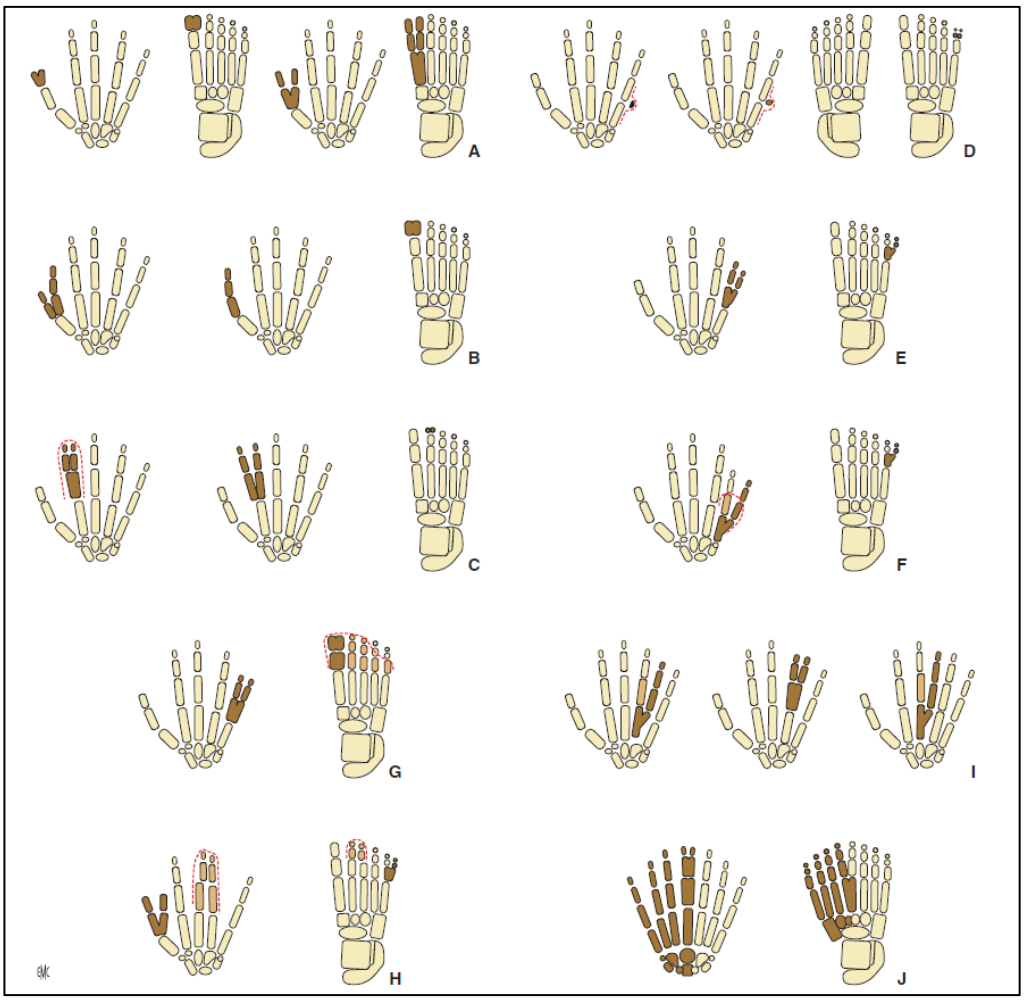

Figure 5 : Classification de Blauth pour les hypoplasies des pouces

Type I : discret raccourcissement isolé ; Type II : diminution de taille, hypoplasie de l'éminence thénar, brièveté de la première commissure, articulation métacarpo-phalangienne plus ou moins stable ; Type III : aplasie totale de l'éminence thénar, brièveté de la première commissure, instabilité constante de l'articulation métacarpophalangienne, interphalangienne plus ou moins raide. Les muscles extrinsèques sont souvent absents. On distingue les sous-types III A et III B selon la présence ou non d'une articulation carpo-métacarpienne ; Type IV : pouce flottant, relié à la main par un simple pédicule cutané, absence de premier métacarpien ; Type V : aplasie totale du pouce (17).

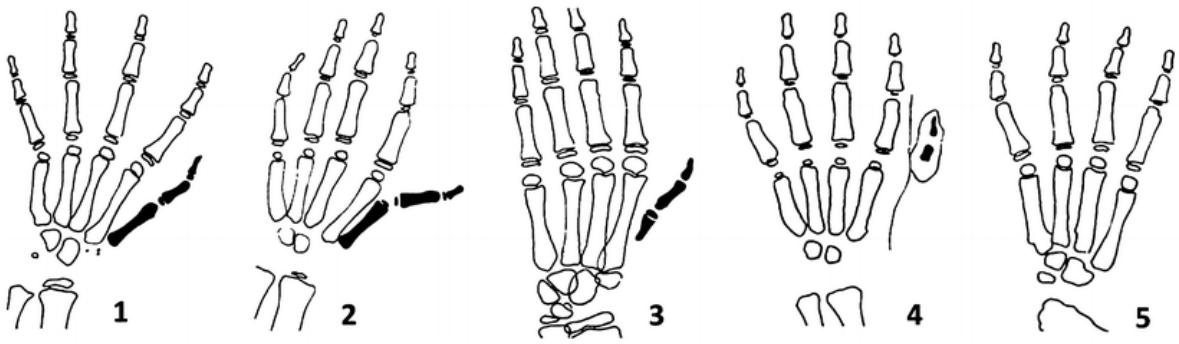

Le pronostic de ces patients est lié à l'impact fonctionnel et esthétique de la malformation, mais aussi à la présence et au type d'atteinte associée. Le pronostic fonctionnel est notamment lié à l'atteinte de la pince pouce-index, indispensable à de nombreux gestes du quotidien. Une intervention chirurgicale peut être parfois proposée, comme la pollicisation de l'index en cas de pouce non fonctionnel, les cures de syndactylies, le traitement des duplications pré ou post axiales ou des clinodactylies. Le port d'un appareillage peut être discuté en fonction de l'acceptabilité du patient. L'appareillage doit continuellement être adapté à la croissance de l'enfant mais aussi à son développement psycho-moteur. Ainsi, l'association à un trouble du neuro-développement par exemple peut orienter la prise en charge rééducative.

Au moins une atteinte associée est rapportée chez 88-92 % des patients porteurs de malformations des membres (18,19). Elles peuvent être variables : malformations cardiaques, rénales, atteintes neuro-sensorielles, hématologiques, … Dans ce

contexte, le bilan malformatif orienté et l'éventuelle identification d'une cause génétique est cruciale pour la prise en charge adaptée du patient. Par ailleurs, l'identification d'une étiologie génétique au syndrome malformatif permettra de préciser le conseil génétique, c'est-à-dire le risque de récurrence de la pathologie dans la fratrie ou la descendance du cas index, source d'inquiétude importante des patients, particulièrement dans le cadre de malformation des membres (20).

c. Démarche étiologique des malformations des membres supérieurs

La démarche étiologique fait appel aux compétences du généticien clinicien, qui s'aidera des antécédents familiaux, du déroulement de la grossesse, du type de malformation du membre supérieur et des éventuels signes associés pour orienter les investigations moléculaires. Certaines présentations cliniques, telles que l'agénésie transverse de membre supérieur, le syndrome de Poland ou la maladie des brides amniotiques, sont évocatrices d'une cause clastique, environnementale, vasculaire ou multifactorielle. Une origine tératogène peut également être suspectée, notamment dans les embryofoetopathies à la thalidomide ou au valproate.

Devant une anomalie radiale, le bilan malformatif comprendra classiquement une échographie cardiaque, une échographie abdominale, des radiographies de rachis, un bilan sensoriel (ORL et ophtalmologique) et hématologique (numération formule sanguine et plaquettaire). Sur le plan génétique, une analyse chromosomique par puce à ADN est généralement demandée en première intention. La recherche de fragilité chromosomique peut être demandée devant une anomalie radiale, isolée ou associée à un retard de croissance, une microcéphalie ou autres signes associés évocateurs d'anémie de Fanconi. Actuellement, l'étude des gènes impliqués dans les syndromes comprenant une malformation des membres supérieurs peut encore être réalisée de façon ciblée par séquençage à haut débit d'un panel de gènes.

Selon les dernières études de cohorte, le taux diagnostique après étude de panel de gènes était de 32,7% pour les anomalies radiales (21). L'étude du génome entier peut maintenant être proposée aux patients dans le cadre du Plan France Medecine Génomique 2025, dans les pré-indications « Syndromes malformatifs » de la filière Maladies Rares AnDDI-rares si elles sont syndromiques, ou « Maladies Osseuses

Constitutionnelles » si elles sont isolées. L'interprétation de ces données nécessite une expertise en génétique du développement des membres, car beaucoup de ces gènes sont des facteurs de transcription avec des domaines fonctionnels spécifiques et éventuellement des hotspots mutationnels. Certaines régions régulatrices de ces gènes sont également bien caractérisées et sont analysées en pratique de routine (notamment la ZRS, région régulatrice du gène *SHH* spécifique des membres). Certains gènes sont associés à un type particulier de variants (variants tronquants pour *SALL1*, expansion de répétitions d'Alanine pour *HOXD13*, …). Enfin, il existe des corrélations génotype / phénotype bien décrites pour certains gènes (*GLI3, ROR2*).

Dans une première étude au cours de laquelle 69 patients atteints de malformations des membres ont bénéficié du séquençage de génome, alors que les analyses de routine étaient négatives, des variants probablement pathogènes ou pathogènes ont été identifiés chez 12 cas (17.4%) incluant 4 variants dans des gènes déjà connus en pathologie, une répétition d'alanine dans *HOXD13* et deux réarrangements complexes de structure (3%). Par ailleurs, un nouveau gène a été associé à l'ectrodactylie chez 3 patients issus de familles différentes et des variants d'intérêt ont été identifiés dans 3 gènes candidats. En revanche, aucun variant non-codant n'a été identifié (22).

Par ailleurs, s'agissant de gènes exprimés principalement au cours du développement embryonnaire, l'accès à l'ARN chez les patients peut être difficile. L'expression des gènes dans différents tissus accessibles chez l'enfant ou l'adulte (sang, urines, salive, cellules buccales) n'est pas toujours connue, rendant les études du transcriptome difficiles d'accès chez les patients.

d. Variants génomiques de signification incertaine

Depuis 2015, l'interprétation des variants génomiques a été standardisée par l'American College of Medical Genetics and Genomics, par l'utilisation de différents critères permettant de classer les variants de 1 à 5 : bénin, probablement bénin, signification incertaine, probablement pathogène, pathogène (23). La liste de ces critères et le mode de classification sont explicités par le Tableau 1 et le Tableau 2.

Les études de génome montrent des taux de variants de signification incertaine (VSI) de 6 à 50%, démontrant la variabilité d'interprétation entre les centres. Alors que

certains centres ne rapportent que les variants pathogènes, pouvant expliquer le phénotype, d'autres rapportent des VSI situés dans des gènes connus comme impliqués dans la pathologie, alors que certains rapportent également des VSI dans des gènes candidats (24).

De larges bases de données sont accessibles afin d'évaluer la fréquence du variant d'intérêt dans la population générale : GnomAD (25) ; mais aussi dans des populations de patients : ClinVar (26), DECIPHER (27), LOVD (28).

Tableau 1 : Liste des critères ACMG pour la classification des variants génomiques.

Issue de Richards et al, 2015 (23).

Criteria	Strength	Details
PM1	Moderate	Located in a mutational hot spot and/or critical and well-established functional domain (e.g., active site of an enzyme) without benign variation
PM5	Moderate	Novel missense change at an amino acid residue where a different missense change determined to be pathogenic has been seen before
PM2	Supporting	Absent from controls (or at extremely low frequency if recessive) in Exome Sequencing Project, 1000 Genomes Project, or Exome Aggregation Consortium
PP1	Supporting	Cosegregation with disease in multiple affected family members in a gene definitively known to cause the disease
PP2	Supporting	Missense variant in a gene that has a low rate of benign missense variation and in which missense variants are a common mechanism of disease
PP3	Supporting	Multiple lines of computational evidence support a deleterious effect on the gene or gene product (conservation, evolutionary, splicing impact, etc.)
BP4	Supporting	Multiple lines of computational evidence suggest no impact on gene or gene product (conservation, evolutionary, splicing impact, etc.)
PP4	Supporting	Patient's phenotype or family history is highly specific for a disease with a single genetic etiology
PS3	Supporting	Well-established in vitro or in vivo functional studies supportive of a damaging effect on the gene or gene product
BS3	Supporting	Well-established in vitro or in vivo functional studies show no damaging effect on protein function or splicing

Tableau 2 : Mode de classification ACMG.

Issue de Richards et al, 2015 (23).

Pathogenic	(i) 1 Very strong (PVS1) *AND* (a) ≥1 Strong (PS1–PS4) *OR* (b) ≥2 Moderate (PM1–PM6) *OR* (c) 1 Moderate (PM1–PM6) and 1 supporting (PP1–PP5) *OR* (d) ≥2 Supporting (PP1–PP5) (ii) ≥2 Strong (PS1–PS4) *OR* (iii) 1 Strong (PS1–PS4) *AND* (a)≥3 Moderate (PM1–PM6) *OR* (b)2 Moderate (PM1–PM6) *AND* ≥2 Supporting (PP1–PP5) *OR* (c)1 Moderate (PM1–PM6) *AND* ≥4 supporting (PP1–PP5)	Benign	(i) 1 Stand-alone (BA1) *OR* (ii) ≥2 Strong (BS1–BS4)
Likely pathogenic	(i) 1 Very strong (PVS1) *AND* 1 moderate (PM1–PM6) *OR* (ii) 1 Strong (PS1–PS4) *AND* 1–2 moderate (PM1–PM6) *OR* (iii) 1 Strong (PS1–PS4) *AND* ≥2 supporting (PP1–PP5) *OR* (iv) ≥3 Moderate (PM1–PM6) *OR* (v) 2 Moderate (PM1–PM6) *AND* ≥2 supporting (PP1–PP5) *OR* (vi) 1 Moderate (PM1–PM6) *AND* ≥4 supporting (PP1–PP5)	Likely benign	(i) 1 Strong (BS1–BS4) and 1 supporting (BP1–BP7) *OR* (ii) ≥2 Supporting (BP1–BP7)
		Uncertain significance	(i) Other criteria shown above are not met OR (ii) the criteria for benign and pathogenic are contradictory

Des outils de prédiction *in silico* ont été développés pour évaluer l'impact des variants faux-sens selon le degré de conservation inter-espèces, la localisation du variant (domaine fonctionnel, site actif, interactions protéiques, …), l'écart physico-chimique entre les acides aminés : EVE (29), VARITY (30). Plus récemment, des outils basés sur le calcul de méta-scores combinent les données de conservation, de fréquence en population générale et d'impact physico-chimique du variant : CADD (31), REVEL (32),... Alors que REVEL a été créé pour l'interprétation des variants faux-sens, CADD peut prédire l'impact d'InDels ou d'autres types de variants tels que les variants non-sens ou affectant l'épissage. Ces outils sont entrainés par des machines virtuelles à partir de variants déjà connus, mais ne prennent pas en compte les données fonctionnelles ou de structure. Des outils spécifiques ont été développés pour la prédiction de structure à partir des structures décrites dans la littérature : Phyre2 (33), Alphafold (34), Missense 3D (35,36). Plus récemment, des outils basés sur des machines virtuelles permettent d'intégrer la prédiction de modification de structure : AlphaMissense (37). Pour prédire l'effet d'un variant sur l'épissage, plusieurs outils sont disponibles : MaxEntScan (38), SPIP (39), Splice AI (40). Selon l'orientation des prédictions vers un caractère pathogène ou bénin, les critères PP3 ou BP4 peuvent être respectivement appliqués.

Par ailleurs, des tests fonctionnels, adaptés au gène et au mécanisme moléculaire de la pathologie peuvent être réalisés pour argumenter quant au caractère probablement bénin ou probablement pathogène. Les critères PS3 ou BS3 peuvent être appliqués, mais répondent à des exigences strictes (41).

e. Tests fonctionnels

Alors que certains tests sont capables de refléter l'environnement biologique (activité enzymatique chez un patient ou un modèle animal par exemple), d'autres ne peuvent être réalisés que *in vitro* et n'explorent parfois qu'une partie des fonctions de la protéine étudiée. La reproductibilité et la robustesse de ces tests doivent donc être explicités pour évaluer leur performance. Des groupes d'experts ont publié des recommandations par gène et ont souligné l'importance d'une bonne connaissance du gène et de la pathologie pour le choix et l'interprétation des tests fonctionnels, selon la fonction du gène et les mécanismes moléculaires de la pathologie (42). Des

recommandations spécifiques ont été données par un groupe de travail SVI (Sequence Variant Interpretation) du Clinical Genome Resource (ClinGen) pour préciser le terme « well-established » du critère PS3/BS3 des critères ACMG concernant les tests fonctionnels (41). Ils doivent être idéalement réalisés à partir de cellules issues du patient, permettant d'évaluer l'impact du variant dans son contexte physiologique (autres variants en *cis* ou en *trans*, épigénétique, type cellulaire, …). Lorsqu'un modèle animal est utilisé, il peut être parfois difficile d'évaluer s'il reflète le contexte humain, notamment dans le cas de différences anatomiques comme cela est observé pour les membres.

L'impact du variant peut être évalué à différents niveaux : sur la régulation de l'expression génique, sur la fonction de la protéine ou sur le phénotype cellulaire. La régulation de l'expression d'un gène cible peut être étudiée si la cible est bien connue, pour un variant identifié dans une séquence régulatrice. A l'échelle de la fonction protéique, les tests fonctionnels pourront être quantitatifs (Western Blot) ou qualitatifs (localisation cellulaire, stabilité, interaction avec d'autres protéines, capacité à se lier à l'ADN pour les facteurs de transcription par exemple). A l'échelle du phénotype cellulaire, la survie, la morphologie cellulaire, la croissance ou encore des fonctions spécifiques du type cellulaire peuvent être étudiés.

Les tests *in vitro* sont élaborés à façon, et nécessitent généralement l'utilisation de constructions plasmidiques contenant le gène étudié, dans lequel le variant d'intérêt est introduit par mutagénèse. Ces constructions sauvages et mutées sont ensuite transfectées dans un type cellulaire donné, afin de permettre l'analyse fonctionnelle choisie.

Les variants d'épissage peuvent avoir un impact sur la quantité de protéine (s'ils entraînent un codon stop prématuré déclenchant le mécanisme de NMD, *nonsense mediated mRNA decay*) ou altérer la séquence ou la structure protéique (saut d'exon, rétention intronique, insertion de pseudo-exon). Pour étudier l'impact de variants suspects d'altérer l'épissage, plusieurs techniques peuvent être utilisées. Si le gène est exprimé dans un tissu accessible à un prélèvement, l'étude de l'ARN par RT-PCR et/ou RNA-seq sera privilégié. En l'absence d'accès à l'ARN, des tests *in vitro*, appelés tests minigènes, peuvent être réalisés (43). Ils nécessitent généralement le clonage d'une séquence d'intérêt (sauvage ou mutée) entre 2 exons d'une construction plasmidique d'expression, puis, après transfection cellulaire, à l'étude de l'ARN issu

de chacune de ces conditions afin de comparer la taille des fragments puis leur séquence à la recherche d'un épissage alternatif (Figure 5). La caractérisation des variants d'épissage a fait récemment l'objet de nombreuses publications dans le domaine des maladies rares, notamment pour l'étude des variants introniques profonds (44). Néanmoins, les résultats des tests minigènes ont également des limites puisqu'ils ne reflètent pas directement l'impact fonctionnel. Un épissage alternatif du dernier exon peut, par exemple, générer une protéine tronquée dont la fonction serait conservée. Les transcrits anormaux peuvent également être soumis au NMD.

Figure 6 : Tests Minigènes.

Adapté de Gaildrat *et al.*, 2010 (43).

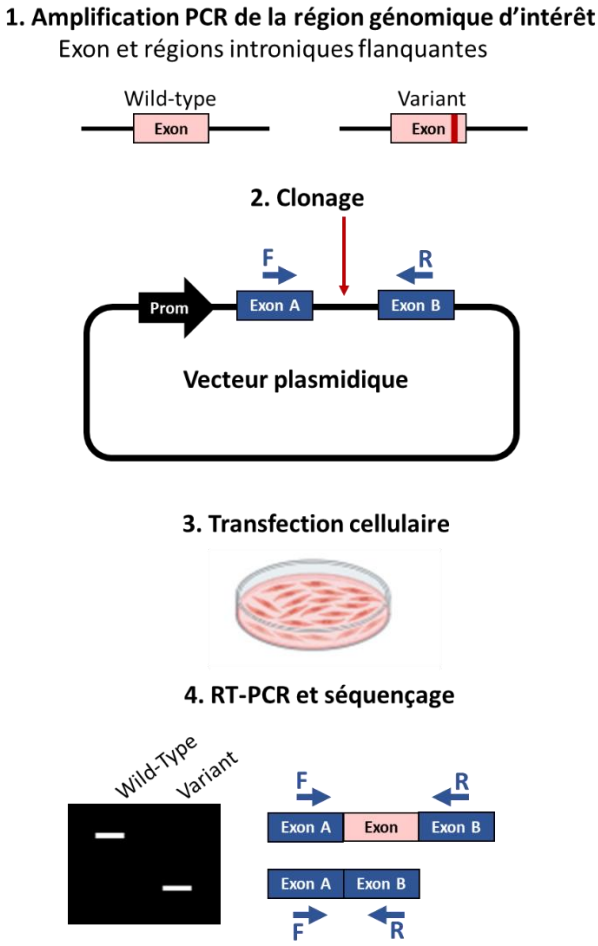

Ainsi, le développement et la mise au point en recherche de ces techniques d'étude fonctionnelle est indispensable pour envisager leur application en pratique courante.

f. Outils d'interprétation du génome non codant

L'interprétation des variants localisés dans le génome non codant est actuellement l'un des défis de la génomique humaine. Les éléments régulateurs pouvant impacter l'expression des gènes incluent les promoteurs, les séquences régulatrices activatrices, répressives ou insulatrices et les facteurs d'organisation de la chromatine. Leur rôle peut être spécifique d'un tissu. Les séquences régulatrices peuvent être situées en amont ou en aval de leur gène cible, et parfois même au sein d'un autre gène, comme cela a pu être décrit pour la ZRS, séquence régulatrice du gène *SHH* spécifique du membre, située dans un intron d'un gène du locus. Leur description peut être basée sur le niveau de conservation inter-espèces, sur la présence de certaines marques chromatiniennes modifiant l'accessibilité de la chromatine, sur l'existence de sites de fixation à des facteurs de transcription d'intérêt.

A la suite du Human Genome Project ayant permis le séquençage complet du génome humain, le projet ENCODE (Encyclopedia of DNA elements) a été initié par le National Human Genome Research Institute, afin de mieux caractériser les éléments régulateurs des génomes murins et humains. Il permet l'accès gratuit en ligne à plus de 15 000 résultats expérimentaux, à partir de plus de 40 technologies de séquençage à haut débit différentes dans plus de 75 types cellulaires ou tissulaires (45,46).

La base de données Limb Enhancer Genie a établi des scores de probabilité de présence d'éléments régulateurs actifs au cours du développement des membres, à partir de la compilation de données de plus de 50 publications de marques chromatiniennes spécifiques du membre, de la conservation inter-espèces de sites de fixation de facteurs de transcription et des données *in vivo* de la base de données VISTA ayant permis de valider certains de ces éléments régulateurs (47,48).

La description de ces éléments régulateurs est donc encore récente et est encore incomplète. L'impact d'un variant au sein d'une séquence régulatrice est d'autant plus complexe à prédire, mais l'accumulation récente d'exemples de pathologies rares liées à une altération d'un élément régulateur pose les jalons de recommandations de bonne pratique (49).

OBJECTIFS

Au sein des malformations des membres supérieurs, les anomalies radiales semblent être plus fréquemment associées à une cause génétique, notamment lorsqu'elles sont bilatérales.

Nous avons pu constituer une cohorte de patients présentant une anomalie radiale, grâce à des collaborations nationales et internationales.

Le fil conducteur des travaux présentés ci-dessous a été l'identification d'un déterminisme moléculaire pour les patients de cette cohorte en errance diagnostique, après l'étude des régions codantes d'un panel de gènes impliqués dans le développement des membres :

- Par une meilleure connaissance clinique et moléculaire des pathologies avec anomalies radiales déjà décrites
- Par la mise en place de tests fonctionnels adaptés
- Par la caractérisation de nouveaux gènes impliqués dans le développement des membres
- Par l'utilisation du séquençage de génome entier pour l'exploration des régions non codantes

PARTIE I. LA DYSPLASIE RADIALE : de la biologie du développement à la pathologie humaine

Le rayon radial a connu une évolution morphologique majeure chez les primates, avec l'émergence de la bipédie et l'enrichissement des fonctions des membres supérieurs, permettant notamment l'opposition du pouce pour des manipulations de précision chez l'Homme. Potentiellement en lien avec cette évolution accélérée, le rayon radial est particulièrement sensible aux altérations des mécanismes moléculaires impliqués dans le développement des membres supérieurs. Ainsi, les anomalies radiales concernent entre 1/5000 et 1/11000 naissances (13,18,19). Elles peuvent être observées dans de nombreux syndromes dont les phénotypes sont chevauchants.

Dans cette revue, nous présentons de quelle façon les connaissances en génétique du développement des membres ont nourri la description des gènes associés aux pathologies malformatives humaines dans ce domaine.

Radial ray: from developmental biology to human disease

Clémence Vanlerberghe[1], Elise Pisan[1], Florence Petit[1]

[1] Univ. Lille, CHU Lille, ULR 7364 - RADEME, F-59000 Lille, France

ABSTRACT

The radial ray has undergone a major morphological evolution in primates, with the emergence of bipedalism and the enrichment of upper limb functions, notably enabling opposition of the thumb for precision manipulation in humans. Potentially linked to this accelerated evolution, the radial ray is particularly sensitive to alterations in the molecular mechanisms involved in upper limb development. Thus, radial defects are among the most frequent limb malformations and can be observed in many syndromes with overlapping phenotypes. In this review, we describe the molecular mechanisms involved in upper limb development, as well as the main diagnoses associated with radial defects. A good clinical knowledge and molecular studies are necessary to enable accurate diagnosis in patients, in order to adapt their management and monitoring.

KEY WORDS

Radial ray, radius, thumb, genetic rare disease, limb development, limb malformation

INTRODUCTION

In vertebrates, the radial ray is crucial to forelimb function, involved in arm strength and thumb precision. Developmental biology studies have enabled us to understand the complex biological processes implicated in the initiation of limb buds and their differentiation into upper or lower limbs. Numerous molecular pathways play a role in the formation of arms and fingers, particularly the thumb, essential for prehension in mammals.

Approximately 10 to 20% of newborns affected with congenital malformations have upper limb defects [1]. Large epidemiological studies have estimated the incidence of radial dysplasia between on average 1/5000 to 1/11000 births [2–4], depending on variable inclusion criteria (including or not isolated polydactyly or syndactyly, brachydactyly, clinodactyly, mild hypoplasia). Most cases are bilateral (59%). Sex ratio is male biased overall (6/4) [3], however a female preponderance is observed for isolated thumb deficiencies, whereas a male preponderance is suspected for the radial club hand [2]. At least one associated feature is reported in 88-92% [3,5]. Infant mortality is observed in 38% of children with bilateral radial ray deficiency, notably due to potentially associated heart defects [3]. A family history of radial malformation is rare (1-6%) [2,3].

Prenatal detection rate of upper limb defects is estimated at between 31-42 % [6,7]. Detection of a longitudinal reductional defect in the upper limbs leads to termination of pregnancy in 65% of cases in Austria [8]. Distal abnormalities are more challenging to detect prenatally [7].

In the OMIM database, radial involvement is a feature reported in about 400 conditions, with various modes of inheritance: autosomal dominant, autosomal recessive, X linked [9]. The

Genome England Panel App (version 1.24) includes 60 genes that can cause radial dysplasia [10]. The diagnostic yield in patients with radial defects suspected of having a specific genetic disease has been estimated at around 30%, through targeted high-throughput sequencing [11]. No data are yet available on the diagnostic performance of genome sequencing under these clinical conditions.

Etiological diagnosis is crucial for the fetus or the patient for appropriate medical management, in view of the frequency of associated features requiring early detection to avoid complications and the possible association with cognitive impairment. As radial dysplasia can be detected during pregnancy, a better understanding of its molecular basis is essential for interpreting the results of prenatal exome or genome sequencing.

Here, we review current knowledge on upper limb development and the molecular pathways involved in radial dysplasia in humans. The combination of recent advances, both fundamental and medical, on radial dysplasia could help researchers guide futures studies in the field.

1 - UPPER LIMB DEVELOPMENT

1A Limb developmental biology

The induction and subsequent growth and differentiation of the limb bud requires a complex and coordinated spatiotemporal organization, involving numerous players and multiple epithelial-mesenchymal interactions [12]. In tetrapods, after the gastrulation stage, the mesoderm divides into 3 compartments: paraxial, intermediate and lateral (depending on their location relative to the neural tube). Limb buds develop from the lateral mesoderm at a precise rostro-caudal location determined by a pattern of Hox gene expression [13]. They

develop along 3 main axes: proximodistal, anterior-posterior and dorsoventral (**Figure 1, Left**)[12].

The apical ectodermal ridge (AER) guides proximodistal growth. During limb bud induction, the *Fgf10* gene is expressed in the lateral mesoderm and induces the expression of *Fgf8* in the ectoderm. Fgf8/Fgf10 growth factors then generate an epithelial-mesenchymal activation loop, enabling cell proliferation and limb bud outgrowth (**Figure 1, Middle**). Inactivation of *Fgf10* in animal models results in the complete absence of limbs [14,15]. Limb bud initiation and the onset of distal outgrowth also depend on retinoic acid [16,17]. The formation of a functional AER depends on the bone morphogenetic protein (Bmp) signaling pathway in the mesenchyme [18].

The limb bud contains a region of rapid cell proliferation called the progression zone, from which cells differentiate to give rise to the various limb structures. While bones, tendons and part of the vasculature originate from the mesoderm, muscle precursors are derived from a more medial compartment of the somites [19].

Anterior-posterior limb polarization is under the control of the morphogen *Shh* secreted by the zone of polarizing activity (ZPA), located in the posterior part of the limb bud. The anterior compartment, that will give rise to the radial ray, requires no *Shh* activity: in this compartment, Shh is antagonized by Gli3R expression (**Figure 1, Right**)[20].

The Bmp pathway is essential for dorsoventral polarization, inducing the expression of specific genes in the ventral (*En1*) and dorsal (*Wnt7a*) ectoderm [12].

T-box proteins play a major role in embryogenesis and limb development. The *T, Tbx2, Tbx3, Tbx4, Tbx5, Tbx15* and *Tbx18* genes are expressed in the limb bud and participate in its development [21]. The *T* gene is essential for mesoderm formation at an early stage of

development, while *Tbx2* and *Tbx3* play a role in finger identity via the Shh and Bmp signaling pathways [21]. In human disease, pathogenic variants in some of these genes are responsible for syndromic limb malformations: *TBX3* in Ulnar-Mammary syndrome (MIM#181450), *TBX4* in Ischio-coxo-podo-patellar syndrome (MIM#147891), *TBX5* in Holt-Oram syndrome (MIM#142900) for example.

1B Upper limb specificities

Initially, the four limb buds appear to be identical clusters of cells. But as the limbs grow, the progenitor cells differentiate into a network of bone, tendon, muscle and vascular tissues, resulting in two limb types: upper/forelimb and lower/hindlimb.

Most of the genes involved in limb development are similarly expressed in the upper and lower limbs, but this is not the case for *TBX5*, expressed exclusively in the upper limbs, while *TBX4* and *PITX1* are expressed exclusively in the lower limbs. Initially, it was suggested that these genes were essential players in limb identity [12]. However, using transgenic animal models, some authors have demonstrated that Tbx4 can replace Tbx5 in the forelimb bud initiation [13]. Thus, signaling pathways and their target genes appear to be common to upper and lower limb development, with limb identity resulting from modulation of the regulation of this common gene network.

In the chick embryo, cells from the lateral mesoderm region implanted at an ectopic position on the craniocaudal axis always develop into the limb-type where they come from [22]. Limb identity is therefore programmed very early in development and determined by the mesoderm. Hox genes are expressed along the entire craniocaudal axis, according to a temporal and spatial colinear distribution. These genes act upstream of *Tbx5* in controlling the

upper limb bud initiation [23]. A minimal regulatory sequence has been described within intron 2 of *Tbx5* that can be targeted by *Hox* genes. Rostral *Hox* genes, like the *Hox4* and *Hox5* paralogs, share the same spatial expression as *Tbx5*. They appear to have redundant functions, since deletion of all paralogs is needed to reproduce the absence of upper limbs observed in the *Tbx5* conditional knock-out mice[23]. In the caudal lateral plate mesoderm, the Hoxc9 transcription factor has been shown to bind to this regulatory element and repress *Tbx5* expression [24].

Tbx4 and Tbx5 are essential during limb bud initiation to establish the Fgf10/Fgf8 loop. Conditional knock-out in the presumptive forelimbs has shown that *Tbx5* expression can induce limb bud only during a precise spatiotemporal window in mice (E9.5-E10.5) [25]. However, this loop is subsequently completely autonomous and the expression of *Tbx4* and *Tbx5* is no longer required [26]. At a later stage of development (E11.5-E12.5), the conditional deletion of *Tbx5* specifically affects muscle and tendon patterning without disrupting skeletal development or limb growth [27].

The transcription factors Sall1 and Sall4 act downstream of Tbx5 during the upper limb bud development (**Figure 1, Middle**). The Sall proteins are characterized by zinc finger domains and a glutamine-rich region implicated in self-dimerization and heterodimerization [28]. These proteins are essential for Fgf10 expression through synergistic activation with Tbx5 [29,30].

In conclusion, the radial ray develops mainly under the influence of *HOX* genes, *TBX5*, *SALL1*, *SALL4*, *FGF10*, *FGF8* and requires no *SHH* activity (**Figure 1**). The alteration of these genes or their regulatory elements is responsible for limb malformations in human disease.

2 - GENETIC CONDITIONS WITH RADIAL DEFECT

Radial defects comprise a spectrum of radius and/or thumb malformations, ranging from aplasia/hypoplasia to duplicated or triphalangeal thumb (**Figure 2**). Various conditions have been associated with these malformations, most of them having a genetic etiology.

The diagnostic of a radial defect must lead to a meticulous clinical examination that should look notably for lower limb involvement, growth retardation and ear dysplasia. Minimal screening analyses comprise blood cell count, ophthalmologic tests (ocular mobility defect, lacrimal ducts), hearing tests, renal ultrasound and spine radiographs. Genetic analyses may subsequently be guided by the presence and the type of associated features, under the supervision of the clinical geneticist.

2A Chromosomal abnormalities

Chromosomal microarray is largely used as a first-line genetic test in case of congenital anomalies. It is usually performed when a radial defect is diagnosed, during pregnancy or at birth. Many chromosomal anomalies may include a radial defect, the most classical being trisomy 18 (Edwards syndrome). It is characterized by the association of intrauterine growth retardation, heart defect, esophageal atresia, diaphragmatic hernia, and neural tube defect. Abnormalities of the extremities have been observed in 56% of patients [31]. The most predominant anomaly of the upper limbs is clenched fist with overlapping fingers [32]. Radial defects are found in 22% of patients.

2B Monogenic disorders

According to large epidemiological studies, the classic syndromic conditions associated with radial anomalies are, from the most to the least frequent: VACTERL association, Holt-Oram

syndrome, TAR syndrome, Blackfan-Diamond syndrome and Fanconi anemia [33]. However, a radial defect may be part of many other rare conditions that we review herein according to the disrupted molecular pathways (**Table 1**). Apart from the genes and regulatory elements involved in limb specification and pattern formation, the alteration of genome maintenance, transcription and translation are responsible for radial defects.

Clinical conditions where there is a general defect of the forearm long-bones and hand, such as amelia of the upper-limb and transversal hemimelia, have been excluded from this review.

Limb specification and pattern formation

A. Holt-Oram syndrome

Holt-Oram syndrome (HOS) is the most frequent monogenic disorder identified in congenital radial defects. This autosomal dominant condition is characterized by the association of highly variable bilateral preaxial defects (from thumb hypoplasia to phocomelia) and heart defects in 90% of the patients (congenital heart malformation and/or conduction abnormalities)[34,35]. Radial hypoplasia/agenesis is observed in 20-30% of the patients. Thumb involvement is constant in HOS, comprising thumb hypoplasia/agenesis, I-II syndactyly, thenar hypoplasia, triphalangeal or digitalized thumbs. In our experience, thumb duplication is not observed in this condition. Sloping shoulders, clavicle defects and/or limitation of elbow mobility can be observed. Cardiac defects include atrial and/or ventricular septal defects or more rarely complex cardiac malformations. Conduction disturbance (5% of HOS patients), such as sinus bradycardia, conduction blocks or junctional tachycardia, can occur later in life without any history of cardiac malformation. Molecular confirmation of HOS is crucial to adapt cardiac monitoring.

HOS is due to *TBX5 (T-Box 5)* alterations [36]. These are most often truncating variants leading to haploinsufficiency, and more rarely missense variants leading to loss of function. In patients with typical HOS phenotype, a *TBX5* pathogenic or likely pathogenic variant in coding sequence is found in 70% [35].

B. Duane-Radial Ray; Okihiro syndrome

Duane-Radial Ray (Okihiro, Acro-reno-ocular) syndrome was originally characterized by the association of radial defects, Duane anomaly and deafness. This autosomal dominant condition is due to *SALL4 (Sal-like 4)* gene alterations [37] usually leading to haploinsufficiency or loss-of-function.

Uni- or bilateral radial defects are observed in more than 90% of the patients and range from isolated thenar hypoplasia and/or hypoplasia/aplasia of the thumbs (40%) to hypoplasia/aplasia of the radii (30%), with sometimes ulnar or humeral hypoplasia (10%). Triphalangeal thumbs and pre-axial polydactyly have also been reported (20%). Duane anomaly is observed in 50% of patients (bilateral in 20%). Renal abnormalities may include ectopic kidney, horseshoe kidney and rarely renal hypoplasia. Sensorineural or conductive deafness is observed in 30% of patients, sometimes associated with ear dysplasia. Heart defects (10%), such as ventricular or atrial septal defects, tetralogy of Fallot, or conduction disturbances (5%) have also been reported. Scoliosis is observed in 10% of patients. Anal stenosis or imperforation can be associated [37,38,38–40].

Rarely, mild thrombocytopenia and leukocytosis have been described, leading initially to the description of the “IVIC syndrome” which was later linked to *SALL4* gene and now considered part of the *SALL4*-related disorders spectrum [41].

C. Townes-Brocks syndrome

Townes-Brocks syndrome (TBS, MIM#107480) is an autosomal dominant condition historically characterized by the triad of thumb, external ear and anorectal malformations [42].

Bilateral thumb malformations are present in more than 75% of the cases, with mostly preaxial polydactyly (47%) or triphalangeal thumbs (29%). Deviated thumb or thumb hypoplasia (8%) are more rarely observed. However, no radial involvement is observed in our experience (Leduc et al., *in press*).

External ears are usually dysplastic with variable expressivity: microtia, abnormally folded helix, preauricular tags or pits. Sensorineural and/or conductive hearing impairment is reported in 65% of cases. Anorectal malformations include imperforate anus or anal stenosis in 84% [43].

Other features have subsequently been described, including feet malformations, kidney malformations and/or renal failure, congenital heart defects and male disorders of sex development [44]. Penetrance is reported to be complete, but expressivity is highly variable. Renal failure and deafness can occur at any age, making follow-up of TBS patients essential [45].

TBS is due to heterozygous variants of the *SALL1 (Sal-like 1)* gene [46]. Most of the pathogenic variants are truncating. Some of them escape the nonsense-mediated mRNA decay and may cause a gain-of-function or a dominant-negative effect. However, few TBS patients carry a partial or complete *SALL1* deletion, likely resulting in haploinsufficiency.

D. Lacrimo-auriculo-dento-digital syndrome (LADD)

LADD syndrome is an autosomal dominant condition characterized by the association of hypoplasia, aplasia or atresia of the lacrimal and/or salivary ducts, cup-shaped ears with sensorineural hearing loss, dental anomalies, and digital anomalies [47].

The digital features are incompletely penetrant and show variable expressivity. They include thumb anomalies (aplasia, hypoplasia, duplication, triphalangeal), fifth finger clinodactyly and/or mild syndactyly of fingers and toes. Radius anomalies are not reported in molecularly proven cases.

Obstruction of the nasal lacrimal ducts lead to epiphora and chronic conjunctivitis. Aplasia/hypoplasia of the salivary glands is responsible for dry mouth and frequent caries. Dental features include late tooth eruption, small and peg-shaped lateral maxillary incisors and mild enamel dysplasia.

LADD syndrome is due to altered FGF signaling and displays some genetic heterogeneity, with heterozygous pathogenic variants reported in *FGF10, FGFR2* or *FGFR3* [48,49].

E. Preaxial polydactyly

Isolated preaxial polydactylies are classified according to the Wassel classification, from bifid or duplicated proximal and/or distal phalanges (type I to IV) to bifid or duplicated metacarpus (type V and VI) and triphalangeal thumbs (type VII)[50]. Feet can also be affected with polydactyly [51].

Gain-of-function pathogenic variants [52] or copy number gain [53] in the ZRS (Zone of polarizing activity Regulatory Sequence), a non-coding sequence regulating the expression of *SHH* in the posterior limb bud, are responsible for preaxial polydactylies, due to anterior ectopic *SHH* expression. Related to genotype-phenotype correlations, the phenotype may be more severe with polysyndactylies and anterior-posterior polarization alteration of the long bones (tibial hypoplasia/aplasia, fibula duplication). However, radius malformations have not been reported.

F. Hand-foot-genital syndrome

Hand-foot-genital syndrome (HFGS) is an autosomal dominant condition characterized by distal limb and urogenital malformations [54].

Limb malformations are usually bilateral and symmetric, consisting of thumb hypoplasia without radius defect, associated with ulnar deviation of the second fingers and brachymesophalangy of the fifth fingers, together with short halluces. There is also delayed ossification and fusion of the carpals and tarsals. Urogenital malformations have variable expressivity and incomplete penetrance, including hypospadias in males, Mullerian duct fusion defects resulting in bicornuate or uterus didelphys in females, vesicoureteral reflux and pelvi-ureteric junction obstruction [55].

Various molecular alterations involving the *HOXA13* gene have been described: truncating or missense variants, polyalanine tract expansions and 7p15.2 microdeletions [55,56], responsible for either loss of function, haploinsufficiency or gain of function with dominant negative effect.

G. *LEF1*-related radial defects

In 8 individuals from two unrelated families affected with radial defects of variable expressivity, ranging from radial hypoplasia, thumb hypoplasia or duplication, to thenar hypoplasia, a heterozygous missense variant in the DNA-binding domain of *LEF1* has recently been described [57]. *LEF1* encodes a transcription factor acting downstream of the WNT-β-catenin signaling pathway. Transcriptome profiling in fibroblast cells from one affected individual shows alteration in the WNT-β-catenin signaling pathway. Together with radial defects, syndactyly of fingers or toes may be observed as well as preaxial polydactyly of feet.

Also, patients have mild features of ectodermal dysplasia, consisting of hypoplastic nipples, sparse eyebrows and body hair.

Genome maintenance

A. Fanconi anemia

Fanconi anemia associates bone marrow failure and increased risk for malignancy with congenital anomalies. Malformations occur in 75% of cases [58]. Patients present with pre- and postnatal growth retardation associated with microcephaly. Skeletal anomalies can be asymmetric and mostly concern the upper limbs. Radial ray defects are present in half of the patients [58,59]. Thumb anomalies range from proximally placed, triphalangeal, bifid or duplicated thumb, to thumb hypoplasia and aplasia. Radial hypoplasia/aplasia is always associated with thumb anomalies. Lower limbs (5%) and vertebral (2%) anomalies have been described. Endocrine disorders affect up to 75% of the patients with growth hormone deficiency, hypothyroidism, diabetes, impaired glucose tolerance/insulin resistance, dyslipidemia, delayed puberty or impaired fertility [60]. Common features include café-au-lait macules, hyper or hypopigmentation (40%), ocular anomalies (20%, microphthalmia, strabismus) and genitourinary tract malformations (20%, dysplastic/ectopic/hypoplastic/absent kidney, hypogenitalism). Although less frequent, hearing loss and congenital heart defects have been described.

Bone marrow failure usually appears around 7 years old and can lead to myelodysplastic syndrome or acute myelogenous leukemia [61]. Patients are also at increased risk to develop solid tumors, especially ENT, skin and genitourinary tract tumors [62].

Fanconi anemia belongs to breakage syndromes which imply increased chromosome instability. After exposure to crossed-linking agent, karyotype shows chromosome breakage

and radial forms. Fanconi anemia is a genetically heterogeneous disorder with 23 genes described so far. These genes are involved in DNA repair in the FANC/BRCA pathway. Variants in *FANCA* are the most frequent and are involved in around 70% of cases [63]. Fanconi anemia is usually autosomal recessive, but autosomal dominant or X-linked inheritance are also observed, associated with variants in *RAD51* or *FANCB* genes respectively [64,65].

B. *RECQL4*-related disorders: Baller-Gerold syndrome, RAPADILINO, Rothmund Thomson type 2

Three overlapping phenotypes with autosomal recessive inheritance are caused by pathogenic variants in the *RECQL4* gene, encoding a DNA helicase which plays a crucial role in the maintenance of nuclear and mitochondrial genomes (DNA replication, transcription, recombination and repair) [66]. Common features include growth restriction, radial defects, patella hypoplasia/aplasia and chronic diarrhea. Radial defects consist of thumb hypoplasia/aplasia and radius hypoplasia/aplasia. Intelligence is usually normal, and an increased risk of cancer is described.

RAPADILINO stands for RAdial ray defect, PAtellar hypoplasia/aplasia and high arched PAlate/cleft, chronic DIarrhea and DIslocated joints, LIttle size and LImb anomalies, NOrmal intelligence and long, slender Nose [67]. Radial defects are virtually present in every patient. Growth delay is present pre- and postnatally. Patients often present with feeding problems. A founder mutation has been identified in Finnish populations [68]. Patients have a higher risk of developing osteosarcoma or lymphoma [69].

Rothmund-Thomson type 2 syndrome [70] is characterized by poikiloderma, usually starting on the face during the first months of life and secondly spreading to limbs and extremities. The trunk is typically not affected. Hyperkeratosis on the soles of the feet is frequent. Patients

present with sparse hair, nail dysplasia and dental anomalies (microdontia, dental eruption delay, supernumerary or missing teeth, caries). Cataract has been described in up to 50% of patients. It is usually bilateral, more frequently juvenile but can occur at any age [71]. Radial defects are present in 20% of the patients [72]. An increased risk of cancer, especially of osteosarcoma and skin cancer, is described. More recently, bi-allelic variants in *ANAPC1*, *CRIPT* and *DNA2* have also been associated with Rothmund-Thomson syndrome [73–75].

Baller-Gerold syndrome is characterized by craniosynostosis, mostly affecting the coronal sutures, and poikiloderma, which usually appears in the first year of life [76]. Imperforate or anteriorly placed anus can be associated. Facial features consist of prominent forehead, proptosis, concave nasal ridge, short nose, thin vermilion of the lips and high arched palate. Only one case of lymphoma has been described so far [77].

C. Cornelia de Lange

Cornelia de Lange syndrome (CDLS) is characterized by pre and postnatal growth restriction, microcephaly, distinct facial features, hypertrichosis, intellectual disability and multiple congenital malformations [78,79]. Facial features are recognizable with synophrys and hirsutism, high-arched eyebrows, long eyelashes, anteverted nares, long smooth philtrum, thin vermilion of the upper lip, retrognathia. Intellectual disability is almost constant, and language is particularly affected.

Limb malformations mostly affect the upper limbs and range from micromelia, short first metacarpal, 5th digit clinodactyly to oligodactyly, monodactyly, radioulnar synostosis, radial or ulnar hypoplasia and complete absence of the forearm. Mild upper limb malformations are observed in almost all patients whereas severe malformations are present in 25% of patients [79]. Lower limbs can be mildly affected with short feet and syndactyly 2-3 of toes. Limb

malformations are asymmetric in 65% of patients [80]. In these cases, the right side is usually more severely affected.

Other congenital malformations consist of congenital heart defect (30%, [81]); urogenital anomalies (cryptorchidism, hypogenitalism, bicornuate uterus), ophthalmological problems (60%, ptosis, myopia, [82]). Hearing impairment affects 80% of patients (conductive or sensorineural, [83]). Growth restriction is frequently aggravated by feeding difficulties and gastroesophageal reflux [84].

Six genes are described so far in CDLS. They are associated with autosomal dominant (*NIPBL*, *SMC3*, *RAD21*, *BRD4*) or X-linked inheritance (*SMC1A*, *HDAC8*). Most of these genes encode for subunits of the cohesin complex, involved in gene transcription, DNA repair and genome stability [85].

Spliceosomopathies and ribosomopathies

A. Diamond-Blackfan syndrome

Diamond-Blackfan syndrome (DBS) is originally characterized by bone marrow failure manifesting as severe anemia usually notable in infancy. The classic definition has been challenged in recent years by the increasing reports of patients with pathogenic variants in DBS genes, who exhibit multisystem anomalies expected in DBS but with subtle or no hematological abnormalities. DBS can manifest with a range of clinical features, including one or more congenital malformations (44.4%), growth retardation (8.7%), and an increased predisposition to hematological and solid malignancies (2-5%). Among the associated malformations, craniofacial, upper limb, heart, and genitourinary are the most prevalent. Radial defects are observed in approximately 15% of the patients and may comprise: flat

thenar eminence to triphalangeal, duplicated, hypoplastic or absent thumb, hypoplastic radius, radio-ulnar synostosis [86,87].

To date, more than twenty genes have been implicated in DBS, most of them encoding ribosomal proteins. *RPS19* (DBA1, MIM#105650), *RPL5* (DBA6, MIM#612561), *RPS26* (DBA10, MIM#613309) and *RPL11* (DBA7, MIM#612562) are the most frequently identified. Inheritance is usually dominant autosomal but X-linked inheritance is also described. Penetrance of loss-of-function variants in those genes is very high, while it seems incomplete for damaging missense variants [87].

B. Nager syndrome

Nager syndrome belongs to the acrofacial dysostoses. This autosomal dominant condition is characterized by craniofacial anomalies (down-slanting palpebral fissures, palpebral clefts, malar hypoplasia, ear anomalies, microretrognathism, cleft palate), conductive deafness and preaxial limb anomalies that are variable and often asymmetrical [88,89].

In the upper limbs, there may be a hypoplasia/aplasia of the radius often associated with proximal radioulnar synostosis, absent/hypoplastic/triphalangeal or duplicated thumb. Lower limb involvement is usually mild: clubfoot, hypoplasia of the hallux.

Highly variable intrafamilial expressivity is observed.

Nager syndrome is due to haploinsufficiency of the *SF3B4* gene, encoding a component of the pre-mRNA spliceosome complex [88].

C. Thrombocytopenia Absent Radius (TAR) syndrome

TAR syndrome is clinically recognizable because of radial defects contrasting with the presence of thumbs [90]. Limb malformations range from radial hypoplasia/aplasia, radio-ulnar

or radio-humeral synostosis to phocomelia. Affected individuals may also have lower-limb defects and visceral malformations (heart, genitourinary). Thrombocytopenia may be congenital or develop in infancy and the episodes usually decrease with age. Cow's milk allergy is frequent.

The inheritance is recessive autosomal, due to haploinsufficiency of *RBM8A* gene encoding a subunit of the exon-junction complex involved in mRNA maturation [91]. Cases are compound heterozygotes for a null allele (most often a 1q21.1 deletion) and a hypomorphic allele (whose frequency may be significant in the population) of the *RBM8A* gene [91,92].

2C OTHER SYNDROMIC CONDITIONS

VACTERL association is classically characterized by the presence of at least 3 of the following features: Vertebral anomalies, Anal anomalies, Cardiac defects, Tracheoesophageal fistula, Esophageal atresia, Renal malformations and Limb malformations. Its prevalence is estimated between 1/10000 and 1/40000. Carli *et al.* described the limb phenotypes of 25 patients with VACTERL association, affecting the radial ray. They are mostly unilateral and include thumb anomalies (79%; usually hypoplastic, more rarely duplicated) or radial agenesis (33%). They are most of the time associated with costo-vertebral malformations [93].

However, relatively little is known about the causes of this condition, and its clinical heterogeneity could be explained by the overlap of several unrecognized disorders (Townes-Brocks syndrome, Fanconi anemia...) rather than a distinct etiologic entity [94]. Molecular approaches have identified various copy number variations or single nucleotide variants in novel human candidate genes: *FOXF1, HSPA6, HAAO, KYNU, TRAP1,* and *ZIC3* [95–98]. However, these reports explain only a few VACTERL cases [99].

Several of these genes (*HSPA6, HAAO, KYNU, TRAP1)* are implicated in the NAD synthesis pathway, involved in endochondral ossification. NAD inhibition in mouse induce dramatic limb shortening due to death of growth plate chondrocytes [100].

ZIC3 variants have been linked to a X-linked VACTERL form. This gene is closely related to Gli-superfamily members. *In situ* hybridization studies in mouse embryos between E9.5 and E14.5 reveal Zic3 expression in the autopod and apical ectodermal ridge at early stages, and then become confined to the presumptive wrist region and digital tips [96]. During limb development, post-translational modifications of Gli3 posteriorly restrict Shh expression, an anterior repression that is crucial for the radius and thumb development. Zic3 regulates digits number via its modifying effect on Gli3 and Shh expression levels [101]. Animal models furthermore link the VACTERL phenotype to *Shh* signaling [102].

Oculo-auriculo-vertebral syndrome (or Goldenhar syndrome), a developmental disorder involving the first and second branchial arches derivatives, is characterized by hemifacial microsomia, anomalies of the ear (mostly microtia) and vertebral defects. Its incidence is evaluated around 1/26 500 [103]. Anomalies of the extremities, including the thumb, are described in 12% of cases [104]. Although rare, the most common limb anomalies observed are thumb hypoplasia/agenesis and hypoplasia/agenesis of the radius, but also triphalangeal or duplicated thumb [105]. This condition has a large phenotypic variability and probably also genetic heterogeneity.

The description of a few familial cases suggests the existence of a genetic basis for OAVS. To date, variants in 10 different genes have been identified in patients but explain very few cases [106]. Bifid thumbs and bilateral additional flexion creases on thumbs are reported in 2 different patients with *SF3B2* variants [107]. However, the role and expression of *SF3B2* during limb

development is not known. No obvious limb defects have been described in the animal models for these OATS-related genes, but they could be very subtle.

Other OATS-related genes, notably *MYT1* and *ZYG11B* genes, are involved in the retinoic acid pathway, required upstream of *Tbx5* during forelimb bud initiation [17]. *ZYG11B* gene, a member of an E3 ubiquitin ligase complex, is also involved in cell differentiation through the Patched1 receptor for Shh [108].

Nongenetic causes are also hypothesized for OATS, including maternal diabetes, placental vascular disruption and exposure to toxic substances during pregnancy such as retinoic acid [106].

VACTERL and OATS have phenotypic overlap and, although a genetic determinism is rarely identified, the genes described so far are implicated in common pathways at very early stages of development.

Besides, some environmental factors have been highlighted as significant risk factors for radial dysplasia: valproic acid medication, thalidomide, maternal diabetes. Smoking, alcohol consumption and air pollution have been suggested as additional risk factors, but with less robust associations [109].

Various other clinical entities including a radial defect without molecular basis are reported in the OMIM database. They may correspond to old observations whose molecular basis has since been resolved, or to incomplete presentations of known conditions such as Okihiro, Townes-Brocks, Nager syndromes or the large VACTERL/OATS spectrum. For example, an X-linked form of radial hypoplasia/aplasia has been suggested in one report but, since hydrocephaly and anorectal malformations were associated, the implication of the *ZIC3* gene could be hypothesized [110].

DISCUSSION

The evolution towards bipedalism in Humans has freed the upper-limb and the thumb for grasping, allowing cupping, precision and power grip. The evolution of thumb functions has been accompanied by morphological changes, from bone and muscle perspectives, leading to an elongated first ray capable of pad-to-pad opposition with the other fingers [111]. The radial ray has undergone dramatic morphological and size changes among species evolution and seems less constrained compared to other forelimb bones that are mostly unmodified across taxa. The price to pay for this striking evolutionary plasticity may be the enrichment for radial defects in human malformations, suggesting a lack of robustness in the regulation of its developmental mechanisms.

The upper limb and especially the radius seem to have an increased sensitivity to developmental anomalies compared to the lower limb and more generally to other long bones. In support of this hypothesis, among all longitudinal hemimelia, radial hemimelia is much more frequently observed and associated with a higher number of syndromic conditions than ulnar, tibial or fibular hemimelia [33].

While many genes involved in upper limb development are also implicated in lower limb development, leg and feet malformations are mild or even absent in several examples where these genes are altered (i.e. *FGF10*, *SALL1*, *SALL4*...). Additionally, gain of function variants of the ZRS in preaxial polydactyly is the only example known so far, where a single nucleotide variation in a regulatory element is responsible for the altered regulation of a major developmental process (i.e. *SHH* signaling pathway) [52]. Altogether, this points to a lack of robustness in the molecular mechanisms regulating the development of the radial ray, who therefore may be more sensitive to genome maintenance, transcription or translation defects.

As demonstrated here, there is a high genetic heterogeneity in radial defects. A wide variable expressivity and overlapping features are observed in many of the syndromes described. Although some conditions including a radial defect are clinically recognizable, molecular investigations are essential to distinguish overlapping phenotypes to offer appropriate medical management and genetic counselling. Indeed, beyond the congenital malformations visible at birth, some conditions include features occurring later in life: rhythm disturbances in Holt-Oram syndrome, hearing and/or renal impairment in Townes-Brocks syndrome for example. Another example of a threatening associated feature is bone marrow failure, which can be associated with several conditions comprising radial defects: Fanconi anemia, Diamond-Blackfan syndrome, *RECQL4*-related disorders, TAR syndrome and others. The risk of myelodysplastic syndrome and solid cancer is also increased for the first 3 examples. Depending on the syndrome and the variable expressivity, bone marrow failure may be either single lineage or pancytopenia and may develop as early as the neonatal period or later in infancy, childhood or even adulthood. In view of this observation, a hematological check-up should be carried out systematically in the event of radial ray defect. Careful interpretation of the reports is needed to look for minor anomalies (macrocytosis, decreased hemoglobin levels, platelet counts or neutrophil counts), especially since those patients may undergo invasive surgeries given the associated malformations.

The molecular mechanisms involved in these diseases (i.e. genome maintenance, DNA replication, transcription, translation) have relevance to the development of bone marrow failure or malignancies, but the relation to the radial defect is less apparent. Again, an increased sensitivity to subtle deregulation of gene expression related to the molecular mechanisms may be hypothesized.

Despite advances in the genetic characterization of human malformations, much more than half of the cases with radial defects remain unsolved [11]. The diagnostic rate is lower in isolated compared to syndromic limb malformations, leading to the interesting hypothesis that many isolated conditions may be due to the alteration of limb-specific regulatory elements, rather than the alteration of genes themselves. Supporting this, several regulatory anomalies have been demonstrated to be responsible for limb malformations, highlighting the limb as a paradigmatic model for such mechanisms, ranging from single nucleotide variations to structural variations or chromatin architecture disruption [112]. The general evolution towards genome sequencing in routine diagnosis for developmental anomalies may help decipher more conditions associated with these molecular mechanisms. In that regard, the identification of regulatory elements is mandatory to interpret genomic alterations especially in the noncoding genome.

Efforts have long been made by researchers in the field of limb development to identify and characterize forelimb specific enhancers, therefore likely involved in the limb identity. The most interesting target gene is *Tbx5*, a marker of the forelimb identity, for which two candidate forelimb enhancers have been described in the literature. The first one, a 361 bp element located in intron 2, was identified through transgenic mice studies using DNA elements joined to reporter genes inserted randomly in the genome [23]. This element was sufficient to initiate the early forelimb-restricted expression of Tbx5 from E8.5. *Hox* genes (*Hoxa4, Hoxa5, Hoxb4, Hoxb5, Hoxc4, Hoxc5*) are direct upstream regulators of *Tbx5*, binding to this element. The second one (cns12sh), located downstream of *Tbx5* and conserved from fish to mammals, was described using the same technique in zebrafish [113]. These enhancers were attractive candidates for severe forelimb malformations if altered. However, knock-out studies in mice were very disappointing since embryos harboring either intron 2 or cns12sh

homozygous deletion, exhibit normal expression of *Tbx5* in the forelimb, normal forelimb bud initiation at E9.5 and normal forelimb skeleton formation at E14. Thus, even though the intron 2 and cns12sh elements can activate transcription when placed near basal promoters in ectopic genomic locations, they may not be necessary and sufficient to control forelimb Tbx5 activation in their normal genomic locations [114]. Redundancy in mammalian enhancers may explain the absence of phenotype in these animal models. According to genome editing experiments with both single and combinatorial enhancer deletions at distinct loci required for limb development, a median of eight distinct enhancers per gene is observed for genes encoding transcription factors [115]. This functional redundancy reduces the likelihood of severe consequences resulting from genetic alterations. These findings suggest that noncoding regulatory variants in humans will cause at most very subtle phenotypes, especially for enhancers regulating genes that are fundamental for the early limb development like *Tbx5*. In this respect, the fact that *Shh* expression is directed in the limb by a single enhancer (i.e. the ZRS), for which genomic alterations are responsible for developmental abnormalities, is quite unique.

In addition, the fact that fundamental knowledge on limb developmental biology relies on animal studies using mainly mouse and chick models, constitutes a further limitation in the identification of enhancers involved in human disease. Particularly for the radial ray, the prehension capacity acquired by the primates suggests evolutionary specificities in the genetic regulation of forelimb bud development. Recent data on human embryonic tissues, such as transcriptome and chromatin conformation capture, could guide future studies [116].

Finally, apart from Mendelian hypotheses (i.e. single alteration of a gene or regulatory region), oligogenic or multigenic alterations may explain the diagnostic deadlocks remaining in some multiple congenital anomalies. For example, some cases affected with VACTERL association

have been linked to rare monogenic variants in genes involved in the *SHH* signaling pathway, suggesting that the deregulation of this pathway may be the pathophysiological mechanism involved in this condition. Similar to the holoprosencephaly model [117], we can hypothesize that most of the VACTERL cases could be due to the accumulation of variants in genes or regulatory elements involved in the same developmental pathway, leading to an altered signaling. In support of this hypothesis, enrichment for rare variants in genes involved in *SHH* and *WNT* pathways has been observed by exome sequencing studies [118]. Therefore, combining genomic approaches like genome sequencing and transcriptome profiling, together with the development of functional testing of the signaling pathways may help resolve these cases in the future.

FIGURES AND TABLE LEGENDS

Figure 1: Limb bud development.
Left panel: The 3 axes of limb development and their signaling centers; Middle panel: Initiation of the upper-limb development; Right panel: Anterior-posterior polarization under the control of a reciprocal antagonism between SHH and GLI3R. Numbers refer to the developing rays. AER: Apical Ectodermal Ridge; ZPA: Zone of Polarizing Activity;

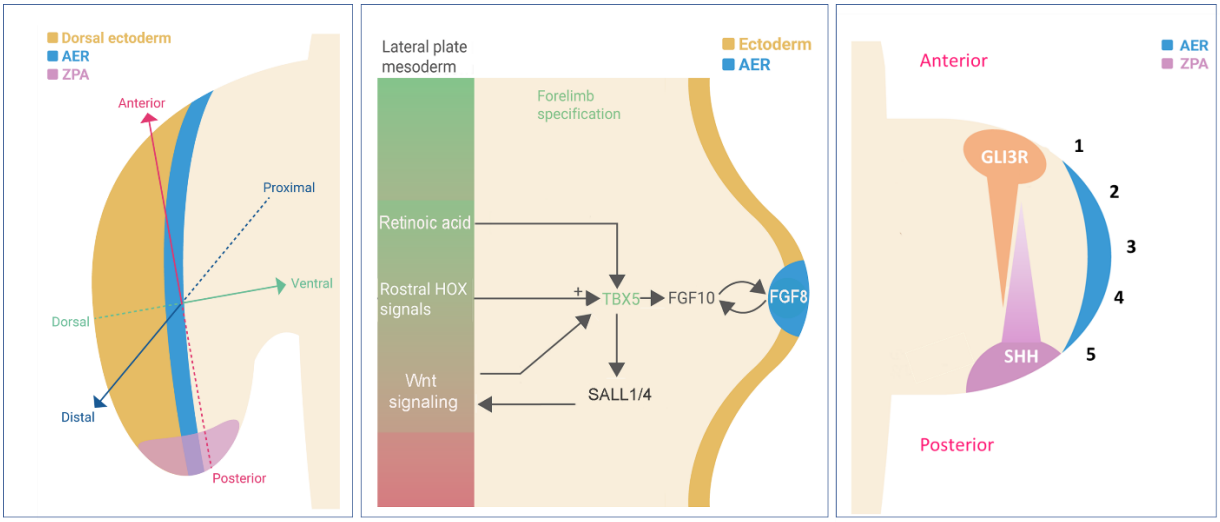

Figure 2: Variable expressivity of radial defects.
A: Radius and thumb agenesis; B: Radius agenesis with thumb present, typical of TAR syndrome; C: Radius hypoplasia with thumb agenesis; D: Severe thumb hypoplasia; E: Thumb hypoplasia; F: Thumb duplication; G: Triphalangeal and digitalized thumb.

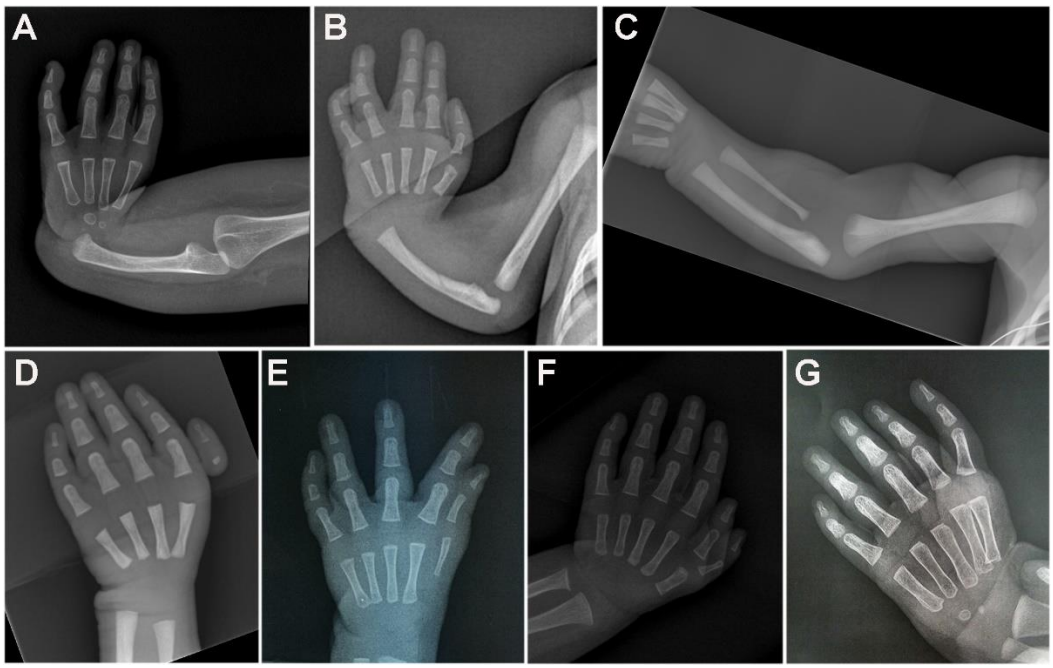

Table 1: Syndromes associated with radial defects.

* regulatory sequence; N.A.: non applicable; "-": feature absent; "+": feature present; AR: autosomal recessive; AD: autosomal dominant; XL: X-linked;

Syndromes	MIM#	Radial defect	Thumb malformations	Other skeletal defects	Associated features	Risk of malignancy	Genes	Inheritance
Limb specification and pattern formation								
Holt-Oram syndrome	142900	Radial aplasia/hypoplasia	Thumb hypoplasia/agenesis, triphalangeal thumb, I-II syndactyly	Phocomelia, ulnar/humeral hypoplasia, sploping shoulders, clavicle defects, limitation of elbow mobility	Congenital heart defect, cardiac conduction disease	-	*TBX5*	AD
Duane-Radial Ray; Okihiro syndrome	607323	Radial aplasia/hypoplasia	Thumb hypoplasia/agenesis, triphalangeal or duplicated thumb	Ulnar or humeral hypoplasia	Duane anomaly, hearing impairment, kidney defects	-	*SALL4*	AD
Townes-Brocks syndrome	107480	-	Triphalangeal or duplicated thumb, rarely thumb hypoplasia	Feet anomalies	Imperforate anus, dysplastic ears, hearing impairment, kidney disease	-	*SALL1*	AD
LADD syndrome	149730	-	Thumb hypoplasia/aplasia, triphalangeal or duplicated thumb	Other fingers involvement	hypoplasia, aplasia or atresia of the lacrimal and/or salivary system	-	*FGF10, FGFR2, FGFR3*	AD
LEF1-related radial defects	N.A.	Radial hypoplasia	Thumb hypoplasia or duplication	Syndactyly of fingers / toes, preaxial polydactyly of feet.	Ectodermal dysplasia	-	*LEF1*	AD
Preaxial polydactyly type I/II	174500	-	Triphalangeal or duplicated thumb	Duplicated hallux	-	-	ZRS*	AD
Hand-foot-genital syndrome	140000	-	Thumb hypoplasia	Ulnar deviation of the 2nd fingers, brachymesophalangy of the 5th fingers, short halluces. Delayed ossification and fusion of the carpals and tarsals.	Urogenital malformations, hypospadias, Mullerian duct fusion defects, vesicoureteric reflux and pelvi-ureteric junction obstruction.	-	*HOXA13*	AD
Spliceosomopathies and ribosomopathies								
Nager syndrome	154400	Radial hypoplasia/aplasia, radio-ulnar synostosis	Thumb hypoplasia/aplasia, triphalangeal or duplicated thumb	Mandibulofacial dysostosis, clubfoot, hypoplasia of the hallux	Hearing impairment, congenital heart defect	-	*SF3B4*	AD
TAR syndrome	274000	Radia hypoplasia/aplasia	Thumbs present	Phocomelia	Thrombocytopenia, congenital heart defect, cow's milk intolerance	-	*RBM8A*	AR
Diamond-Blackfan syndrome	105650	Radial hypoplasia/aplasia,radio-ulnar synostosis	Thumb hypoplasia/aplasia, triphalangeal or duplicated thumb	Mandibulofacial dysostosis	Growth retardation, craniofacial, heart, and genitourinary malformations	+	heterogenous	AD, XLD

Syndromes	MIM#	Radial defect	Thumb malformations	Other skeletal defects	Associated features	Risk of malignancy	Genes	Inheritance
Genome maintenance								
Cornelia de Lange syndrome	122470, 300590, 610759, 614701, 300882, 620568	Radial aplasia, radioulnar synostosis	Short first metacarpal, thumb hypoplasia	Micromelia, oligodactyly, monodactyly, syndactyly 2-3 of toes	Growth deficiency, microcephaly, facial dysmorphism, hirsutism, congenital heart defect, urogenital malformation, hearing impairment, intellectual disability	-	*NIPBL, SMC1A, SMC3, RAD21, HDAC8, BRD4*	AD, XLD
Fanconi syndrome	227650	Radia hypoplasia/aplasia	Thumb hypoplasia/aplasia, triphalangeal or duplicated thumb	Scoliosis, hemivertebrae, rib anomalies, hip dislocation/dysplasia, club feet, toe syndactyly	Growth deficiency, microcephaly, variable congenital anomalies, endocrine disorders	+	heterogenous	AR, AD, XL
Baller-Gerold syndrome	218600	Radia hypoplasia/aplasia	Thumb hypoplasia/aplasia	Patella hypoplasia/aplasia	Growth deficiency, craniosynostosis, anteriorly placed or imperforate anus, diarrhea, facial dysmorphism	-	*RECQL4*	AR
RAPADILINO	266280	Radia hypoplasia/aplasia	Thumb hypoplasia/aplasia	Patella hypoplasia/aplasia	Growth deficiency, cleft palate, diarrhea, joint dislocations, facial dysmorphism	+	*RECQL4*	AR
Rothmund-Thomson syndrome type 2	268400	Radia hypoplasia/aplasia	Thumb hypoplasia/aplasia	Patella hypoplasia/aplasia	Growth deficiency, poikiloderma, hyperkeratosis of feet soles, sparse hair, nail dysplasia, dental anomalies, cataract	+	*RECQL4*	AR
Multifactorial determinism								
VACTERL Association	192350	Radia hypoplasia/aplasia, radioulnar synostosis	Thumb hypoplasia/aplasia, triphalageal or duplicated thumb	Costo-vertebral anomalies	Congenital heart defect, kidney malformations, anal atresia, tracheo-esophageal fistula or esophageal atresia	-	unknown	unknown
OATS / Goldenhar	141400	Radia hypoplasia/aplasia	Thumb hypoplasia/aplasia, triphalageal or duplicated thumb	Vertebral anomalies	Hemifacial microsomia, microtia, preauricular tag/pit, oral cleft	-	unknown	unknown

REFERENCES

1. Kozin SH. Upper-extremity congenital anomalies. J Bone Joint Surg Am. août 2003;85(8):1564-76.

2. Ekblom AG, Laurell T, Arner M. Epidemiology of Congenital Upper Limb Anomalies in 562 Children Born in 1997 to 2007: A Total Population Study from Stockholm, Sweden. J Hand Surg. 1 nov 2010;35(11):1742-54.

3. Koskimies E, Lindfors N, Gissler M, Peltonen J, Nietosvaara Y. Congenital upper limb deficiencies and associated malformations in Finland: a population-based study. J Hand Surg. juin 2011;36(6):1058-65.

4. Bedard T, Lowry RB, Sibbald B, Kiefer GN, Metcalfe A. Congenital limb deficiencies in Alberta-a review of 33 years (1980-2012) from the Alberta Congenital Anomalies Surveillance System (ACASS). Am J Med Genet A. nov 2015;167A(11):2599-609.

5. Paladini D, Greco E, Sglavo G, D' Armiento MR, Penner I, Nappi C. Congenital anomalies of upper extremities: prenatal ultrasound diagnosis, significance, and outcome. Am J Obstet Gynecol. 1 juin 2010;202(6):596.e1-596.e10.

6. Gray BL, Calfee RP, Dicke JM, Steffen J, Goldfarb CA. The utility of prenatal ultrasound as a screening tool for upper extremity congenital anomalies. J Hand Surg. nov 2013;38(11):2106-11.

7. Piper SL, Dicke JM, Wall LB, Shen TS, Goldfarb CA. Prenatal Detection of Upper Limb Differences With Obstetric Ultrasound. J Hand Surg. juill 2015;40(7):1310-1317.e3.

8. Farr A, Wachutka E, Bettelheim D, Windsperger K, Farr S. Perinatal outcomes of infants with congenital limb malformations: an observational study from a tertiary referral center in Central Europe. BMC Pregnancy Childbirth. 13 janv 2020;20(1):35.

9. Hamosh A, Scott AF, Amberger J, Valle D, McKusick VA. Online Mendelian Inheritance in Man (OMIM). Hum Mutat. 2000;15(1):57-61.

10. Martin AR, Williams E, Foulger RE, Leigh S, Daugherty LC, Niblock O, et al. PanelApp crowdsources expert knowledge to establish consensus diagnostic gene panels. Nat Genet. nov 2019;51(11):1560-5.

11. Jourdain AS, Petit F, Odou MF, Balduyck M, Brunelle P, Dufour W, et al. Multiplex targeted high-throughput sequencing in a series of 352 patients with congenital limb malformations. Hum Mutat. janv 2020;41(1):222-39.

12. Duboc V, Logan MPO. Regulation of limb bud initiation and limb-type morphology. Dev Dyn Off Publ Am Assoc Anat. mai 2011;240(5):1017-27.

13. Minguillon C, Del Buono J, Logan MP. Tbx5 and Tbx4 are not sufficient to determine limb-specific morphologies but have common roles in initiating limb outgrowth. Dev Cell. janv 2005;8(1):75-84.

14. Min H, Danilenko DM, Scully SA, Bolon B, Ring BD, Tarpley JE, et al. Fgf-10 is required for both limb and lung development and exhibits striking functional similarity to Drosophila branchless. Genes Dev. 15 oct 1998;12(20):3156-61.

15. Sekine K, Ohuchi H, Fujiwara M, Yamasaki M, Yoshizawa T, Sato T, et al. Fgf10 is essential for limb and lung formation. Nat Genet. janv 1999;21(1):138-41.

16. Mic FA, Sirbu IO, Duester G. Retinoic acid synthesis controlled by Raldh2 is required early for limb bud initiation and then later as a proximodistal signal during apical ectodermal ridge formation. J Biol Chem. 18 juin 2004;279(25):26698-706.

17. Zhao X, Sirbu IO, Mic FA, Molotkova N, Molotkov A, Kumar S, et al. Retinoic acid promotes limb induction through effects on body axis extension but is unnecessary for limb patterning. Curr Biol CB. 23 juin 2009;19(12):1050-7.

18. Benazet JD, Zeller R. Dual requirement of ectodermal Smad4 during AER formation and termination of feedback signaling in mouse limb buds. Genes N Y N 2000. sept 2013;51(9):660-6.

19. Pearse RV, Scherz PJ, Campbell JK, Tabin CJ. A cellular lineage analysis of the chick limb bud. Dev Biol. 15 oct 2007;310(2):388-400.

20. Litingtung Y, Dahn RD, Li Y, Fallon JF, Chiang C. Shh and Gli3 are dispensable for limb skeleton formation but regulate digit number and identity. Nature. 29 août 2002;418(6901):979-83.

21. King M, Arnold JS, Shanske A, Morrow BE. T-genes and limb bud development. Am J Med Genet A. 1 juill 2006;140(13):1407-13.

22. Saito D, Yonei-Tamura S, Takahashi Y, Tamura K. Level-specific role of paraxial mesoderm in regulation of Tbx5/Tbx4 expression and limb initiation. Dev Biol. 1 avr 2006;292(1):79-89.

23. Minguillon C, Nishimoto S, Wood S, Vendrell E, Gibson-Brown JJ, Logan MPO. Hox genes regulate the onset of Tbx5 expression in the forelimb. Dev Camb Engl. sept 2012;139(17):3180-8.

24. Nishimoto S, Minguillon C, Wood S, Logan MPO. A combination of activation and repression by a colinear Hox code controls forelimb-restricted expression of Tbx5 and reveals Hox protein specificity. PLoS Genet. mars 2014;10(3):e1004245.

25. Rallis C, Bruneau BG, Del Buono J, Seidman CE, Seidman JG, Nissim S, et al. Tbx5 is required for forelimb bud formation and continued outgrowth. Dev Camb Engl. juin 2003;130(12):2741-51.

26. Hasson P, Del Buono J, Logan MPO. Tbx5 is dispensable for forelimb outgrowth. Dev Camb Engl. janv 2007;134(1):85-92.

27. Hasson P, DeLaurier A, Bennett M, Grigorieva E, Naiche LA, Papaioannou VE, et al. Tbx4 and tbx5 acting in connective tissue are required for limb muscle and tendon patterning. Dev Cell. 19 janv 2010;18(1):148-56.

28. de Celis JF, Barrio R. Regulation and function of Spalt proteins during animal development. Int J Dev Biol. 2009;53(8-10):1385-98.

29. Harvey SA, Logan MPO. sall4 acts downstream of tbx5 and is required for pectoral fin outgrowth. Dev Camb Engl. mars 2006;133(6):1165-73.

30. Koshiba-Takeuchi K, Takeuchi JK, Arruda EP, Kathiriya IS, Mo R, Hui C chung, et al. Cooperative and antagonistic interactions between Sall4 and Tbx5 pattern the mouse limb and heart. Nat Genet. févr 2006;38(2):175-83.

31. Shravya MS, Girisha KM, Nayak SS. Comprehensive phenotyping of fetuses with trisomy 18: a perinatal center experience. Clin Dysmorphol. 1 janv 2024;33(1):16-26.

32. Rosa RFM, Rosa RCM, Lorenzen MB, Zen PRG, Oliveira CAV de, Graziadio C, et al. Limb abnormalities on trisomy 18: evidence for early diagnosis. J Pediatr (Rio J). 2012;88(5):401-5.

33. Wildenauer L, Mavrommatis S, Bae DS, Steinman SE, Wall LB, Van Heest AE. Syndromic Involvement of Patients Presenting With Congenital Upper Limb Anomalies: An Analysis of 4,317 Cases. J Hand Surg. 1 avr 2024;49(4):311-20.

34. McDermott DA, Fong JC, Basson CT. Holt-Oram Syndrome. In: Adam MP, Feldman J, Mirzaa GM, Pagon RA, Wallace SE, Bean LJ, et al., éditeurs. GeneReviews® [Internet]. Seattle (WA): University of Washington, Seattle; 1993 [cité 13 juill 2024]. Disponible sur: http://www.ncbi.nlm.nih.gov/books/NBK1111/

35. Vanlerberghe C, Jourdain AS, Ghoumid J, Frenois F, Mezel A, Vaksmann G, et al. Holt-Oram syndrome: clinical and molecular description of 78 patients with TBX5 variants. Eur J Hum Genet EJHG. 2019;27(3):360-8.

36. Basson CT, Bachinsky DR, Lin RC, Levi T, Elkins JA, Soults J, et al. Mutations in human TBX5 [corrected] cause limb and cardiac malformation in Holt-Oram syndrome. Nat Genet. janv 1997;15(1):30-5.

37. Al-Baradie R, Yamada K, St Hilaire C, Chan WM, Andrews C, McIntosh N, et al. Duane radial ray syndrome (Okihiro syndrome) maps to 20q13 and results from mutations in SALL4, a new member of the SAL family. Am J Hum Genet. nov 2002;71(5):1195-9.

38. Kohlhase J. SALL4-Related Disorders. In: Adam MP, Feldman J, Mirzaa GM, Pagon RA, Wallace SE, Bean LJ, et al., éditeurs. GeneReviews® [Internet]. Seattle (WA): University of Washington, Seattle; 1993 [cité 13 juill 2024]. Disponible sur: http://www.ncbi.nlm.nih.gov/books/NBK1373/

39. Borozdin W, Wright MJ, Hennekam RCM, Hannibal MC, Crow YJ, Neumann TE, et al. Novel mutations in the gene SALL4 provide further evidence for acro-renal-ocular and Okihiro syndromes being allelic entities, and extend the phenotypic spectrum. J Med Genet. août 2004;41(8):e102.

40. Kohlhase J, Chitayat D, Kotzot D, Ceylaner S, Froster UG, Fuchs S, et al. SALL4 mutations in Okihiro syndrome (Duane-radial ray syndrome), acro-renal-ocular syndrome, and related disorders. Hum Mutat. sept 2005;26(3):176-83.

41. Paradisi I, Arias S. IVIC syndrome is caused by a c.2607delA mutation in the SALL4 locus. Am J Med Genet A. 15 févr 2007;143(4):326-32.

42. Townes PL, Brocks ER. Hereditary syndrome of imperforate anus with hand, foot, and ear anomalies. J Pediatr. août 1972;81(2):321-6.

43. Kohlhase J. Townes-Brocks Syndrome. In: Adam MP, Feldman J, Mirzaa GM, Pagon RA, Wallace SE, Bean LJ, et al., éditeurs. GeneReviews® [Internet]. Seattle (WA): University of Washington, Seattle; 1993 [cité 13 juill 2024]. Disponible sur: http://www.ncbi.nlm.nih.gov/books/NBK1445/

44. Miller EM, Hopkin R, Bao L, Ware SM. Implications for genotype-phenotype predictions in Townes-Brocks syndrome: case report of a novel SALL1 deletion and review of the literature. Am J Med Genet A. mars 2012;158A(3):533-40.

45. Beaudoux O, Lebre AS, Doco Fenzy M, Spodenkiewicz M, Canivet E, Colosio C, et al. Adult diagnosis of Townes-Brocks syndrome with renal failure: Two related cases and review of literature. Am J Med Genet A. mars 2021;185(3):937-44.

46. Kohlhase J, Wischermann A, Reichenbach H, Froster U, Engel W. Mutations in the SALL1 putative transcription factor gene cause Townes-Brocks syndrome. Nat Genet. janv 1998;18(1):81-3.

47. Hollister DW, Klein SH, De Jager HJ, Lachman RS, Rimoin DL. The lacrimo-auriculo-dento-digital syndrome. J Pediatr. sept 1973;83(3):438-44.

48. Milunsky JM, Zhao G, Maher TA, Colby R, Everman DB. LADD syndrome is caused by FGF10 mutations. Clin Genet. avr 2006;69(4):349-54.

49. Rohmann E, Brunner HG, Kayserili H, Uyguner O, Nürnberg G, Lew ED, et al. Mutations in different components of FGF signaling in LADD syndrome. Nat Genet. avr 2006;38(4):414-7.

50. Wassel HD. The results of surgery for polydactyly of the thumb. A review. Clin Orthop. 1969;64:175-93.

51. Umair M, Ahmad F, Bilal M, Ahmad W, Alfadhel M. Clinical Genetics of Polydactyly: An Updated Review. Front Genet. 2018;9:447.

52. Lettice LA, Heaney SJH, Purdie LA, Li L, de Beer P, Oostra BA, et al. A long-range Shh enhancer regulates expression in the developing limb and fin and is associated with preaxial polydactyly. Hum Mol Genet. 15 juill 2003;12(14):1725-35.

53. Sun M, Ma F, Zeng X, Liu Q, Zhao XL, Wu FX, et al. Triphalangeal thumb-polysyndactyly syndrome and syndactyly type IV are caused by genomic duplications involving the long range, limb-specific SHH enhancer. J Med Genet. sept 2008;45(9):589-95.

54. Stern AM, Gall JC, Perry BL, Stimson CW, Weitkamp LR, Poznanski AK. The hand-food-uterus syndrome: a new hereditary disorder characterized by hand and foot dysplasia, dermatoglyphic abnormalities, and partial duplication of the female genital tract. J Pediatr. juill 1970;77(1):109-16.

55. Goodman FR, Bacchelli C, Brady AF, Brueton LA, Fryns JP, Mortlock DP, et al. Novel HOXA13 mutations and the phenotypic spectrum of hand-foot-genital syndrome. Am J Hum Genet. juill 2000;67(1):197-202.

56. Tas E, Sebastian J, Madan-Khetarpal S, Sweet P, Yatsenko AN, Pollock N, et al. Familial deletion of the HOXA gene cluster associated with Hand-Foot-Genital syndrome and phenotypic variability. Am J Med Genet A. janv 2017;173(1):221-4.

57. Dufour W, Alawbathani S, Jourdain AS, Asif M, Baujat G, Becker C, et al. Monoallelic and biallelic variants in LEF1 are associated with a new syndrome combining ectodermal dysplasia and limb malformations caused by altered WNT signaling. Genet Med Off J Am Coll Med Genet. août 2022;24(8):1708-21.

58. Fiesco-Roa MO, Giri N, McReynolds LJ, Best AF, Alter BP. Genotype-Phenotype Associations in Fanconi Anemia: A Literature Review. Blood Rev. sept 2019;37:100589.

59. Bourke G, Wilks D, Kinsey S, Feltbower RG, Giri N, Alter BP. The incidence and spectrum of congenital hand differences in patients with Fanconi anaemia: analysis of 48 patients. J Hand Surg Eur Vol. juill 2022;47(7):711-5.

60. Petryk A, Kanakatti Shankar R, Giri N, Hollenberg AN, Rutter MM, Nathan B, et al. Endocrine Disorders in Fanconi Anemia: Recommendations for Screening and Treatment. J Clin Endocrinol Metab. 1 mars 2015;100(3):803-11.

61. Shimamura A, Alter BP. Pathophysiology and management of inherited bone marrow failure syndromes. Blood Rev. mai 2010;24(3):101-22.

62. Alter BP. Arm anomalies and bone marrow failure may go hand in hand. J Hand Surg. mai 1992;17(3):566-71.

63. Joenje H, Patel KJ. The emerging genetic and molecular basis of Fanconi anaemia. Nat Rev Genet. juin 2001;2(6):446-58.

64. Wang H, Hunter AG, Clifford B, McLaughlin M, Thompson D. VACTERL with hydrocephalus: spontaneous chromosome breakage and rearrangement in a family showing apparent sex-linked recessive inheritance. Am J Med Genet. 1 août 1993;47(1):114-7.

65. Wang AT, Kim T, Wagner JE, Conti BA, Lach FP, Huang AL, et al. A Dominant Mutation in Human RAD51 Reveals Its Function in DNA Interstrand Crosslink Repair Independent of Homologous Recombination. Mol Cell. 6 août 2015;59(3):478-90.

66. Mo D, Zhao Y, Balajee AS. Human RecQL4 helicase plays multifaceted roles in the genomic stability of normal and cancer cells. Cancer Lett. janv 2018;413:1-10.

67. Kääriäinen H, Ryöppy S, Norio R. RAPADILINO syndrome with radial and patellar aplasia/hypoplasia as main manifestations. Am J Med Genet. 1989;33(3):346-51.

68. Siitonen HA. Molecular defect of RAPADILINO syndrome expands the phenotype spectrum of RECQL diseases. Hum Mol Genet. 9 sept 2003;12(21):2837-44.

69. Siitonen HA, Sotkasiira J, Biervliet M, Benmansour A, Capri Y, Cormier-Daire V, et al. The mutation spectrum in RECQL4 diseases. Eur J Hum Genet EJHG. févr 2009;17(2):151-8.

70. Thomson MS. An Hitherto Undescribed Familial Disease. Br J Dermatol. 1923;35(12):455-62.

71. Vennos EM, Collins M, James WD. Rothmund-Thomson syndrome: Review of the world literature. J Am Acad Dermatol. 1 nov 1992;27(5, Part 1):750-62.

72. Wang LL, Levy ML, Lewis RA, Chintagumpala MM, Lev D, Rogers M, et al. Clinical manifestations in a cohort of 41 Rothmund-Thomson syndrome patients. Am J Med Genet. 2001;102(1):11-7.

73. Ajeawung NF, Nguyen TTM, Lu L, Kucharski TJ, Rousseau J, Molidperee S, et al. Mutations in ANAPC1, Encoding a Scaffold Subunit of the Anaphase-Promoting Complex, Cause Rothmund-Thomson Syndrome Type 1. Am J Hum Genet. 5 sept 2019;105(3):625-30.

74. Averdunk L, Huetzen MA, Moreno-Andrés D, Kalb R, McKee S, Hsieh TC, et al. Biallelic variants in *CRIPT* cause a Rothmund-Thomson-like syndrome with increased cellular senescence. Genet Med. 1 juill 2023;25(7):100836.

75. Filho RDL, Yamamoto GL, Silva TJ, Rocha LA, Linnenkamp BDW, Castro MAA, et al. Biallelic variants in DNA2 cause poikiloderma with congenital cataracts and severe growth failure reminiscent of Rothmund-Thomson syndrome. J Med Genet. 1 nov 2023;60(11):1127-32.

76. Maldergem LV, Siitonen HA, Jalkh N, Chouery E, Roy MD, Delague V, et al. Revisiting the craniosynostosis-radial ray hypoplasia association: Baller-Gerold syndrome caused by mutations in the RECQL4 gene. J Med Genet. 1 févr 2006;43(2):148-52.

77. Debeljak M, Zver A, Jazbec J. A patient with Baller-Gerold syndrome and midline NK/T lymphoma. Am J Med Genet A. 15 févr 2009;149A(4):755-9.

78. Ptacek LJ, Opitz JM, Smith DW, Gerritsen T, Waisman HA. The Cornelia de Lange syndrome. J Pediatr. 1 nov 1963;63(5):1000-20.

79. Jackson L, Kline AD, Barr MA, Koch S. de Lange syndrome: a clinical review of 310 individuals. Am J Med Genet. 15 nov 1993;47(7):940-6.

80. Mehta D, Vergano SAS, Deardorff M, Aggarwal S, Barot A, Johnson DM, et al. Characterization of limb differences in children with Cornelia de Lange Syndrome. Am J Med Genet C Semin Med Genet. 2016;172(2):155-62.

81. Chatfield KC, Schrier SA, Li J, Clark D, Kaur M, Kline AD, et al. Congenital heart disease in Cornelia de Lange syndrome: Phenotype and genotype analysis. Am J Med Genet A. 2012;158A(10):2499-505.

82. Shi A, Levin AV. Ophthalmologic findings in the Cornelia de Lange syndrome. Ophthalmic Genet. 2 janv 2019;40(1):1-6.

83. Marchisio P, Selicorni A, Bianchini S, Milani D, Baggi E, Cerutti M, et al. Audiological findings, genotype and clinical severity score in Cornelia de Lange syndrome. Int J Pediatr Otorhinolaryngol. 1 juill 2014;78(7):1045-8.

84. Luzzani S, Macchini F, Valadè A, Milani D, Selicorni A. Gastroesophageal reflux and Cornelia de Lange syndrome: typical and atypical symptoms. Am J Med Genet A. 15 juin 2003;119A(3):283-7.

85. Di Nardo M, Musio A. Cohesin - bridging the gap among gene transcription, genome stability, and human diseases. FEBS Lett. 9 juin 2024;

86. Sieff C. Diamond-Blackfan Anemia. In: Adam MP, Feldman J, Mirzaa GM, Pagon RA, Wallace SE, Bean LJ, et al., éditeurs. GeneReviews® [Internet]. Seattle (WA): University of Washington, Seattle; 1993 [cité 13 juill 2024]. Disponible sur: http://www.ncbi.nlm.nih.gov/books/NBK7047/

87. Ulirsch JC, Verboon JM, Kazerounian S, Guo MH, Yuan D, Ludwig LS, et al. The Genetic Landscape of Diamond-Blackfan Anemia. Am J Hum Genet. 6 déc 2018;103(6):930-47.

88. Bernier FP, Caluseriu O, Ng S, Schwartzentruber J, Buckingham KJ, Innes AM, et al. Haploinsufficiency of SF3B4, a component of the pre-mRNA spliceosomal complex, causes Nager syndrome. Am J Hum Genet. 4 mai 2012;90(5):925-33.

89. Petit F, Escande F, Jourdain AS, Porchet N, Amiel J, Doray B, et al. Nager syndrome: confirmation of SF3B4 haploinsufficiency as the major cause. Clin Genet. sept 2014;86(3):246-51.

90. Petit F, Boussion S. Thrombocytopenia Absent Radius Syndrome. In: Adam MP, Feldman J, Mirzaa GM, Pagon RA, Wallace SE, Bean LJ, et al., éditeurs. GeneReviews® [Internet]. Seattle (WA): University of Washington, Seattle; 1993 [cité 13 juill 2024]. Disponible sur: http://www.ncbi.nlm.nih.gov/books/NBK23758/

91. Albers CA, Paul DS, Schulze H, Freson K, Stephens JC, Smethurst PA, et al. Compound inheritance of a low-frequency regulatory SNP and a rare null mutation in exon-junction complex subunit RBM8A causes TAR syndrome. Nat Genet. 26 févr 2012;44(4):435-9, S1-2.

92. Boussion S, Escande F, Jourdain AS, Smol T, Brunelle P, Duhamel C, et al. TAR syndrome: Clinical and molecular characterization of a cohort of 26 patients and description of novel noncoding variants of RBM8A. Hum Mutat. juill 2020;41(7):1220-5.

93. Carli D, Garagnani L, Lando M, Fairplay T, Bernasconi S, Landi A, et al. VACTERL (vertebral defects, anal atresia, tracheoesophageal fistula with esophageal atresia, cardiac defects, renal and limb anomalies) association: disease spectrum in 25 patients ascertained for their upper limb involvement. J Pediatr. mars 2014;164(3):458-462.e1-2.

94. Solomon BD. The etiology of VACTERL association: Current knowledge and hypotheses. Am J Med Genet C Semin Med Genet. déc 2018;178(4):440-6.

95. Saisawat P, Kohl S, Hilger AC, Hwang DY, Yung Gee H, Dworschak GC, et al. Whole-exome resequencing reveals recessive mutations in *TRAP1* in individuals with CAKUT and VACTERL association. Kidney Int. 1 juin 2014;85(6):1310-7.

96. Ac H, J H, T P, A van der V, G S, Da B, et al. Targeted Resequencing of 29 Candidate Genes and Mouse Expression Studies Implicate ZIC3 and FOXF1 in Human VATER/VACTERL Association. Hum Mutat [Internet]. déc 2015 [cité 19 juin 2024];36(12). Disponible sur: https://pubmed.ncbi.nlm.nih.gov/26294094/

97. Shi H, Enriquez A, Rapadas M, Martin EMMA, Wang R, Moreau J, et al. NAD Deficiency, Congenital Malformations, and Niacin Supplementation. N Engl J Med. 10 août 2017;377(6):544-52.

98. Kause F, Zhang R, Ludwig M, Schmiedeke E, Rissmann A, Thiele H, et al. HSPA6: A new autosomal recessive candidate gene for the VATER/VACTERL malformation spectrum. Birth Defects Res. 1 juin 2019;111(10):591-7.

99. Thiem CE, Stegmann JD, Hilger AC, Waffenschmidt L, Bendixen C, Köllges R, et al. Re-sequencing of candidate genes FOXF1, HSPA6, HAAO, and KYNU in 522 individuals with VATER/VACTERL, VACTER/VACTERL-like association, and isolated anorectal malformation. Birth Defects Res. juin 2022;114(10):478-86.

100. Warren A, Porter RM, Reyes-Castro O, Ali MM, Marques-Carvalho A, Kim HN, et al. The NAD salvage pathway in mesenchymal cells is indispensable for skeletal development in mice. Nat Commun. 17 juin 2023;14(1):3616.

101. Quinn ME, Haaning A, Ware SM. Preaxial polydactyly caused by Gli3 haploinsufficiency is rescued by Zic3 loss of function in mice. Hum Mol Genet. 15 avr 2012;21(8):1888-96.

102. Kim J, Kim P, Hui CC. The VACTERL association: lessons from the Sonic hedgehog pathway. Clin Genet. mai 2001;59(5):306-15.

103. Barisic I, Odak L, Loane M, Garne E, Wellesley D, Calzolari E, et al. Prevalence, prenatal diagnosis and clinical features of oculo-auriculo-vertebral spectrum: a registry-based study in Europe. Eur J Hum Genet EJHG. août 2014;22(8):1026-33.

104. Tasse C, Böhringer S, Fischer S, Lüdecke HJ, Albrecht B, Horn D, et al. Oculo-auriculo-vertebral spectrum (OAVS): clinical evaluation and severity scoring of 53 patients and proposal for a new classification. Eur J Med Genet. 2005;48(4):397-411.

105. Vendramini S, Richieri-Costa A, Guion-Almeida ML. Oculoauriculovertebral spectrum with radial defects: a new syndrome or an extension of the oculoauriculovertebral spectrum? Report of fourteen Brazilian cases and review of the literature. Eur J Hum Genet EJHG. avr 2007;15(4):411-21.

106. Tingaud-Sequeira A, Trimouille A, Sagardoy T, Lacombe D, Rooryck C. Oculo-auriculo-vertebral spectrum: new genes and literature review on a complex disease. J Med Genet. mai 2022;59(5):417-27.

107. Timberlake AT, Griffin C, Heike CL, Hing AV, Cunningham ML, Chitayat D, et al. Haploinsufficiency of SF3B2 causes craniofacial microsomia. Nat Commun. 3 août 2021;12(1):4680.

108. Yamaki Y, Kagawa H, Hatta T, Natsume T, Kawahara H. The C-terminal cytoplasmic tail of hedgehog receptor Patched1 is a platform for E3 ubiquitin ligase complexes. Mol Cell Biochem. mars 2016;414(1-2):1-12.

109. Syvänen J, Raitio A, Helenius I, Löyttyniemi E, Lahesmaa-Korpinen AM, Gissler M, et al. Prevalence and risk factors of radial ray deficiencies: A population-based case-control study. Am J Med Genet A. mars 2021;185(3):759-65.

110. Gibson CC, Genest DR, Bieber FR, Holmes LB. X-linked phenotype of absent radius and anogenital anomalies. Am J Med Genet. 15 mars 1993;45(6):743-4.

111. Chavez TJ, Morrell NT. The Evolution of the Human Hand From an Anthropologic Perspective. J Hand Surg. févr 2022;47(2):181-5.

112. Petit F, Sears KE, Ahituv N. Limb development: a paradigm of gene regulation. Nat Rev Genet. 2017;18(4):245-58.

113. Adachi N, Robinson M, Goolsbee A, Shubin NH. Regulatory evolution of Tbx5 and the origin of paired appendages. Proc Natl Acad Sci U S A. 06 2016;113(36):10115-20.

114. Cunningham TJ, Lancman JJ, Berenguer M, Dong PDS, Duester G. Genomic Knockout of Two Presumed Forelimb Tbx5 Enhancers Reveals They Are Nonessential for Limb Development. Cell Rep. 12 2018;23(11):3146-51.

115. Osterwalder M, Barozzi I, Tissières V, Fukuda-Yuzawa Y, Mannion BJ, Afzal SY, et al. Enhancer redundancy provides phenotypic robustness in mammalian development. Nature. 8 févr 2018;554(7691):239-43.

116. Zhang B, He P, Lawrence JEG, Wang S, Tuck E, Williams BA, et al. A human embryonic limb cell atlas resolved in space and time. Nature. 6 déc 2023;

117. Dubourg C, Kim A, Watrin E, de Tayrac M, Odent S, David V, et al. Recent advances in understanding inheritance of holoprosencephaly. Am J Med Genet C Semin Med Genet. juin 2018;178(2):258-69.

118. Ritter J, Lisec K, Klinner M, Heinrich M, von Schweinitz D, Kappler R, et al. Genetic Disruption of Cilia-Associated Signaling Pathways in Patients with VACTERL Association. Child Basel Switz. 14 mai 2023;10(5):882.

Ce travail a permis de lister l'ensemble des gènes impliqués dans les syndromes avec anomalies radiales et d'identifier des voies de signalisation préférentiellement dérégulées dans ces pathologies.

Nous retenons les chevauchements phénotypiques entre ces pathologies, justifiant d'une description phénotypique précise pour différencier les tableaux cliniques, orienter les investigations moléculaires et adapter la surveillance. Nous notons également un rendement diagnostique relatif faible dans les dysplasies radiales, notamment lorsqu'elles sont observées de façon isolée.

Au vu du rôle majeur du gène *TBX5* dans le développement des membres supérieurs, nous nous sommes intéressés en premier lieu aux patients suspects de syndrome de Holt-Oram, afin de constituer une cohorte de patients présentant une atteinte radiale bilatérale, plus ou moins associée à une atteinte cardiaque, et de préciser le phénotype lié aux altérations du gène *TBX5*.

PARTIE II. LE SYNDROME DE HOLT-ORAM : critères diagnostiques cliniques et moléculaires d'une cause majeure d'atteinte radiale

a. Caractérisation clinique du syndrome de Holt-Oram

Le syndrome de Holt-Oram (HOS) est une affection autosomique dominante caractérisée par la présence d'une anomalie radiale, éventuellement associée à une malformation cardiaque congénitale, avec ou sans troubles du rythme, liée aux variants du gène *TBX5*. Ce diagnostic peut être difficile à établir en raison de la variabilité d'expression et de l'important chevauchement phénotypique avec d'autres affections, comme le syndrome d'Okihiro, le syndrome TAR ou la maladie de Fanconi.

Du fait de l'expertise clinico-biologique de notre équipe, nous avons étudié rétrospectivement 212 observations de patients adressés pour suspicion de HOS entre 2002 et 2014, ayant bénéficié de l'analyse moléculaire du gène *TBX5*.

Nous présentons, dans ce second article, les caractéristiques cliniques et moléculaires des 78 patients porteurs d'un variant de *TBX5*. A notre connaissance, il s'agit de la plus grande série moléculaire jamais décrite. Dans cette cohorte, 61 patients répondaient aux critères diagnostiques précédemment décrits et 17 ont été considérés comme ayant un diagnostic de HOS incertain. Une malformation cardiaque était présente chez 91 % des patients présentant un variant de *TBX5*, la communication interauriculaire étant la plus fréquente (61,5 %). L'étude de corrélation génotype-phénotype met en évidence certaines caractéristiques du syndrome de Holt-Oram : l'atteinte septale préférentielle de la cardiopathie, le caractère bilatéral et asymétrique de l'atteinte radiale et la présence d'un défaut de mobilité de l'épaule ou du coude. En outre, 21 patients étaient concernés par un diagnostic différentiel. Parmi eux, 13 avaient une présentation typique de HOS.

Nous discutons des stratégies qui pourraient être adoptées pour améliorer la caractérisation moléculaire des patients typiques restants.

European Journal of Human Genetics (2019) 27:360–368
https://doi.org/10.1038/s41431-018-0303-3

ESHG

ARTICLE

Holt-Oram syndrome: clinical and molecular description of 78 patients with *TBX5* variants

Clémence Vanlerberghe[1,2] · Anne-Sophie Jourdain[2,3] · Jamal Ghoumid[1,2] · Frédéric Frenois[2] · Aurélie Mezel[4] · Guy Vaksmann[5] · Bruno Lenne[6] · Bruno Delobel[6] · Nicole Porchet[3] · Valérie Cormier-Daire[7] · Thomas Smol[2,8] · Fabienne Escande[2,3] · Sylvie Manouvrier-Hanu[1,2] · Florence Petit[1]

Received: 8 March 2018 / Revised: 12 October 2018 / Accepted: 25 October 2018 / Published online: 14 December 2018

Abstract

Holt-Oram syndrome (HOS) is an autosomal dominant condition characterised by the association of congenital heart defect (CHD), with or without rhythm disturbances and radial defects, due to *TBX5* variants. The diagnosis is challenged by the variability of expression and the large phenotypic overlap with other conditions, like Okihiro syndrome, TAR syndrome or Fanconi disease. We retrospectively reviewed 212 patients referred for suspicion of HOS between 2002 and 2014, who underwent *TBX5* screening. A *TBX5* variant has been identified in 78 patients, representing the largest molecular series ever described. In the cohort, 61 met the previously described diagnostic criteria and 17 have been considered with an uncertain HOS diagnosis. A CHD was present in 91% of the patients with a *TBX5* variant, atrial septal defects being the most common (61.5%). The genotype–phenotype study highlights the importance of some critical features in HOS: the septal characteristic of the CHD, the bilateral and asymmetric characteristics of the radial defect and the presence of shoulder or elbow mobility defect. Besides, 21 patients presented with an overlapping condition. Among them, 13 had a typical HOS presentation. We discuss the strategies that could be adopted to improve the molecular delineation of the remaining typical patients.

Introduction

Congenital heart disease (CHD) is the most common congenital anomaly with an estimated prevalence of 9 per 1000 at birth [1]. Septal defects represent 47% of CHD [1]. Several genes contribute to heart development. Although *NKX2–5* and *GATA4* have been associated with isolated CHD, their partner *TBX5* is implicated in Holt-Oram syndrome (HOS) (MIM #142900). This autosomal dominant condition is characterised by the association of CHD and anterior upper limb defect, with a high penetrance and a wide variability of expression [2]. Its prevalence has been estimated at 1 in 100,000 births [3]. A CHD is present in 70–95% of the individuals according to the literature [4–10]. The most common are septal defects: *ostium secundum* atrial septal defect (44.4%) and ventricular septal defect (29.4%). More severe CHD have also been reported: atrioventricular septal defect, Fallot tetralogy, left ventricle hypoplasia, and aortic coarctation. Rhythm disturbances (39%) can be found isolated or associated with a CHD, and may appear over the course of life. The most common are sinus bradycardia and right bundle branch block [4, 6, 7, 9, 11]. Upper limb involvement is constant but very

Electronic supplementary material The online version of this article (https://doi.org/10.1038/s41431-018-0303-3) contains supplementary material, which is available to authorized users.

✉ Clémence Vanlerberghe
clemence.vanlerberghe@chru-lille.fr

1 CHU Lille, Clinique de Génétique, 59000 Lille, France

2 Univ. Lille, RADEME, EA 7364, 59000 Lille, France

3 CHU Lille, Institut de Biochimie et Génétique Moléculaire, 59000 Lille, France

4 CHU Lille, Unité de chirurgie orthopédique infantile, 59000 Lille, France

5 Hôpital privé de La Louvière, unité de cardiologie pédiatrique, Lille, France

6 Centre de Génétique Chromosomique, Hôpital Saint Vincent de Paul, Lille, France

7 Service de Génétique, U781, Fondation Imagine, Hôpital Necker-Enfants malades AP-HP, Paris, France

8 CHU Lille, Institut de Génétique Médicale, 59000 Lille, France

variable. Its spectrum extends from an isolated thenar hypoplasia, a mobility defect affecting the thumb, elbow, or shoulder, up to phocomelia. The most common defects are thumb hypoplasia at various degrees or a triphalangeal/fingerlike thumb, associated or not with radial hypoplasia. A left-right asymmetry may be observed, with usually more severe defects on the left-hand side [4, 6]. No correlation between the severity of the skeletal and the cardiac defects has been observed [6].

Variants in the *TBX5* gene (chromosome 12q24) have been found to cause HOS in 1997 [12, 13]. *TBX5* encodes a transcription factor belonging to the T-box family, regulating a large variety of developmental processes in vertebrates [14]. During heart development, *Tbx5* expression appears uniformly at the early stages, then is left-biased as the heart tube loops, being totally absent from the right ventricle [15]. Its role is crucial for cardiomyocytes proliferation and differentiation, septum formation and the establishment of the conduction system (reviewed in the ref. [16]). During limb development, *Tbx5* is expressed in forelimbs and not in hindlimbs. Its action is essential at early stages of limb initiation (E9.5–E10.5) to trigger the epithelio-mesenchymal growth loop between Fgf10 in the mesenchyme and Fgf8 in the apical ectodermal ridge. At later stages (E11.2–E12.5), Tbx5 is involved in muscle and tendon patterning and no longer needed for limb outgrowth [17].

About 300 HOS patients have been described in the literature. However, for most of them, the diagnosis was only established on clinical features [4–11]. The molecular confirmation of HOS diagnosis is crucial because of the cardiac monitoring required by this condition, and its impact on the genetic counselling. The detection yield of *TBX5* variants in HOS patients ranges from 22 to 74% depending on the studies [8, 11, 18–20]. The diagnostic criteria were consistent in most studies (uni or bilateral anterior upper limb defect, associated with a personal or familial history of CHD or rhythm disturbances). Mc Dermott et al. showed that the variant detection rate increases to 74% when the absence of associated features (except for spinal deformities) was added to the previous criteria. Of note, the molecular analysis methods were heterogeneous in the reported series of the literature and none of them included intragenic rearrangements screening.

Here, we report on the clinical and molecular characterisation of 78 unrelated HOS individuals harbouring a *TBX5* variant, allowing the description of the largest molecular series so far. These data allow detailed genotype–phenotype correlations and support the idea that molecular analyses are essential to distinguish HOS from overlapping conditions, which could be clinically confused.

Patients and methods

Patients

A multicentre, retrospective study was set up to collect data on 228 patients addressed to our laboratory for suspicion of HOS, between 2002 and 2014. This collaboration involved 56 departments of clinical genetics. Sixteen patients were excluded because of a non-appropriate diagnosis of HOS, in presence of postaxial upper limb involvement, lower limb defect or multiple associated malformations. Patient phenotypes were divided into three groups: typical HOS with heart defect, typical HOS without heart defect, uncertain HOS. Typical HOS patients met the diagnostic criteria established by Mc Dermott et al. HOS was considered as uncertain, if the preaxial defect, associated with a heart defect, was unilateral and/or in presence of one or two minor additional features. The associated features were considered as minor if they were previously described in a patient with a *TBX5* variant or if they are common in general population (growth retardation, urogenital malformations for example). Data from 212 patients were recorded. Clinical and radiological information were collected at the time of diagnosis and updated thanks to a clinical questionnaire as part of the study (available on request).

Ethics statement

Our study was performed using the Declaration of Helsinki protocol. Written informed consents were obtained from the patients or their parents prior to the molecular diagnostic analysis.

Genotyping

Peripheral blood was collected from patients and relatives. We performed Sanger sequencing of all *TBX5* coding exons and their flanking intronic regions. Primers sequences are available on request. Variants are given according to reference sequence NM_000192.3 (Hg19). Large intragenic *TBX5* rearrangements were tested by a multiplex ligation-dependent probe amplification (MLPA) kit (PE180 Limb malformations probemix, MRC-Holland). *TBX5* variants were submitted to ClinVar database, available at the following link: http://www.ncbi.nlm.nih.gov/clinvar/?term=TBX5[gene]. For the interpretation of missense variants, pathogenicity prediction software (SIFT, Polyphen) and proteic structure prediction software (PHYRE2, SuperPose) were used.

Statistical analysis

Comparisons between the different groups of patients have been assessed by the Chi-square test, with Yates correction when the application conditions were not respected.

Results

Among the 212 patients, 105 met the established diagnostic criteria (79 with heart defect, 26 without heart defect) and 107 were considered with an uncertain HOS diagnosis. *TBX5* molecular analysis identified 78 probands with *TBX5* variants: 61 who meet the diagnostic criteria and 17 who were clinically considered as uncertain. According to the diagnostic criteria established by Mc Dermott et al., the detection rate of *TBX5* variant was 58%. This detection rate was better in the subgroup associating bilateral anterior upper limb defect and CHD (70%).

Description of the patients with *TBX5* variants

Within the 78 probands with *TBX5* variants, 47 were sporadic cases. The clinical and radiological features observed in the patients and their 16 affected relatives are detailed in Tables 1 and 2. A cardiac defect was observed in 91% (71/78) of the patients. ASD was the most frequent (61.5% of the cases). Rhythm disturbances were observed in 30% of the living patients. The range of the limb phenotypes is depicted in Fig. 1. The upper limb defects were bilateral in 96% (75/78) of the patients. A left/right asymmetry was observed in 91% (31/34) of the patients when this information was available. The observed malformations were most often reduction defects (79.5%). None of the patients presented with preaxial polydactyly. Fourteen patients did not fit into the strict diagnostic criteria: 7 presented with the association of one or two skeletal features (scoliosis [4], *pectus excavatum* [3], costal deformities [1]), or one or two non-skeletal features (growth retardation [2], bilateral pyelic dilatation [1], familial form of Kallmann syndrome [1], laryngomalacia [1], pulmonary malformation [2], micropenis [1]). We describe 11 prenatal cases: 4 were revealed by an isolated upper limb defect (thumb agenesis, radial hypoplasia, phocomelia), 2 by an isolated CHD (VSD, AVD), 5 by the association of upper limb defect and CHD. The severity of the upper limb defects led to pregnancy termination for 6 foetuses. Data regarding the management and the evolution of the patients were often missing in the questionnaire filled in mainly by clinical geneticists. Orthopaedic surgery was reported for 25% (18/71) of the patients and consisted for 72% of them in pollicisation of the index finger. Cardiac surgery was performed in 47% (31/66) of the living patients with CHD and a pacemaker was placed for 38% (8/21) of the patients with rhythm disturbances. Two deaths occurred, including one during a cardiac surgery, due to the severity of the CHD consisting of atrioventricular septal defect either isolated or associated with a tight isthmic coarctation.

Among the observed *TBX5* variants, 87% were point changes. Most of them were truncating (37% nonsense, 26% frameshift, 10% splice site), while 14% were missense variants. MLPA analysis identified *TBX5* intragenic deletions in 8% and intragenic duplications in 4%. Finally, an apparently balanced translocation t(2;12)(q31;q24.3) implicating the *TBX5* locus did segregate in 3 affected cases of the same family. All described variants are illustrated in the Fig. 2. We identified 49 novel variants. Two novel variants responsible for an extended TBX5 protein were found: one familial case (c.1303delC, p.(Leu435Trpfs*147), triphalangeal thumbs, radial hypoplasia, single auricle with sinusal bradycardia) and one sporadic foetus (c.1346delA, p.(Gln449Argfs*70) de novo, bilateral thumbs and radial hypoplasia, complex CHD and a micropenis). Eight distinct missense variants have been identified in 11 unrelated patients. Their pathogenicity was appreciated according to criteria developed in Supp table 1. Two of them occurred de novo in sporadic cases, therefore considered as likely pathogenic. Two of them concerned the amino acid 237, crucial for DNA interaction. Functional tests for these 2 variants have been previously published, allowing us to consider them as pathogenic. The remaining 4 variations have been considered to be of uncertain significance.

Lack of penetrance—Mosaicism

In our series, 4 non-related parents of an affected child harboured the familial variant but no clinical HOS features. Two of them had normal skeletal X rays, cardiac ultrasound and electrocardiogram, whereas their children had typical features of HOS, up to phocomelia. This lack of penetrance was observed for 4 different variants: c.713dupG (p.(Ser239Glnfs*2)), duplication of exons 1 to 7 (c.(?_−667)_(755+1_756–1)dup), deletion of exon 7 (c.(663+1_664–1)_(755+1_756–1)del) and c.710G>A (p.(Arg237Gln)). Furthermore, one asymptomatic father of a proband presented with a somatic mosaicism (around 10% of the alleles in blood sample) for the variant identified in his son c.537C>A (p.(Tyr179*)).

Differential diagnosis

Among the 212 patients, 21 turned out to present a differential diagnosis (Supp table 2). Thirteen of them had

Table 1 Frequency of cardiac phenotypes in the 78 probands and their affected relatives in our series, compared to the literature [4–11]

	Patients from our study		Literature [4–11]
	Probands ($N = 78$)	Probands and relatives ($N = 94$)	
Congenital heart disease (CHD)			
General			
Single septal defect	38/78 (48.7)	44/94 (46.8)	nd
Multiple septal defect	12/78 (15.4)	16/94 (17)	nd
Septal defect, associated with another CHD	15/78 (19.2)	17/94 (18)	nd
Isolated valvular defect	2/78 (2.6)	2/94 (2.1)	nd
Details			
Septal defects			
Atrial septal defect	48/78 (61.5)	58/94 (61.7)	44.4%
Ventricular septal defect	27/78 (34.6)	32/94 (34)	29.4%
Atrioventricular septal defect	4/78 (5.1)	4/94 (4.3)	3.3%
Other			
Mitral valve abnormalities	3/78 (3.8)	3/94 (3.2)	4.1%
Patent ductus arteriosus	3/78 (3.8)	3/94 (3.2)	3.6%
Pulmonary stenosis	2/78 (2.6)	3/94 (3.2)	1.8%
Dextrocardia	2/78 (2.6)	2/94 (2.1)	1.8%
Left ventricle hypoplasia	2/78 (2.6)	2/94 (2.1)	nd
Aortic coarctation	4/78 (5.1)	4/94 (4.3)	nd
Left superior vena cava	3/78 (3.8)	3/94 (3.2)	nd
Complex CHD	1/78 (1.3)	1/94 (1)	nd
Conduction disturbances			
General			
Isolated	3/71 (4.2)	5/87 (5.7)	nd
Associated with CHD	18/71 (25.3)	20/87 (23)	nd
Details			
Sinus bradycardia	6/71 (8.5)	7/87 (8)	nd
Atrial flutter	2/71 (2.8)	2/87 (2.3)	nd
Atrioventricular block	2/71 (2.8)	4/87 (4.6)	nd
Right bundle branch block	5/71 (7)	6/87 (6.9)	nd
Junctional tachycardia	5/71 (7)	5/87 (5.7)	nd
Long QT	1/71 (1.4)	1/87 (1.1)	nd

Numbers in brackets are expressed in percent

nd not determined

typical presentation of HOS. Okihiro syndrome was confirmed molecularly for eight patients. Fanconi anemia was diagnosed in presence of increased chromosome breakage on karyotype with mitomycin C. TAR syndrome was confirmed in presence of a 1q21.1 microdeletion involving *RBM8A*, even if the second hit (hypomorphic SNP) was not observed.

Genotype–phenotype correlations

First, we compared the phenotypes between variant-positive and variant-negative patients, in the 3 phenotypic groups of patients. Some items were significantly more common in the variant-positive patients: the presence of a familial history, the presence of a septal defect, the association of a rhythm disturbance with a CHD, the bilateral characteristics of the radial defect and the presence of a shoulder or elbow mobility defect ($p < 0.05$) (Supp Table 3).

In addition, we compared the phenotypes according to the type of *TBX5* variant: truncating (nonsense, frameshift, splice site point variants, intragenic deletions or duplications) versus missense variants. We observed that isolated septal CHD are more common in the truncating than in the missense variants ($p = 0.02$). Besides, complex CHD associated to septal defect seems to be more common in case of missense variants ($p = 0.053$). Thus, we observed a tendency of less severe CHD in patients with truncating variants compared to the patients with missense variants. No significant difference was observed in the type or the severity of upper limb defects between the two groups.

Discussion

This description of the largest molecular HOS series ever reported allows a better delineation of the HOS phenotype and genotype, and helps to direct appropriate molecular analyses by using more accurate diagnostic criteria for HOS and overlapping conditions.

Our clinical study highlights the importance of some critical features: the septal involvement for the CHD, the bilateral characteristics of the radial ray defects and the

Table 2 Frequency of skeletal phenotypes in the 78 probands and their affected relatives in our series, compared to the literature [4–11]

	Patients from our study				Literature [4–11]
	Probands ($N = 78$)		Probands and relatives ($N = 94$)		Right and left
	Right	Left	Right	Left	
Hand					
Reduction defect of the thumbs					
Thenar hypoplasia	22/78 (28.2)	20/78 (25.6)	23/94 (24.4)	21/94 (22.3)	34.2%
Thumb hypoplasia	23/78 (29.5)	26/78 (33.3)	26/94 (27.7)	30/94 (31.9)	31.9%
Thumb agenesis	17/78 (21.8)	25/78 (32.1)	18/94 (19.1)	27/94 (28.7)	32.3%
I-II syndactyly	12/78 (15.4)	11/78 (14.1)	14/94 (14.9)	12/94 (12.8)	13.3%
First metacarpal agenesis	4/78 (5.1)	3/78 (3.8)	4/94 (4.3)	3/94 (3.2)	nd
Additional defect of the thumbs					
Triphalangeal thumb	21/78 (26.9)	19/78 (24.3)	21/94 (22.3)	20/94 (21.3)	23.6%
Digitalised thumb	5/78 (6.4)	2/78 (2.6)	5/94 (5.3)	4/94 (4.3)	31.9%
Bifid thumb	–	–	–	–	5%
II–III syndactyly	2/78 (2.6)	3/78 (3.8)	2/94 (2.1)	3/94 (3.2)	nd
Carpal bones malformation	3/78 (3.8)	3/78 (3.8)	5/94 (5.3)	5/94 (5.3)	35.3%
Forearm					
Radial defects					
Hypoplasia	17/78 (21.8)	17/78 (21.8)	19/94 (20.2)	20/94 (20.2)	34.2%
Agenesis	4/78 (5.1)	8/78 (10.3)	4/94 (4.3)	8/94 (8.5)	15.2%
Ulnar defects	–	1/78 (1.3)	–	1/94 (1.1)	nd
Radio-ulnar synostosis	3/78 (3.8)	5/78 (6.4)	3/94 (3.2)	5/94 (5.3)	nd
Limitation of pro-supination	14/78 (17.9)	16/78 (20.5)	19/94 (20.2)	20/94 (21.3)	25.8%
Limitation of elbow mobility	9/78 (11.5)	12/78 (15.4)	12/94 (12.8)	14/94 (14.9)	nd
Arm					
Humeral hypoplasia	–	1/78 (1.3)	–	1/94 (1)	32%
Phocomelia	3/78 (3.8)	4/78 (5.1)	4/94 (4.3)	5/94 (5.3)	8.4 %
Shoulder					
Limitation of elbow mobility	4/78 (5.1)	5/78 (6.4)	4/94 (4.3)	5/94 (5.3)	28.6%
Sloping shoulders	20/78 (25.6)	18/78 (23)	20/94 (20.2)	18/94 (19.1)	7.5%
Clavicle defects	8/78 (10.3)	8/78 (10.3)	10/94 (10.6)	10/94 (10.6)	31.6%
Muscular hypoplasia	5/78 (6.4)	5/78 (6.4)	5/94 (5.3)	5/94 (5.3)	38.2%

Numbers in brackets are expressed in percent

nd not determined

shoulder or elbow mobility defect (even in the absence of any skeletal involvement). Preaxial polydactyly, previously described in HOS in the literature [10], has not been observed in any of our patients with *TBX5* variants. We observed that the presence of pectus excavatum, spinal deformities or pulmonary malformations should not rule out the HOS hypothesis. The presence of *pectus excavatum* in HOS has been largely overestimated (30%) in the clinical series of the literature, probably because some of these patients had an overlapping condition [4, 6]. In our series, only 3 patients out of 78 (4%) presented with pectus excavatum, which is still higher than its frequency in the general population (0.3%) [21]. This association can be explained by the involvement of *Tbx5* in sternum development, demonstrated by the presence of abnormal sternal formation in a *Tbx5* conditional mutant [22]. Four patients out of 78 (5%) presented with *scoliosis*, which is not significantly different than its frequency in the general population (2–3%) [23], suggesting that this feature is independent from HOS. Four patients from the literature presented with vertebral defects: fusion of cervical vertebrae, defect of anterior vertebral bodies, hemivertebra [4, 8, 10, 19], while *Tbx5* expression has never been reported in the spinal column. Two patients of our series presented with a *pulmonary malformation*. A right lung agenesis, a right lung hypoplasia and a horseshoe lung have been previously described in HOS [24–26]. *Tbx5* expression has been described in the mesenchyme of the developing lungs and trachea, and could participate, through Fgf10 pathway, to lung branching [27]. The other associated features were likely incidental.

We described a lack of penetrance in 4 different HOS families in our series, and a somatic mosaicism in the father of one proband. HOS has generally been described as a condition with complete penetrance, but 2 families presenting with missense variants and an incomplete penetrance have already been reported [8, 28]. Somatic mosaicism for a variant has previously been reported in an

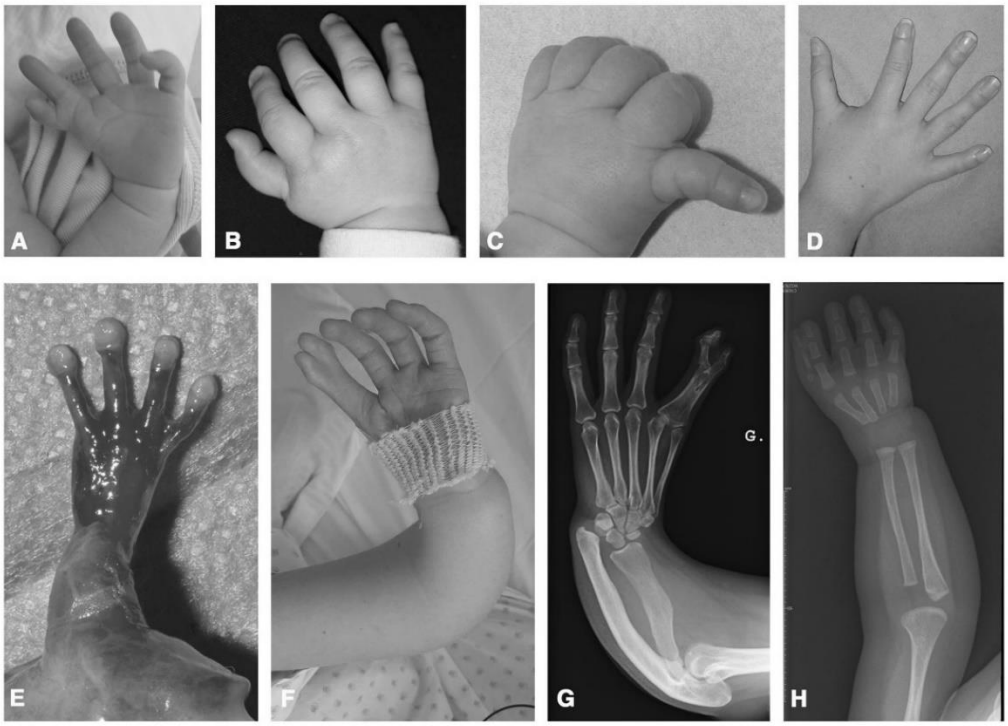

Fig. 1 Clinical and radiological phenotypes in HOS patients. **a** Left triphalangeal thumb, I–II syndactyly, elbow mobility defect; **b** Right thumb hypoplasia; **c** Left thumb hypoplasia; **d** Left triphalangeal thumb; **e** Left thumb agenesis in a foetus: **f** Left digitalised thumb, I–II syndactyly, radial hypoplasia; **g** Radial and ulnar hypoplasia, I–II phalangeal syndactyly; **h** Right thumb hypoplasia

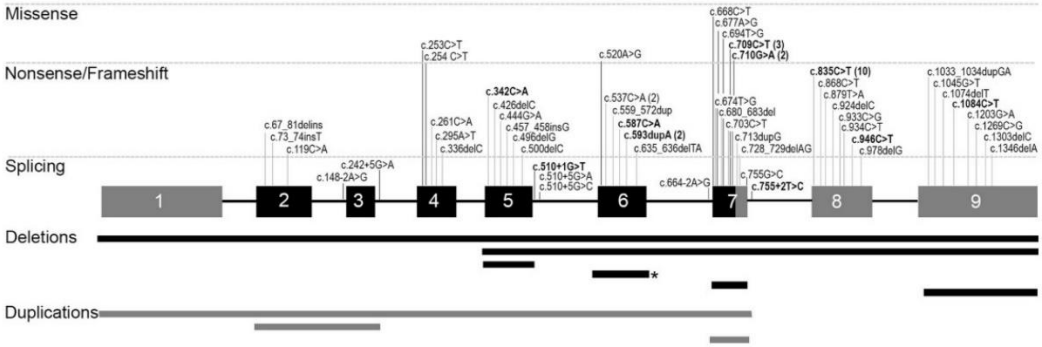

Fig. 2 Representation of the *TBX5* variants identified in our series of 78 HOS patients. Dark exons represent the T-box domain. Point variants are represented at the superior part of the figure. Intragenic deletions or duplications are represented at the inferior part. Variants in bold and deletions highlighted by a star have been described previously in the literature. The exons/introns are not at scale

asymptomatic parent in the literature [9]. This highlights the importance of the parental molecular analyses for all the probands with *TBX5* variants, even if the case seems to be sporadic, to be able to give an accurate genetic counselling to these families.

TBX5 variants are distributed throughout the gene, but the majority are found within the T-box DNA binding domain. Nonsense variants are the most common in our series (37%), whereas missense variants are the most frequently reported *TBX5* variants in the literature (30%,

Table 3 Summary and frequency of associated features that can be observed in the main differential diagnoses for HOS

	MIM#	Gene/Locus	Inheritance	Cardiac anomalies	Radial defects	Characteristic clinical features	References
Okihiro syndrome	607323	*SALL4*	AD	23%	80%	Duane anomaly, renal anomalies	[8, 31]
Fanconi pancytopenia	227650	FA core complex genes	AR, XL	6%	35%	Pancytopenia, growth retardation, microcephaly	[38]
Polydactyly, preaxial type II Syndactyly type IV	174500 and 186200	ZRS locus	AD	–	100%	Isolated pre-axial polydactyly with or without triphalangeal thumbs, mirror image polydactyly	[39]
Valproate embryopathy	–	–	sporadic	14–26%	30%	Developmental delay, neural tube defects, vertebral defects, hypospadias, cleft palate	[40, 41]
VACTERL association	192350	–	sporadic	40–80%	40–50%	Vertebral defects, anal atresia/ stenosis, cardiac anomalies, tracheo-Esophageal fistula, renal anomalies, limb defects	[42]
Townes-Brockes syndrome	107480	*SALL1*	AD	9–40%	50–90%	Anal atresia, ears malformations, deafness, triphalangeal thumbs, renal anomalies	[43]
TAR syndrome	274000	*RBM8A*	AR	15–30%	100%	Thrombocytopenia, preserved thumbs, lower limbs defects	[44, 45]
Nager syndrome	154400	*SF3B4*	AD	15%	100%	Mandibulofacial dysostosis, deafness	[46]
LADD syndrome	149730	*FGF10, FGFR2, FGFR3*	AD	-	95%	Lacrymal ducts atresia, ears malformations, deafness, abnormal teeth, thumb anomalies	[47, 48]
Roberts syndrome	268300	*ESCO2*	AR	26%	100%	Growth retardation, craniofacial malformations, upper and lower limbs reduction defects	[49, 5, 50]

versus 14% in our series), due to the larger propensity of publication of missense variant functional analyses (reviewed in the ref. [29]). Nonetheless, most of the reported *TBX5* variants (70%) lead to haploinsufficiency by synthesis of a non-functional truncated protein or by triggering the nonsense-mediated mRNA decay, by nonsense, frameshift or splice site variants [29]. Missense *TBX5* variants can cause loss-of-function or exceptionally gain-of-function. Sequence point variations leading to an extended protein and large intra and intergenic deletion/duplication have also been occasionally reported [29]. We observed a higher propensity of missense variants to be responsible for complex CHD associated to septal defect. In the literature, the few *TBX5* variants described in patients presenting with a non-septal CHD (Fallot tetralogy, cardiomyopathy) are also missense variants. Also, frameshift variants leading to an extended TBX5 protein seem to be associated with more severe CHD and associated malformations [30]. This suggests a potential dominant-negative effect for these variants.

HOS is a challenging diagnosis by its variability of expression and the large phenotypic overlap with other conditions. Among the patients addressed to our laboratory for HOS suspicion, 21 turned out to present a differential diagnosis (Supp table 3). More than 50% of these patients met the HOS diagnostic criteria. The most common is Okihiro syndrome (MIM#607323), characterised by constant bilateral anterior upper limb defects, possibly associated with abnormality of the ocular motility named Duane anomaly (65% of the cases), morphological renal defects (28%), but also with cardiac (17%) or spinal defects and ear dysplasia or deafness [8, 31]. This autosomal dominant condition is due to variants affecting *SALL4*, which encodes a transcription factor acting synergistically with TBX5 during heart and limb development [32, 33]. HOS can be mistaken with many other overlapping conditions (summarized in Table 3) and clinical assessment of patients should be standardized, as detailed in Fig. 3.

Finally, some patients with typical HOS features had no *TBX5* variant or identified overlapping condition after

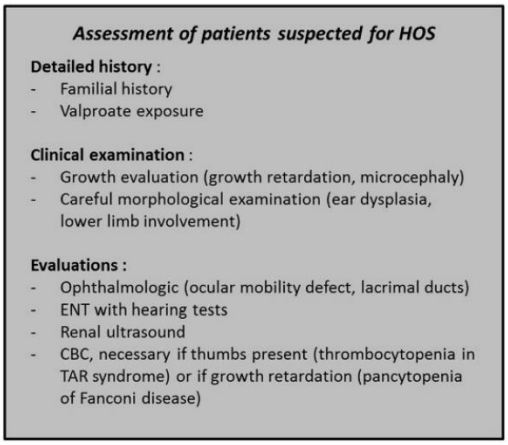

Fig. 3 Assessment of patients suspected for HOS

additional screening by array-CGH and the targeted high-throughput sequencing of 124 genes involved in limb development (data not shown). Previously, Terrett et al. identified 2 families with a typical presentation of HOS that were not linked to the 12q24 locus [34], supporting the hypothesis of a genetic heterogeneity. However, we performed whole exome sequencing in 13 selected typical cases, revealing no candidate gene (data not shown). Recent data showed that regulatory variants may explain a large part of congenital malformations [35]. Three *TBX5* heart-specific enhancers have been described, and one homozygous rare variant in one of these sequences has been reported in a patient presenting with an isolated VSD [36]. A minimal regulatory sequence has been identified in intron 2, where Hox factors bind to activate *Tbx5* expression during mouse upper limb initiation [37]. No variant in this element has been reported so far. Whole genome sequencing will probably help to unravel the variant-negative cases by allowing the exploration of regulatory elements, and the detailed screening of balanced chromosomal rearrangements.

Our study illustrates the inconsistencies and issues of the molecular diagnosis of HOS, by both its clinical (variability of expression, lack of penetrance, numerous overlapping conditions) and molecular aspects (diversity of *TBX5* variants, potential genetic heterogeneity or regulatory variant). The diagnosis of HOS cannot be certainly affirmed or ruled out by strict diagnostic criteria and need to be confirmed by *TBX5* molecular analysis, since the typical presentation of HOS can be sometimes incomplete or associated with other features in patients with *TBX5* variants.

Acknowledgements We greatly thank all the clinicians, the patients and their families for their contribution to this study.

Compliance with ethical standards

Conflict of interest The authors declare that they have no conflict of interest.

References

1. van der Linde D, Konings EEM, Slager MA, et al. Birth prevalence of congenital heart disease worldwide: a systematic review and meta-analysis. J Am Coll Cardiol. 2011;58:2241–7.
2. Holt M, Oram S. Familial heart disease with skeletal malformations. Br Heart J. 1960;22:236–42.
3. Elek C, Vitéz M, Czeizel E. Holt-Oram syndrome. Orv Hetil. 1991;132:73–74. 77–78
4. Smith AT, Sack GH, Taylor GJ. Holt-Oram syndrome. J Pediatr. 1979;95:538–43.
5. Hurst JA, Hall CM, Baraitser M. The Holt-Oram syndrome. J Med Genet. 1991;28:406–10.
6. Newbury-Ecob RA, Leanage R, Raeburn JA, Young ID. Holt-Oram syndrome: a clinical genetic study. J Med Genet. 1996;33:300–7.
7. Basson CT, Cowley GS, Solomon SD, et al. The clinical and genetic spectrum of the Holt-Oram syndrome (heart-hand syndrome). N Engl J Med. 1994;330:885–91.
8. Brassington A-ME, Sung SS, Toydemir RM, et al. Expressivity of Holt-Oram syndrome is not predicted by TBX5 genotype. Am J Hum Genet. 2003;73:74–85.
9. Borozdin W, Bravo Ferrer Acosta AM, Bamshad MJ, et al. Expanding the spectrum of TBX5 mutations in Holt-Oram syndrome: detection of two intragenic deletions by quantitative real time PCR, and report of eight novel point mutations. Hum Mutat. 2006;27:975–6.
10. Barisic I, Boban L, Greenlees R, et al. Holt Oram syndrome: a registry-based study in Europe. Orphanet J Rare Dis. 2014;9:156.
11. Heinritz W, Moschik A, Kujat A, et al. Identification of new mutations in the TBX5 gene in patients with Holt-Oram syndrome. Heart Br Card Soc. 2005;91:383–4.
12. Li QY, Newbury-Ecob RA, Terrett JA, et al. Holt-Oram syndrome is caused by mutations in TBX5, a member of the Brachyury (T) gene family. Nat Genet. 1997;15:21–29.
13. Basson CT, Bachinsky DR, Lin RC, et al. Mutations in human TBX5 [corrected] cause limb and cardiac malformation in Holt-Oram syndrome. Nat Genet. 1997;15:30–35.
14. Naiche LA, Harrelson Z, Kelly RG, Papaioannou VE. T-box genes in vertebrate development. Annu Rev Genet. 2005;39:219–39.
15. Bruneau BG, Logan M, Davis N, et al. Chamber-specific cardiac expression of Tbx5 and heart defects in Holt-Oram syndrome. Dev Biol. 1999;211:100–8.
16. Greulich F, Rudat C, Kispert A. Mechanisms of T-box gene function in the developing heart. Cardiovasc Res. 2011;91:212–22.
17. Hasson P, DeLaurier A, Bennett M, et al. Tbx4 and Tbx5 acting in connective tissue are required for limb muscle and tendon patterning. Dev Cell. 2010;18:148–56.
18. Cross SJ, Ching YH, Li QY, et al. The mutation spectrum in Holt-Oram syndrome. J Med Genet. 2000;37:785–7.
19. McDermott DA, Bressan MC, He J, et al. TBX5 genetic testing validates strict clinical criteria for Holt-Oram syndrome. Pediatr Res. 2005;58:981–6.
20. Debeer P, Race V, Gewillig M, Devriendt K, Frijns J-P. Novel TBX5 mutations in patients with Holt-Oram syndrome. Clin Orthop. 2007;462:20–26.
21. Ellis DG. Chest wall deformities. Pediatr Rev. 1989;11:147–51.

22. Bickley SRB, Logan MPO. Regulatory modulation of the T-box gene Tbx5 links development, evolution, and adaptation of the sternum. Proc Natl Acad Sci USA. 2014;111:17917–22.
23. Weinstein SL, Dolan LA, Cheng JCY, Danielsson A, Morcuende JA. Adolescent idiopathic scoliosis. Lancet Lond Engl. 2008;371: 1527–37.
24. Tseng Y-R, Su Y-N, Lu FL, et al. Holt-Oram syndrome with right lung agenesis caused by a de novo mutation in the TBX5 gene. Am J Med Genet A. 2007;143A:1012–4.
25. Qin X, Wei W, Fangqi G. Horseshoe lung associated with Holt-Oram syndrome. Iran J Pediatr. 2015;25:e251.
26. Böhm J, Heinritz W, Craig A, et al. Functional analysis of the novel TBX5 c.1333delC mutation resulting in an extended TBX5 protein. BMC Med Genet. 2008;9:88.
27. Arora R, Metzger RJ, Papaioannou VE. Multiple roles and interactions of Tbx4 and Tbx5 in development of the respiratory system. PLoS Genet. 2012;8:e1002866.
28. Boogerd CJJ, Dooijes D, Ilgun A, et al. Functional analysis of novel TBX5 T-box mutations associated with Holt-Oram syndrome. Cardiovasc Res. 2010;88:130–9.
29. Barnett P, Postma AV. Molecular genetics of Holt-Oram syndrome. In: John Wiley & Sons Ltd (ed). *eLS*. Wiley, Chichester, 2014. http://doi.wiley.com/10.1002/9780470015902.a0024329. Accessed 31 May 2016.
30. Al-Qattan MM, Abou Al-Shaar H. Molecular basis of the clinical features of Holt-Oram syndrome resulting from missense and extended protein mutations of the TBX5 gene as well as TBX5 intragenic duplications. Gene. 2015;560:129–36.
31. Borozdin W, Wright MJ, Hennekam RCM, et al. Novel mutations in the gene SALL4 provide further evidence for acro-renal-ocular and Okihiro syndromes being allelic entities, and extend the phenotypic spectrum. J Med Genet. 2004;41:e102.
32. Al-Baradie R, Yamada K, St Hilaire C, et al. Duane radial ray syndrome (Okihiro syndrome) maps to 20q13 and results from mutations in SALL4, a new member of the SAL family. Am J Hum Genet. 2002;71:1195–9.
33. Koshiba-Takeuchi K, Takeuchi JK, Arruda EP, et al. Cooperative and antagonistic interactions between Sall4 and Tbx5 pattern the mouse limb and heart. Nat Genet. 2006;38:175–83.
34. Terrett JA, Newbury-Ecob R, Cross GS, et al. Holt-Oram syndrome is a genetically heterogeneous disease with one locus mapping to human chromosome 12q. Nat Genet. 1994;6: 401–4.
35. Spielmann M, Mundlos S. Looking beyond the genes: the role of non-coding variants in human disease. Hum Mol Genet. 2016;25: R157–R165.
36. Smemo S, Campos LC, Moskowitz IP, Krieger JE, Pereira AC, Nobrega MA. Regulatory variation in a TBX5 enhancer leads to isolated congenital heart disease. Hum Mol Genet. 2012;21:3255–63.
37. Minguillon C, Nishimoto S, Wood S, Vendrell E, Gibson-Brown JJ, Logan MPO. Hox genes regulate the onset of Tbx5 expression in the forelimb. Dev Camb Engl. 2012;139:3180–8.
38. Shimamura A, Alter BP. Pathophysiology and management of inherited bone marrow failure syndromes. Blood Rev. 2010;24:101–22.
39. VanderMeer JE, Ahituv N. cis-regulatory mutations are a genetic cause of human limb malformations. Dev Dyn Publ Am Assoc Anat. 2011;240:920–30.
40. Kozma C. Valproic acid embryopathy: report of two siblings with further expansion of the phenotypic abnormalities and a review of the literature. Am J Med Genet. 2001;98:168–75.
41. Mohd Yunos H, Green A. Fetal valproate syndrome: the Irish experience. Ir J Med Sci. 2018;187:965–8
42. Carli D, Garagnani L, Lando M, et al. VACTERL (vertebral defects, anal atresia, tracheoesophageal fistula with esophageal atresia, cardiac defects, renal and limb anomalies) association: disease spectrum in 25 patients ascertained for their upper limb involvement. J Pediatr. 2014;164:458–462.
43. Kohlhase J, Taschner PE, Burfeind P, et al. Molecular analysis of SALL1 mutations in Townes-Brocks syndrome. Am J Hum Genet. 1999;64:435–45.
44. Hall JG. Thrombocytopenia and absent radius (TAR) syndrome. J Med Genet. 1987;24:79–83.
45. Albers CA, Paul DS, Schulze H, et al. Compound inheritance of a low-frequency regulatory SNP and a rare null mutation in exon-junction complex subunit RBM8A causes TAR syndrome. Nat Genet. 2012;44:435–9, S1–2.
46. Petit F, Escande F, Jourdain AS, et al. Nager syndrome: confirmation of SF3B4 haploinsufficiency as the major cause. Clin Genet. 2014;86:246–51.
47. Wiedemann HR, Drescher J. LADD syndrome: report of new cases and review of the clinical spectrum. Eur J Pediatr. 1986;144:579–82.
48. Rohmann E, Brunner HG, Kayserili H, et al. Mutations in different components of FGF signaling in LADD syndrome. Nat Genet. 2006;38:414–7.
49. Vega H, Waisfisz Q, Gordillo M, et al. Roberts syndrome is caused by mutations in ESCO2, a human homolog of yeast ECO1 that is essential for the establishment of sister chromatid cohesion. Nat Genet. 2005;37:468–70.
50. Vega H, Trainer AH, Gordillo M, et al. Phenotypic variability in 49 cases of ESCO2 mutations, including novel missense and codon deletion in the acetyltransferase domain, correlates with ESCO2 expression and establishes the clinical criteria for Roberts syndrome. J Med Genet. 2010;47:30–37.

SUPPLEMENTARY DATA

Supp 1 – Missense variants reported in our series.

Supp 2 – Differential diagnoses observed in our series. AD: autosomal dominant; ASD: atrial spetal defect; VSD: ventricular septal defect; TAR syndrome: Thrombocytopenia-absent radius syndrome; LADD syndrome: Lacrimo-auriculo-dento-digital syndrome

Supp 3– Statistical comparison of the clinical features according to the presence or absence of *TBX5* variant, according to the 3 phenotypic groups: typical with heart defect, typical without heart defect, uncertain.

Supp 1 – Missense variants reported in our series.

Patients	Phenotype	Familial (F) or sporadic (S)	*TBX5* variant	Inheritance	Localisation	Prediction softwares: SIFT (0), Polyphen (1)	Prediction on proteic structure	Functional tests	Conclusion
50	Bilateral anterior upper limb involvment, ASD	S	c.253C>T;p.(Pro85Ser)	*de novo*	T-box	deleterious (0), probably damaging (1), conserved nucleotide, significant physicochemical gap	Modified	-	Likely pathogenic
192	Bilateral anterior upper limb involvment, ASD, hypoplasia of left ventricule	S	c.254C>T;p.(Pro85Leu)	-	T-box	deleterious (0), probably damaging (1), conserved nucleotide, significant physicochemical gap	Not modified	-	Uncertain significance
193	Bilateral anterior upper limb involvment, dextrocardia	S	c.520A>G;p.(Asn174Asp)	-	T-box	deleterious (0), probably damaging (1), conserved nucleotide, minor physicochemical gap	Not modified	-	Uncertain significance
158	Bilateral anterior upper limb involvment, ASD, VSD	F	c.668C>T;p.(Thr223Met)	-	T-box	deleterious (0), probably damaging (1), conserved nucleotide, significant physicochemical gap	Not modified	-	Uncertain significance
130	Bilateral phocomelia, ASD, VSD	S	c.677A>G;p.(Lys226Arg)	*de novo*	T-box	deleterious (0), probably damaging (1), moderately conserved nucleotide, minor physicochemical gap	Not modified	-	Likely pathogenic
107	Bilateral anterior upper limb involvment, VSD, aortic coarctation	S	c.694T>G;p.(Phe232Val)	-	T-box	deleterious (0), probably damaging (1), conserved nucleotide, minor physicochemical gap	Modified	-	Uncertain significance
231	Bilateral anterior upper limb involvment, without cardiac defect	F	c.710G>A;p.(Arg237Gln)	-	T-box	deleterious (0), probably damaging (1), conserved nucleotide, minor physicochemical gap	Modified	Published	Pathogenic
171	Bilateral anterior upper limb involvment, without cardiac defect	F	c.710 G>A;p.(Arg237Gln)	-	T-box	deleterious (0), probably damaging (1), conserved nucleotide, minor physicochemical gap	Modified	Published	Pathogenic
114	Bilateral anterior upper limb involvment, ASD	F	c.709C>T;p.(Arg237Trp)	-	T-box	deleterious (0), probably damaging (1), moderately conserved nucleotide, significant physicochemical gap	Modified	Published	Pathogenic
229	Bilateral anterior upper limb involvment, ASD, VSD, aortic coarctation	S	c.709C>T;p.(Arg237Trp)	-	T-box	deleterious (0), probably damaging (1), moderately conserved nucleotide, significant physicochemical gap	Modified	Published	Pathogenic
145	Bilateral anterior upper limb involvment, ASD	S	c.709C>T;p.(Arg237Trp)	-	T-box	deleterious (0), probably damaging (1), moderately conserved nucleotide, significant physicochemical gap	Modified	Published	Pathogenic

Supp 2 – Differential diagnoses observed in our series. AD: autosomal dominant; ASD: atrial spetal defect; VSD: ventricular septal defect; TAR syndrome: Thrombocytopenia-absent radius syndrome; LADD syndrome: Lacrimo-auriculo-dento-digital syndrome

Case#	Pedigree	Cardiac defects	Limb malformations	Other clinical features	Molecular anomaly	Final diagnosis
24	Sporadic	Aortic incompetence	Thumbs agenesis, hypoplastic 2nd fingers, left radius aplasia	-	*SALL4* ; c.1411del (p.(Ser471Leufs*2))	Okihiro syndrome
120	Familial AD	-	Thumbs agenesis, hypoplastic radii	-	*SALL4* ; c.1412_1415delCTTT (p.(Ser471*))	Okihiro syndrome
147	Familial AD	-	Thumbs hypoplasia, right syndactyly of digits 1-2	Pelvic kidney	*SALL4* ; c.1410_1411delTT (p.(Ser471Phefs*23))	Okihiro syndrome
150	Sporadic	-	Thumbs agenesis	Strabismus, ears dysplasia	*SALL4* ; c.2491C>T (p.(Arg831*))	Okihiro syndrome
155	Sporadic	-	Thumbs agenesis, hypoplastic radii	Ears dysplasia, abnormal ribs	*SALL4* ; c.620delG (p.(Gly207Valfs*33))	Okihiro syndrome
156	Familial AD	-	Radii and thumbs agenesis, syndactyly of digits 2-3	-	*SALL4* ; c.1514delG (p.(Gly505Valfs*45))	Okihiro syndrome
216	Familial AD	ASD	Radii hypoplasia, triphalangeal thumbs, syndactyly of digits 1-2	-	*SALL4* ; c.1230dupC (p.(Val411Argfs*53))	Okihiro syndrome
245	Familial AD	-	Right thumb agenesis, left thumb hypoplasia	-	*SALL4* ; c.2484delG p.(Phe829Leufs*27)	Okihiro syndrome
56	Sporadic	-	Thumbs and radii agenesis	-	-	Valproate embryofoetopathy
100	Sporadic	-	Thumbs hypoplasia, right preaxial polydactyly	Hypospadias, tracheomalacia	-	Valproate embryofoetopathy
104	Sporadic	ASD	Left thumb hypoplasia, triphalangeal right thumb	-	-	Valproate embryofoetopathy
215	Sporadic	ASD	Right thumb agenesis	Laryngomalacia	-	Valproate embryofoetopathy
3	Sporadic	ASD	Hypoplastic thumbs, left radius hypoplasia	Growth retardation, microcephaly	Increased chromosome breakage on karyotype with mitomycin C	Fanconi pancytopenia
84	Sporadic	ASD	Thumbs and radii agenesis	Left kidney agenesis, intrauterine growth retardation	Increased chromosome breakage on karyotype with mitomycin C	Fanconi pancytopenia
121	Sporadic	Left superior vena cava	Right thumb agenesis, left thumb hypoplasia	-	Increased chromosome breakage on karyotype with mitomycin C	Fanconi pancytopenia
152	Sporadic	-	Radii agenesis, preserved thumbs	-	Compound heterozygous *RBM8A* variants	TAR syndrome
209	Sporadic	-	Radii agenesis, preserved thumbs	Thrombocytopenia	Del 1q21.1, no *RBM8A* variant	TAR syndrome
196	Familial AD	ASD	Bilateral preaxial polydactyly	-	*LMBR1* , c.423+4859T>C (ZRS)	Preaxial polydactyly type 2
227	Sporadic	VSD	First metacarpals agenesis, triphalangeal left thumb	Intrauterine growth retardation, partial sacral agenesis	-	VACTERL association
71	Sporadic	ASD	Triphalangeal thumbs	-	*FGF10* ; c.577C>T (p.(Ala193*))	LADD syndrome
222	Sporadic	ASD	Radii hypoplasia, left thumb agenesis, triphalangeal left thumb	Hypoplastic nipples, hypohidrosis, hypotrichosis	Deletion involving *TBX5* and *TBX3*	Microdeletion

Supp 3– Statistical comparison of the clinical features according to the presence or absence of *TBX5* variant, according to the 3 phenotypic groups: typical with heart defect, typical without heart defect, uncertain.

	TYPICAL WITH HEART DEFECT			TYPICAL WITHOUT HEART DEFECT			UNCERTAIN		
	WITH TBX5 VARIANT	WITHOUT TBX5 VARIANT	STAT	WITH TBX5 VARIANT	WITHOUT TBX5 VARIANT	STAT	WITH TBX5 VARIANT	WITHOUT TBX5 VARIANT	STAT
Familial history	**21/56**	**5/19**	**p=0.376**	**5/6**	**1/12**	**p=0.008**	**5/17**	**10/82**	**p=0.153**
SKELETAL DEFECT									
- Bilateral	56/56	19/19	-	6/6	12/12	-	13/17	35/82	**p=0.01**
- Left/Right asymetry	20/21	5/6	**p=0.922**	3/3	1/5	**p=0.144**	8/10	25/61	**p=0.051**
- Limitation of elbow and shoulder mobility and/or muscular hypoplasia	27/56	4/19	**p=0.037**	4/6	2/12	**p=0.112**	4/17	14/82	**p=0.77**
HEART DEFECT									
Congenital heart malformation									
- Isolated septal defect	25/56	6/19	**p=0.317**	-	-	-	14/17	32/82	**p=0.001**
- non septal defect	-	3/19	**p=0.018**	-	-	-	-	12/82	**p=0.2**
Isolated valvular anomaly	2/56	2/19	**p=0.565**	-	-	-	-	3/82	**p=0.981**
Conduction disturbances									
- Isolated	2/56	1/19	**p=0.725**	-	-	-	1/17	2/82	**p=0.981**
- associated with a heart malformation	15/56	-	**p=0.028**	-	-	-	3/17	4/82	**p=0.177**

Ce travail a permis de préciser le phénotype associé aux variants de *TBX5*, avec notamment l'absence de bifidité/duplication des pouces, contrairement à certains diagnostics différentiels proches (syndrome d'Okihiro, syndrome de Townes-Brocks).

A l'issue de ce premier travail, plusieurs variants faux-sens et variants d'épissage restaient de signification incertaine.

b. Caractérisation moléculaire de variants du gène *TBX5*

Prédire les effets des variants génomiques est devenu un véritable défi dans le diagnostic des maladies rares. La majorité des variants de *TBX5* responsables du syndrome de Holt-Oram sont tronquants et responsables d'une haploinsuffisance. La pathogénicité des variants faux-sens ou d'épissage est plus difficile à démontrer.

Dans ce troisième article, 14 variants de signification incertaine (5 faux-sens, 9 variants d'épissage) et 6 variants faux-sens probablement pathogènes de *TBX5* ont été sélectionnés. Au vu de sa fonction de facteur de transcription, nous avons étudié, pour les variants faux-sens, la localisation cellulaire par immunohistochimie, la quantification protéique par Western Blot et l'activation transcriptionnelle par test rapporteur à la luciférase. Pour les variants suspects d'altérer l'épissage, nous avons réalisé des tests minigènes. Les résultats de ces tests fonctionnels ont été comparés aux prédictions *in silico*.

Nous montrons ici la complémentarité des approches bio-informatiques et biologiques, associées à une bonne connaissance de la pathologie, pour la classification ACMG des variants de *TBX5*.

Functional characterization vs *in silico* prediction for *TBX5* missense and splice variants in Holt-Oram syndrome

Clémence VANLERBERGHE[1,2], Anne Sophie JOURDAIN[2,3], Frédéric FRENOIS[2], Emilie AIT-YAHYA[2,4], Mike BAMSHAD[5], Anne DIEUX[1,2], William DUFOUR[1,2], Fiona LEDUC[1,2], Sylvie MANOUVRIER-HANU[1,2], Karynne PATTERSON[6], Jamal GHOUMID[1,2], Fabienne ESCANDE[2,7], Thomas SMOL[2,3], Perrine BRUNELLE[2,3], Florence PETIT[1,2]

[1] CHU Lille, Centre de Référence des Anomalies du Développement, F-59000 Lille, France

[2] Univ. Lille, CHU Lille, ULR 7364 - RADEME - Maladies RAres du DÉveloppement embryonnaire et du Métabolisme, F-59000 Lille, France

[3] CHU Lille, Institut de génétique médicale, F-59000 Lille, France

[4] CHU Lille, cellule bioinformatique, plateau commun de séquençage, F-59000 Lille, France

[5] Department of Pediatrics, University of Washington Center for Mendelian Genomics, USA

[6] Department of Genome Sciences, University of Washington Center for Mendelian, USA Genomics

[7] CHU Lille, UF Oncologie moléculaire, F-59000 Lille, France

ABSTRACT

Purpose: Predicting effects of genomic variants has become a real challenge in the diagnosis of rare human diseases. Holt-Oram syndrome (HOS) is an autosomal condition characterized by the association of radial and heart defects, due to variants in *TBX5*. Most variants are predicted to be truncating and result in haploinsufficiency. The pathogenicity of missense or splice variants is harder to demonstrate. **Methods:** Fourteen *TBX5* variants of uncertain significance (VUS) (5 missense, 9 splice) and 6 likely pathogenic missense variants were selected for functional testing, depending on the variant-type (immunolocalization, western blot, reporter assays, minigene splice assays and RT-PCR). Results were compared with *in silico* predictions. **Results:** Functional tests allowed to reclassify 9/14 VUS in *TBX5* as likely pathogenic, confirming their role in HOS. We demonstrated loss-of-function (n=8) or gain-of-function (n=1) for 9 of the 11 missense variants, whereas no functional impact was shown for the 2 variants: p.(Gly195Ala) and p.(Ser261Cys), as suggested by contradictory predictions of *in silico* approaches. Of 9 splice variants predicted to affect splicing by SpliceAI, we observed partial or complete exon skipping (n=6), intron retention (n=2) or exon shortening (n=1), inducing frame-shifting with premature stop codons. **Conclusion:** Bioinformatic and biological approaches are complementary, together with a good knowledge of clinical conditions, for accurate ACMG classification in human rare diseases.

KEY-WORDS : Holt-Oram syndrome, *TBX5*, minigene, variant of uncertain significance, variant classification

INTRODUCTION

In human genetics, predicting effects of variants of uncertain significance (VUS) has become crucial to increase the diagnostic rate of rare diseases, as shown by the huge interest in deep learning prediction tools development. Thus, functional characterization of VUS, tailored to the specific protein type (e.g. enzyme, channel, transcription factor), is essential for confirming the impact of these variants on protein function.

Holt-Oram syndrome (HOS, MIM#142900) is a rare autosomal dominant condition characterized by the combination of radial defects (from thumb hypoplasia to phocomelia) and, in 90% of patients, heart defects (congenital heart malformation and/or conduction abnormalities). Its prevalence has been estimated at 1 in 100,000 births[1]. A high penetrance and a wide variability of expression have been described.[2] HOS is due to alterations in the *TBX5* gene (MIM*601620, HGNC:11604), encoding a transcription factor belonging to the T-box family.[3]

T-box transcription factors play crucial roles during development and share a highly homologous DNA-binding domain that is highly conserved among species.[4] During limb development, Tbx5 triggers *Fgf10* (HGNC:3666) expression in the limb mesenchyme and establishes the epithelial-mesenchymal feedback loop between Fgf10 and Fgf8 (HGNC:3686), which is then self-maintaining.[5] During cardiac development, *NPPA* (HGNC:7939) and *GJA5* (HGNC:4279) genes, respectively encoding the atrial natriuretic factor (ANF)[6] and the connexin 40 (Cx40)[7], are direct TBX5-target genes.

Around 300 HOS patients have been reported in the literature, and a molecular genetic diagnosis has been made in around 150 of these cases. [8–11] Variants in *TBX5* coding sequence are found in 70% of patients with typical HOS phenotypes.[11] Most of the reported variants result in a premature stop codon due to either nonsense or frameshift variants, leading to loss-of-function through the synthesis of a truncated protein, or haploinsufficiency through the nonsense-mediated mRNA decay. However, other types of variants have been observed: missense variants, splice variants, intragenic deletion or duplication, extended protein.[12]

Specific functional tests have been developed to characterize *TBX5* missense variants, mostly located in the DNA-binding domain. This includes TBX5 nuclear localization by immunohistochemistry, DNA-binding by Electrophoretic Mobility Shift Assays, TBX5 interactions with its cofactors (NKX2.5, GATA4 - HGNC:2488 and 4173) by pull-down assays, or transcriptional activation of target genes (*NPPA, FGF10, GJA5*) by reporter assays [13,14]. Two 3D structures of the TBX5 protein have been determined by radiocrystallography: isolated TBX5 (PDB:2X6U) and TBX5 linked to a DNA segment (PDB:2X6V), allowing mutated protein structure predictions[15].

In silico metapredictors have been developed to help adjudicate VUS interpretation. They were first based on evolutionary conservation, functional annotations (domains, protein interactions, active sites) and physicochemical differences between amino acids. More recently, they include the prediction of secondary protein structure.[16]

In 2015, the American College of Medical Genetics and Genomics (ACMG) and the Association for Molecular Pathology (AMP) published a joint guideline that provides a framework for Sequence Variant Interpretation, combining several criteria to assess the predicted pathogenicity of

sequence variants. Both PS3/BS3 criteria for functional test results and PP3/BP4 criteria for *in silico* metapredictors data impact on the clinical interpretation of genetic variants.[17,18]

In HOS, the molecular confirmation of the diagnosis is important for patient management, especially since conduction disturbances can occur late in life and early detection could avoid complications. Furthermore, given that some HOS features could be detected prenatally, and that they could overlap many syndromic genetic conditions with more severe outcomes (Fanconi anemia for example), there is a need to improve VUS interpretation after prenatal Exome/Genome sequencing in order to clarify the diagnosis and its consequences[11].

Here we performed functional tests on 11 selected missense and 9 splice VUS of *TBX5* and compared our results to the results of *in silico* metapredictors. Our results provide guidance on the interpretation of VUS in *TBX5* and their relationship to HOS.

MATERIALS AND METHODS

TBX5 variants selection

We used HGMD professional database (December 2022) to select previously reported *TBX5* missense and splice variants identified in simplex and familial cases.[19] We selected exonic or intronic splice variants located outside canonical sites, and we excluded *de novo* or previously functionally characterized variants. We identified 28 *TBX5* missense variants (Supp Data 1) and 23 variants possibly affecting splicing. We selected 8 missense variants with no previously published functional tests and 5 splice variants located outside canonical splice sites (-1, -2, +1, +2).[8,9,11,20–25] Previous reports of variants were published between 1999 and 2021. We added 3

missense variants from our previously published series.[11] We used our local database to identify additional missense and splice variants that had not been previously characterized. We added 4 variants identified in our laboratory in the molecular biology department of Lille university hospital (France). Three splice variants were identified by targeted high-throughput sequencing of a limb gene panel. One deep intronic variant was identified in a familial HOS by genome sequencing (aligned on reference genome hg38), performed in collaboration with the University of Washington Center for Mendelian Genomics (UW-CMG) (USA), since previous sequencing of the *TBX5* coding region failed to identify any variants (pedigree and phenotypes detailed in Supp Data 2). We reported the 4 unpublished variants in ClinVar Database (from SCV004035065 to SCV004035068).

The MANE select transcript ID for *TBX5* is NM_181486.4, however, we have used NM_000192.3 in this manuscript since we have assessed variants previously reported using the latter. Of note, the nomenclature is identical using either of these transcript references.

Informed consent statement

Written informed consents for research use were obtained from the patients or their parents prior to the *TBX5* molecular analysis. The research protocol was reviewed and accepted by the Institutional Review Board and Data Protection Manager of Lille University Hospital (DEC19-366).

In silico analysis

The assessment of *TBX5* variants was conducted using MobiDetails,[26] a bioinformatic tool for querying multiple databases and prediction software (lastly assessed September 2023), CADD,

REVEL and AlphaMissense[16] databases. Databases references are detailed in Supp Data 3. Variants were also evaluated with EVE, an unsupervised deep learning algorithm based on the sequences of 140K species across evolution, ranging from the most pathogenic (score=1), to the most benign (score=0). Additionally, VARITY_ER, a specialized tool for predicting extremely rare missense variants, was employed.

Structure predictions of the missense *TBX5* variants were conducted using the Phyre2 server (Protein Homology/analogy Recognition Engine V2.0), with the deduced amino acid sequence of each protein as the input. The predicted 3D structure of TBX5 proteins was compared with the 3D resolved structure of the human TBX5 native protein (PDB code: 2X6U) (99% identity sequence between native TBX5 protein and the mutated proteins) using the molecular visualization system, PyMOL (The PyMOL Molecular Graphics System, Version 3.0 Schrödinger, LLC).
Additionally, AlphaFold v2.1.0 protein folding algorithms, with a restrained energy minimization procedure (OpenMM molecular mechanics simulation package), were employed to construct a 3D computer model of the native and missense variants of the TBX5 protein[27]. The sequences were directly run as per the directions on the Colab notebook.

The Missense 3D database was also used to ascertain the likelihood of a missense variant having a damaging effect on the stability of the folded protein, based on both experimentally determined structures and homology-predicted models.

To compare the sequences of several T-box proteins (TBX1, TBX2, TBX3, TBX4, TBX6, TBX15 and TBX22; HGNC:11592, 11597, 11602, 11603, 11605, 11594, 11600), we used Clustal Omega program from EMBL's European Bioinformatics Institute.

The following algorithms were used to assess the strength of canonical and potential novel/cryptic splicing sites and predict the impact of potential splice variants: MaxEntScan, SPiP, SpliceAI [28] and SpliceAI visual.

We referred to the gnomAD v3 database to assess the frequency of the variant in the general population. We consulted the ClinVar, DECIPHER and LOVD databases to assess the description of selected variants reported by other molecular biology laboratories.

Characterization of missense variants

a. *TBX5* plasmid constructs

Wild type and mutant *TBX5*-expressing plasmids pRP[Exp]–CMV>3xFLAG/hTBX5[NM_000192.3] were constructed and packaged by Vectorbuilder. The mutant plasmids used as positive controls, carrying variant c.710G>C p.(Arg237Pro) or c.835C>T p.(Arg279*), were obtained through mutagenesis with Q5 site-directed mutagenesis technology (NEB) according to the manufacturer's instructions. Both variants have been previously reported in HOS patients and functionally characterized [14,29]. The vectors and primers are detailed in Supp Data 4. All plasmids were isolated using the Nucleobond Xtra Maxi Plus EF for plasmid DNA (Macherey-Nagel) and subjected to Sanger sequencing for verification purposes.

b. Cell culture and transfection

HEK293T cells (ATCC, CRL-1573) were subcultured in DMEM supplemented with 10% fetal bovine serum, 1% L-glutamine, and 0.5% antibiotics (penicillin/streptomycin) using standard procedures. For Western Blot and Immunofluorescence analyses, 5×10^5 cells were seeded on 6-well plates

24h prior to transfection. Cells were transfected with 2µg of plasmid DNA using Lipofectamine 2000 (Invitrogen) according to the manufacturer's instructions.

c. Western Blot

48h after transfection, HEK293T cells were lysed for total protein extract with RIPA Lysis and Extraction Buffer (Thermo Fisher Scientific) complemented with protease inhibitor. The protein concentration was determined using a BCA Protein Assay Kit (Thermo Fisher Scientific), and 10µg were electrophoresed in NuPAGE 4% to 12% Bis-Tris Protein Gels (Invitrogen), then transferred to nitrocellulose membrane with iBlot 2 Gel Transfer Device (Invitrogen). The membranes were blocked with a 5% milk solution, and primary antibody incubations were performed overnight at 4◦C (β-Tubulin, 1:200, AB-233-6 (8B2), Diagomics; anti-FLAG, 1:5000, F1804 (M2), Sigma). Secondary antibody horseradish peroxidase–conjugated anti-rabbit mouse (1:1000, Santa Cruz Biotechnologies sc-2357) was incubated for 1h and detected with SuperSignal West Dura (Thermo Fisher Scientific). The protein bands were visualized using the iBright CL1500 Imaging System (Thermo Fisher Scientific). Western blots were performed 3 times, with 3 independent transfections and 3 independent plasmid preparations. Quantification and statistical analysis using the One-way ANOVA with uncorrected Fisher's least significant difference were performed using ImageJ and Prism software. A significance threshold (p-value) of 0.05 was used.

d. Immunofluorescence

HEK293T transfected cells were fixed for 40min in phosphate-buffered saline (PBS)–4% paraformaldehyde, washed 3 times in ice-cold PBS, permeabilized in PBS–0.1% Triton for 20min, blocked with PBS–4% bovine serum albumin–Tween 0.05% for 1h and incubated with mouse

primary antibody at 4◦C overnight (monoclonal anti-FLAG antibody, 1:500, F1804 (M2), Sigma). After washing, the cells were incubated with a secondary antibody for 1h (Mouse Alexa 488, 1:1000, Thermo Fisher Scientific A-11094). Following counterstaining with 3µL of Vectashield antifade mounting media with DAPI (1.5 µg/ml, Vector Laboratories), cells were visualized using confocal microscopy (Zeiss LSM170 Airyscan). The immunofluorescence experiments were performed 3 times, with 3 independent transfections and 3 independent plasmid preparations. Cellular localization was determined for each cell on at least 4 fields (on average 36 cells per variant) and proportions of nuclear versus cytoplasmic localization were compared for each variant to the WT using a One-way ANOVA with uncorrected Fisher's least significant difference calculated with Prism software. A significance threshold (p-value) of 0.05 was used.

e. Luciferase assays

To assess the transactivation capacity of TBX5 proteins, we used the pGl3-Nppa construct in which the *Nppa* promoter drives the firefly luciferase reporter gene, kindly provided by A. Postma. HEK293T cells were seeded on 24-well plates 24h prior to transfection. The cells were transfected with 400ng of *TBX5*-expressing plasmid and 400ng of the pGl3-Nppa using Lipofectamine 2000 (Invitrogen) according to the manufacturer's instructions. The Renilla-expressing pRL-SV40 Vector (Addgene, E2231) was co-transfected at a 1/100 ratio.

The cells were harvested 48h after transfection. The Firefly and Renilla activities were quantified using the Dual-Luciferase® Reporter Assay System (Promega®) and the Glomax Navigator (Promega®) luminometer, following the manufacturers' recommendations.

The Firefly luciferase activity was normalized to the Renilla luciferase activity. The difference between each normalized mean value of "F/R" and the wild-type condition was analyzed using a one-way ANOVA with uncorrected Fisher's least significant difference using Prism software. A significance threshold (p-value) of 0.05 was used.

Characterization of splice variants

Primers for cloning and site-directed mutagenesis of *TBX5* splice variants are detailed in Supp Data 5.

Since *TBX5* is not expressed in blood, the impact of variants on splicing was assessed *in vitro* by a multi-exonic minigene assay using the previously described vector pCAS2 (methods detailed in Supp Data 6)[30].

In vivo transcript analysis was conducted for one fetal case (F12-III2) carrying a deep intronic variant. RNA was extracted from fetal lung tissue in individual F12-III2 and a sex- and gestational age-matched control fetus, using the Trizol™ reagent (Thermo Fisher Scientific) according to the manufacturer's recommendations. Reverse transcription was performed on 1µg of RNA using the SuperScript™ III Reverse Transcriptase (Thermo Fisher Scientific) with random hexamers. A forward primer was designed to overlap the exon 4-exon 5 junction, and a reverse primer was placed in the predicted pseudo-exon in intron 6 (C7) (Supp Data 7). cDNA was amplified with the High-Fidelity AccuPrime DNA polymerase (Invitrogen), following 35 cycles, annealing temperature 58°C. PCR products were run on a 2% agarose gel.

Nomenclature and ACMG classification

The molecular classification of the variants investigated was performed following the ACMG Guidelines.[17] ACMG criteria are outlined in Supp Data 8. In accordance with the results of functional assays for missense variants, the PS3_supporting criterion was employed when *in vitro* functional studies provided pathogenic evidence, given that the assays included both normal and positive controls and technical replicates. Conversely, the BS3_supporting criterion was utilized when *in vitro* functional studies did not support any pathogenic evidence.[31] For splicing variants, the specific recommendations of the ClinGen group were applied to support pathogenic evidence according to the minigene assays results.[32] As recommended, PS3 criterion was not used for splice variants, but instead the PVS1 decision tree was employed in order to determine code strength (strong, moderate or N/A).

RESULTS

The clinical and molecular data are presented in Table 1 for missense variants and in Table 2 for splice variants.

Associated phenotypes were typical for HOS, with or without cardiac defects, with the exception of 2 sporadic cases that carried the p.(Gly195Ala) and p.(Gly238Ala) variants respectively, and one family that carried the p.(Ser261Cys) variant. In the latter cases, atypical features or skeletal involvement were observed (Table 1).

The *TBX5* variants selected are presented in Figure 1: 10/11 missense variants and 7/9 splice variants were located in the DNA-binding domain, and 3 of them were in the nuclear localization signal (p.(Arg81Trp), p.(Pro85Leu), p.(Val89Glu)).

In silico analysis of missense variants

According to the metapredictors, 9/11 missense variants were predicted to be damaging. The p.(Gly195Ala) and p.(Ser261Cys) variants yielded contradictory predictions, potentially due to the lack of conservation of these residues among the T-box family, as evidenced by the weak EVE prediction score(Supp data 9).

Furthermore, *in silico* predictions for previously characterized *TBX5* missense variants were evaluated (Supp data 10). Among the 17 variants investigated, one variant, c.145C>A p.(Gln49Lys), was identified as having a discrepancy between the *in silico* predictions and the functional test results. This variant is located outside the T-box domain, at the last position of exon 2, and may potentially impact splicing, despite SpliceAI indicating no splice defect. The variant c.755G>T p.(Ser252Ile), which is located at the last position of exon 7, is predicted to affect splicing (SpliceAI, Donor Loss score 0.93).We performed a minigene assay for another *TBX5* variant located at the same position c.755G>C.

We compared *in silico* tools for protein structure prediction (Supp data 11). The topology (orientation of helices and beta sheets) is conserved between the native TBX5 protein and the 3D predicted models as illustrated in Supp Data 11. To ascertain whether the native and the mutated TBX5 proteins exhibit structural homology, an alignment was conducted with PyMOL to measure

the root-mean-square-deviation (*RMSD), corresponding to the average distance between the alpha carbon atoms (the backbone atoms) of superimposed proteins. The number of RMSD cut-off cycles required for alignment with Phyre2 varies depending on the variant, with 2 to 5 cycles typically sufficient. The value of the 5 RMSD cut-off for the native and mutated proteins are indicated in the table in Supp Data 11C. The p.(Pro85Thr) and p.(Arg237Pro) variants, which have previously been characterized as missense positive controls, exhibit a slightly higher RMSD value than the other variants. The results obtained with Phyre2 and AlphaFold did not indicate major structural damage for our variants. The Missense 3D prediction indicated slight structural damage for several variants: p.(Met74Val), p.(Pro85Leu), p.(Val89Glu), p.(Trp121Gly), p.(Gly195Ala) and p.(Lys226Asn). Nevertheless, it is noteworthy that some residues involved in this study have been previously described as crucial for DNA binding, including Arg81, Lys226 and Phe232.[15] Furthermore Met74, Arg81, Pro85, Val89, Trp121, Asn174, and Lys226 are highly conserved amino acids and their replacement could potentially impact the protein's stability.

None of the selected variants were reported in controls in gnomAD v3. In the ClinVar database, the p.(Ser261Cys) variant has been reported 4 times as a VUS (ID518540). Besides, variants affecting the same residue but with a different amino acid change have been designated as “likely pathogenic” and “pathogenic”: p.(Lys226Glu) (ID430377) and p.(Phe232Leu) (ID2573991). No clinical details were available for the p.(Lys226Glu) variant whereas a HOS phenotype was described without details for p.(Phe232Leu), in an autosomal dominant pattern in three generations, affecting the 10 family members investigated. The p.(Pro85Thr) (ID626359), p.(Pro85Ser) and p.(Lys226Arg) variants have been previously published as occurring *de novo*.[11,33] The p.(Gly238Ser) variant (ID636673) has been reported as of uncertain significance.

In silico analysis of splice variants

The predictions of SpliceAI and SPiP regarding the splice effects for all variants are consistent, with the exception of one variant: c.664-342G>T. For this deep intronic variant, SpliceAI predicts the creation of a new splice donor site in intron 6 and the recruitment of a new acceptor site 95bp upstream of the donor site, whereas SPiP does not predict any impact. Besides, for the 2 missense variants located at the second-to-last base of exons 3 (c.241A>T) and 4 (c.361T>G), SpliceAI predicts no impact on splicing whereas SPiP predicts an impact for c.241A>T. The visual representations of SpliceAI are provided in Supp data 12.

Among the selected splice variants, c.755G>C has been documented in the ClinVar database (ID 265264), though the accompanying clinical details are lacking. Variants affecting the same nucleotide have also been reported at position c.755G>A (ID213819) and c.755G>T (ID411099). Interestingly, the latter has been published several times and functional tests demonstrated a loss-of-function.[13,34,35]

Functional characterization of missense variants

Immunofluorescence on HEK293T transfected cells shows a preferential cytoplasmic localization of TBX5 protein for 4 variants studied, p.(Arg81Trp), p.(Pro85Leu), p.(Val89Glu) and p.(Lys226Asn) compared to the wild-type condition, suggesting an alteration of the nuclear localization signal for p.(Arg81Trp), p.(Pro85Leu), p.(Val89Glu) and an alteration of nuclear distribution for p.(Lys226Asn)(Figure 2A,B).

Luciferase assays revealed that variants p.(Met74Val), p.(Arg81Trp), p.(Pro85Leu), p.(Trp121Gly), p.(Lys226Asn) and p.(Phe232Val) induce a decrease in the transcriptional activation of TBX5-target gene, leading to a loss-of-function. In contrast, the p.(Gly238Ala) variant exhibited an increase in TBX5 transactivation activity, suggesting a gain-of-function mechanism (Figure 2E). We confirm that the previously described variant p.(Arg237Pro) causes a decrease in the transcriptional activation of *TBX5*-target gene, whereas the p.(Arg279*) variant retains a strong DNA-binding activity, consistent with its location downstream of the T-box domain. It is noteworthy that the background activity observed for the "non-transfected" condition (i.e. cells transfected with the reporter plasmid containing the *Nppa* promoter, but without the *TBX5*-expressing plasmid) is likely attributable to the activation of the *Nppa* promoter by endogenous transcription factors present in the cell line.

Immunoblots of HEK293T transfected cells revealed a reduction in TBX5 protein expression only for the p.(Asn174Asp) variant, and an increased protein expression for the p.(Pro85Leu) variant ($p<0.005$). However, it should be noted that some of the standard deviations were large (Figure 2C,D). The previously described p.(Arg279*) variant was confirmed to cause the synthesis of a truncated protein *in vitro*, as there was no activation of the nonsense-mediated mRNA decay given the absence of introns in the plasmid construct. We also confirm that the missense positive control p.(Arg237Pro) has no impact on the protein expression level.

Overall, the p.(Met74Val), p.(Arg81Trp), p.(Pro85Leu), p.(Val89Glu), p.(Trp121Gly), p.(Asn174Asp), p.(Lys226Asn) and p.(Phe232Val) variants appear to result in a loss-of-function, as observed in the positive control variants p.(Arg279*) and p.(Arg237Pro), and p.(Gly238Ala) in a

gain-of-function. *In vitro* functional assays did not yield any notable consequences for p.(Gly195Ala) and p.(Ser261Cys).

Functional characterization of splice variants

Minigene assays confirmed a splice defect for 6/9 variants (Table 2, Figure 3): c.664-342G>T, c.353A>G, c.362G>T, c.510+5G>T, c.755G>C, c.756-3C>G. The identified mechanisms include exon skipping resulting from the loss of canonical donor or acceptor sites (c.362G>T, c.510+5G>T, c.756-3C>G), intron retention (c.755G>C), and exon shortening through the creation of new cryptic intronic or exonic donor sites (c.353A>G, c.510+5G>T, c.756-3C>G). The deep intronic variant in intron 6, c.664-342G>T, results in the creation of a new donor site and a new acceptor site, leading to the incorporation of a pseudo-exon. A partial exon skipping is observed for 3 splice variants: c.242G>T, c.242+5G>A, and c.510+5G>A. All of the aforementioned events result in frame-shifting and premature stop codons. Minigene assays indicate that the 2 missense variants localized at the second-to-last base position of exons 3 and 4 (c.241A>T p.(Arg81Trp) and c.361T>G p.(Trp121Gly)), have no impact on splicing. However, their impact on TBX5 function has been demonstrated by the luciferase assays described above (Figure 2E). The results of the minigene splice assays and fragment analyses are presented in Supp data 13.

RT-PCR was performed on fetal lung tissue from an individual carrying the familial deep intronic *TBX5* variant c.664-342G>T (Figure 3A, Supp data 14). The variant creates cryptic splice donor and acceptor sites, leading to the insertion of a pseudo-exon into the cDNA sequence, as predicted by SpliceAI software (Figure 3B, Supp data 14).

ACMG classification

All variants were categorized as PM2_supporting due to their absence in controls (GnomAD_v3). First, the PP4-supporting criterion was applied to all variants, except for p.(Gly195Ala), p.(Gly238Ala) and p.(Ser261Cys), due to the presence of atypical associated clinical features or absence of radial involvement. It is noteworthy that the PP4-supporting criterion was applied for the variant p.(Gly238Ala) due to the previous documentation of a gain-of-function mechanism in a patient exhibiting a very similar phenotype.[36] The PM1 criterion was added for the variants located within the DNA-binding domain. The PP3 criterion was applied for all variants, except p.(Gly195Ala) and p.(Ser261Cys) because of contradictory predictions. Given that the p.(Arg81Trp), p.(Trp121Gly) and p.(Ser261Cys) variants were observed in familial cases, with more than two affected relatives carrying the variant, the PP1 criterion was added. In the literature, 4 variants involving the same residues have been reported *de novo,* thus allowing the application of the PM5 criterion: p.(Met74Ile), p.(Pro85Ser), p.(Pro85Thr) and (p.Lys226Arg).[11,14,33] The variant p.(Phe232Leu) has recently been reported in 10 affected members of a large family with atypical HOS.[37] Finally, the PS3_supporting criterion was added to the functionally validated missense variants, whereas the BS3_supporting criterion was applied to p.(Gly195Ala) and p.(Ser261Cys) because our *in vitro* assays do not show any functional consequences. As recommended by the specific ACMG guidelines, the PVS1_strength (RNA) criterion was used instead of the PS3 criterion to characterize the functional assays results for splice variants.[32]

Considering our functional data, 3 missense VUS could be reclassified as likely pathogenic, whereas 2 remained of uncertain significance. Six splice variants could be reclassified as likely

pathogenic, whereas 3 remained of uncertain significance due to partial exon skipping on RNA analyses.

DISCUSSION

Twenty *TBX5* variants were characterized by functional assays and the results were compared with various variant effect prediction software. Overall, 9 of the 14 selected *TBX5* VUS could be reclassified as likely pathogenic, by the addition of the PS3_supporting and PP4_supporting (for the gain-of-function variant) ACMG criteria for missense variants or the PVS1_strong criterion for splice variants.

For missense variants, *in silico* variant effect predictions were largely consistent with the results of functional assays. Conflicting predictions were observed for the only 2 variants that had no functional consequences *in vitro*, p.(Gly195Ala) and p.(Ser261Cys). This finding is consistent with the observation that the clinical presentation of these patients was not typical for HOS. The variant p.(Gly195Ala) has been documented in a simplex case exhibiting both typical (association of bilateral radial defect and heart defect) and unusual (abdominal situs inversus) features of HOS. Structural damage was predicted by Missense 3D, but since this residue is not conserved between *T-box* genes, CADD and EVE scores were low. The variant p.(Ser261Cys) has been reported in a family with unusual features: isolated hypoplastic distal phalanges and nail hypoplasia without radial or heart involvement. However, it has been reported 4 times as VUS in ClinVar (ID518540), but without information on clinical findings. This variant is located in a NuRD (Nucleosome remodeling and deacetylase) interaction domain, which suggests the potential for an impact on TBX5 binding to the NuRD repressor complex. This complex is essential to cardiac development

and evolution of the mammalian heart.[38] Further studies are needed to address this question, as this specific mechanism could be responsible for an atypical HOS phenotype.

Our functional tests demonstrated that the p.(Gly238Ala) variant results in TBX5 gain-of-function. To our knowledge, in the literature only one variant, p.(Gly125Arg), has been associated with a gain-of-function, the luciferase assay showing an increased transactivation of TBX5 on its target genes *NPPA* and *GJA5*.[36] This mechanism has been explained by an interaction between *TBX5* and the histone deacetylase HDAC3 (HGNC:4854), a *TBX5* transcriptional repressor.[39] Here, this mechanism could not be considered since the residue 238 is not close to an acetylated lysine. Interestingly, the phenotypes in these 2 families were very similar and atypical for HOS: scapular dysplasia and scoliosis without radial involvement, associated with paroxysmal atrial fibrillation/ventricular tachyarrhythmia. This information allowed us to apply the PP4_supporting criteria to this variant despite the clinical findings reported as atypical for HOS. This observation suggests a genotype-phenotype relationship and highlights the power of functional tests in elucidating the underlying molecular mechanisms, in contrast to the limitations of variant effect predictors.

Our immunofluorescence experiments showed relocalization in the cytoplasm for 4 missense variants studied, of which 3 variants located in the nuclear localization signal. Previous studies reported mislocalization as a common consequence for coding variations, affecting about one-sixth of all pathogenic missense variants.[40] However, in our study, the proportion of nuclear and cytoplasmic localization of the WT protein were quite similar. *In vivo* Tbx5 cytoplasmic localization has been previously reported during heart development.[41] Interaction between Tbx5 and Pdlim7

(HGNC:22958), a cytoplasmic protein associated with the actin cytoskeleton, described in vertebrate limb and heart development, could regulate Tbx5 activity through its subcellular localization.[42,43] The preferential cytoplasmic localization of the variant p.(Lys226Asn) could be due to an alteration of TBX5 protein stability or an increased affinity for PDLIM7 binding for example. For now, TBX5 structure has been characterized by radiocrystallography only for the isolated TBX5 protein and the TBX5 DNA-binding domain linked to DNA. However the alteration of other interaction domains could affect TBX5 structure, as described for the NuRD interaction domain.[38] Therefore, predicting the impact of missense variants on protein structure may be challenging, especially for variants located outside the T-box binding domain.

For splice variants, the functional test results were consistent with the predictions made by SpliceAI software, even for exonic or deep intronic variants.[44] This enabled us to characterize as pathogenic a deep intronic variant in a family with a typical HOS phenotype, as well as a splice variant located 9bp upstream of the end of exon 4, both responsible for the creation of new donor splice sites.

We observed partial exon skipping for 3 variants, which raises concerns about the interpretation of *in vitro* splice assays. Since *TBX5* is not expressed during adult life, *in vivo* transcript or protein studies could not be used to assess the pathogenicity of these variants. However, based on the results of variant effect predictors and clinical features consistent with HOS, all three variants are likely pathogenic.

Exonic variants, either located at the last position or 9bp before the end of the exon, were characterized as splice variants by creating strong donor splice sites. The variant c.755G>T,

located at the identical position as one of the selected variants c.755G>C, is documented in the literature as a missense variant. However, this variant could rather affect splicing.[13,35]

While *in silico* predictors are not able to assess the pathogenicity of a variant on their own, they provide a valuable contribution to the overall ACMG classification. Recent publications have benchmarked the performance of variant effect predictors using data generated by Deep Mutational Scanning (DMS) studies, demonstrating a strong correlation and a high level of accuracy in identifying clinically relevant variants, promoting the power of tools such as VARITY_ER, EVE or REVEL.[45]

Lacking access to the TBX5 transcript or protein *in vivo*, functional *in vitro* assays were used to specifically study the biological consequences of *TBX5* variants at the cellular level. However, these systems are artificial and may not accurately reflect *in vivo* molecular mechanisms. Besides, variant effect assays are often resources- and time-consuming, because of their low throughput. Also, they are usually performed after the identification of individual variants. Now available, the multiplexed assays of variant effect (MAVEs) enable the functional characterization of every possible single nucleotide change within a functional element of interest, with the ambition to create an “Atlas” of variant effect maps for every protein-encoding gene and regulatory element in the human genome.[46] For example, DMS could assist in the interpretation of *TBX5* missense or splice variants located in the DNA-binding domain, as it has been performed for *PAX6* (HGNC:8620) variants using a yeast one-hybrid assay to assess DNA-binding capacity.[47] However, the molecular mechanism of the disease need to be previously investigated to adapt the readout of the screenings.

Overall, our results highlight the value of using complementary bioinformatic and biological approaches and the importance of a good knowledge of clinical conditions for accurate ACMG classification in rare human diseases.[48]

DATA AVAILABILITY

All data presented in this paper are available to qualified researchers upon request to Clémence Vanlerberghe (clemence.vanlerberghe@chu-lille.fr). Genomic variants are reported in the ClinVar Database.

ACKNOWLEDGEMENTS

pGL3-Nppa promoter plasmid was kindly provided by Dr Alex Vincent Postma (Department of Clinical Genetics, Amsterdam, UMC).

pCAS2 vector was kindly provided by the Department of Genetics and Institute for Biomedical Research, Rouen University Hospital, Inserm U614, IFRMP, University of Rouen, Northwest Canceropole, France.

We thank the BioImaging Center Lille (BiCeL, US 41 - UAR 2014 – PLBS) of Lille University for providing access to confocal imaging.

For family F12, sequencing and data analysis were provided by the University of Washington Center for Rare Disease Research (UW-CRDR) with support from NHGRI grants U01 HG011744, UM1 HG006493 and U24 HG011746. The content is solely the responsibility of the authors and does not necessarily represent the official views of the National Institutes of Health.

We thank the geneticists and the fetopathologists who examined the patients and fetus.

We thank the patients and their families.

FUNDING

This study was supported by a grant from the GIRCI Nord-Ouest (AAP-AE-17-18) and by the Health PhD grant from the Isite Foundation.

AUTHOR CONTRIBUTIONS

Conceptualization: C.V., A.S.J., F.E., P.B., F.P.; Data curation: C.V., E.A.Y., A.D., S.M.H.; Formal analysis: C.V., A.S.J, F.F., M.B., K.P., F.E., P.B., W.D., F.L., F.P.; Funding acquisition: C.V., S.M.H., J.G., F.P.; Supervision: J.G., T.S., F.P.; Visualization: C.V., A.S.J., F.F., T.S., F.P. Writing-original draft: C.V., F.P.; Writing-review & editing: F.L., S.M.H., J.G., T.S., P.B.

ETHICS DECLARATION

Written informed consents for research use were obtained from the patients or their parents prior to the *TBX5* molecular analysis. The research protocol was reviewed and accepted by the Institutional Review Board and Data Protection Manager of Lille University Hospital (DEC19-366). The study was conducted in accordance with the Declaration of Helsinki.

CONFLICT OF INTEREST

The authors declare no conflict of interest.

TABLE 1 – *TBX5* missense variants

Description of variants selected from the literature or from our local series, prediction data and results of functional tests (Western Blot, Luciferase reporter assays, immunofluorescence). Considering location of variant, *in silico* predictions, results of functional tests and ACMG classification: features in white are in favor of pathogenicity, light grey are equivocal, dark grey are in favor of benign variants.

ASD: Atrial Septal Defect; PFO: Permeability of Foramen Oval; N/A: Not Available; NLS: Nuclear Localization Signal; OS-ASD: Ostium Secundum Atrial Septal Defect; VSD: Ventricular Septal Defect; supp: supporting; RSA: relative solvent accessibility;

[a] CADD score: the raw score is single numerical deleteriousness score, correlating with the likelihood that the variant is pathogenic or disruptive to gene function. A conversion table translates to a scaled CADD-score, a variants' relative rank among all potential SNV alterations presented on PHRED-scale (−10 * log10(1/rank)).

[b] VARITY_ER: the final score is obtained after a transformation of a log(odds) ("lod") score via a sigmoid transformation, and represent the probability to be pathogenic: variants with a score close to 1 are inferred to be pathogenic.

Genomic position (hg38) (NC_000012.12)	g.114401848T>C	g.114401827T>A	g.114399621G>A	g.114399609A>T	g.114399514A>C	g.114394884T>C	g.114394820C>G	g.114385553C>A	g.114385537A>C	g.114385518C>G	g.114366366T>A
HGVS DNA (NM_000192.3)	**c.220A>G**	**c.241A>T**	**c.254C>T**	**c.266T>A**	**c.361T>G**	**c.520A>G**	**c.584G>C**	**c.678G>T**	**c.694T>G**	**c.713G>C**	**c.781A>T**
HGVS protein (NP_000183.2)	p.(Met74Val)	p.(Arg81Trp)	p.(Pro85Leu)	p.(Val89Glu)	p.(Trp121Gly)	p.(Asn174Asp)	p.(Gly195Ala)	p.(Lys226Asn)	p.(Phe232Val)	p.(Gly238Ala)	p.(Ser261Cys)
Reference	(21)	(22)	(11)	(23)	(8)	(11)	(8)	(24)	(11)	(25)	(8)
PHENOTYPE (PP4)											
Limb phenotype	Thumb hypoplasia	Bilateral radial and thumb defect (left side more severely affected) with carpal bones involvement	Bilateral radial defect	Bilateral radial and thumb defect	Left radial hypoplasia	Bilateral radial defect	Bilateral thumb hypoplasia	Triphalangeal thumbs	Bilateral radial defect	No	Left radial hypoplasia and left index aplasia
Heart phenotype	ASD, VSD	VSD	ASD, hypoplasia of left ventricle	No	ASD	Dextrocardia	PFO, asymmetrical aortic valve	OS-ASD, atrioventricular septal defect, pulmonary stenosis, hypertension, and mitral insufficiency	VSD, aortic coarctation	Mitral and tricuspid valve insufficiency and atrial septal thinning, life-threatening tachyarrhythmias	Double outlet right ventricle, atrioventricular canal
Uncommon features	No	No	No	No	No	No	Abdominal situs inversus, vertebral defects (C2-C3 and C6-C7 fusion)	11 pairs of ribs, shortened scapular bone	No	Thoracic spine deformity (scoliosis) and scapula dysplasia	Cleft palate, facial asymmetry, micrognathia, hypoplastic nails
SEGREGATION (PP1)											
Family history	Simplex	Familial	Simplex	Simplex	Familial	Simplex	Simplex	Familial	Simplex	Simplex	Familial
Variant inheritance	N/A	Two other affected members	N/A	N/A	Four other affected members	N/A	N/A	One other affected member	N/A	N/A	Two other affected members

LOCATION (PM1)											
Exon	exon 3	exon 3	exon 4	exon 4	exon 4	exon 6	exon 6	exon 7	exon 7	exon 7	exon 8
Domain	DNA binding domain	DNA binding domain; NLS	DNA binding domain; NLS	DNA binding domain; NLS	DNA binding domain	DNA binding domain	DNA binding domain	DNA binding domain	DNA binding domain	DNA binding domain	No functional domain
***IN SILICO* DATABASES AND PREDICTIONS (PM2 and PP3)**											
gnomAD v3	No match	No match	No match	No match	No match	No match	No match	No match	No match	No match	No match
CADD : raw-score (PHRED score)[a]	3.20 (23.90)	5.59 (34)	4.67 (32)	4.45 (32)	5.20 (33)	4.09 (27.7)	2.49 (22.4)	4 (26.9)	4.22 (28.90)	3.72 (25.5)	4.27 (29.30)
REVEL	Damaging (0.919)	Damaging (0.927)	Damaging (0.962)	Damaging (0.957)	Damaging (0.963)	Damaging (0.812)	Uncertain (0.49)	Damaging (0.885)	Damaging (0.95)	Damaging (0.843)	Damaging (0.876)
EVE	Pathogenic (0.643)	Uncertain (0.631)	Uncertain (0.638)	Uncertain (0.603)	Uncertain (0.639)	Uncertain (0.637)	Benign (0.314)	Uncertain (0.635)	Pathogenic (0.647)	Uncertain (0.601)	Benign (0.233)
VARITY_ER[b]	0.939	0.926	0.958	0.977	0.953	0.98	0.389	0.889	0.967	0.76	0.47
AlphaMissense	Likely pathogenic (0.999)	Likely pathogenic (1.0)	Likely pathogenic (1.0)	Likely pathogenic (0.999)	Likely pathogenic (0.998)	Likely pathogenic (0.999)	Likely pathogenic (0.908)	Likely pathogenic (1.0)	Likely pathogenic (1.0)	Likely pathogenic (0.985)	Ambiguous (0.349)
Missense 3D (PDB:2X6U)	Structural damage: buried H-bond breakage (RSA 1.0%), expansion of cavity volume by 103.68 Å^3	No structural damage	Structural damage: replacement of a cis proline.	Structural damage: buried charge introduced (this substitution replaces a buried uncharged residue (Val, RSA 0.0%) with a charged residue (Glu))	Structural damage: expansion of cavity volume by 102.168 Å^3.	No structural damage	Structural damage: the phi/psi angles in favored region for wild-type residue but outlier region for mutant residue, replacement of a glycine originally located in a bend curvature	Structural damage: buried H-bond breakage (RSA 6.3%), buried exposed switch (Lys is buried (RSA 6.3%) and Asn is exposed (RSA 19.7%))	No structural damage	No structural damage	No available protein structure prediction
FUNCTIONAL TEST RESULTS (PS3)											
Western Blot	Normal expression	Normal expression	Increased expression	Normal expression	Normal expression	Reduced expression	Normal expression	Normal expression	Normal expression	Normal expression	Normal expression

Luciferase assay	Reduced activity	Reduced activity	Reduced activity	No modification	Reduced activity	No modification	No modification	Reduced activity	Reduced activity	Increased activity	No modification
Cellular localization	Normal	Cytoplasmic relocalization	Cytoplasmic relocalization	Cytoplasmic relocalization	Normal	Normal	Normal	Cytoplasmic relocalization	Normal	Normal	Normal
ACMG RECLASSIFICATION											
ACMG criteria without functional tests	PP4, PM1, PM2_supp, PP3, PM5	PP4, PP1, PM1, PM2_supp, PP3	PP4, PM1, PM2_supp, PP3, PM5	PP4, PM1, PM2_supp, PP3	PP4, PP1, PM1, PM2_supp, PP3	PP4, PM1, PM2_supp, PP3	PM1, PM2_supp	PP4, PM1, PM2_supp, PP3, PM5	PP4, PM1, PM2_supp, PP3, PM5	PM1, PM2_supp, PP3	PP1, PM2_supp
ACMG classification without functional tests	Likely pathogenic	Likely pathogenic	Likely pathogenic	Uncertain significance	Likely pathogenic	Uncertain significance	Uncertain significance	Likely pathogenic	Likely pathogenic	Uncertain significance	Uncertain significance
ACMG criteria with functional tests	PP4, PM1, PM2_supp, PP3, PM5, PS3_supp	PP4, PP1, PM1, PM2_supp, PP3, PS3_supp	PP4, PM1, PM2_supp, PP3, PM5, PS3_supp	PP4, PM1, PM2_supp, PP3, PS3_supp	PP4, PP1, PM1, PM2_supp, PP3, PS3_supp	PP4, PM1, PM2_supp, PP3, PS3_supp	PM1, PM2_supp, BS3_supp	PP4, PM1, PM2_supp, PP3, PM5, PS3_supp	PP4, PM1, PM2_supp, PP3, PM5, PS3_supp	PM1, PM2_supp, PP3, PS3_supp, PP4	PP1, PM2_supp, BS3_supp
ACMG classification prediction with functional tests	Likely pathogenic	Likely pathogenic	Likely pathogenic	Likely pathogenic	Likely pathogenic	Likely pathogenic	Uncertain significance	Likely pathogenic	Likely pathogenic	Likely pathogenic	Uncertain significance

TABLE 2 - *TBX5* splice variants

Description of variants selected from the literature or from our local series, prediction data and results of functional tests (minigene assays, RT-PCR).

ASD: Atrial Septal Defect; N/A: Not Available; NLS: Nuclear Localization Signal; OS-ASD: Ostium Secundum Atrial Septal Defect; VSD: Ventricular Septal Defect; supp: supporting; WT: wild-type; Mut: mutant;

[a] PhyloP: phyloP scores measure evolutionary conservation at individual alignment sites compared to the evolution that is expected under neutral drift. Positive scores highlight a slower evolution than expected, at sites that are predicted to be conserved. Negative scores highlight a faster evolution than expected, at sites that are predicted to be fast-evolving.

[b] SPIP gives the probability between 0 and 100% of splice site use

[c] SpliceAI gives the probability between 0 and 1 of acceptor loss or gain and donor loss or gain within the region (we set up the analysis to look for new splice sites 5000 bp upstream and downstream the variant position)

Genomic position (hg38) (NC_000012.12)	g.114385909 C>A	g.114401827 T>A	g.114401826C >A	g.114401821 C>T	g.114399522 T>C	g.114399514 A>C	g.114399513 C>A	g.114398568 C>T	g.114398568 C>A	g.114385476 C>G	g.114366394 G>C
HGVS DNA (NM_000192.3)	c.664-342G>T	c.241A>T	c.242G>T	c.242+5G>A	c.353A>G	c.361T>G	c.362G>T	c.510+5G>A	c.510+5G>T	c.755G>C	c.756-3C>G
HGVS protein (NP_000183.2)	p.?	p.(Arg81Trp)	p.(Arg81Met)	p.?	p.(Asp118Gly)	p.(Trp121Gly)	p.(Trp121Leu)	p.?	p.?	p.(Ser252Thr)	p.?
Position	intron 6	exon 3 (second to last base)	exon 3 (last base)	intron 3	exon 4 (9bp upstream the end of the exon)	exon 4 (second to last base)	exon 4 (last base)	intron 5	intron 5	exon 7 (last base)	intron 7
Reference	This study	(22)	This study	(11)	This study	(8)	This study	(11)	(20)	(11)	(9)
PHENOTYPE (PP4)											
Limb phenotype	Bilateral thenar hypoplasia	Right thumb and radial agenesis, carpal bone abnormalities and left humeral hypoplasia, ulnar and radial agenesis, fusion of carpal bones, triphalangeal thumbs and oligodactyly	Bilateral I-II syndactyly, bilateral radial hypoplasia,	Bilateral thumb hypoplasia, sloping shoulders, limitation of shoulder mobility	Right thenar hypoplasia, left I-II fingers syndactyly and radial hypoplasia and digitalized thumb	Thumb hypoplasia, radial hypoplasia, radio-ulnar synostosis, narrow shoulders	Bilateral thumb agenesis, bilateral fingers I-II syndactyly radial hypoplasia (more severe on the left side)	Bilateral thumb hypoplasia	Dysplasia of all carpal bones and an extra carpal bone	Bilateral thenar hypoplasia, bilateral triphalangeal thumbs	Bilateral thumb defects
Cardiac phenotype	ASD	VSD	Large ASD, muscular VSD, pulmonary artery hypoplasia	Moderate mitral valve prolapse, left ventricle hypoplasia	Large VSD, large ASD, tight pulmonary stenosis	ASD	No	ASD, VSD, pulmonary stenosis, junctional tachycardia	ASD, sinus bradycardia, symptomatic sinus node disease, atrial fibrillation	OS, ASD	ASD, VSD

SEGREGATION (PP1)											
Family history	Familial	Familial	Simplex	Familial	Simplex	Familial	Familial	Simplex	Familial	Simplex	Simplex
Inheritance	All affected members	Two other affected members (father and sister)	N/A	One other affected member (mother), absent in her unaffected sister	N/A	Four other affected members	One other affected member (mother)	N/A	One other affected member (daughter)	N/A	N/A
IN SILICO DATABASES (PM2 and PP3)											
gnomAD v3	0	0	0	0	0	0	0	0	0	0	0
Conservation PhyloP [a]	-1,07	3,21	7,8	4,96	7,67	8,95	7,57	7,57	7,57	7,48	2,71
In Silico consequence	Creation of a new splice donor site (2bp upstream), integration of a pseudo exon of 95 bp	Alteration of the consensus splice site	Alteration of the consensus splice site (exon 3 skipping?)	Alteration of the consensus splice site (exon 3 skipping?)	Creation of a new donor splice site + Alteration of an exonic splicing regulatory element (shortening of exon 4? frameshift?)	No effect on splicing but missense predictions: damaging	Alteration of the consensus splice site (exon 4 skipping?)	Alteration of the consensus splice site (exon 5 skipping?)	Alteration of the consensus splice site (exon 5 skipping?)	Alteration of the consensus splice site (new donor site, 56 bp downstream?)	Alteration of the consensus splice site
MaxEntScan (WT/Mut)	5'SS (-1.59/6.05)	5'SS (8.68/7.23)	5'SS (8.68/3.37)	5'SS (8.68/4.51) and 3'SS (3.35/4.36)	5'SS (0.37/8.55)	0	5'SS (7.42/0.43)	5'SS (7.83/-0.39)	5'SS (7.83/-1.86)	5'SS (9.45/3.85)	3'SS (11/-1.84)
SPIP [b]	0%	69.33%. (61.29-76.59%)	98.41% (91.47-99.96%)	98.41% (91.47-99.96%)	98.54% (94.83%-99.82%)	9.3% (2.59-22.14%)	98.41% (91.47-99.96%)	98.41% (91.47-99.96%)	98.41% (91.47-99.96%)	98.41% (91.47-99.96%)	98.41% (91.47-99.96%)
SpliceAI [c] Acceptor Loss	0	0	0.61-0.67 (94bp)	0.42-0.50 (99bp)	0.02 (-110bp)	0.00 (118bp)	0.00 (119bp)	0	0 (152bp)	0	**0.82-0.91 (-3 bp)**
SpliceAI Donor Loss	0.03 (-125bp)	**0.24-0.27 (-1bp)**	**0.79 (0bp)**	**0.53-0.55 (5bp)**	**0.57 (-9bp)**	0.02 (-1bp)	**0.67 (0 bp)**	**0,72 - 0,81 (5bp)**	**0.75 - 0.83 (5bp)**	**0,95 (0 bp)**	0
SpliceAI Acceptor Gain	0.32 (93bp)	0	0	0	0.01 (110 bp)	0.01 (1219bp)	0.03-0.04 (1220 bp)	0	0.02 (2165 bp)	0,01 (526 bp)	0,19 (-8 bp)

SpliceAI Donor Gain	**0.62 (2bp)**	0.02 (-864 bp)	0.02 (-8bp)	0.02-0.03 (-3bp)	**0.99 (1bp)**	0.01 (-709bp)	0.02 (92bp)	0,02 - 0,03 (9bp)	0.03 - 0.05 (9bp)	0,86 (-56bp)	0
CADD Phred score	3.34	34.00	36	22.6	34.0	33.00	35.0	25.20	25.60	34.00	25.40
FUNCTIONAL ASSAYS (PVS1)											
Minigene splice assay	Introduction of a pseudo exon in intron 6	No effect	Partial exon skipping	Partial exon skipping	Deletion of the last 10 pb of exon 4	No effect	Exon skipping	Partial exon skipping	Exon skipping or deletion of 4 bp due to a new cryptic donor site	Addition of 56 pb from intron 7	Exon skipping or deletion of 5 bp due to a new cryptic acceptor site
RT-PCR	Introduction of a pseudo exon in intron 6	N/A	N/A	N/A	N/A	N/A	N/A	N/A	N/A	N/A	N/A
Predicted protein consequence	Frameshift p.(Ile222Lysfs*35)	Missense p.(Arg81Trp)	Frameshift p.(Met51Glyfs*8)	Frameshift p.(Met51Glyfs*8)	Frameshift p.(Asp118Glyfs*3)	Missense p.(Trp121Gly)	Frameshift p.(Arg82Valfs*7)	Frameshift p.(Ser122Tyrfs*12)	Frameshift p.?	Frameshift p.(Ser252Thrfs*2)	Frameshift p.?
ACMG CLASSIFICATION											
ACMG criteria without functional tests	PP4, PP1, PM2_supp, PP3	see Table 1	PP4, PM2_supp, PP3	PP4, PP1, PM2_supp, PP3	PP4, PM2_supp, PP3	see Table 1	PP4, PM2_supp, PP3	PP4, PM2_supp, PP3	PP4, PM2_supp, PP3	PP4, PM2_supp, PP3	PP4, PM2_supp, PP3
ACMG classification without functional tests	Uncertain significance	see Table 1	Uncertain significance	Uncertain significance	Uncertain significance	see Table 1	Uncertain significance	Uncertain significance	Uncertain significance	Uncertain significance	Uncertain significance
ACMG criteria with functional tests	PP4, PP1, PM2_supporting, PVS1_strong (RNA)	see Table 1	PP4, PM2_supporting, PVS1_N/A (RNA)	PP4, PP1, PM2_supporting, PVS1_N/A (RNA)	PP4, PM2_supporting, PVS1_strong (RNA)	see Table 1	PP4, PM2_supporting, PVS1_strong (RNA)	PP4, PM2_supporting, PVS1_N/A (RNA)	PP4, PM2_supporting, PVS1_strong (RNA)	PP4, PM2_supporting, PVS1_strong (RNA)	PP4, PM2_supporting, PVS1_strong (RNA)
ACMG classification with functional tests	Likely pathogenic	see missense variant table	Uncertain significance	Uncertain significance	Likely pathogenic	see Table 1	Likely pathogenic	Uncertain significance	Likely pathogenic	Likely pathogenic	Likely pathogenic

FIGURES

Figure 1 - Localization of functionally characterized *TBX5* missense and splice variants

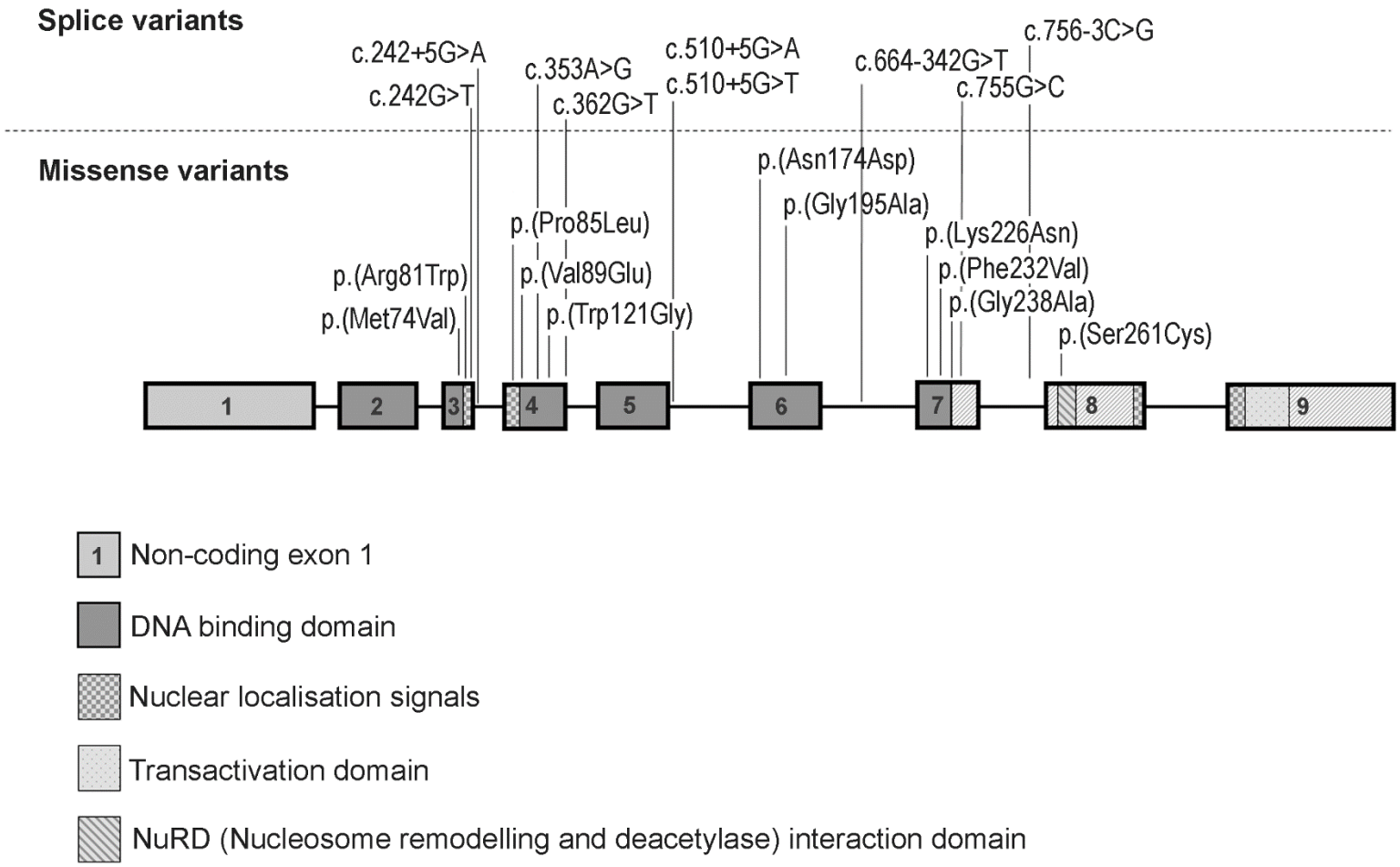

Figure 2 – Functional assays performed on selected *TBX5* missense variants: subcellular localization, Western Blot and luciferase reporter assays

A. Subcellular localization has been studied by immunofluorescence in HEK293T transfected cells. Nucleus are stained in blue (DAPI). TBX5-FLAG proteins are stained in green. WT: wild-type. **B.** Percentage of cells with TBX5 cytoplasmic localization and statistical comparison of variants with the WT. **C.** Western blot for TBX5 and Tubulin (control), performed on HEK293T transfected cells. **D.** Normalized TBX5 protein expression and statistical analysis from 3 western blot biological replicates. **E.** Luciferase reporter assays performed on HEK293T cells, co-transfected with the TBX5-expressing plasmid and the Nppa-reporter plasmid. Normalized luciferase activity from 3 biological replicates.

Histograms: mean with standard deviation. Grey bars: TBX5 variants studied; Black bars: controls (WT: wild-type TBX5; p.(Arg279*): truncating variant, control for TBX5 haploinsufficiency; p.(Arg237Pro): missense variant, control for TBX5 loss-of-function; NT: non-transfected cells). One-way ANOVA for comparison of variants to the WT condition: *$p<0.05$, **$p<0.005$, *** $p<0.0005$, **** $p<0.00005$.

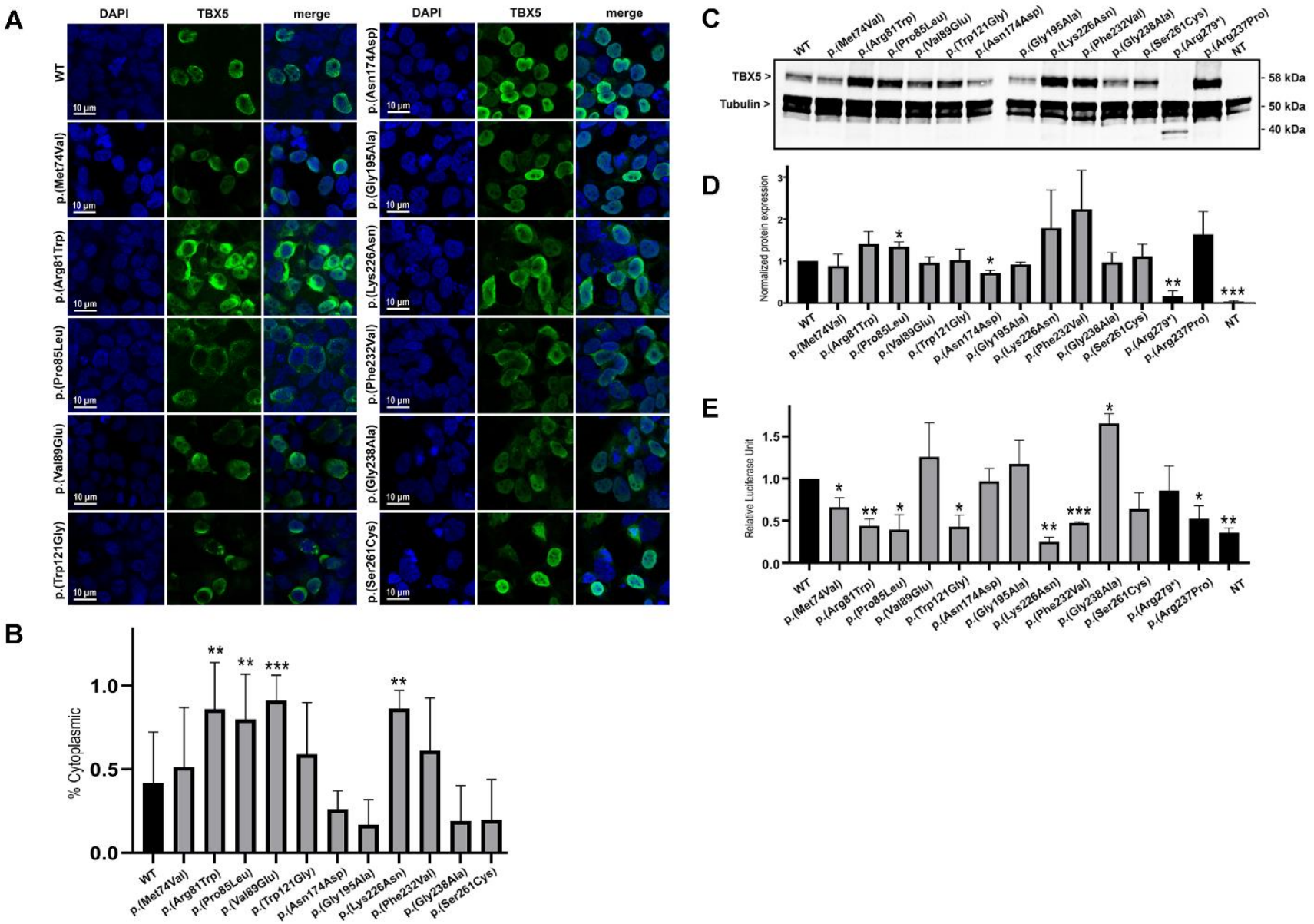
A
DAPI
TBX5
merge
WT
p.(Met74Val)
p.(Arg81Trp)
p.(Pro85Leu)
p.(Val89Glu)
p.(Trp121Gly)
p.(Asn174Asp)
p.(Gly195Ala)
p.(Lys226Asn)
p.(Phe232Val)
p.(Gly238Ala)
p.(Ser261Cys)
10 µm
B
% Cytoplasmic
1.0
0.5
0.0
C
TBX5 >
Tubulin >
58 kDa
50 kDa
40 kDa
D
Normalized protein expression
E
Relative Luciferase Unit
p.(Arg279*)
p.(Arg237Pro)
NT

Figure 3 – Schematic results of the functional assays for splice variants.

Partial pre-mRNA are represented on the left, with normal splicing (up) and abnormal splicing (down) patterns indicated by dashed lines. Black arrows indicate the location of variants. V indicate the introduction of cryptic splice sites. Partial mRNA observed by functional assays are represented on the right, with the percentage of alternative splicing indicated when relevant. E: exon; ins: insertion; del: deletion; PE: pseudo exon; IR: intron retention.

A. Introduction of cryptic splice sites

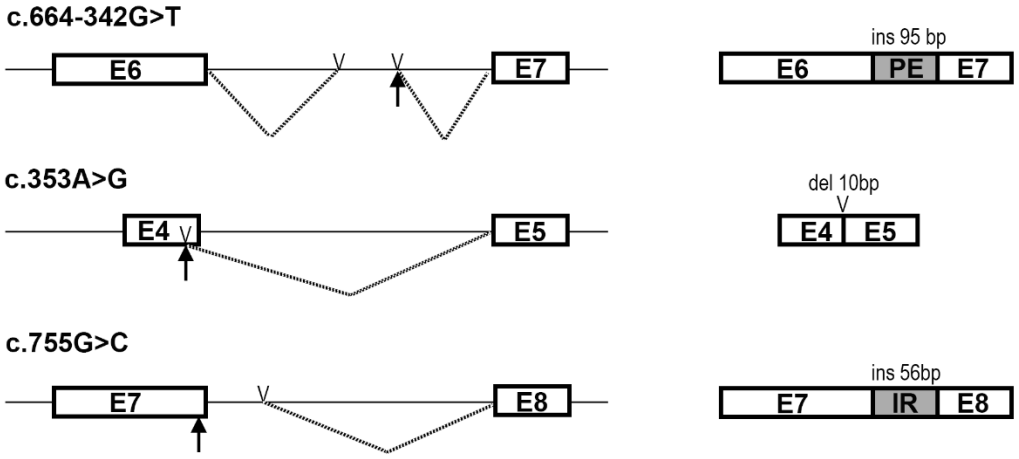

B. Abolition of canonical splice sites

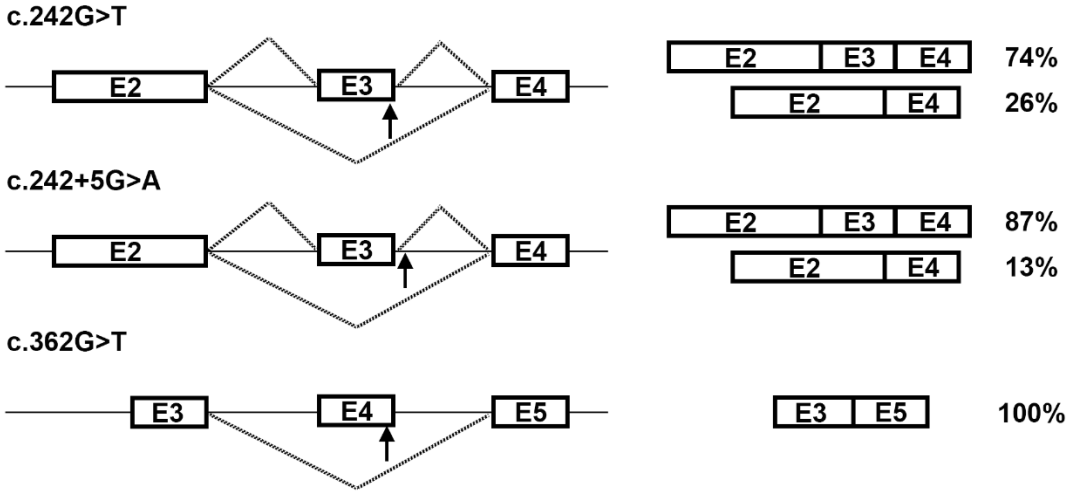

C. Abolition of canonical splice sites AND introduction of cryptic spice sites

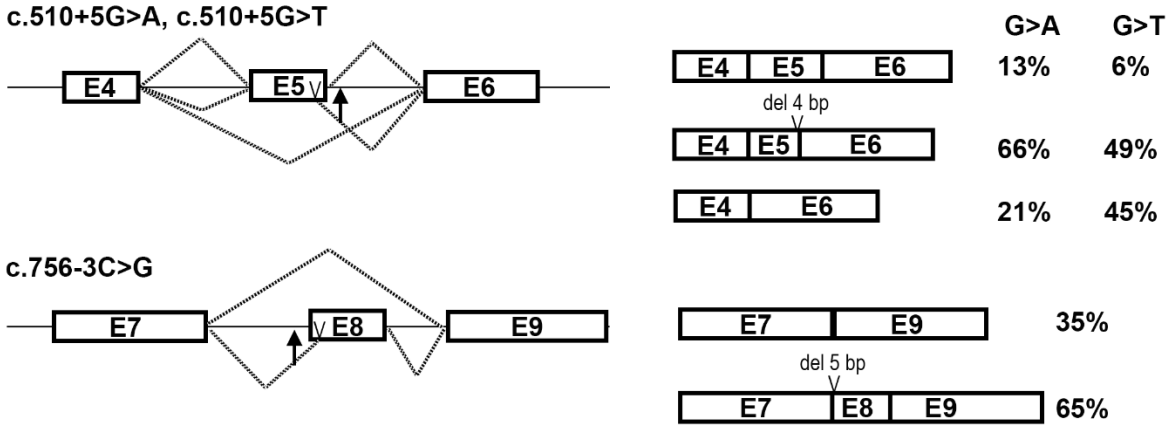

REFERENCES

1. Elek C, Vitéz M, Czeizel E. [Holt-Oram syndrome]. *Orv Hetil*. 1991;132(2):73-74, 77-78.

2. McDermott DA, Bressan MC, He J, et al. TBX5 genetic testing validates strict clinical criteria for Holt-Oram syndrome. *Pediatr Res*. 2005;58(5):981-986. doi:10.1203/01.PDR.0000182593.95441.64

3. Basson CT, Bachinsky DR, Lin RC, et al. Mutations in human TBX5 [corrected] cause limb and cardiac malformation in Holt-Oram syndrome. *Nat Genet*. 1997;15(1):30-35. doi:10.1038/ng0197-30

4. Naiche LA, Harrelson Z, Kelly RG, Papaioannou VE. T-box genes in vertebrate development. *Annu Rev Genet*. 2005;39:219-239. doi:10.1146/annurev.genet.39.073003.105925

5. Ohuchi H, Nakagawa T, Yamamoto A, et al. The mesenchymal factor, FGF10, initiates and maintains the outgrowth of the chick limb bud through interaction with FGF8, an apical ectodermal factor. *Dev Camb Engl*. 1997;124(11):2235-2244.

6. Hiroi Y, Kudoh S, Monzen K, et al. Tbx5 associates with Nkx2-5 and synergistically promotes cardiomyocyte differentiation. *Nat Genet*. 2001;28(3):276-280. doi:10.1038/90123

7. Linhares VLF, Almeida NAS, Menezes DC, et al. Transcriptional regulation of the murine Connexin40 promoter by cardiac factors Nkx2-5, GATA4 and Tbx5. *Cardiovasc Res*. 2004;64(3):402-411. doi:10.1016/j.cardiores.2004.09.021

8. Brassington AME, Sung SS, Toydemir RM, et al. Expressivity of Holt-Oram syndrome is not predicted by TBX5 genotype. *Am J Hum Genet*. 2003;73(1):74-85. doi:10.1086/376436

9. Heinritz W, Moschik A, Kujat A, et al. Identification of new mutations in the TBX5 gene in patients with Holt-Oram syndrome. *Heart Br Card Soc*. 2005;91(3):383-384. doi:10.1136/hrt.2004.036855

10. Borozdin W, Bravo Ferrer Acosta AM, Bamshad MJ, et al. Expanding the spectrum of TBX5 mutations in Holt-Oram syndrome: detection of two intragenic deletions by quantitative real time PCR, and report of eight novel point mutations. *Hum Mutat*. 2006;27(9):975-976. doi:10.1002/humu.9449

11. Vanlerberghe C, Jourdain AS, Ghoumid J, et al. Holt-Oram syndrome: clinical and molecular description of 78 patients with TBX5 variants. *Eur J Hum Genet EJHG*. 2019;27(3):360-368. doi:10.1038/s41431-018-0303-3

12. Barnett P, Postma AV. Molecular Genetics of Holt-Oram Syndrome. In: John Wiley & Sons Ltd, ed. *eLS*. John Wiley & Sons, Ltd; 2014. Accessed August 3, 2016. http://doi.wiley.com/10.1002/9780470015902.a0024329

13. Fan C, Liu M, Wang Q. Functional analysis of TBX5 missense mutations associated with Holt-Oram syndrome. *J Biol Chem*. 2003;278(10):8780-8785. doi:10.1074/jbc.M208120200

14. Boogerd CJJ, Dooijes D, Ilgun A, et al. Functional analysis of novel TBX5 T-box mutations associated with Holt-Oram syndrome. *Cardiovasc Res*. 2010;88(1):130-139. doi:10.1093/cvr/cvq178

15. Stirnimann CU, Ptchelkine D, Grimm C, Müller CW. Structural basis of TBX5-DNA recognition: the T-box domain in its DNA-bound and -unbound form. *J Mol Biol*. 2010;400(1):71-81. doi:10.1016/j.jmb.2010.04.052

16. Cheng J, Novati G, Pan J, et al. Accurate proteome-wide missense variant effect prediction with AlphaMissense. *Science*. 2023;381(6664):eadg7492. doi:10.1126/science.adg7492

17. Richards S, Aziz N, Bale S, et al. Standards and guidelines for the interpretation of sequence variants: a joint consensus recommendation of the American College of Medical Genetics and Genomics and the Association for Molecular Pathology. *Genet Med Off J Am Coll Med Genet*. 2015;17(5):405-424. doi:10.1038/gim.2015.30

18. Wilcox EH, Sarmady M, Wulf B, et al. Evaluating the impact of in silico predictors on clinical variant classification. *Genet Med*. 2022;24(4):924-930. doi:10.1016/j.gim.2021.11.018

19. Cooper DN, Ball EV, Krawczak M. The human gene mutation database. *Nucleic Acids Res*. 1998;26(1):285-287. doi:10.1093/nar/26.1.285

20. Ross SB, Bagnall RD, Yeates L, Sy RW, Semsarian C. Holt-Oram syndrome in two families diagnosed with left ventricular noncompaction and conduction disease. *Hear Case Rep*. 2018;4(4):146-151. doi:10.1016/j.hrcr.2017.12.002

21. Debeer P, Race V, Gewillig M, Devriendt K, Frijns JP. Novel TBX5 mutations in patients with Holt-Oram syndrome. *Clin Orthop*. 2007;462:20-26. doi:10.1097/BLO.0b013e3181123ffe

22. Ersoy AÖ, Topçu V, Kale İ, Ersoy E, Özler S, Danışman N. A novel mutated sequence in the T-box transcription factor-5 (TBX-5) gene (c.241A>T) in Holt-Oram syndrome. *J Turk-Ger Gynecol Assoc*. 2016;17(1):55-57. doi:10.5152/jtgga.2015.15233

23. Furniss D, Kan SH, Taylor IB, et al. Genetic screening of 202 individuals with congenital limb malformations and requiring reconstructive surgery. *J Med Genet*. 2009;46(11):730-735. doi:10.1136/jmg.2009.066027

24. Porto MPR, Vergani N, Carvalho ACC, Cernach MCSP, Brunoni D, Perez ABA. Novel mutations in the TBX5 gene in patients with Holt-Oram Syndrome. *Genet Mol Biol*. 2010;33(2):232-236. doi:10.1590/S1415-47572010005000051

25. Chakova N, Dolmatovich T, Niyazova S, Komissarova S, Rebeko E, Savchenko A. New Missense Mutation Gly238Ala in the TBX5 Gene and Its Phenotypical Characteristics. *Russ J Genet*. 2021;57:949-954. doi:10.1134/S1022795421070061

26. Baux D, Van Goethem C, Ardouin O, et al. MobiDetails: online DNA variants interpretation. *Eur J Hum Genet EJHG*. 2021;29(2):356-360. doi:10.1038/s41431-020-00755-z

27. Tunyasuvunakool K, Adler J, Wu Z, et al. Highly accurate protein structure prediction for the human proteome. *Nature*. 2021;596(7873):590-596. doi:10.1038/s41586-021-03828-1

28. Jaganathan K, Kyriazopoulou Panagiotopoulou S, McRae JF, et al. Predicting Splicing from Primary Sequence with Deep Learning. *Cell*. 2019;176(3):535-548.e24. doi:10.1016/j.cell.2018.12.015

29. Ghosh TK. Characterization of the TBX5 binding site and analysis of mutations that cause Holt-Oram syndrome. *Hum Mol Genet*. 2001;10(18):1983-1994. doi:10.1093/hmg/10.18.1983

30. Gaildrat P, Killian A, Martins A, Tournier I, Frébourg T, Tosi M. Use of splicing reporter minigene assay to evaluate the effect on splicing of unclassified genetic variants. *Methods Mol Biol Clifton NJ*. 2010;653:249-257. doi:10.1007/978-1-60761-759-4_15

31. Brnich SE, Abou Tayoun AN, Couch FJ, et al. Recommendations for application of the functional evidence PS3/BS3 criterion using the ACMG/AMP sequence variant interpretation framework. *Genome Med*. 2019;12(1):3. doi:10.1186/s13073-019-0690-2

32. Walker LC, de la Hoya M, Wiggins GAR, et al. APPLICATION OF THE ACMG/AMP FRAMEWORK TO CAPTURE EVIDENCE RELEVANT TO PREDICTED AND OBSERVED IMPACT ON SPLICING: RECOMMENDATIONS FROM THE CLINGEN SVI SPLICING SUBGROUP. *MedRxiv Prepr Serv Health Sci*. Published online February 26, 2023:2023.02.24.23286431. doi:10.1101/2023.02.24.23286431

33. Dreßen M, Lahm H, Lahm A, et al. A novel de novo TBX5 mutation in a patient with Holt-Oram syndrome leading to a dramatically reduced biological function. *Mol Genet Genomic Med*. 2016;4(5):557-567. doi:10.1002/mgg3.234

34. Cross SJ, Ching YH, Li QY, et al. The mutation spectrum in Holt-Oram syndrome. *J Med Genet*. 2000;37(10):785-787.

35. Fan C, Chen Q, Wang QK. Functional role of transcriptional factor TBX5 in pre-mRNA splicing and Holt-Oram syndrome via association with SC35. *J Biol Chem*. 2009;284(38):25653-25663. doi:10.1074/jbc.M109.041368

36. Postma AV, van de Meerakker JBA, Mathijssen IB, et al. A gain-of-function TBX5 mutation is associated with atypical Holt-Oram syndrome and paroxysmal atrial fibrillation. *Circ Res*. 2008;102(11):1433-1442. doi:10.1161/CIRCRESAHA.107.168294

37. Møller Nielsen AK, Dehn AM, Hjortdal V, Larsen LA. *TBX5* variants and cardiac phenotype: A systematic review of the literature and a novel variant. *Eur J Med Genet*. 2024;68:104920. doi:10.1016/j.ejmg.2024.104920

38. Waldron L, Steimle JD, Greco TM, et al. The Cardiac TBX5 Interactome Reveals a Chromatin Remodeling Network Essential for Cardiac Septation. *Dev Cell*. 2016;36(3):262-275. doi:10.1016/j.devcel.2016.01.009

39. Lewandowski SL, Janardhan HP, Smee KM, et al. Histone deacetylase 3 modulates Tbx5 activity to regulate early cardiogenesis. *Hum Mol Genet*. 2014;23(14):3801-3809. doi:10.1093/hmg/ddu093

40. Lacoste J, Haghighi M, Haider S, et al. Pervasive mislocalization of pathogenic coding variants underlying human disorders. *BioRxiv Prepr Serv Biol*. Published online September 5, 2023:2023.09.05.556368. doi:10.1101/2023.09.05.556368

41. Bimber B, Dettman RW, Simon HG. Differential regulation of Tbx5 protein expression and sub-cellular localization during heart development. *Dev Biol*. 2007;302(1):230-242. doi:10.1016/j.ydbio.2006.09.023

42. Camarata T, Bimber B, Kulisz A, Chew TL, Yeung J, Simon HG. LMP4 regulates Tbx5 protein subcellular localization and activity. *J Cell Biol*. 2006;174(3):339-348. doi:10.1083/jcb.200511109

43. Camarata T, Snyder D, Schwend T, Klosowiak J, Holtrup B, Simon HG. Pdlim7 is required for maintenance of the mesenchymal/epidermal Fgf signaling feedback loop during zebrafish pectoral fin development. *BMC Dev Biol*. 2010;10:104. doi:10.1186/1471-213X-10-104

44. Soukarieh O, Gaildrat P, Hamieh M, et al. Exonic Splicing Mutations Are More Prevalent than Currently Estimated and Can Be Predicted by Using In Silico Tools. *PLoS Genet*. 2016;12(1):e1005756. doi:10.1371/journal.pgen.1005756

45. Livesey BJ, Marsh JA. Updated benchmarking of variant effect predictors using deep mutational scanning. *Mol Syst Biol*. 2023;19(8):e11474. doi:10.15252/msb.202211474

46. Fowler DM, Adams DJ, Gloyn AL, et al. An Atlas of Variant Effects to understand the genome at nucleotide resolution. *Genome Biol*. 2023;24(1):147. doi:10.1186/s13059-023-02986-x

47. McDonnell AF, Plech M, Livesey BJ, et al. Deep mutational scanning quantifies DNA binding and predicts clinical outcomes of PAX6 variants. Published online July 26, 2023:2023.07.25.550478. doi:10.1101/2023.07.25.550478

48. Patel MJ, DiStefano MT, Oza AM, et al. Disease-specific ACMG/AMP guidelines improve sequence variant interpretation for hearing loss. *Genet Med Off J Am Coll Med Genet*. 2021;23(11):2208-2212. doi:10.1038/s41436-021-01254-2

SUPPLEMENTARY MATERIALS

Supp Data 1 – *TBX5* (HGNC:11604) missense variants previously reported in the literature with functional validation (NM_000192.3). ND: not determined; Ref.: reference.

Genomic position (hg38) NC_000012.12	HGVS DNA NM_000192.3	Exon	HGVS protein NP_000183.2	Ref.	Published functional characterization	Published protein studies	Family history	Variant segregation
g.114841559G>T	c.145C>A	2	p.(Gln49Ly)s	[1,2]	Loss of function			
g.114839712A>G	c.161T>C	3	p.(Ile54Thr)	[1,2]	Loss of function			
g.114839658G>T	c.215C>A	3	p.(Thr72Lys)	[3]	no			De novo
g.114839653T>C	c.220A>G	3	p.(Met74Val)	[4]		No impact on stability [5]	Sporadic	ND
g.114839651C>G	c.222G>C	3	p.(Met74Ile)	[6]	Loss of function			De novo
g.114839635C>T	c.238G>A	3	p.(Gly80Arg)	[2,7,8]	Loss of function			
g.114839632T>A	c.241A>T	3	p.(Arg81Trp)	[9]		critical residues for DNA binding	Familial	3 affected members
g.114837427G>A	c.253C>T	4	p.(Pro85Ser)	[10]	no			De novo
g.114837427G>T	c.253C>A	4	p.(Pro85Thr)	[11]	Loss of function			De novo
g.114837426G>A	c.254C>T	4	p.(Pro85Leu)	[10]			Sporadic	ND
g.114837414A>T	c.266T>A	4	p.(Val89Glu)	[12]			Sporadic	ND
g.114837399A>C	c.281T>G	4	p.(Leu94Arg)	[6]	Loss of function			De novo
g.114837319A>C	c.361T>G	4	p.(Trp121Gly)	[13]		impact on stability [5]	Familial	5 affected members
g.114836515C>G	c.373G>C	5	p.(Gly125Arg)	[14]	Gain of function			
g.114836407T>G	c.481A>C	5	p.(Thr161Pro)	[15]	no			De novo
g.114836383C>T	c.505G>A	5	p.(Gly169Arg)	[2(p200),8,16]	Loss of function			
g.114832689T>C	c.520A>G	6	p.(Asn174Asp)	[10]			NI	ND
g.114832625C>G	c.584G>C	6	p.(Gly195Ala)	[13]			Sporadic	ND
g.114823368G>A	c.668C>T	7	p.(Thr223Met)	[10,13,17]	Loss of function			
g.114823359T>C	c.677A>G	7	p.(Lys226Arg)	[10]	no			De novo
g.114823358C>A	c.678G>T	7	p.(Lys226Asn)	[18]		critical residues for DNA binding	Familial	2 affected members
g.114823342A>C	c.694T>G	7	p.(Phe232Val)	[10]		critical residues for DNA binding	Sporadic	ND
g.114823327G>A	c.709C>T	7	p.(Arg237Trp)	[2,7,8,10]	Loss of function			
g.114823326C>T	c.710G>A	7	p.(Arg237Gln)	[2,8,10,19(p1)]	Loss of function			
g.114823326C>G	c.710G>C	7	p.(Arg237Pro)	[6]	Loss of function			De novo
g.114823323C>G	c.713G>C	7	p.(Gly238Ala)	[20]			Sporadic	ND
g.114823281C>A	c.755G>T	7	p.(Ser252Cys)	[2,8,16]	Loss of function			
g.114804171T>A	c.781A>T	8	p.(Ser261Cys)	[13]			Familial	3 affected members

Supp Data 2 – Pedigree and phenotypes of affected family members with *TBX5* deep intronic variant. Patients circled in red have been studied through Genome sequencing (alignment on reference genome hg38)

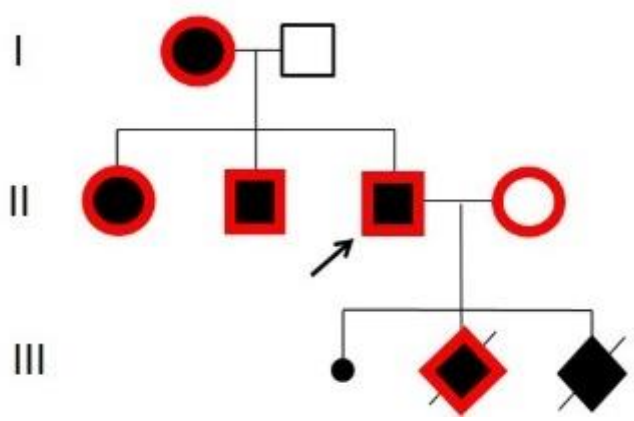

Patients	Limb phenotype	Heart phenotype
I1	Bilateral thenar hypoplasia	No
II1	Bilateral thumb hypoplasia, limited flexion on left	Patent ductus arteriosus
II2	Bilateral thenar hypoplasia	Ventricular septal defect
II3	Bilateral thenar hypoplasia	Atrial septal defect
III2 Fetus 26WG	No severe radial defect, but thumbs not precisely examined	Complex cardiac malformation (single ventricle, mitral atresia)
III3 Fetus 10WG	Bilateral phocomelia with absent thumbs	Congenital cardiac malformation: pulmonary atresia, ventricular septal defect

Supp Data 3 – *In silico* databases used in this study

- **Missense variants effect in silico predictors**:
  - CADD [21]
  - REVEL [22]
  - EVE [23]
  - VARITY [24]
  - AlphaMissense [25]

- **Structure predictions:**
  - Phyre2 [26]
  - Alphafold [27]
  - Missense 3D [28,29]

- **Sequence conservation:**
  - Clustal Omega (EMBL-EBI) [30]

- **Splice variant effect in silico predictors:**
  - MaxEntScan [31]
  - SPIP [32]
  - Splice AI [33]
  - Splice AI visual [34]

- **Population and patient databases:**
  - GnomAD [35]
  - ClinVar [36]
  - DECIPHER [37]
  - LOVD [38]

Supp Data 4– Primers used for site-directed mutagenesis (SDM) in pRP TBX5 wild type wildtype constructs of *TBX5* missense variants with Q5 site-directed mutagenesis (NEB)

Wild type and mutant TBX5-expressing plasmids pRP[Exp]–CMV>3xFLAG/hTBX5[NM_000192.3] were constructed and packaged by Vectorbuilder.

IDs to retrieve detailed information about the vectors on vectorbuilder.com: VB230130-1017aem, VB230130-1019bpu, VB230130-1020uxt, VB230130-1021wve, VB230130-1022xug, VB230130-1023vvb, VB230130-1024bgv, VB230130-1025npq, VB230130-1026wxr, VB230130-1027cae, VB230130-1028qgz, VB230130-1029dck.

***TBX5* Variants**	**Wildtype construct**	**SDM_Forward primer**	**SDM_Reverse primer**
c.710G>C	pRP-TBX5-WT	AAAGGATTTCCGGGCAGTGATG	GGCAAAGGGATTATTCTC
c.835C>T	pRP-TBX5-WT	CAGCGAGTCTTGAGCTCTCTC	CTGAAAGGACTGTGGTTG

Supp Data 5 – Primers for cloning and site directed mutagenesis of *TBX5* splice variants

A. Minigene amplicons: design and primer sequences

minigene amplicon	size (bp)	Forward primer	Reverse primer
TBX5 intron 6	393	[CGCGGATCC]-AGAACTAGGAAACGCTATCTGC	[CGCACGCGT]-ACGGGACCCACCACTTCAT
TBX5 exon 3	463	[CGCGGATCC]-GCTGTTGGGTGCTCCAGATA	[CGCACGCGT]-TGGAGGAATCTCCTTGTGCC
TBX5 exon 4	472	[CGCGGATCC]-CGGGATGGATCTTGCGGAG	[CGCACGCGT]-CATCTGGAAAACCGGAGCTAA
TBX5 exon 5	552	[CGCGGATCC]-GGGATGCGAGAGGCTGTAAG	[CGCACGCGT]-TCCAGATCAAGAAGGTAGAGGC
TBX5 exon 7	598	[CGCGGATCC]-CCCAGCTGGAATGATGCAGA	[CGCACGCGT]-ACTCTTCGTACCTTCTCTCCAC

B. Primers used for site-directed mutagenesis (SDM) in pCAS2 wildtype constructs with Quick Change site-directed mutagenesis (Agilent)

TBX5 Variant	Wildtype construct	SDM_Forward primer	SDM_Reverse primer
c.241A>T	TBX5 exon 3	caacaaaccatctcaccatccagccttggttatgatc	gatcataaccaaggctggatggtgagatggtttgttg
c.361T>G	TBX5 exon 4	cccagtgcctacccttattatctgcgaatttgtatctg	cagatacaaattcgcagataataaagggtaggcactggg

C. Primers used for site-directed mutagenesis (SDM) in pCAS2 wildtype constructs with Q5 site-directed mutagenesis (NEB)

TBX5 Variant	wildtype construct	SDM_Forward primer	SDM_Reverse primer
c.510+5G>C	TBX5 exon 5	GGGCATGTGACTACCGTGGCC	AAATGGGTCCAGGTGG
c.510+5G>T	TBX5 exon 5	GGGCATGTGATTACCGTGGCC	AAATGGGTCCAGGTGGTTG

Supp Data 6 – *In vitro* minigene assays

Minigene splice assays were carried out pCAS2 vector carries two exons (named A and B) with a sequence derived from the human *SERPING1/C1NH* gene (HGNC:1228), separated by an intron with BamHI and MluI cloning sites, under the control of a CMV promoter. The translation initiation codon is disrupted so that the RNA products are resistant to nonsense-mediated mRNA decay. Genomic fragments encompassing the variants studied and flanking intronic regions were amplified by PCR using the AmpliTaq Gold DNA polymerase (ThermoFisher) and cloned into the pCAS2 by a restriction digestion/ligation strategy using BamHI and MluI (Biolabs). Forward primers include a tail of 10 nts with restriction site BamHI (AGTCGGATCC). Reverse primers carry a tail with restriction site MluI (AGCTACGCGT). Wild-type constructs were obtained from the wild-type alleles. Mutant constructs were obtained either from the patients' DNA when available, or through mutagenesis with QuickChange II Site-directed mutagenesis kit (Agilent) or Q5 site directed mutagenesis technology (NEB) according to the manufacturers' instructions. The primers used for genomic amplification and site-directed mutagenesis are listed in Supp Data 2. Plasmid DNA were isolated with Nucleospin Plasmid Minikit for plasmid DNA (Macherey-Nagel) and Sanger sequenced for verification with the vector-specific sequence primers pCAS-seq-F: 5'- GGGGTCAATAGCAGTGAGAG-3'; pCAS-seq-R: 5'-GCTCCATTTCACAGGTAGAGA-3'. The wild-type and mutant minigene constructs were transfected into HeLa cells using the Effectene transfection reagent (Qiagen) (250ng of plasmid per well in a 24-well plate). Cells were collected 24h after transfection. Total RNA was extracted using Nucleospin RNA, Minikit for RNA purification (Macherey Nagel), according to the manufacturer's instructions. Between 500-750ng was used to synthetize cDNA, with SuperScript VILO (Thermofisher Scientific), according to the manufacturer's instructions. RT-PCR analysis of the minigene transcripts was performed using AmpliTaq Gold DNA polymerase and vector-specific primers located in the flanking exons A and B (pCAS-KOI-F: 5'-TGACGTCGCCGCCCATCAC-3' and pCAS-2R: 5'- ATTGGTTGTTGAGTTGGTTGTC-3'). RT-PCR products were separated by electrophoresis on 2% agarose gels and Sanger sequenced. In case of partial exon skipping, a fragment analysis has been performed, using ONE STEP (Qiagen) with a fluorescent forward primer pCAS-KOI-F. Size standards and sample fragments were loaded in a

capillary run (3730 Series Genetic Analyzers, Thermo Fisher Scientific) under the same electrophoretic forces, allowing to determine the size of each fragment.

Supp Data 7 - Primers for in vivo *TBX5* transcripts analysis

Primer	Location	Primer sequence
Forward primer	Exon 4 – exon 5 junction	TAAATGGTCTGTGACGGGCA
Reverse primer	Predicted pseudo-exon in intron 6	GATCGTTGCACATCAGGCAG

Supp Data 8 – ACMG criteria (from Richards *et al.* 2015)

Criteria	Strength	Detail
PM1	Moderate	Located in a mutational hot spot and/or critical and well-established functional domain (e.g., active site of an enzyme) without benign variation
PM2	Supporting	Absent from controls (or at extremely low frequency if recessive) in Exome Sequencing Project, 1000 Genomes Project, or Exome Aggregation Consortium
PM5	Moderate	Novel missense change at an amino acid residue where a different missense change determined to be pathogenic has been seen before
PP1	Supporting	Cosegregation with disease in multiple affected family members in a gene definitively known to cause the disease
PP2	Supporting	Missense variant in a gene that has a low rate of benign missense variation and in which missense variants are a common mechanism of disease
PP3	Supporting	Multiple lines of computational evidence support a deleterious effect on the gene or gene product (conservation, evolutionary, splicing impact, etc.)
BP4	Supporting	Multiple lines of computational evidence suggest no impact on gene or gene product (conservation, evolutionary, splicing impact, etc.)
PP4	Supporting	Patient's phenotype or family history is highly specific for a disease with a single genetic etiology
PS3	Supporting	Well-established in vitro or in vivo functional studies supportive of a damaging effect on the gene or gene product
BS3	Supporting	Well-established in vitro or in vivo functional studies show no damaging effect on protein function or splicing

Supp Data 9 – Sequence comparison between TBX5 and other human T-box proteins described in human genetic conditions (TBX1, TBX2, TBX3, TBX4, TBX6, TBX15, TBX22; HGNC:11592, 11597, 11602, 11603, 11605, 11594, 11600). The residues of interest in our study are highlighted in yellow.

```
sp|Q99593|TBX5_HUMAN       -------ALGAPSK-SPSS-----PQAAFTQQGMEGIKVFLHERELWLKFHEVGTEMIIT 77
sp|O43435|TBX1_HUMAN       -------AAE-PEGPGASCA-AAAKAPVKKNAKVAGVSVQLEMKALWDEFNQLGTEMIVT 133
sp|Q13207|TBX2_HUMAN       EAGLHVSALG-PHPPAAHL--RSLKSLEPEDEVEDDPKVTLEAKELWDQFHKLGTEMVIT 128
sp|O15119|TBX3_HUMAN       ETGIPFSSLG----PQAHL--RPLKTMEPEEEVEDDPKVHLEAKELWDQFHKRGTEMVIT 126
sp|P57082|TBX4_HUMAN       APGLSGAALGSPPGPGADV-----VAAAAAEQTIENIKVGLHEKELWKKFHEAGTEMIIT 90
sp|O95947|TBX6_HUMAN       -------AMG---------T-EPAPSAPEALHSLPGVSLSLENRELWKEFSSVGTEMIIT 114
sp|Q96SF7|TBX15_HUMAN      RTSCSFSTHT-------DLASGAAGPVPAAMSSMEEIQVELQCADLWKRFHDIGTEMIIT 136
sp|Q9Y458|TBX22_HUMAN      SSGCGS-----------D--SGY-G-NSSESLEEKDIQMELQGSELWKRFHDIGTEMIIT 115
                                                  .: *.   ** .* . ****::*

sp|Q99593|TBX5_HUMAN       KAGRRMFPSYKVKVTGLNPKTKYILLMDIVPADDHR--YKFADNKWSVTGKAEP-AMPGR 134
sp|O43435|TBX1_HUMAN       KAGRRMFPTFQVKLFGMDPMADYMLLMDFVPVDDKRYRYAFHSSSWLVAGKADP-ATPGR 192
sp|Q13207|TBX2_HUMAN       KSGRRMFPPFKVRVSGLDKKAKYILLMDIVAADDCR--YKFHNSRWMVAGKADP-EMPKR 185
sp|O15119|TBX3_HUMAN       KSGRRMFPPFKVRCSGLDKKAKYILLMDIIAADDCR--YKFHNSRWMVAGKADP-EMPKR 183
sp|P57082|TBX4_HUMAN       KAGRRMFPSYKVKVTGMNPKTKYILLIDIVPADDHR--YKFCDNKWMVAGKAEP-AMPGR 147
sp|O95947|TBX6_HUMAN       KAGRRMFPACRVSVTGLDPEARYLFLLDVIPVDGAR--YRWQGRRWEPSGKAEP-RLPDR 171
sp|Q96SF7|TBX15_HUMAN      KAGRRMFPAMRVKITGLDPHQQYYIAMDIVPVDNKRYRYVYHSSKWMVAGNADS-PVPPR 195
sp|Q9Y458|TBX22_HUMAN      KAGRRMFPSVRVKVKGLDPGKQYHVAIDVVPVDSKRYRYVYHSSQWMVAGNTDHLCIIPR 175
                           *:*****  :*   *::    * . :*.: .*. *  * : .  *  :*:::      *

sp|Q99593|TBX5_HUMAN       LYVHPDSPATGAHWMRQLVSFQKLKLTNNHLDPFGHI--------------------ILN 174
sp|O43435|TBX1_HUMAN       VHYHPDSPAKGAQWMKQIVSFDKLKLTNNLLDDNGHI--------------------ILN 232
sp|Q13207|TBX2_HUMAN       MYIHPDSPATGEQWMAKPVAFHKLKLTNNISDKHGFT--------------------ILN 225
sp|O15119|TBX3_HUMAN       MYIHPDSPATGEQWMSKVVTFHKLKLTNNISDKHGFTLAFPSDHATWQGNYSFGTQTILN 243
sp|P57082|TBX4_HUMAN       LYVHPDSPATGAHWMRQLVSFQKLKLTNNHLDPFGHI--------------------ILN 187
sp|O95947|TBX6_HUMAN       VYIHPDSPATGAHWMRQPVSFHRVKLTNSTLDPHGHL--------------------ILH 211
sp|Q96SF7|TBX15_HUMAN      VYIHPDSLASGDTWMRQVVSFDKLKLTNNELDDQGHI--------------------ILH 235
sp|Q9Y458|TBX22_HUMAN      FYVHPDSPCSGETWMRQIISFDRMKLTNNEMDDKGHI--------------------ILQ 215
                           .: **** ..*  ** : ::*.::****.  *  *.                    **:

sp|Q99593|TBX5_HUMAN       SMHKYQPRLHIVKADENNGFGSK-----NTAFCTHVFPETAFIAVTSYQNHKITQLKIEN 229
sp|O43435|TBX1_HUMAN       SMHRYQPRFHVVYVDPRKDSEKY---A-EENFKTFVFEETRFTAVTAYQNHRITQLKIAS 288
sp|Q13207|TBX2_HUMAN       SMHKYQPRFHIVRAN---DILKL---P-YSTFRTYVFPETDFIAVTAYQNDKITQLKIDN 278
sp|O15119|TBX3_HUMAN       SMHKYQPRFHIVRAN---DILKL---P-YSTFRTYLFPETEFIAVTAYQNDKITQLKIDN 296
sp|P57082|TBX4_HUMAN       SMHKYQPRLHIVKADENNAFGSK-----NTAFCTHVFPETSFISVTSYQNHKITQLKIEN 242
sp|O95947|TBX6_HUMAN       SMHKYQPRIHLVRAA---QLCSQ---H-WGGMASFRFPETTFISVTAYQNPQITQLKIAA 264
sp|Q96SF7|TBX15_HUMAN      SMHKYQPRVHVIRKDFSSDLSPTKPVPVGDGVKTFNFPETVFTTVTAYQNQQITRLKIDR 295
sp|Q9Y458|TBX22_HUMAN      SMHKYKPRVHVIEQGSSVDLSQIQSLP-TEGVKTFSFKETEFTTVTAYQNQQITKLKIER 274
                           ***:*:**.*::              . :. * ** * :**:*** :**:***

sp|Q99593|TBX5_HUMAN       NPFAKGFRGSDDMELHRMSRMQS----KEYPVVPRSTVRQKVASNHSPFSSESRALSTSS 285
sp|O43435|TBX1_HUMAN       NPFAKGFRDCDPEDWPRNHRPGALPLMSAFARS-----RNPVASPTQP----------SG 333
sp|Q13207|TBX2_HUMAN       NPFAKGFRDTGNGRREKRK-QLTLPSLRLYEEH-----CKPERDGAES----------DA 322
sp|O15119|TBX3_HUMAN       NPFAKGFRDTGNGRREKRK-QLTLQSMRVFDER-----HKKENGTSDE----------SS 340
sp|P57082|TBX4_HUMAN       NPFAKGFRGSDDSDL-RVARLQS----KEYPVISKSIMRQRLISPQLSATPDVGPLLGTH 297
sp|O95947|TBX6_HUMAN       NPFAKGFRENGRNCKRERDARVK-------RKL-----RGPEPAATEA----------YG 302
sp|Q96SF7|TBX15_HUMAN      NPFAKGFRDSGRNRTGLEAIME------TYAFW-----RPPVRTLTFE----------DF 334
sp|Q9Y458|TBX22_HUMAN      NPFAKGFRDTGRNRGVLDGLLE------TYP-W-----RPSF-TLDFK----------TF 311
                           ********  .
```

Supp Data 10 – In silico predictions for *TBX5* missense variants that have been previously characterized in the literature

Genomic position (hg38) NC_000012.12	HGVS DNA NM_000192.3	HGVS protein NP_000183.2	Reference	Functional characterization	Sporadic / Familial	Domain	AlphaMissense	CADD	REVEL
g.114841559G>T	c.145C>A	p.(Gln49Lys)	[1,2]	loss of function	NI	no	0,361 (Ambiguous)	27,5	0,509 (Ambiguous)
g.114839712A>G	c.161T>C	p.(Ile54Thr)	[1,2]	loss of function	NI	no	0,979 (Likely pathogenic)	24,7	0,732 (Damaging)
g.114839658G>T	c.215C>A	p.(Thr72Lys)	[3]	N	de novo	T Box	0,999 (Likely pathogenic)	31	0,94 (Damaging)
g.114839651C>G	c.222G>C	p.(Met74Ile)	[6]	loss of function	de novo	T Box	1 (Likely pathogenic)	23,9	0,936 (Damaging)
g.114839635C>T	c.238G>A	p.(Gly80Arg)	[2,7,8]	loss of function		T Box	1 (Likely pathogenic)	32	0,982 (Damaging)
g.114837427G>A	c.253C>T	p.(Pro85Ser)	[10]	N	de novo	T Box	1 (Likely pathogenic)	31	0,971 (Damaging)
g.114837427G>T	c.253C>A	p.(Pro85Thr)	[11]	loss of function	de novo	T Box	1 (Likely pathogenic)	31	0,969 (Damaging)
g.114837399A>C	c.281T>G	p.(Leu94Arg)	[6]	loss of function	de novo	T Box	0,999 (Likely pathogenic)	31	0,983 (Damaging)
g.114836515C>G	c.373G>C	p.(Gly125Arg)	[14]	gain of function		T Box	1 (Likely pathogenic)	27,2	0,898 (Damaging)
g.114836407T>G	c.481A>C	p.(Thr161Pro)	[15]	N	de novo	T Box	0,999 (Likely pathogenic)	31	0,96 (Damaging)
g.114836383C>T	c.505G>A	p.(Gly169Arg)	[2(p200),8,16]	loss of function		T Box	1 (Likely pathogenic)	31	0,939 (Damaging)
g.114823368G>A	c.668C>T	p.(Thr223Met)	[10,13,17]	loss of function		T Box	1 (Likely pathogenic)	28,5	0,959 (Damaging)
g.114823359T>C	c.677A>G	p.(Lys226Arg)	[10]	N	de novo	T Box	0,996 (Likely pathogenic)	29,1	0,879 (Damaging)
g.114823327G>A	c.709C>T	p.(Arg237Trp)	[2,7,8,10]	loss of function		T Box	0,999 (Likely pathogenic)	32	0,914 (Damaging)
g.114823326C>T	c.710G>A	p.(Arg237Gln)	[2,8,10,19(p1)]	loss of function		T Box	0,999 (Likely pathogenic)	29,5	0,924 (Damaging)
g.114823326C>G	c.710G>C	p.(Arg237Pro)	[6]	loss of function	de novo	T Box	1 (Likely pathogenic)	28,9	0,947 (Damaging)
g.114823281C>A	c.755G>T	p.(Ser252Ile)	[2,8,16]	loss of function		no	0,839 (Likely pathogenic)	34	0,73 (Damaging)

Supp data 11 - Predicted consequences of the *TBX5* variants studied and 2 positive controls p.(Pro85Thr) and p.(Arg237Pro) on protein structure.

(A) structural predictions of human TBX5 protein (amino-acids 54-239) in grey and the human missense variants of TBX5 protein (amino-acids 54-239) in magenta carried out with Phyre2 server.
(B) structural predictions of human TBX5 protein (amino-acids 54-239) in grey and the human missense variants of TBX5 protein (amino-acids 54-239) in blue carried out with AlphaFold v2.1.0.
(C) 5 RMSD cut-off values for studied *TBX5* variants

A.

TBX5 p.(Met74Ala)

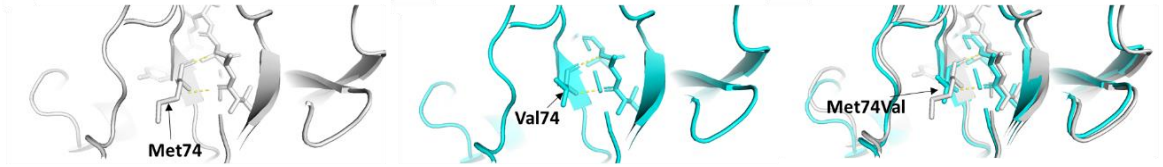

TBX5 p.(Arg81Trp)

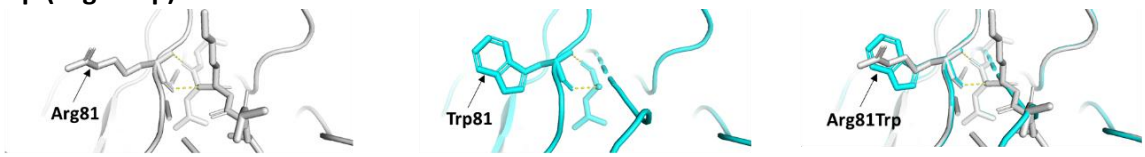

TBX5 p.(Pro85Leu)

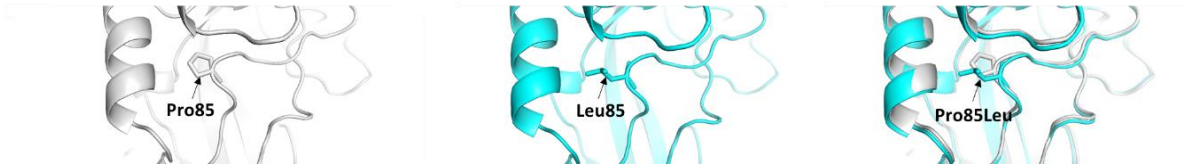

TBX5 p.(Val89Glu)

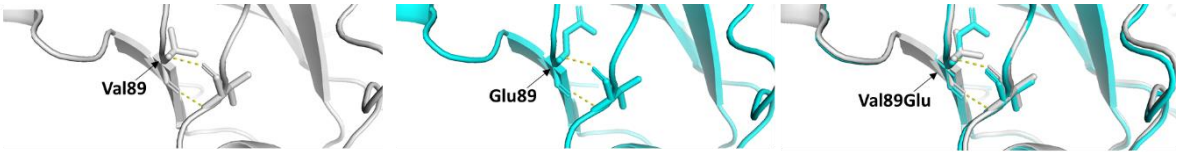

TBX5 p.(Trp121Gly)

TBX5 p.(Asn174Asp)

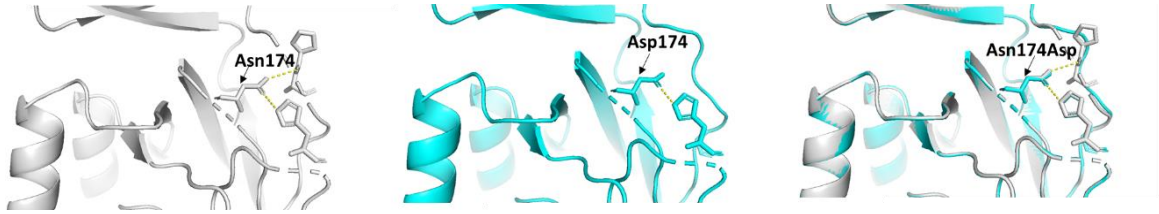

TBX5 p.(Gly195Ala)

TBX5 p.(Lys226Asn)

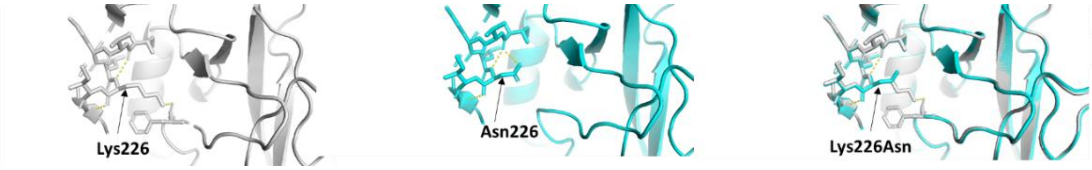

TBX5 p.(Phe232Val)

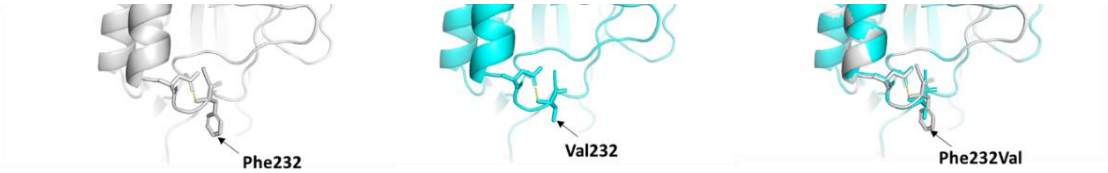

TBX5 p.(Gly238Ala)

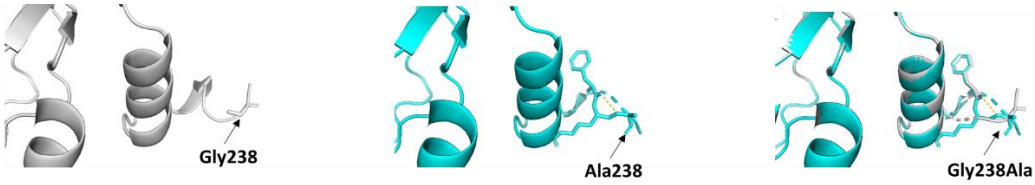

Positive control missense variants:

TBX5 p.(Pro85Thr)

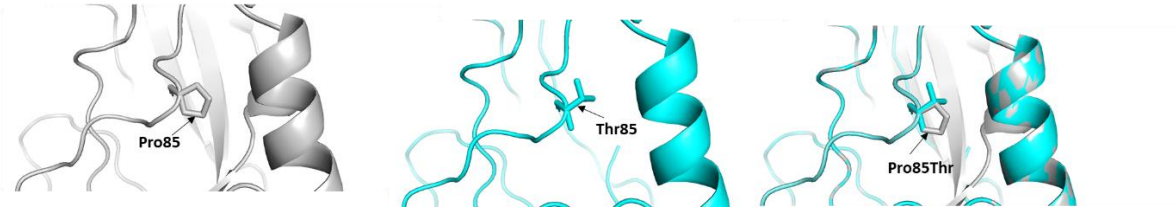

TBX5 p.(Arg237Pro)

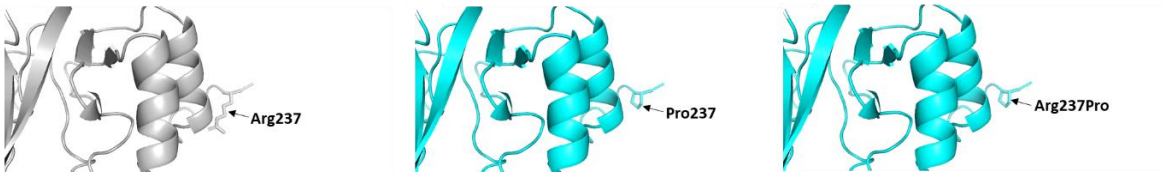

B.

TBX5 p.(Met74Val)

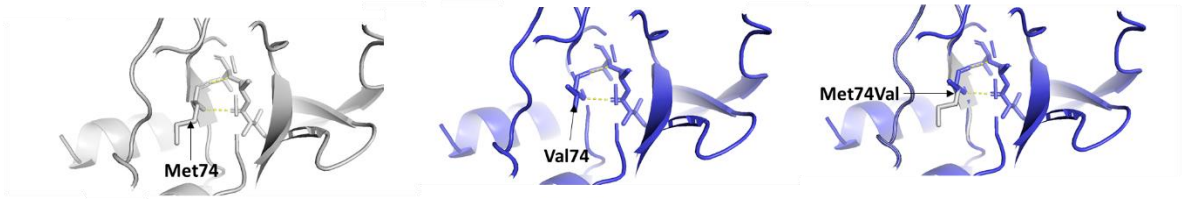

TBX5 p.(Arg81Trp)

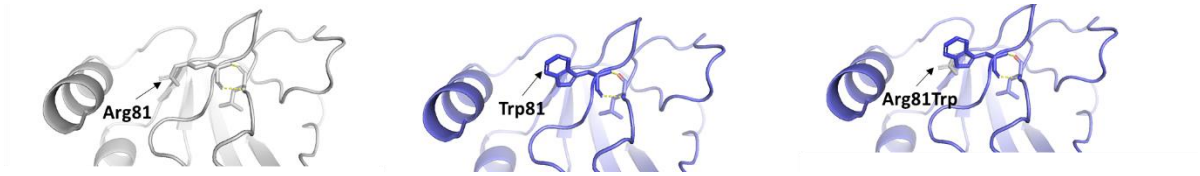

TBX5 p.(Pro85Leu)

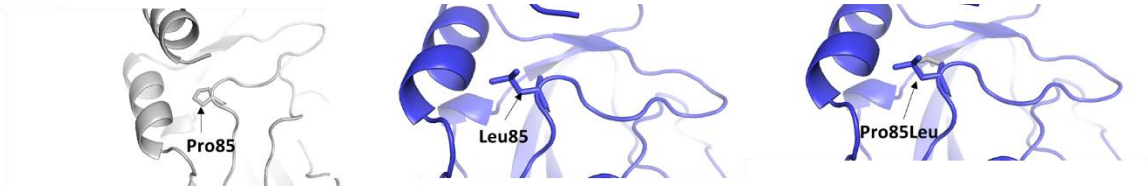

TBX5 p.(Val89Glu)

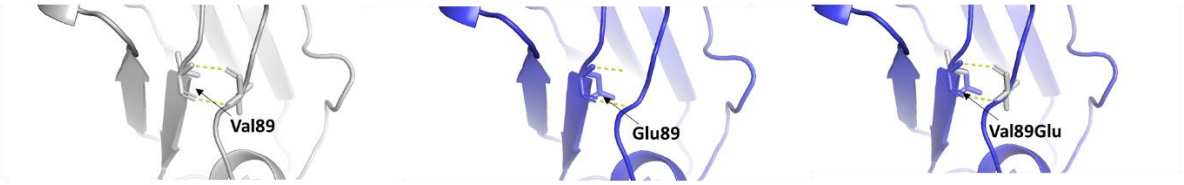

TBX5 p.(Trp121Gly)

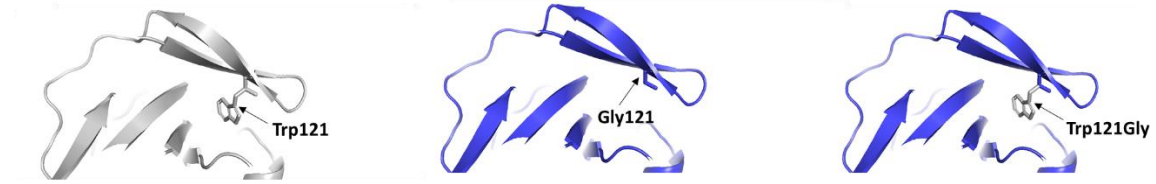

TBX5 p.(Asn174Asp)

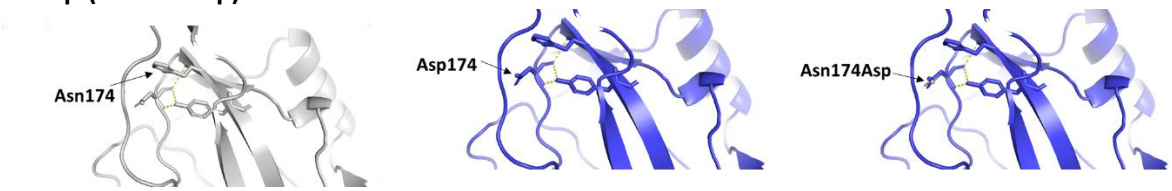

TBX5 p.(Gly195Ala)

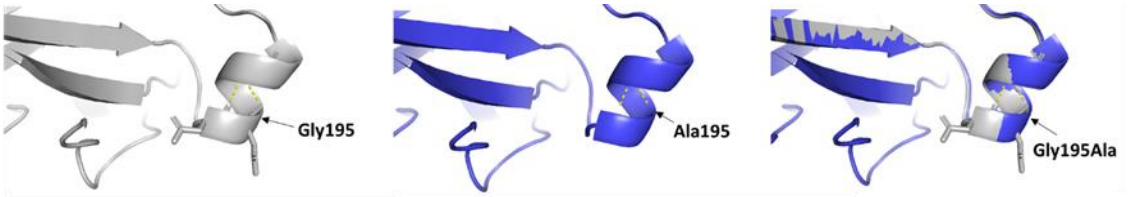

TBX5 p.(Lys226Asn)

TBX5 p.(Phe232Val)

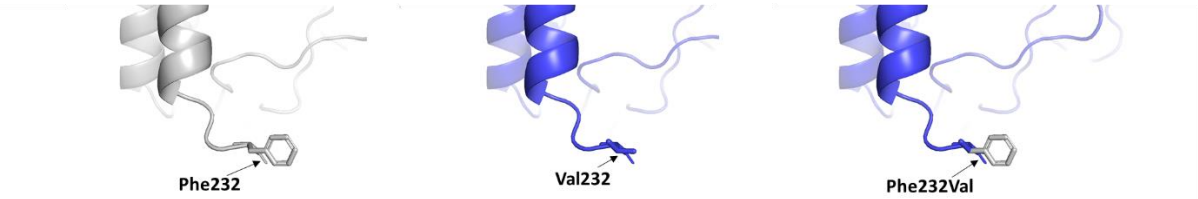

TBX5 p.(Gly238Ala)

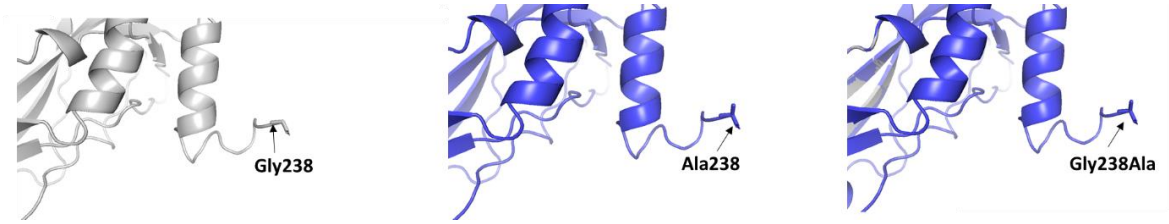

Positive control missense variants:

TBX5 p.(Pro85Thr)

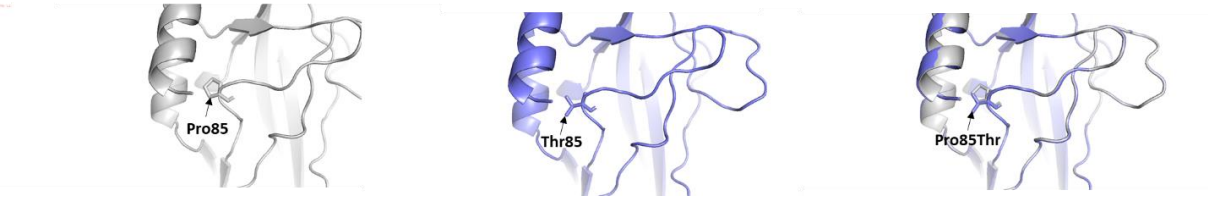

TBX5 p.(Arg237Pro)

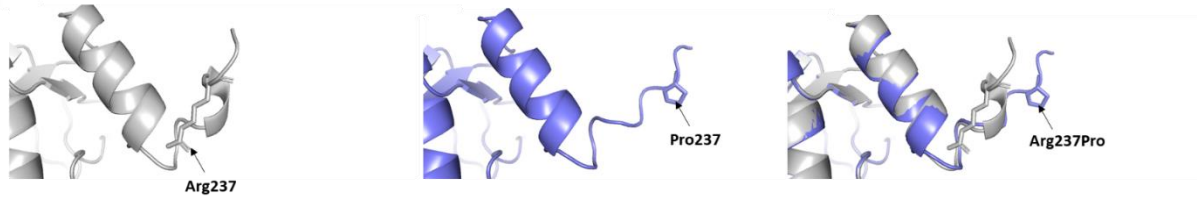

C.

***TBX5* Variants**	**5 RMSD cut-off values (mutant vs WT)**
Variants of our study	
p.(Met74Val)	0.15
p.(Arg81Trp)	0.15
p.(Pro85Leu)	0.05
p.(Val89Glu)	0.09
p.(Trp121Gly)	0.35
p.(Asn174Asp)	0.373
p.(Gly195Ala)	0.01
p.(Lys226Asn)	0.496
p.(Phe232Val)	0.13
p.(Gly238Ala)	0.02
p.(Ser261Cys)	No available protein structure prediction
Variants previously characterized in the literature	
p.(Pro85Thr)	1.35
p.(Arg237Pro)	1.06

Supp Data 12 - Splice AI visual

Predicted acceptor sites are represented in orange; predicted donor sites are represented in blue. Variant position is pointed by a green (wild-type) or a pink (mutated) rectangle.

NM_181486.4:c.664-342G>T

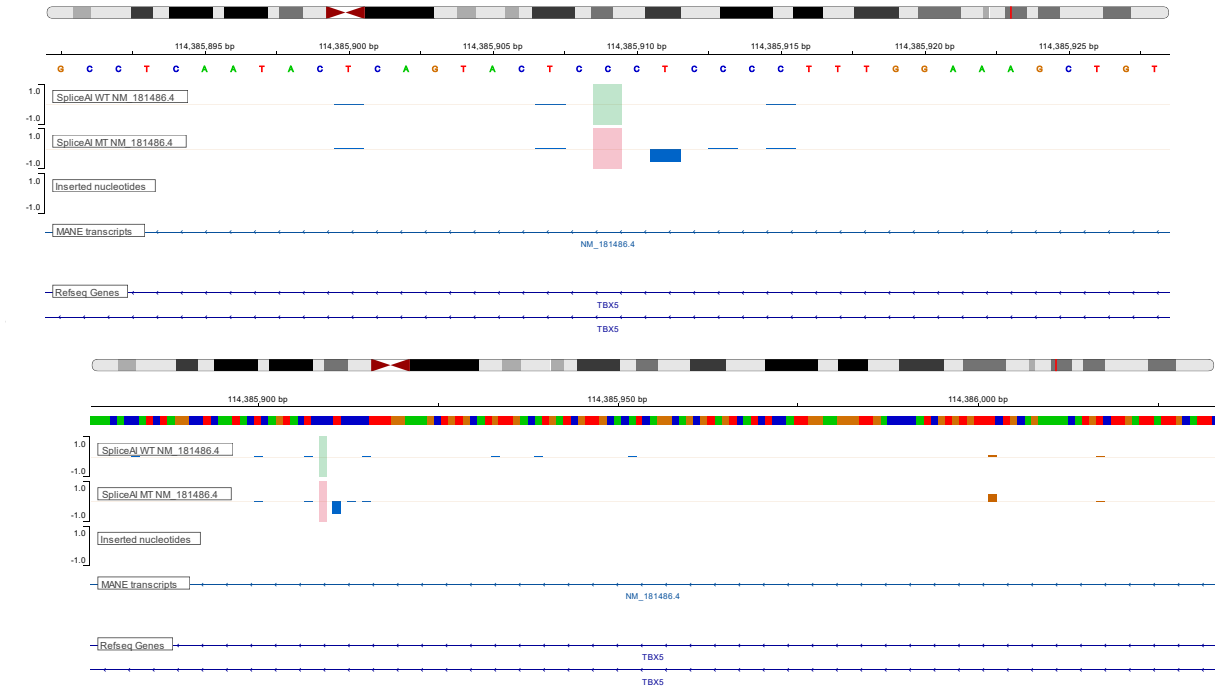

NM_181486.4:c.242G>T

NM_181486.4:c.242+5G>A

NM_181486.4:c.353A>G

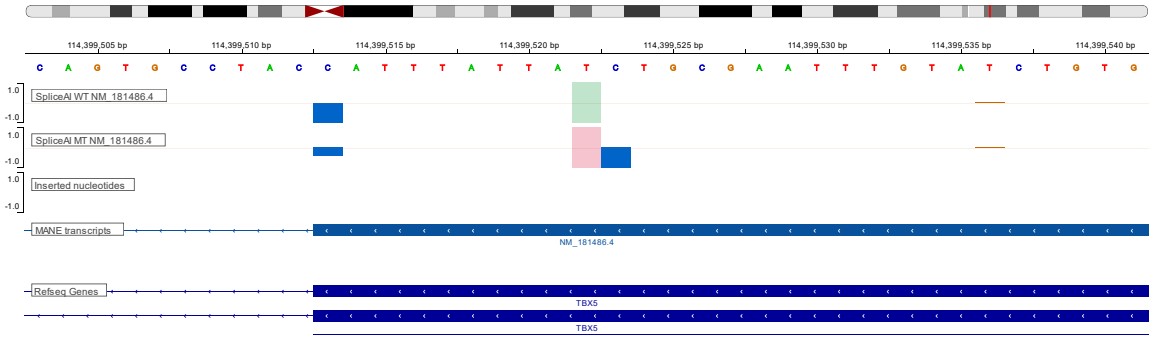

NM_181486.4:c.362G>T

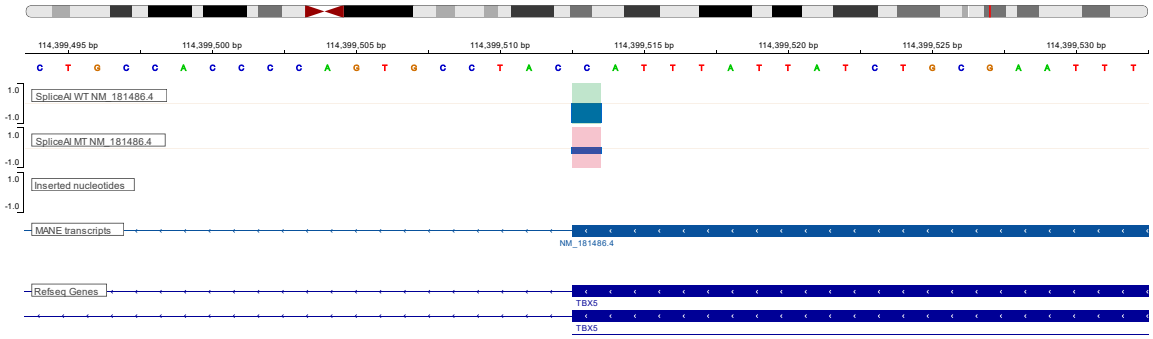

NM_181486.4:c.510+5G>A

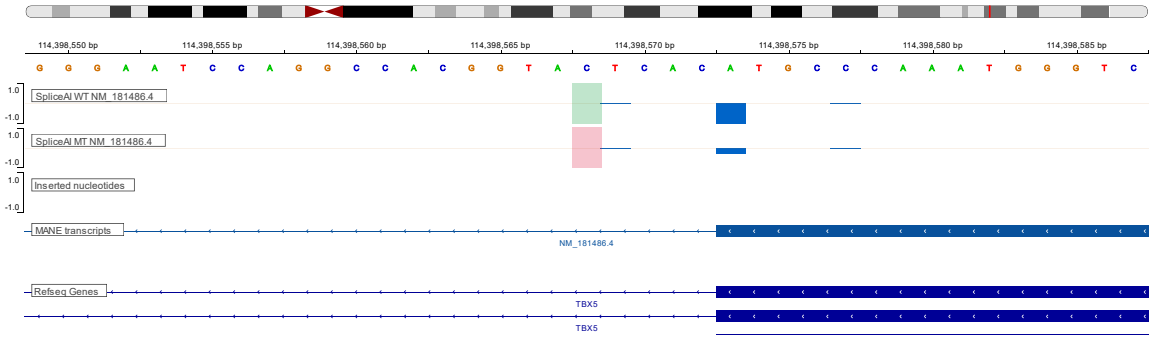

NM_181486.4:c.510+5G>T

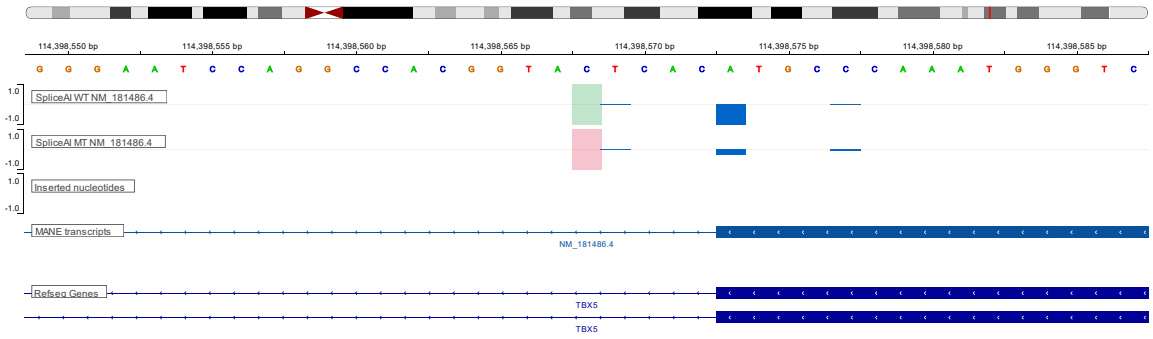

NM_181486.4:c.755G>C

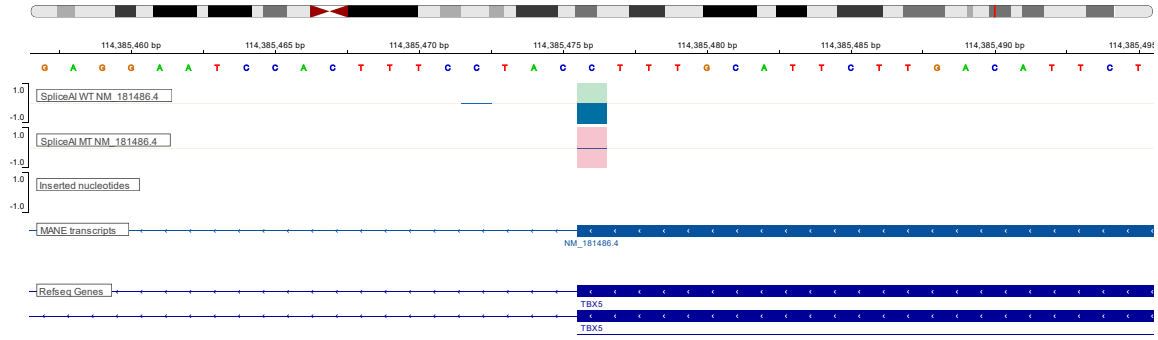

NM_181486.4:c.756-3C>G

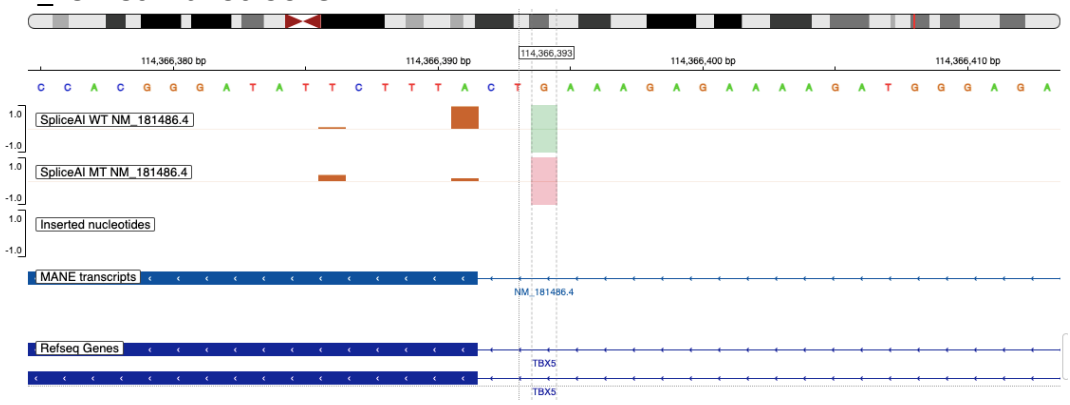

Supp Data 13 - Splice variants: minigene assays results for wild-type (WT) and *TBX5* variants.

Semi quantitative analysis has been performed if partial exon skipping.

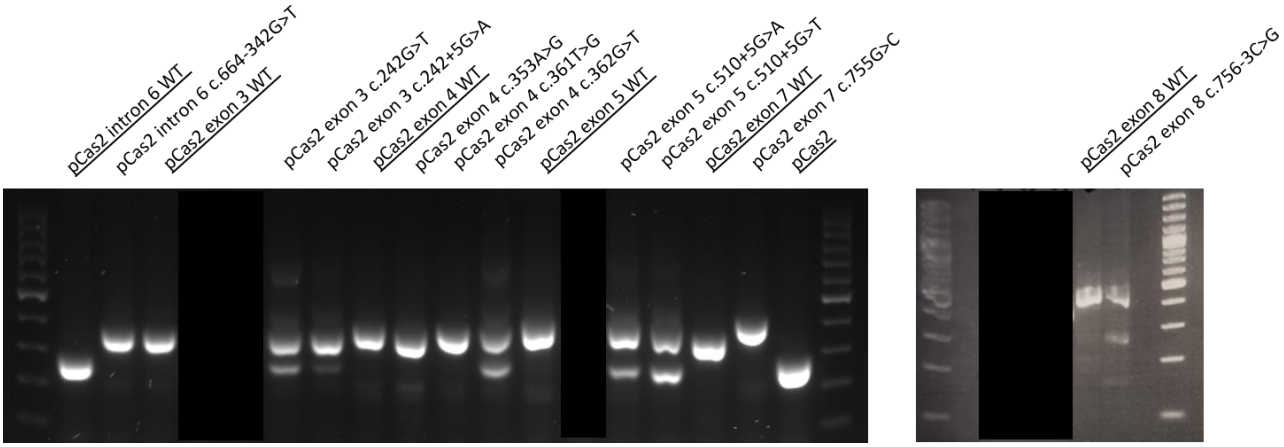

NM_181486.4:c.242G>T

Fragment analysis

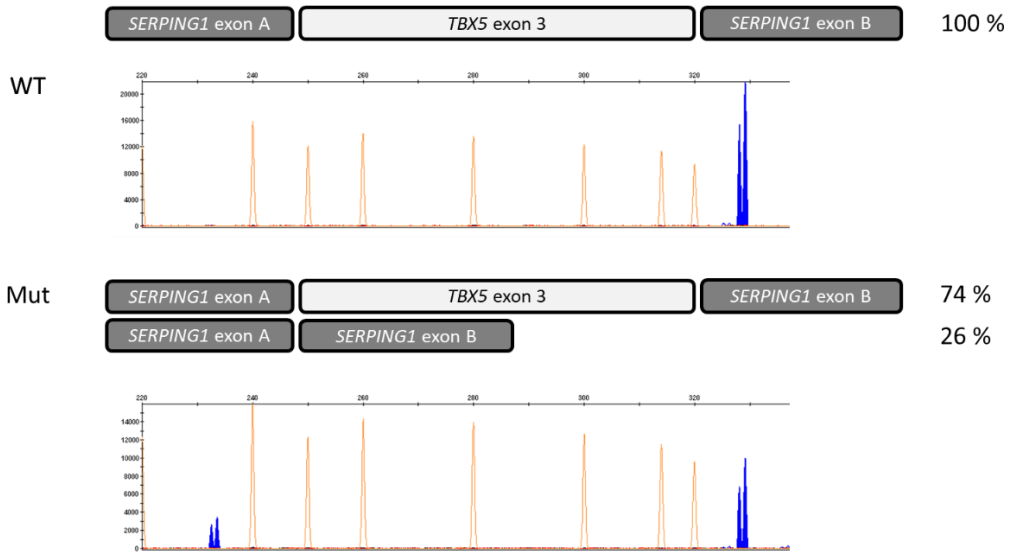

NM_181486.4:c.242+5G>A

Fragment analysis

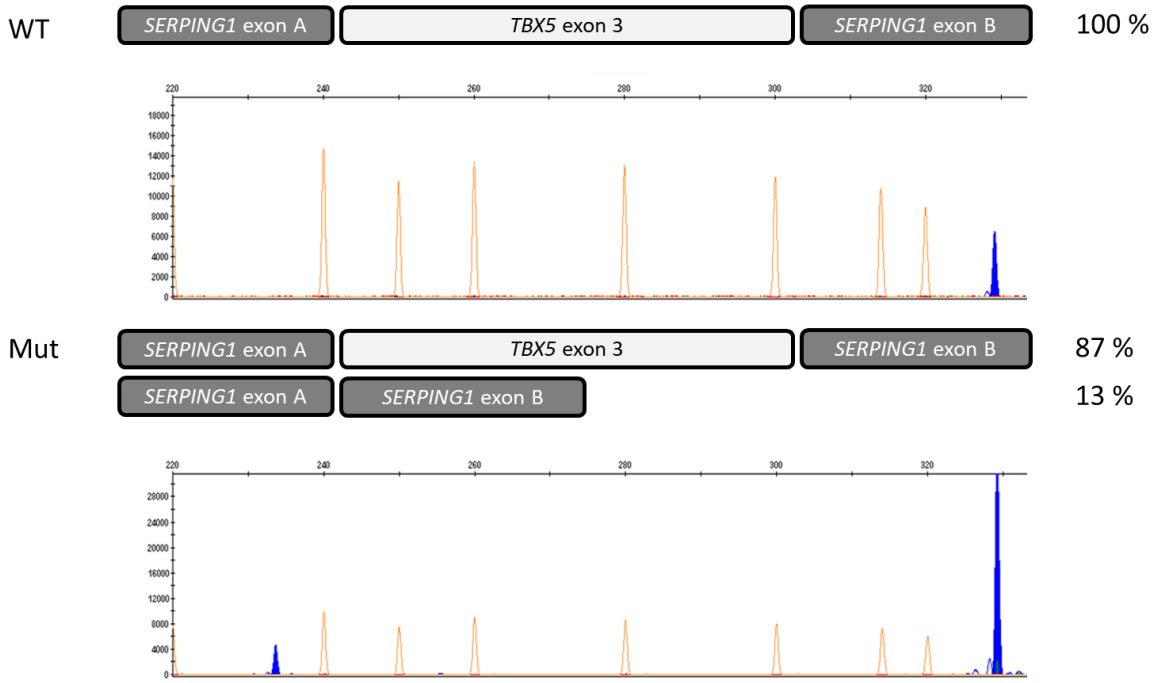

NM_181486.4:c.362G>T

Fragment analysis

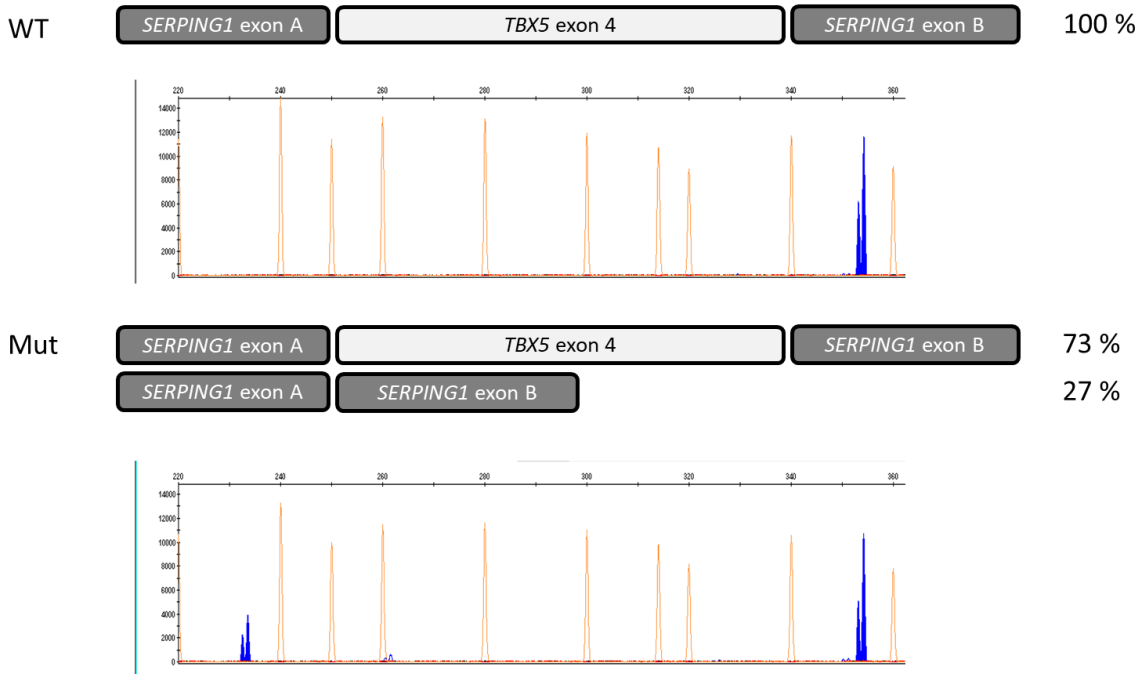

NM_181486.4:c.510+5G>A

Fragment analysis

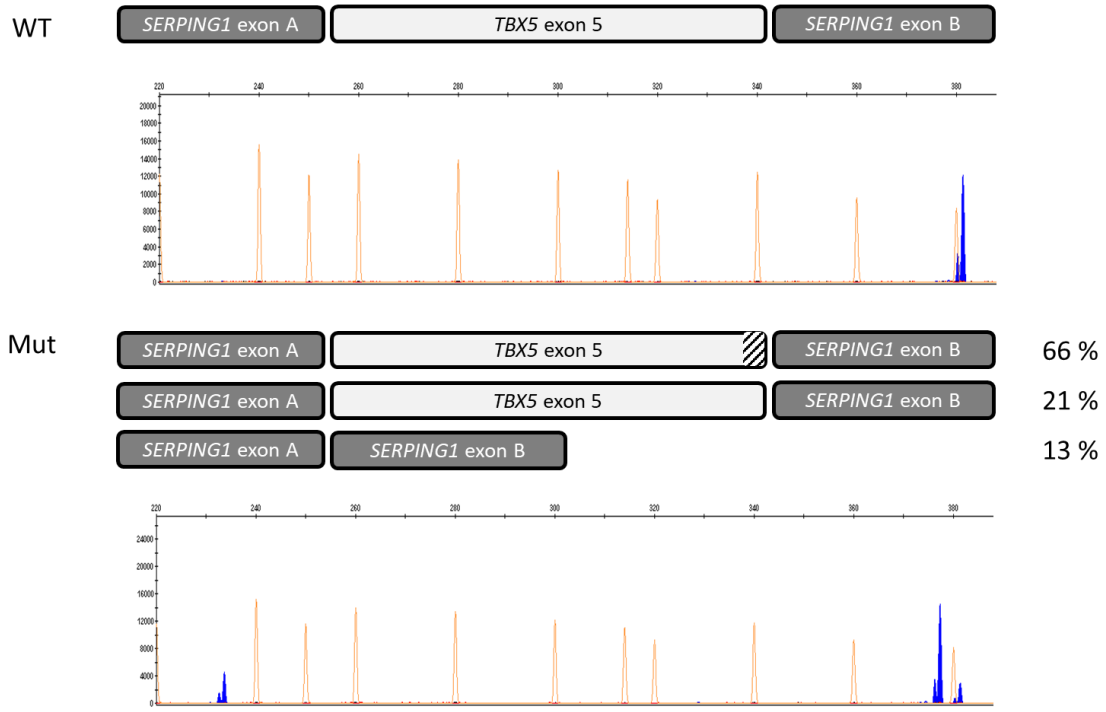

NM_181486.4:c.510+5G>T

Fragment analysis

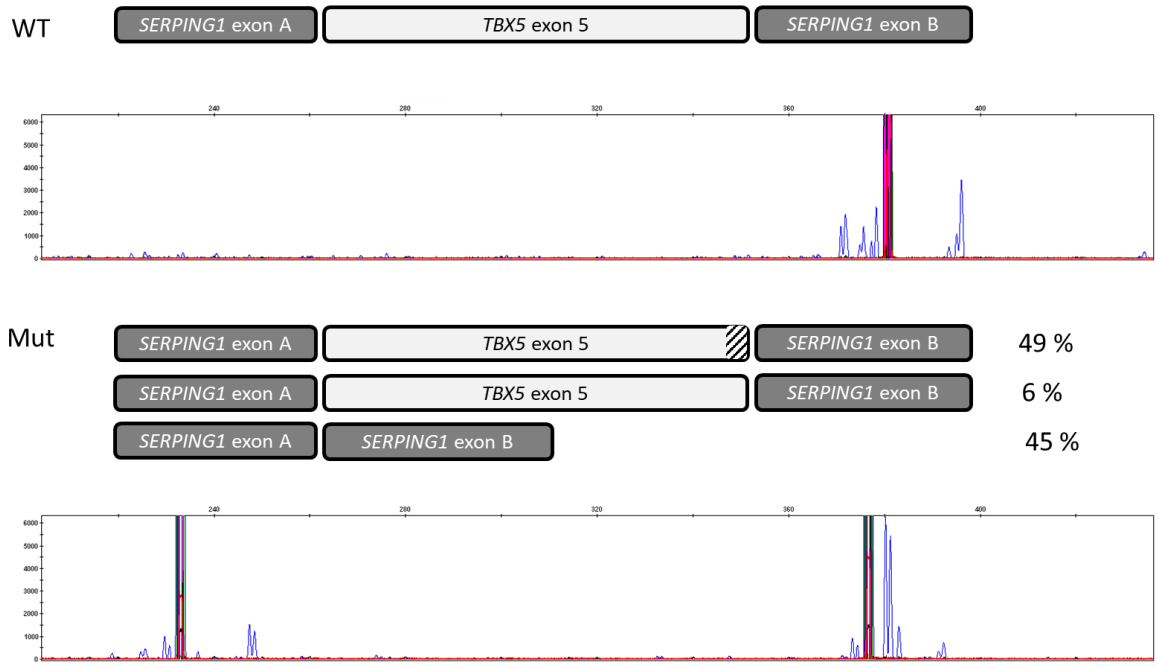

NM_181486.4: c.756-3C>G

Fragment analysis

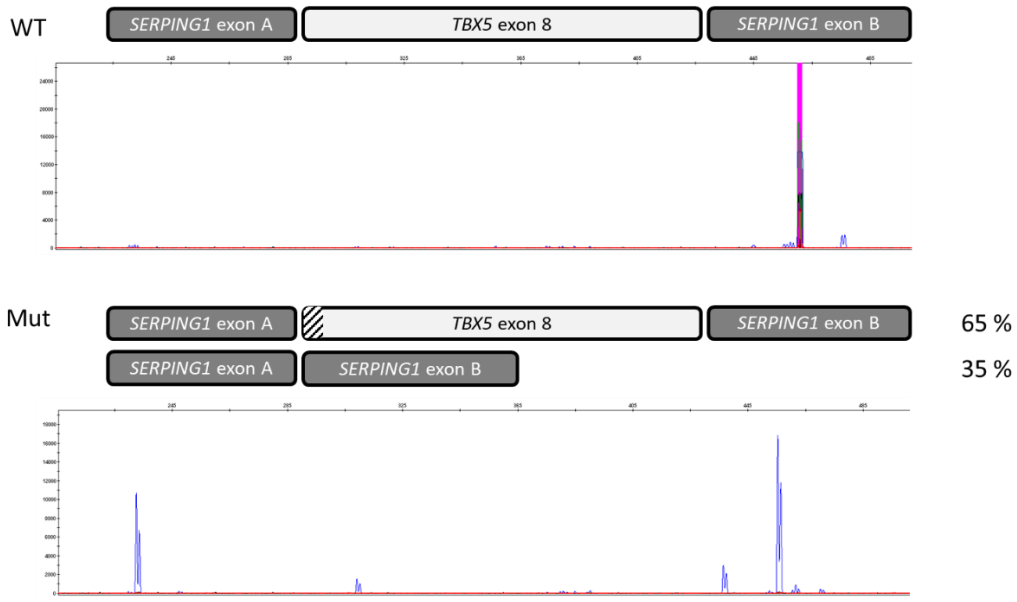

Supp data 14 – RT-PCR results of a *TBX5* deep intronic variant c.664-342G>T

A – RT-PCR with forward primer at the junction of exon 4 and 5 and a reverse primer designed in the predicted pseudo-exon. cDNA sequence at the junction of exon 6 and the pseudoexon.
B – Annotated *TBX5* sequence with the identified variant, the predicted splice donor and acceptor sites, the pseudo-exon, upstream exon 7.

A

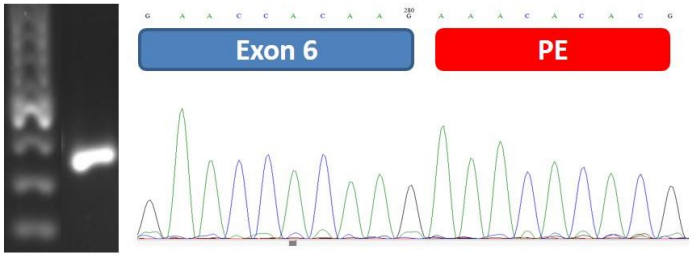

B

TTTCATTAGGCACCATTTTCCACCAGAACTAGGAAACGCTATCTGCAAAACTATGAAATG
AACATGAAATGAGGCATAATAGAATTTTTGAATGCAATAATCAAGACATGTTTTCTGCAG
/AAACACACGATGGGGTCAACCCTTCCAATGGAGATGACTACGCTGCCTGATGTGCAACGA
TCATGTCAACATGCACAGCTTTCCAAAGGGGA/GGGAGTACTGAGTATTGAGGCCTAGATG
GTGTTTAAAACACAAAATGCAAGATTGGAAAAAAAAAAAAAAGAACCCAGCTGGAATGAT
GCAGAGTATGACTCCAATTAATGGGCAAACCAAACCCAGGTGTTTTTCCCCTTTTAAAAG
CAGTCCAATGGAGGACATTTTTCAAAGCCTCCACTTGAATGAAGTGGTGGGTCCCGTTGA
CGTGACTGGCTTAATTTGCTTCTTTTGGTTGCCAGAGGCTGCATTTCCATGATATTTATT
ATTAGCTCATGTCCTGAGGTGGTCTTGCAGCAATCAAGTGAAAACCAGCTTGTTCTCTCT
TCCTCTTTCCTTCAGATCACGCAATTAAAGATTGAGAATAATCCCTTTGCCAAAGGATTT
CGGGGCAGTGATGACATGGAGCTGCACAGAATGTCAAGAATGCAAAGGTAGGAAAGTGGA

AAA... : Pseudo exon sequence

CTG... : Primer C7

G/A : new acceptor site

A/G : new donor site

G : mutated position
NM_000192.3(TBX5):c.664-342G>T

ATCA... : Exon 7

References Supp Data

1. Yang J, Hu D, Xia J, et al. Three novel TBX5 mutations in Chinese patients with Holt-Oram syndrome. *Am J Med Genet*. 2000;92(4):237-240. doi:10.1002/(SICI)1096-8628(20000605)92:4<237::AID-AJMG2>3.0.CO;2-G

2. Fan C, Liu M, Wang Q. Functional analysis of TBX5 missense mutations associated with Holt-Oram syndrome. *J Biol Chem*. 2003;278(10):8780-8785. doi:10.1074/jbc.M208120200

3. Al-Qattan MM, Abou Al-Shaar H. Molecular basis of the clinical features of Holt-Oram syndrome resulting from missense and extended protein mutations of the TBX5 gene as well as TBX5 intragenic duplications. *Gene*. 2015;560(2):129-136. doi:10.1016/j.gene.2015.02.017

4. Debeer P, Race V, Gewillig M, Devriendt K, Frijns JP. Novel TBX5 mutations in patients with Holt-Oram syndrome. *Clin Orthop*. 2007;462:20-26. doi:10.1097/BLO.0b013e3181123ffe

5. Stirnimann CU, Ptchelkine D, Grimm C, Müller CW. Structural Basis of TBX5–DNA Recognition: The T-Box Domain in Its DNA-Bound and -Unbound Form. *J Mol Biol*. 2010;400(1):71-81. doi:10.1016/j.jmb.2010.04.052

6. Boogerd CJJ, Dooijes D, Ilgun A, et al. Functional analysis of novel TBX5 T-box mutations associated with Holt-Oram syndrome. *Cardiovasc Res*. 2010;88(1):130-139. doi:10.1093/cvr/cvq178

7. Basson CT, Huang T, Lin RC, et al. Different TBX5 interactions in heart and limb defined by Holt-Oram syndrome mutations. *Proc Natl Acad Sci U S A*. 1999;96(6):2919-2924.

8. Fan C, Chen Q, Wang QK. Functional Role of Transcriptional Factor TBX5 in Pre-mRNA Splicing and Holt-Oram Syndrome via Association with SC35. *J Biol Chem*. 2009;284(38):25653-25663. doi:10.1074/jbc.M109.041368

9. Ersoy AÖ, Topçu V, Kale İ, Ersoy E, Özler S, Danışman N. A novel mutated sequence in the T-box transcription factor-5 (TBX-5) gene (c.241A>T) in Holt-Oram syndrome. *J Turk-Ger Gynecol Assoc*. 2016;17(1):55-57. doi:10.5152/jtgga.2015.15233

10. Vanlerberghe C, Jourdain AS, Ghoumid J, et al. Holt-Oram syndrome: clinical and molecular description of 78 patients with TBX5 variants. *Eur J Hum Genet EJHG*. 2019;27(3):360-368. doi:10.1038/s41431-018-0303-3

11. Dreßen M, Lahm H, Lahm A, et al. A novel de novo TBX5 mutation in a patient with Holt-Oram syndrome leading to a dramatically reduced biological function. *Mol Genet Genomic Med*. 2016;4(5):557-567. doi:10.1002/mgg3.234

12. Furniss D, Kan SH, Taylor IB, et al. Genetic screening of 202 individuals with congenital limb malformations and requiring reconstructive surgery. *J Med Genet*. 2009;46(11):730-735. doi:10.1136/jmg.2009.066027

13. Brassington AME, Sung SS, Toydemir RM, et al. Expressivity of Holt-Oram syndrome is not predicted by TBX5 genotype. *Am J Hum Genet*. 2003;73(1):74-85. doi:10.1086/376436

14. Postma AV, van de Meerakker JBA, Mathijssen IB, et al. A Gain-of-Function TBX5 Mutation Is Associated With Atypical Holt–Oram Syndrome and Paroxysmal Atrial Fibrillation. *Circ Res*. 2008;102(11):1433-1442. doi:10.1161/CIRCRESAHA.107.168294

15. Koçak Eker H, Altunoglu U, Toksoy G, Kayserili H. Holt-Oram syndrome because of the novel TBX5 mutation c.481A>C. *Clin Dysmorphol*. 2016;25(4):192-194. doi:10.1097/MCD.0000000000000121

16. Cross SJ, Ching YH, Li QY, et al. The mutation spectrum in Holt-Oram syndrome. *J Med Genet*. 2000;37(10):785-787.

17. Markunas AM, Manivannan PKR, Ezekian JE, et al. TBX5-encoded T-box transcription factor 5 variant T223M is associated with long QT syndrome and pediatric sudden cardiac death. *Am J Med Genet A*. 2021;185(3):923-929. doi:10.1002/ajmg.a.62037

18. Porto MPR, Vergani N, Carvalho ACC, Cernach MCSP, Brunoni D, Perez ABA. Novel mutations in the TBX5 gene in patients with Holt-Oram Syndrome. *Genet Mol Biol*. 2010;33(2):232-236. doi:10.1590/S1415-47572010005000051

19. Basson CT, Bachinsky DR, Lin RC, et al. Mutations in human TBX5 [corrected] cause limb and cardiac malformation in Holt-Oram syndrome. *Nat Genet*. 1997;15(1):30-35. doi:10.1038/ng0197-30

20. Chakova N, Dolmatovich T, Niyazova S, Komissarova S, Rebeko E, Savchenko A. New Missense Mutation Gly238Ala in the TBX5 Gene and Its Phenotypical Characteristics. *Russ J Genet*. 2021;57:949-954. doi:10.1134/S1022795421070061

21. Rentzsch P, Witten D, Cooper GM, Shendure J, Kircher M. CADD: predicting the deleteriousness of variants throughout the human genome. *Nucleic Acids Res*. 2019;47(Database issue):D886-D894. doi:10.1093/nar/gky1016

22. Ioannidis NM, Rothstein JH, Pejaver V, et al. REVEL: An Ensemble Method for Predicting the Pathogenicity of Rare Missense Variants. *Am J Hum Genet*. 2016;99(4):877-885. doi:10.1016/j.ajhg.2016.08.016

23. Frazer J, Notin P, Dias M, et al. Disease variant prediction with deep generative models of evolutionary data. *Nature*. 2021;599(7883):91-95. doi:10.1038/s41586-021-04043-8

24. Wu Y, Li R, Sun S, Weile J, Roth FP. Improved pathogenicity prediction for rare human missense variants. *Am J Hum Genet*. 2021;108(10):1891-1906. doi:10.1016/j.ajhg.2021.08.012

25. Cheng J, Novati G, Pan J, et al. Accurate proteome-wide missense variant effect prediction with AlphaMissense. *Science*. 2023;381(6664):eadg7492. doi:10.1126/science.adg7492

26. Kelley LA, Mezulis S, Yates CM, Wass MN, Sternberg MJE. The Phyre2 web portal for protein modeling, prediction and analysis. *Nat Protoc*. 2015;10(6):845-858. doi:10.1038/nprot.2015.053

27. Jumper J, Evans R, Pritzel A, et al. Highly accurate protein structure prediction with AlphaFold. *Nature*. 2021;596(7873):583-589. doi:10.1038/s41586-021-03819-2

28. Pennica C, Hanna G, Islam SA, Sternberg MJE, David A. Missense3D-PPI: A Web Resource to Predict the Impact of Missense Variants at Protein Interfaces Using 3D Structural Data. *J Mol Biol*. 2023;435(14):168060. doi:10.1016/j.jmb.2023.168060

29. Ittisoponpisan S, Islam SA, Khanna T, Alhuzimi E, David A, Sternberg MJE. Can Predicted Protein 3D Structures Provide Reliable Insights into whether Missense Variants Are Disease Associated? *J Mol Biol*. 2019;431(11):2197-2212. doi:10.1016/j.jmb.2019.04.009

30. Madeira F, Pearce M, Tivey ARN, et al. Search and sequence analysis tools services from EMBL-EBI in 2022. *Nucleic Acids Res*. 2022;50(W1):W276-W279. doi:10.1093/nar/gkac240

31. Yeo G, Burge CB. Maximum entropy modeling of short sequence motifs with applications to RNA splicing signals. *J Comput Biol J Comput Mol Cell Biol*. 2004;11(2-3):377-394. doi:10.1089/1066527041410418

32. Leman R, Parfait B, Vidaud D, et al. SPiP: Splicing Prediction Pipeline, a machine learning tool for massive detection of exonic and intronic variant effects on mRNA splicing. *Hum Mutat*. 2022;43(12):2308-2323. doi:10.1002/humu.24491

33. Jaganathan K, Kyriazopoulou Panagiotopoulou S, McRae JF, et al. Predicting Splicing from Primary Sequence with Deep Learning. *Cell*. 2019;176(3):535-548.e24. doi:10.1016/j.cell.2018.12.015

34. de Sainte Agathe JM, Filser M, Isidor B, et al. SpliceAI-visual: a free online tool to improve SpliceAI splicing variant interpretation. *Hum Genomics*. 2023;17(1):7. doi:10.1186/s40246-023-00451-1

35. Karczewski KJ, Francioli LC, Tiao G, et al. The mutational constraint spectrum quantified from variation in 141,456 humans. *Nature*. 2020;581(7809):434-443. doi:10.1038/s41586-020-2308-7

36. Landrum MJ, Lee JM, Riley GR, et al. ClinVar: public archive of relationships among sequence variation and human phenotype. *Nucleic Acids Res*. 2014;42(Database issue):D980-985. doi:10.1093/nar/gkt1113

37. Firth HV, Richards SM, Bevan AP, et al. DECIPHER: Database of Chromosomal Imbalance and Phenotype in Humans Using Ensembl Resources. *Am J Hum Genet*. 2009;84(4):524-533. doi:10.1016/j.ajhg.2009.03.010

38. Fokkema IFAC, Kroon M, López Hernández JA, et al. The LOVD3 platform: efficient genome-wide sharing of genetic variants. *Eur J Hum Genet EJHG*. 2021;29(12):1796-1803. doi:10.1038/s41431-021-00959-x

Les tests fonctionnels ont permis de reclasser 9/14 VSI de *TBX5* comme probablement pathogènes, confirmant leur implication dans le phénotype HOS. Au total, nous avons démontré une perte de fonction (n=8) ou un gain de fonction (n=1) pour 9 des 11 variants faux-sens, alors qu'aucun impact fonctionnel n'a été démontré pour les 2 variants restants : p.(Gly195Ala) et p.(Ser261Cys), comme suggéré par les prédictions contradictoires des approches *in silico*.

Cette étude a pu montrer l'utilité clinique mais aussi la limite des tests fonctionnels spécifiques, notamment du fait de leur caractère *in vitro*, de leur coût et de leurs difficultés techniques avec parfois un manque de reproductibilité des résultats.

Les conclusions des outils de prédiction *in silico* étaient cohérentes avec les résultats des tests fonctionnels. Néanmoins, ces outils pourraient être améliorés par la prise en compte des résultats des tests fonctionnels déjà réalisés pour les variants d'intérêt. En revanche, la prise en compte des variants déjà décrits chez des patients avec phénotypes similaires est à encadrer, du fait du manque de données cliniques dans certaines bases de données. Le partage des données cliniques et moléculaires des patients atteints de maladies rares dont le phénotype serait bien décrit par le biais de banques de données sécurisées européennes ou internationales serait une aide précieuse à l'interprétation des variants candidats.

En ce qui concerne les 9 variants d'épissage, tous prédits pour affecter l'épissage par SpliceAI, nous avons observé un saut partiel ou complet d'exon (n=6), une rétention d'intron (n=2) ou une délétion partielle d'exon (n=1), induisant un décalage du cadre de lecture et un codon stop prématuré. L'effet partiel observé sur l'épissage à l'échelle de l'ARN ne permet pas de conclure sur l'impact de ces variants, en l'absence de recommandations de bonne pratique dans ces situations. L'étude protéique n'étant pas toujours possible pour les gènes du développement, d'autres approches sont à envisager que nous développerons dans les perspectives.

PARTIE III. LE SYNDROME DE BLACKFAN-DIAMOND : une cause rare d'anomalie radiale parfois isolée

Pour une forme familiale de dysplasie radiale de sévérité très variable en errance diagnostique, un variant du gène *RPL26* a été identifié.

Ce gène est impliqué dans une forme très rare de syndrome de Blackfan-Diamond (DBS) (DBA11, MIM#614900), initialement caractérisé par une insuffisance médullaire plus ou moins associée à diverses malformations congénitales (51). L'incidence du syndrome de Blackfan-Diamond est estimée entre 1:100,000 et 1:200,000 naissances vivantes. Au moins 24 gènes sont impliqués, la majorité d'entre eux codant pour des protéines ribosomiques. *RPL26* code pour la protéine ribosomique L26.

Une seule famille avait été rapportée dans la littérature jusqu'à présent (52). Par le biais d'appels à collaborations nationaux et européens ainsi que par les bases de données GeneMatcher et DECIPHER, nous avons pu recruter 4 autres familles (27,53).

Dans ce quatrième article, nous décrivons les caractéristiques cliniques et moléculaires de ces patients. Un variant de *RPL26* situé dans le 5'UTR a justifié la réalisation de tests fonctionnels : la prolifération et la différenciation érythroïde à partir de cellules CD34+ du sang périphérique ont été étudiées par cytométrie en flux, et l'expression de *RPL26* par qRT-PCR et Western Blot.

***RPL26* variants: a rare cause of Diamond-Blackfan Anemia Syndrome with multiple congenital anomalies at the forefront**

Clémence Vanlerberghe[1], Frédéric Frénois[1], Thomas Smol[1], Anne-Sophie Jourdain[1], Fabienne Escande[1], Emilie Aït-Yahya[2], Abdulrahman A Aldeeri[3,4], Timothy W. Yu[3], Valérie Cormier-Daire[5], Jamal Ghoumid[1], Maureen Jacob[6], Ruth Newbury-Ecob[7], Sylvie Manouvrier[1], Jessica Platon[8], Sebastian Sailer[9], Perrine Brunelle[1], Lydie Da Costa[10], Florence Petit[1]

[1]Univ. Lille, CHU Lille, ULR 7364 - RADEME - Maladies RAres du DÉveloppement embryonnaire et du Métabolisme, F-59000 Lille, France

[2]CHU Lille, cellule bioinformatique, plateau commun de séquençage, Lille, France

[3] Division of Genetics and Genomics, Boston Children's Hospital, Boston, MA, USA; Harvard Medical School, Boston, MA, USA

[4]King Saud University Medical City, Riyadh, Saudi Arabia

[5]Paris Cité University, Reference center for skeletal dysplasia, Imagine Institute, INSERM UMR 1163, Necker Hospital Paris, France

[6]Institute of Human Genetics, Technical University of Munich, School of Medicine, Munich, Germany

[7]Department of Clinical Genetics, University Hospitals Bristol NHS Foundation Trust, St Michael's Hospital, Southwell St, Bristol, UK

[8]HEMATIM UR4666, Université Picardie Jules Verne, Amiens, France

[9]Institute of Human Genetics, Heidelberg University, Germany

[10]AP-HP, Service Hématologie Biologique, Hôpital Bicêtre, Le Kremlin-Bicêtre, France; HEMATIM UR4666, Université Picardie Jules Vernes, Amiens, France; U1170, Université Paris Saclay, Orsay, France;

Abstract

Purpose: Diamond-Blackfan Anemia Syndrome (DBS) is a rare congenital disorder originally characterized by bone marrow failure with or without various congenital anomalies. At least 24 genes are implicated, the vast majority encoding for ribosomal proteins. *RPL26* (*ribosomal protein L26*) is an emerging candidate (DBA11, MIM#614900). We aim to further delineate this rare condition. **Methods:** Patients carrying heterozygous *RPL26* variants were recruited. In one of them, erythroid proliferation and differentiation from peripheral blood $CD34^+$ cells were studied by flow cytometry, and *RPL26* expression by qRT-PCR and immunoblotting. **Results:** We report on eight affected patients from four families. Detailed phenotyping reveals that *RPL26* is mainly associated with multiple congenital anomalies (particularly radial ray anomalies), albeit with variable expression. Mandibulofacial dysostosis and neural tube defects are potential features in DBA11, expanding the growing list of DBS abnormalities. In one individual, we showed that *RPL26* haploinsufficiency was responsible for subclinical impairment in erythroid proliferation and enucleation. The absence of hematological involvement in four adults from this series contributes to the mounting evidence that bone marrow failure is not universally central to all DBS genes. **Conclusion:** We confirm *RPL26* as a DBS gene and expand the phenotypic spectrum of the gene and the disease.

Key Words: *RPL26*, Diamond-Blackfan anemia syndrome, ribosome, mandibulofacial dysostosis

Introduction

Diamond-Blackfan Anemia Syndrome (DBA syndrome, or DBS) is a rare congenital disorder originally described as an inherited bone marrow failure characterized by a moderate to severe anemia usually before 1 year of age. Its incidence is estimated to be 1:100,000 to 1:200,000 live births.[1] The classic definition has been challenged in recent years by the increasing reports of patients with pathogenic variants in ribosomal protein (RP)-encoding genes, who exhibit multisystem anomalies expected in DBS, but with subtle or no hematological abnormalities such as *RPL13* and *RPS23.*[2,3]

When present, the main hematological findings are usually a macrocytic anemia, with profound reticulocytopenia (0 to $20x10^9$/L reticulocytes), elevated erythrocyte adenosine deaminase activity (eADA), persistence of hemoglobin F, and nearly absent or less than 5% erythroid precursors (erythroblastopenia or hypoplastic anemia) in an otherwise normocellular bone marrow. In addition, DBS can manifest with a range of clinical features, including one or more congenital malformations (44.4%), growth retardation (8.7% to 22%), and an increased predisposition to hematological and solid malignancies (2-5%).[1,4–7] Among the associated malformations, craniofacial, upper limb, heart, and genitourinary are the most prevalent.[1] Intrafamilial expression variability is very common, and incomplete penetrance is frequent.[8]

Although all three Mendelian modes of inheritance have been described, autosomal dominant inheritance of pathogenic variants in RP-encoding genes accounts for the vast majority of DBS cases.[9] The mammalian ribosome is composed of 4 ribosomal RNA (rRNA) species and approximately 80 different RP involved in the biogenesis of small (40S) and large (60S) subunits,

which together form the translation-competent 80S ribosome.[10] The RP are ubiquitously expressed, and their proper functioning is critical for normal ribosome biogenesis and function.

To date, more than twenty RP-encoding genes (n=24) have been implicated in DBS,[9] with *RPS19* (DBA1, MIM#105650), *RPL5* (DBA6, MIM#612561), *RPS26* (DBA10, MIM#613309), and *RPL11* (DBA7, MIM#612562) being the most frequently identified. Penetrance of loss-of-function variants in those genes is very high, while it seems incomplete for damaging missense variants.[1] *RPL26*, the gene encoding ribosomal protein L26, has been labeled as a potential candidate gene for DBS (DBA11, MIM#614900) following the description by Gazda et al. in 2012 of one individual. That case emerged in a study involving 96 DBS families, all of whom initially tested negative for known DBS-associated genes. Subsequently, the researchers conducted sequencing of 16 candidate RP-encoding genes, including *RPL26*. They identified a heterozygous pathogenic *RPL26* variant in a 3.5-year-old girl who presented with anemia and multiple congenital anomalies. Functional analysis revealed that the variant causes a defect in ribosome biogenesis due to impaired maturation of the large subunits.[11] Recently, a second individual carrying a heterozygous *RPL26* variant and DBS phenotype was reported.[12] However, the variant remains of uncertain significance due to its missense type and lack of parental segregation and functional analysis. To our knowledge, these are the only *RPL26*-mutated individuals reported so far in the literature.

To further elucidate the clinical and genetic characteristics associated with *RPL26*-related DBS, we present a cohort of eight patients from four unrelated families, including 2 severely affected fetuses. Interestingly, we find that *RPL26* is associated with multiple congenital anomalies, some of which expand the DBS spectrum. Hematological involvement can be subclinical, necessitating more than basic cell counts to be discovered, as we show in one patient.

Patients and Methods

Patients

We report on eight affected patients from four unrelated families carrying a heterozygous *RPL26* variant: five related cases (Family 1) where the phenotype segregates with the variant in an autosomal dominant pattern and three sporadic cases with *de novo* variants. Informed consents for genetics analyses were obtained from all patients.

The clinical features in Family 1 (F1) were reported previously.[13] Radial anomalies ranging from thenar hypoplasia to phocomelia were the most prominent abnormalities and were seen in all affected individuals across 3 generations. The fetal case F1-III3 was not genetically tested (DNA not available) but presumably affected based on phenotypic overlap. He presented with phocomelia of the upper limbs, neural tube defect, and unilateral renal agenesis, leading to the termination of pregnancy at 11 weeks of gestation (WG). Since no hematological abnormalities were present in this family, the diagnosis of DBS was not initially entertained. Chromosomal microarray (Agilent 60K), standard karyotype, and chromosomal breakage analysis induced by mitomycin C were all normal in individual F1-II3. Genome sequencing was performed in 2 affected (F1-I1, F1-II3) and one unaffected individual (F1-III4). Biological analysis revealed a candidate 23bp deletion in *RPL26* gene, right next to the canonical donor splice site of intron 1 (Table 1). Sanger sequencing (primers sequence and PCR conditions available on request) showed that this variant segregates in all affected relatives from whom DNA was available (F1-I1, F1-II2, F1-II3, F1-

III2) and is absent in those unaffected (F1-III1, F1-III4) (**Figure 1**). DNA was not available from the affected fetus F1-III3.

Molecular findings in Patient 6 (P6) were reported previously.[11] Since few clinical details were available in the previous publication, the description is enhanced in this report (Table 1). This case was included in a cohort of DBS patients and hence has a more classic DBS phenotype with anemia and neutropenia secondary to bone marrow failure diagnosed at birth. This patient also had malformations of the DBS spectrum, namely bilateral radial anomalies, unilateral renal agenesis, bicuspid aortic valve, and dysplastic ears. Sanger sequencing of 79 RP-encoding genes was performed and revealed a *de novo* 2 bp deletion in *RPL26* exon 2 (Table 1).

Further cases were collected through international collaborations, facilitated by Genematcher[14] and Decipher[15] databases (last checked in September 2023).

Patient 7 (P7) is a fetus that had multiple severe congenital malformations leading to termination of pregnancy at 34 WG. Ultrasound screening in the third trimester revealed upper-limb phocomelia, semilobar holoprosencephaly, and polyhydramnios. Examination at delivery showed additional malformations, such as macrocephaly, facial dysmorphism (telecanthus, down-slanting palpebral fissures, broad nasal ridge), cleft palate, and dysplastic ears. No fetal autopsy was performed. Karyotype on amniotic fluid identified a balanced 46,XX,t(2;4)(q31;q31) reciprocal translocation. This translocation was then identified in the unaffected mother and was therefore considered unrelated to the phenotype. Trio exome sequencing was performed and revealed a

de novo missense variant affecting the splice acceptor site of *RPL26* exon 1 (Table 1). Analysis of the sequencing data did not show any pathogenic variant in holoprosencephaly-associated genes, nor relevant copy number variants (CNV), including the translocation breakpoint regions.

Patient (P8), a female, was born at 36 weeks after a pregnancy marked by polyhydramnios, with a birth weight of 2.64 kg. Multiple congenital anomalies were noted at birth, including bilateral radial ray defects with absent thumbs, broad halluces, left dysplastic ear and absent ear canal, micrognathia, and choanal atresia requiring stenting. Auditory brainstem response was normal. At 5 weeks, she presented with pallor and was investigated for anemia. Bone marrow failure with trilineage dysplasia was diagnosed, with markedly reduced red cell and granulocyte precursors, normal lymphocytes, and increased megakaryocytes. For the first few years of her life, the patient was transfusion-dependent, and her neutropenia responded to G-CSF. However, these hematological abnormalities resolved later in childhood. Trio exome sequencing was performed and revealed a *de novo* and mosaic truncating variant of *RPL26* exon 2 (Table 1).

Erythroid proliferation and differentiation of CD34$^+$ cells from peripheral blood

CD34$^+$ cells from the peripherical blood of affected patient F1-II3 and healthy donors were isolated by immunomagnetic technique (AutoMacs Miltenyi Biotec). Purified CD34$^+$ cells were cultured in a basal medium containing: IMDM + Glutamax medium (Gibco), 1% penicillin-streptomycin (Pan Biotech), 3% human serum (Sigma Aldrich), 2% plasma (Stemcell technologies), 10µg/ml Insulin recombinant human (Sigma Aldrich), 3U/ml Heparin sodium cell culture (Sigma Aldrich), and 200µg/ml Holo-transferrin human (Sigma Aldrich). From Day (D) 0 to D7, 1ng/ml IL-

3 (Stemcell), 10ng/ml Human SCF (Miltenyi Biotec) and 3U/ml EPO were added to the basal medium. From D7 to D10, 10ng/ml Human SCF (Miltenyi Biotec) and 1U/ml EPO were added to the basal medium. From D10 to D14, 0.1U/ml EPO was added to the basal medium. After D14, cells were cultured in the basal medium.

Viable cells were counted using the trypan blue dye exclusion test as a function of time in culture. Following May-Grünwald-Giemsa staining, the extent of terminal erythroid differentiation was evaluated by morphological assessment.

Erythroid differentiation was also evaluated by flow cytometry (MACSQuant Analyzer 10, Miltenyi Biotec). Cells were immunophenotyped from D7 to D17 using several markers (Miltenyi Biotec): CD117 APC, CD34 PE, CD36 Vioblue, CD123 PE-cyanine7, CD71 PE, CD105 PeVio770, and CD235 APC. Orthochromatophilic erythroblast cell enucleation was determined at D17 with Hoescht (ThermoFischer). Viability was assessed with 7AAD (Miltenyi Biotec).

Lymphoblastoid EBV-infected cell lines

To establish lymphoblastoid cell lines (LCLs), B lymphocytes were isolated from patient F1-II3 total blood by Ficoll gradient centrifugation and submitted to EBV transformation promoted by cyclosporine. Then, LCLs from the patient and control were grown in RPMI (Gibco) supplemented with 10% FBS (Gibco).

Transcript analyses

For qualitative transcript analyses, total RNA from patient F1-II3 and a control sample was extracted from blood using the PAXgene Blood RNA Kit (Qiagen) according to the manufacturer's

recommendations. Reverse transcription was performed on 1 µg of RNA using the SuperScript™ III Reverse Transcriptase (Thermo Fisher Scientific) with random hexamers. cDNA was amplified with PCR primers designed on *RPL26* exon 1 and exon 3 (**Suppl. Materials**), following 35 cycles with an annealing temperature of 58°C. PCR products were run on a 2% agarose gel. Each band obtained was excised, and the PCR products were purified using the NucleoSpin Gel and PCR Clean-up (Macherey-Nagel) and Sanger-sequenced using the same primers.

For semi-quantitative transcript analyses, total RNA from patient F1-II3 and control LCLs was extracted with RNEASY mini kit extraction (Qiagen). cDNA was synthesized with High Capacity cDNA Reverse Transcription Kit (Applied Biosystems). Real-time quantitative RT-PCR was carried out in the Quantstudio 7 Flex (ThermoFischer Scientific), using the SYBR green Real Time Master Mix (Applied Biosystems). The expression level of each gene was normalized using two housekeeping genes – hypoxantine-guanine-phosphoribosyl-transferase 1 (*HPRT1*, MIM*308000) gene and glyceraldehyde-3-phosphate dehydrogenase (*GAPDH*, MIM*138400). Primers are available in **Suppl. Materials**.

Protein extraction and immunoblot analysis

Each pellet of 15,000 erythroid cells from the patient F1-II3 or healthy donor and 250,000 cells from LCLs was lysed in RIPA buffer (Sigma Aldrich), phosphatase (Calbiochem), and protease (Sigma) inhibitors. Samples were run on Tris-glycine 15% SDS-PAGE resolving gel. Following electrophoresis, proteins were transferred into a nitrocellulose membrane by dry transfer (iblot 2, Invitrogen) and stained with Ponceau solution (Sigma Aldrich). Following washing of the membrane with water and then with Tris-buffered saline with 1% Tween-20 (TBST 1X),

membranes were soaked in blocking buffer (5% milk in TBST 1X) for 1h and then immunolabeled overnight at 4°C with different antibodies. Antibodies used for immunoblots were as follows: Phosphorylated p53 (Cell signaling), p53 (Cell signaling), p21 (Santa Cruz), GATA1 (Santa Cruz), PARP (Cell signaling), RPL26 (Bethyl Laboratories, OZYME catalog#BETA300-686A). Following several washes with water, then with TBST 1X, membranes were incubated with appropriate secondary antibodies for 1h. After several washes with water and then with TBST 1X, the membranes were soaked in Super signal West Atto ultimate sensitivity solution (ThermoFischer), and the expression levels of various proteins were determined on the Universal Hood II (Biorad). Western blots on erythroid cells were performed once, while they were replicated twice on LCLs.

In silico predictions

Pathogenicity of all *RPL26* variants was assessed using MobiDetails, a bioinformatic tool for interrogating multiple databases and prediction software (last checked in September 2023).[16]

Results

Clinical and molecular data are summarized in **Figure 1** and **Table 1**.

Clinical features in DBA11 affected patients

We report on eight patients (seven females and one male) from four unrelated families carrying *RPL26* heterozygous variants. Two patients were fetuses subjected to pregnancy termination due to multiple severe congenital anomalies. Age in postnatal cases ranges from 8 months to 91 years. In this series, radial anomalies are present in all individuals (8/8), albeit to a variable degree,

ranging from mild (thenar hypoplasia, triphalangeal thumb) to severe (radial agenesis, phocomelia). Craniofacial anomalies (e.g. hypertelorism, down-slanting palpebral fissures, broad nasal ridge) are present in most patients (6/8), with some expressing prominent features including choanal atresia (2/8), cleft palate (2/8), and dysplastic ears or microtia with absent or narrow auditory meatus (3/8). Unilateral renal agenesis was reported in 2/8 individuals. Surprisingly, only 2/6 of the postnatal cases have clinically observable hematological features (anemia and/or neutropenia with bone marrow hypocellularity). The hematological status was not assessed in the two fetal cases. Blood cell counts were normal in the 4 adults from family F1. In individual F1-II3 eADA was measured, the result being at the upper limit of the normal (1.6 nm/min/mg Hb (0.8-1.6)). Extended erythroid studies were performed in this individual.

RPL26 variants

RPL26 (located on 17p13.1) is composed of 4 exons. Only exons 2 to 4 are coding for the 145 amino acids that make up the large ribosomal subunit protein uL24. None of the four variants described in this report are listed in gnomAD (Table 1) (last checked in September 2023).[17]

The variants identified in P6 and P8 are frameshift deletions causing a premature stop codon in exon 2, therefore likely triggering nonsense-mediated mRNA decay. The variants identified in F1 and P7 affect the intron 1 canonical donor and acceptor splice sites, respectively. Their location upstream of the translation start site makes it challenging to predict their effects. However, *in silico* predictions for the variant NM_000987.5:c.-5-2A>G; p.? seen in P7 are in favor of two effects: the loss of intron 1 acceptor splice site and the use of a cryptic acceptor site that would lead to deletion of the ATG translation initiation codon (**Suppl. Figure 1**). Unfortunately, no tissue

is available from this patient for transcript or protein analysis. For family 1, functional characterization of the variant NM_000987.5:c.-6+3_-6+25del; p.? was performed.

Erythroid defect

Extended hematological studies were performed in individual F1-II3, carrying the variant NM_000987.5:c.-6+3_-6+25del; p.?. We observed a slight increase in the number of $CD34^+$ cells collected per ml of peripheral blood from the patient ($656x10^5$/ml) compared to the control ($566x10^5$/ml) (**Figure 2A**), and a dramatic defect in erythroid proliferation as soon as D7 during the time course of differentiation as usually observed in DBS affected patients (**Figure 2B**). We did not observe delayed erythroid differentiation at D7 on the IL-R3 (CD123) labeling, nor in the number of BFU-e cells ($IL3R^{neg}/CD34^+/CD36^{neg}$ cells), but there was instead a slight acceleration with an increase in CFU-e ($IL3R^{neg}/CD34^{neg}/CD36^+$ cells) in the patient (67%) compared to the control (39%), who exhibited at this time more $CD34^+/CD36^+$ cells (57% versus 27%) (**Figure 2C**). However, this did not affect the number of $CD36^+/CD117^+$ cells at D7 between both individuals (**Figure 2C**), nor the next steps of erythroid differentiation. Indeed, erythroid differentiation at D10, D12, and D14 was very similar between the patient and the control (data not shown). However, at D17, we observed a delay in erythroid enucleation with only 23% of enucleated cells in the patient compared to 52.5% in the control (**Figure 2D**). These findings correlate with the CD71/GPA labeling: the patient exhibits less reticulocytes (which lose the CD71 marker) or more nucleated $CD71^+/GPA^+$ erythroblasts (84%) compared the control (31%). Finally, we observed an increase in the expression level relative to GAPDH of p53, phosphorylated p53, and its target p21

from D7 to D10 compared to the control as the usual DBS feature. GATA1 was not decreased, and PARP was not cleaved (**Figure 2E, Suppl. Figure 2**).

Functional characterization of NM_000987.5:c.-6+3_-6+25del

The NM_000987.5:c.-6+3_-6+25del variant is a 23bp deletion located in the intron 1, right next to the canonical donor splice site of the non-coding exon 1. We performed a RT-PCR and Sanger sequencing and showed that the 23bp-deleted allele is abnormally spliced with two different lengths of partially retained intron 1 (**Figure 3A**). *In silico* translation start prediction (**Suppl. Figure 3**) suggests the utilization of a cryptic ATG start site upstream of the natural initiation site, producing a premature stop codon.

To clarify whether the variant causes haploinsufficiency, we also compared *RPL26* expression in LCLs from the patient F1-II3 to two different LCL controls. We found a large reduction in RPL26 mRNA (**Figure 3B**) and protein (**Figure 3C**) expression compared to the controls GAPDH and HPRT. We also confirmed in LCLs derived from the patient the absence of apoptosis activation on the increase in the anti-apoptotic Bcl-xL mRNA expression (**Figure 3B**).

Discussion

RPL26 has been suggested as a DBS gene based on a single case reported by Gazda et al. in 2012.[11] Since then, only one additional individual carrying a *RPL26* missense variant of uncertain significance has been reported, with insufficient evidence to support the causality due to lack of parental segregation and functional analysis.[12] We here report on eight individuals (including the first case reported in 2012) from four unrelated families affected with congenital malformations

with or without hematological abnormalities, all with *RPL26* heterozygous variants reinforcing that homozygous RP variants are supposedly lethal and that *RPL26* variants are responsible for haploinsufficiency as usually seen in DBS.

In this series, we show that patients with *RPL26* variants share radial anomalies as the only consistent finding across all individuals, although with variable severity even within the same family. In fact, the radial involvement can be so mild that it goes unnoticed. For instance, F1-II2 was considered unaffected until she gave birth to her affected daughter F1-III2. Careful examination of the mother finally identified thenar hypoplasia, a subtle form of radial anomaly.

In addition, other malformations are commonly reported in DBS and present in two-thirds of cases, especially craniofacial anomalies and, less frequently, renal agenesis. However, one of the severe craniofacial anomalies we report is mandibulofacial dysostosis, a condition rarely seen in DBS, except for some individuals with variants in *TSR2* (MIM#300946), *RPS26* (MIM#613309) or *RPS28* genes (MIM#606164). In these patients, dysmorphism is reminiscent of Treacher-Collins syndrome (TCS, MIM#154500), a condition that is mainly caused by variants in *TCOF1* (*Treacle Ribosome Biogenesis Factor 1*) gene, involved in ribosomal DNA gene transcription.[18] Therefore, our report adds another example of ribosomopathy associated with mandibulofacial dysostosis.

We performed extended hematological studies in one affected individual (F1-II3) with normal blood cells count (including normal mean corpuscular volume, reticulocyte count and hemoglobin level) and eADA at the upper limit of the normal. Strikingly, we found the usual large defect in erythroid proliferation *ex vivo*, in association with a p53 activation and its target p21, as seen in DBS patients.[19,20] However, compared to most of the DBS patients,[21] *RPL26*-mutated patient

exhibited no delay in early erythroid differentiation, but a delayed orthochromatophilic erythroblast enucleation, in association with a normal *GATA1* expression and no apoptosis. In this series, only one-third (2/6) of the *RPL26* postnatal cases have clinically observable hematological abnormalities at time of evaluation, highlighting that their absence does not preclude the diagnosis of DBS, and that for some implicated genes, especially *RPL26*, hematological abnormalities may be mild or infrequent. We may hypothesize that, as for *RPL15*,[22] when the fetal period of anemia and hydrops can be overcome, *RPL26*-affected patients may exhibit a normal hemoglobin level. Unfortunately, we could not get any blood samples or bone marrow analyses for the two fetuses reported. Anyway, this is in contrary to some of the earliest DBS patient series, where anemia was considered fully penetrant and usually present in infancy.[4–6] However, this is likely due to biased cohorts that pre-selected and studied individuals with hematological abnormalities as such DBA is primary defined by an erythroblastopenia, while DBS is a larger definition related to RP-haploinsufficiency with or without anemia. Indeed, as research advances, it has become evident that the phenotypic spectrum in DBS is quite broad. Many cases lack hematological abnormalities altogether, while in others, when present, the hematological defects can be overshadowed by other severe physical anomalies. This has led to the current practice of establishing DBS diagnosis based on the identification of a pathogenic variant in any DBS gene in an individual with a compatible phenotype, even in a state of normal hematopoiesis.[9] Indeed, exome and genome sequencing were powerful tools to solve most of the cases in our study that presented with non-classic DBS phenotype.

Like many other DBS genes, we show that *RPL26* exhibits a high degree of inter- and intrafamilial variable expressivity. This is exemplified by Family 1, where four individuals (F1-I1, F1-II1, F1-II4, and F1-III2) have almost isolated radial ray defects, while the presumably affected fetal case F1-III3 had more severe phenotype with multiple congenital anomalies (anencephaly with cervical myelomeningocele and unilateral renal agenesis). Before the *RPL26* variant was identified, the departure of the phenotype in the male fetus from that seen in the affected relatives made the researchers think the fetus was affected by an X-linked condition due to him being the only affected male individual.[13] It would have also been reasonable to hypothesize that this family was affected by an X-linked condition that manifested in the females much more mildly than the male fetus. However, comparing the phenotype of the fetus to the rest of *RPL26* cases, especially P7 who has semilobar holoprosencephaly, it is very likely that neural tube defects are part of the *RPL26*-related DBS spectrum. A literature search identifies one additional case of DBS with occipital meningocele, attributed to a variant in *RPS7* (DBA8, MIM#612563).[23] Similar to many other genetic conditions, inter- and intrafamilial variability in DBS phenotype is not well understood, although it can partially be explained by differences in the severity of the variants affecting the gene and the potential presence of modifier variants. Because of the highly variable expressivity, families with RPL26 pathogenic variants would likely benefit from prenatal ultrasound with a doppler to measure the systolic velocity, with or without prenatal genetic diagnosis. Indeed, ultrasound and the Doppler can both and respectively provide valuable insight into the severity of the physical phenotype and identify intra-uterine anemia and risk of hydrops fetalis if the pregnancy is affected. It may prevent fetal death in these rare families affected with *RPL26* allelic variation.

The prevalence of congenital malformations in DBS is variable across the causal genes. Among the most frequently implicated genes in DBS, *RPL5* and *RPL11* exhibit the highest prevalence of malformations compared to other genes like *RPS19* (83%, 73%, and 34%, respectively).[1] While our series is limited by the small number of individuals, it seems that all *RPL26*-related DBS patients have physical malformations. In syndromes with multisystem involvement, it is helpful to pay special attention to the unique findings as they can narrow the list of possibly causal genes. Since radial anomalies are present in all patients we report, while only seen in 16% of DBS cases caused by all other genes,[4–6] it would be prudent to specifically interrogate *RPL26* gene when radial anomalies are encountered in the appropriate clinical context.

Interestingly, two out of the four variants reported in this study involve non-coding regions before the translation start site. These regions may be non-covered by exome captures or interpreted as insignificant, leading to a false-negative result.

All four *RPL26* variants we report are predicted to lead to premature stop codons and, therefore, cause haploinsufficiency. Decreased RNA and protein expression was demonstrated for one of them on patient-derived LCLs. While several mouse models have been developed to study the consequences of RP haploinsufficiency, no model is available for *Rpl26* so far.[24] However, previous studies in HeLa cells confirmed that RPL26 depletion induced by small interfering RNAs (siRNAs) leads to ribosomal biogenesis impairment affecting maturation of the small and the large ribosomal subunits.[11]

Conclusion

While the involvement of many RP-encoding genes in the pathogenesis of DBS is well known, *RPL26* remained a putative candidate since only one individual has been described to date with convincing functional studies.[11] Our report of several additional cases confirms the causality of *RPL26* gene in some DBS patients, highlights infrequent but unique findings such as mandibulofacial dysostosis, and expands the spectrum of DBS phenotype to include neural tube defects. We also show in four adult cases that hematological abnormalities are not at the forefront in *RPL26*-related DBS. In contrast, radial anomalies are present with variable severity in all cases, which can be a clue to the causal gene.

Data availability

All *RPL26* variants reported in this study are implemented in ClinVar database under the accession or submission numbers: 39740, SCV004099494, SCV004099496, SCV004099497.

Acknowledgements

For family 1, this research was made possible through access to the data generated by the 2025 French Genomic Medicine Initiative. We thank the cell culture facility of Lille University Hospital for the establishment of lymphoblastoid cell lines. Finally, we thank all patients and families who accepted to participate to this project.

Funding Statement

This study was partly supported by a grant from the GIRCI Nord-Ouest (AAP-AE-17-18) and by the Health PhD grant from the I-site Foundation.

This study makes use of data generated by the DECIPHER community. DECIPHER is hosted by EMBL-EBI and funding for the DECIPHER project was provided by the Wellcome Trust [grant number WT223718/Z/21/Z].

Author Contributions

Conceptualization: C.V., F.P., S.M., J.G., L.D.C; Data curation: C.V., F.E., P.B., T.S., F.P., S.M., M.J., S.S., A.A.A. T.Y., V.C.D., R.N.E., J.P., L.D.C; Formal analysis: T.S., P.B., J.P., L.D.C; Funding acquisition: C.V., F.P.; Investigation: C.V., F.P., F.F., A.S.J., J.P., L.D.C; Methodology: F.F., A.S.J., T.S., P.B., J.P., L.D.C; Project administration: C.V., F.P.; Software: E.A.Y., T.S.; Supervision: F.P., F.E., S.M., J.G., L.D.C; Writing-original draft: C.V., F.P., J.P., L.D.C; Writing-review & editing: F.F., A.S.J., F.E., E.A.Y., A.A.A., T.Y., V.C.D., J.G., M.J., R.N.E.; S.M., S.S., P.B., T.S, J.P., L.D.C.

Ethics Declaration

Written informed consents for genetic analyses and permission for publication of photographs or images of patients were obtained from the patients or their parents. The research protocol was reviewed and accepted by the Institutional Review Board (IRB) and Data Protection Manager of Lille University Hospital (Ref DEC19-366). The study was conducted in accordance with the Declaration of Helsinki.

Figure 1: Clinical features in patients with *RPL26* heterozygous variants. A. Pedigree of family 1. **B.** Pictures and X-rays of individual F1-II3 showing triphalangeal thumbs and radio-ulnar synostosis. **C.** Pictures and X-rays of fetus F1-III3 at 11WG showing acrania and phocomelia of the upper limbs. **D.** Pictures of fetus P7 at 34WG showing mandibulofacial dysostosis, dysplastic ears, and phocomelia of the upper limbs with oligodactyly. WG: weeks of gestation.

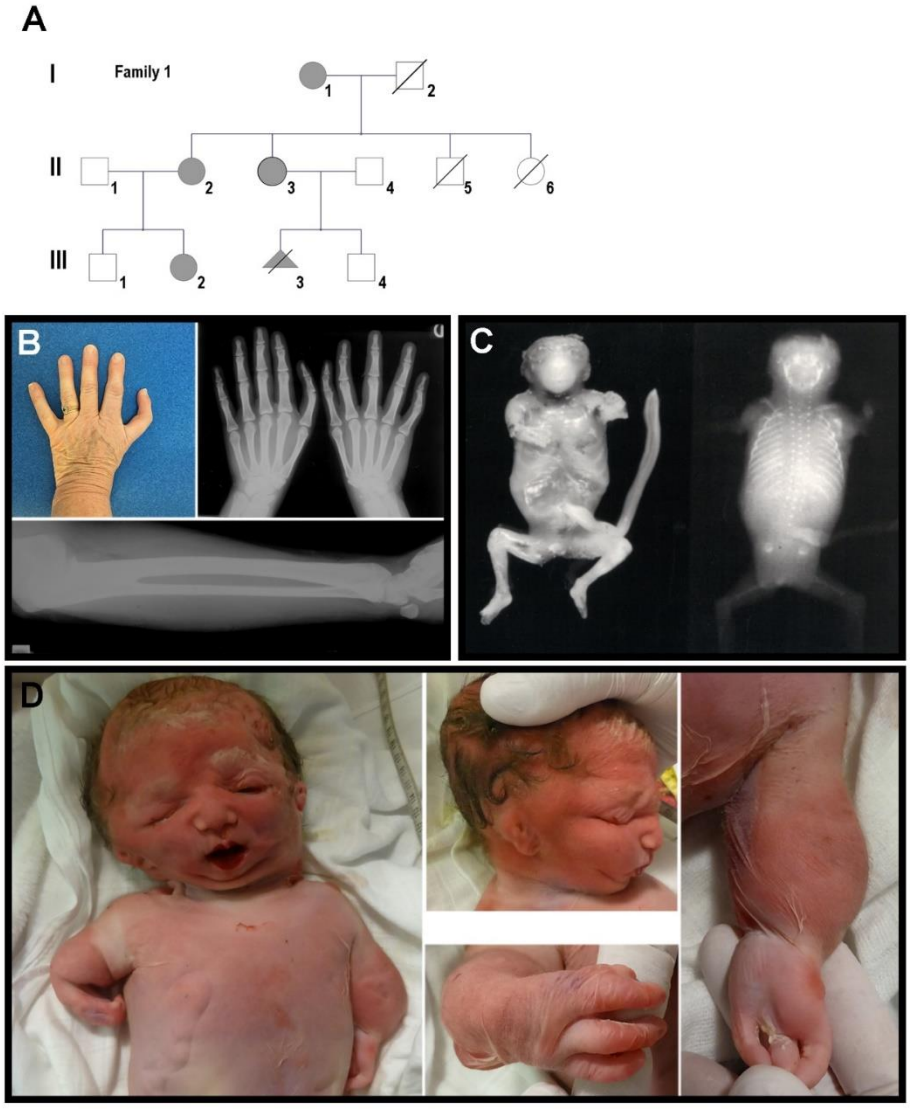

Figure 2: Erythroid studies in individual F1-II3, carrying the variant NM_000987.5(RPL26):c.-6+3_-6+25del. A. $CD34^{+}$ cells count in peripheral blood from the patient $RPL26^{+/Mut}$ compared to the control. **B.** Erythroid proliferation from the patient *$RPL26^{+/Mut}$* compared to the control until D17. **C.** Erythroid differentiation from the patient *$RPL26^{+/Mut}$* compared to the control at D7. Flow cytometry quantification of BFU-e ($CD123^{neg}/CD34^{+}/CD36^{neg}$), more mature BFU-e ($CD123^{neg}/CD34^{+}/CD36^{+}$), and CFU-e ($CD123^{neg}/CD34^{neg}/CD36^{+}$) cells in the patient compared to the control. **D.** Erythroid differentiation at D17. Flow cytometry quantification of nucleated erythroblasts ($CD71^{+}/GPA^{+}$) and orthochromatophilic enucleated erythroblast cells (Hoescht counterstain) in the patient compared to the control. **E.** Expression level of p53, phosphorylated p53, GATA1, PARP and p21 from D7 to D10 or D12, relative to GAPDH and control, in erythroid precursor cells.

D: day; GPA: glycophorin A.

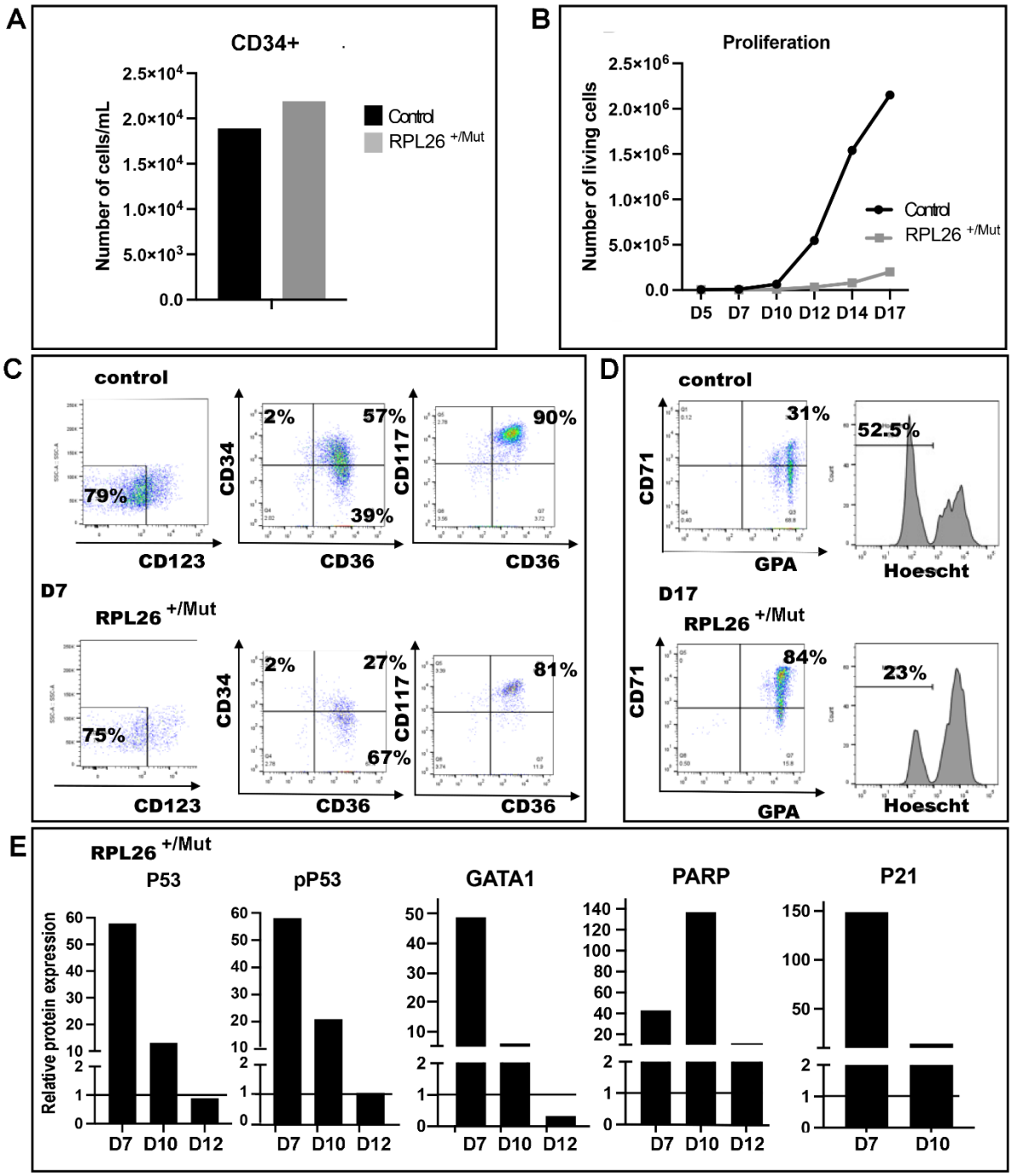
A
CD34+
Number of cells/mL
2.5×10^4
2.0×10^4
1.5×10^4
1.0×10^4
5.0×10^3
0.0
Control
RPL26 +/Mut
B
Proliferation
Number of living cells
2.5×10^6
2.0×10^6
1.5×10^6
1.0×10^6
5.0×10^5
0.0
D5 D7 D10 D12 D14 D17
Control
RPL26 +/Mut
C
control
79%
CD123
CD34
2%
57%
39%
CD36
CD117
90%
CD36
D7
RPL26 +/Mut
75%
CD123
CD34
2%
27%
67%
CD36
CD117
81%
CD36
D
control
CD71
31%
GPA
52.5%
Hoescht
D17
RPL26 +/Mut
CD71
84%
GPA
23%
Hoescht
E
RPL26 +/Mut
P53
pP53
GATA1
PARP
P21
Relative protein expression
D7 D10 D12
D7 D10 D12
D7 D10 D12
D7 D10 D12
D7 D10

Figure 3: Characterization of *RPL26*:c.-6+3_-6+25del variant by RT-PCR and immunoblot. A. RT-PCR for RPL26 exons 1-3 and schematic results from Sanger sequencing. The wild-type allele from patient F1-II3 shows normal splicing. The 23bp-deleted allele is abnormally spliced with two lengths of partial retention of intron 1 (272 and 353 bp) depending on the cryptic splice donor site used. **B.** Semi-quantitative RT-PCR for RPL26 and Bcl-xL (anti-apoptotic marker) on LCLs from patient *RPL26*$^{+/Mut}$ and two controls. **C.** Immunoblots for RPL26 on LCLs from patient *RPL26*$^{+/Mut}$ and two controls, histograms of relative protein expression compared to GAPDH and each control. L: ladder; C: control sample; P: patient sample; E: exon; i: intron; Arrow: deletion of 23 bp; bp: base pairs; LCLs: lymphoblastoid cell lines.

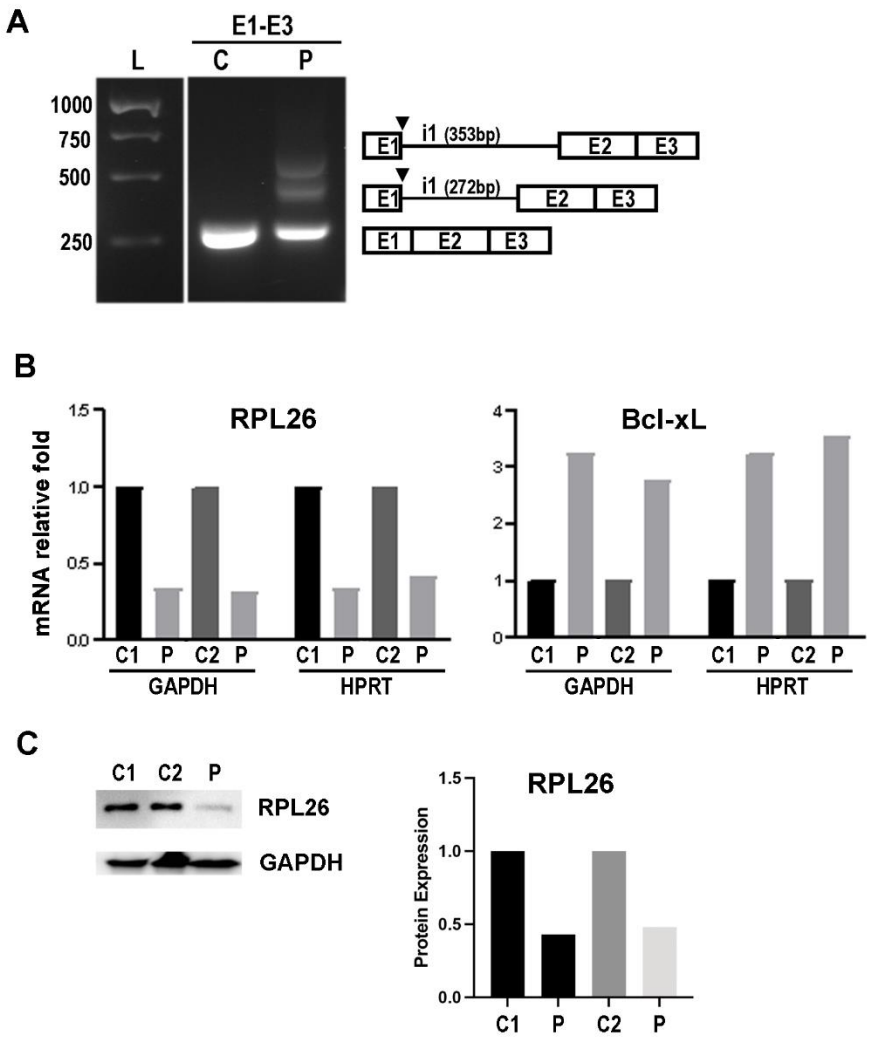
A
E1-E3
L
C
P
1000
750
500
250
i1 (353bp)
E1
E2
E3
i1 (272bp)
E1
E2
E3
E1
E2
E3
B
RPL26
mRNA relative fold
1.5
1.0
0.5
0.0
C1 P C2 P
GAPDH
C1 P C2 P
HPRT
Bcl-xL
4
3
2
1
0
C1 P C2 P
GAPDH
C1 P C2 P
HPRT
C
C1 C2 P
RPL26
GAPDH
RPL26
Protein Expression
1.5
1.0
0.5
0.0
C1 P C2 P

Table 1: Clinical and molecular data of patients with *RPL26* heterozygous variants. Out-of-range hematological parameters are in bold. yo: years old; WG: weeks of gestation; TOP: termination of pregnancy; AD: autosomal dominant; N.D.: not determined; N.A.: not applicable; ACMG: American College of Medical Genetics and Genomics [25].

Case	F1-I1	F1-II2	F1-II3	F1-III2	F1-III3	P6	P7	P8	Total
Sex	F	F	F	F	M	F	F	F	7F/1M
Prenatal	-	-	-	-	TOP		TOP		
Age at last examination	91 yo	64 yo	59 yo	28 yo	11 WG	3.5 yo	34+2 WG	8 months	Range 11WG-91 yo
Height (SD)		165 cm		158 cm	6.5 cm (0 SD)	90 cm (-1 SD)	47 cm (+1 SD)	64.4 cm (-2 SD)	
Weight (SD)					13 g (0 SD)		1970 g (-0,54 SD)	6.7 kg (-3 SD)	
OFC cm (SD)					N.A. (acrania)		37.5 cm (+4,45 SD)	44.2 cm (+1 SD)	
Facial anomalies									6/8
Eye anomalies			strabismus		N.D.		N.D.		
Hypertelorism	N.D.	-	-	+	+		Telecanthus (determination of Hypertelorism not possible)	+	4/6
Downslanting palpebral fissures	N.D.	-	-	+	N.D.	Incomplete lower left eyelid	+	+	4/6
Broad nasal ridge	N.D.	-	+	-			+		2/4
Choanal atresia	-	-	+	-	-		N.D.	+	2/6
Cleft palate	-	-	-	-	-	+	+		2/8
Micro/retrognathia	N.D.	-	-	-	-		+	+	2/5
Ear anomalies	N.D.	-	-	anteverted	-	Absent/narrow auditory meatus	Dysplastic outer ear, absent/ narrow auditory meatus	Left dysplastic ear and absent ear canal	4/8

Other facial anomalies							Caudal malformation or appendage of the tongue		
Skeletal anomalies									8/8
Radial defects	bilateral radioulnar synostosis, right I-II syndactyly, left triphalangeal thumb	bilateral thenar hypoplasia	Bilateral triphalangeal thumbs and radioulnar synostosis	Bilateral thumb aplasia and radioulnar synostosis	Bilateral phocomelia, radial agenesis and oligodactyly (3 rays)	Absent thumbs, right radial agenesis, left radial hypoplasia with radioulnar synostosis	Bilateral phocomelia, bilateral radial aplasia and oligodactyly. Left: 3 rays; Right: 4 rays with syndactyly of the two radial oriented rays.	Absent thumb, radius aplasia/hypoplasia	8/8
Skull anomalies			-	Temporal enlargement, brachycephaly	Absent skull		Brachycephaly		
Other skeletal anomalies	limited shoulder mobility				-		Sacral fistula	Broad halluces	
Visceral anomalies									
Cardiovascular	-	-	-	-	-	Bicuspid aortic valve	-		1/8
Kidney	-	-	-	-	Agenesis of the right kidney	Agenesis of the left kidney	Polyhydramnios		2/8
Other visceral anomalies	-	-	-	-	Common dorsal mesentery		N.D.		
Neurological anomalies									2/6
Neurodevelopment	Normal	Normal	Normal	Normal	N.A.		N.A.		

Cerebral malformations	-	-	-	-	Anencephaly and cervical myelomeningocele		Semilobar holoprosencephaly		2/6
Hematology parameters at last examination									
Hemoglobin (g/dL)	12.2	13.9	13.5	11.8	N.D.	**8.5** g/dL at birth, **4.1** g/dL at 7 weeks, resolved under steroid treatment	N.D.	**5.3**	Anemia 2/6
Mean corpuscular volume (fL)	94	94.2	86.7	**98.9**	N.D.	N.D.	N.D.	92.2	Macrocytosis 1/5
Reticulocytes (.10^9 /L)	N.D.	N.D.	91	N.D.	N.D.	57 at 7 weeks	N.D.	N.D.	
Neutrophils (.10^9 /L)	2.96	2.9	3.8	1.88	N.D.	Neutropenia (**0.2**) at 7 weeks, resolved under steroid treatment	N.D.	**0.5**	Neutropenia 2/6
Platelets (.10^9 /L)	187	235	233	218	N.D.	N.D.	N.D.	157	
Fetal hemoglobin	<0.7%	N.D.	N.D.	N.D.	N.D.	N.D.	N.D.	N.D.	
Erythrocyte adenosine deaminase (eADA) (0.8-1.6 nm/min/mg Hb)	N.D.	N.D.	1.6	N.D.	N.D.	N.D.	N.D.	N.D.	
Bone marrow	N.D.	N.D.	N.D.	N.D.	N.D.	At 7 weeks. Hypocellularity. Markedly reduced red cell and granulocyte precursors.	N.D.	Hypocellularity. Markedly reduced red cell and granulocyte precursors.	
Molecular findings									
RPL26 gene (NM_000987.5)	c.-6+3_-6+25del	c.-6+3_-6+25del	c.-6+3_-6+25del	c.-6+3_-6+25del		c.120_121delGA	c.-5-2A>G	c.87delT	
Location	intron 1	intron 1	intron 1	intron 1		exon 2	intron 1	exon 2	

RPL26 protein	p.(?)	p.(?)	p.(?)	p.(?)		p.(Lys41Valfs*12)	p.(?)	p.(Met30Cysfs*9)	
Inheritance	N.D.	Familial, AD	Familial, AD	Familial, AD		*De novo*	*De novo*	*De novo*, mosaic	
ACMG classification	class 4 (PM2, PP1, PP4, PS3)	class 4 (PM2, PP1, PP4, PS3)	class 4 (PM2, PP1, PP4, PS3)	class 4 (PM2, PP1, PP4, PS3)		class 5 (PM2, PP4, PS2, PVS1)	class 4 (PM2, PP4, PS2)	class 5 (PM2, PP4, PS2, PVS1)	
Additional finding							Reciprocal translocation, 46,XX,t(2;4)(q31;q31), balanced, maternally inherited		

References

1. Ulirsch JC, Verboon JM, Kazerounian S, et al. The Genetic Landscape of Diamond-Blackfan Anemia. *Am J Hum Genet*. 2018;103(6):930-947. doi:10.1016/j.ajhg.2018.10.027

2. Paolini NA, Attwood M, Sondalle SB, et al. A Ribosomopathy Reveals Decoding Defective Ribosomes Driving Human Dysmorphism. *Am J Hum Genet*. 2017;100(3):506-522. doi:10.1016/j.ajhg.2017.01.034

3. Le Caignec C, Ory B, Lamoureux F, et al. RPL13 Variants Cause Spondyloepimetaphyseal Dysplasia with Severe Short Stature. *Am J Hum Genet*. 2019;105(5):1040-1047. doi:10.1016/j.ajhg.2019.09.024

4. Ball SE, McGuckin CP, Jenkins G, Gordon-Smith EC. Diamond-Blackfan anaemia in the U.K.: analysis of 80 cases from a 20-year birth cohort. *Br J Haematol*. 1996;94(4):645-653. doi:10.1046/j.1365-2141.1996.d01-1839.x

5. Ramenghi U, Campagnoli MF, Garelli E, et al. Diamond-Blackfan anemia: report of seven further mutations in the RPS19 gene and evidence of mutation heterogeneity in the Italian population. *Blood Cells Mol Dis*. 2000;26(5):417-422. doi:10.1006/bcmd.2000.0324

6. Lipton JM, Atsidaftos E, Zyskind I, Vlachos A. Improving clinical care and elucidating the pathophysiology of Diamond Blackfan anemia: an update from the Diamond Blackfan Anemia Registry. *Pediatr Blood Cancer*. 2006;46(5):558-564. doi:10.1002/pbc.20642

7. Vlachos A, Rosenberg PS, Atsidaftos E, Alter BP, Lipton JM. Incidence of neoplasia in Diamond Blackfan anemia: a report from the Diamond Blackfan Anemia Registry. *Blood*. 2012;119(16):3815-3819. doi:10.1182/blood-2011-08-375972

8. Sieff C. Diamond-Blackfan Anemia. In: Adam MP, Mirzaa GM, Pagon RA, et al., eds. *GeneReviews®*. University of Washington, Seattle; 1993. Accessed September 16, 2023. http://www.ncbi.nlm.nih.gov/books/NBK7047/

9. Iskander D, Roy NBA, Payne E, et al. Diamond-Blackfan anemia in adults: In pursuit of a common approach for a rare disease. *Blood Reviews*. 2023;61:101097. doi:10.1016/j.blre.2023.101097

10. Dörner K, Ruggeri C, Zemp I, Kutay U. Ribosome biogenesis factors—from names to functions. *The EMBO Journal*. 2023;42(7):e112699. doi:10.15252/embj.2022112699

11. Gazda HT, Preti M, Sheen MR, et al. Frameshift mutation in p53 regulator *RPL26* is associated with multiple physical abnormalities and a specific pre-ribosomal RNA processing defect in diamond-blackfan anemia. *Hum Mutat*. 2012;33(7):1037-1044. doi:10.1002/humu.22081

12. Peñaloza D, Paredes D, Arias-Almeida B, Hosomichi K, Reyes C, Romero VI. Novel ribosomal protein L26 variant and modeling in a patient with Diamond–Blackfan anemia: Case report. *Pediatric Blood & Cancer*. 2023;70(9):e30368. doi:10.1002/pbc.30368

13. Manouvrier S, Moerman A, Coeslier A, Devisme L, Boute O, Le Merrer M. Radioulnar synostosis, radial ray abnormalities, and severe malformations in the male: a new X-linked dominant multiple congenital anomalies syndrome? *Am J Med Genet*. 2000;90(5):351-355. doi:10.1002/(sici)1096-8628(20000228)90:5<351::aid-ajmg1>3.0.co;2-k

14. Sobreira N, Schiettecatte F, Valle D, Hamosh A. GeneMatcher: A Matching Tool for Connecting Investigators with an Interest in the Same Gene. *Human Mutation*. 2015;36(10):928-930. doi:10.1002/humu.22844

15. Firth HV, Richards SM, Bevan AP, et al. DECIPHER: Database of Chromosomal Imbalance and Phenotype in Humans Using Ensembl Resources. *Am J Hum Genet*. 2009;84(4):524-533. doi:10.1016/j.ajhg.2009.03.010

16. Baux D, Van Goethem C, Ardouin O, et al. MobiDetails: online DNA variants interpretation. *Eur J Hum Genet*. 2021;29(2):356-360. doi:10.1038/s41431-020-00755-z

17. Chen S, Francioli LC, Goodrich JK, et al. *A Genome-Wide Mutational Constraint Map Quantified from Variation in 76,156 Human Genomes*. Genetics; 2022. doi:10.1101/2022.03.20.485034

18. Valdez BC, Henning D, So RB, Dixon J, Dixon MJ. The Treacher Collins syndrome (*TCOF1*) gene product is involved in ribosomal DNA gene transcription by interacting with upstream binding factor. *Proc Natl Acad Sci USA*. 2004;101(29):10709-10714. doi:10.1073/pnas.0402492101

19. Moniz H, Gastou M, Leblanc T, et al. Primary hematopoietic cells from DBA patients with mutations in RPL11 and RPS19 genes exhibit distinct erythroid phenotype in vitro. *Cell Death Dis*. 2012;3(7):e356. doi:10.1038/cddis.2012.88

20. Dutt S, Narla A, Lin K, et al. Haploinsufficiency for ribosomal protein genes causes selective activation of p53 in human erythroid progenitor cells. *Blood*. 2011;117(9):2567-2576. doi:10.1182/blood-2010-07-295238

21. Gastou M, Rio S, Dussiot M, et al. The severe phenotype of Diamond-Blackfan anemia is modulated by heat shock protein 70. *Blood Adv*. 2017;1(22):1959-1976. doi:10.1182/bloodadvances.2017008078

22. Wlodarski MW, Da Costa L, O'Donohue MF, et al. Recurring mutations in RPL15 are linked to hydrops fetalis and treatment independence in Diamond-Blackfan anemia. *Haematologica*. 2018;103(6):949-958. doi:10.3324/haematol.2017.177980

23. Akram T, Fatima A, Klar J, et al. Aberrant splicing due to a novel RPS7 variant causes Diamond-Blackfan Anemia associated with spontaneous remission and meningocele. *Int J Hematol*. 2020;112(6):894-899. doi:10.1007/s12185-020-02950-6

24. Liu YL, Shibuya A, Glader B, Wilkes MC, Barna M, Sakamoto KM. Animal models of Diamond-Blackfan anemia: updates and challenges. *haematol*. 2022;108(5):1222-1231. doi:10.3324/haematol.2022.282042

25. Richards S, Aziz N, Bale S, et al. Standards and guidelines for the interpretation of sequence variants: a joint consensus recommendation of the American College of Medical Genetics and Genomics and the Association for Molecular Pathology. *Genet Med*. 2015;17(5):405-424. doi:10.1038/gim.2015.30

Suppl. Materials

Primers used for transcript analyses

RPL26 Forward: 5' CTCTTCCCTTTTGCGGCCAT 3'
RPL26 Reverse: 5' CATTAGCCTTTTCCCGCTGC 3'
Bcl-xL Forward: 5'- AGCGGTTGAAGCGTTCCT 3'
Bcl-xL Reverse: 5' AGCCTTGGATCCAGGAGAA 3'
GAPDH Forward: 5'AAGGTGAAGGTCGGAGTCAA 3'
GAPDH Reverse: 5' CTTGACGGTGCCATGGAATT 3'
HPRT Forward: 5' GCTGAGGATTTGGAAAGGGT 3'
HPRT Reverse: 5' TGTAATCCAGCAGGTCAGCA 3'

Suppl. Figure 1: *In silico* splice predictions for variant NM_000987.5(*RPL26*):c.-5-2A>G.

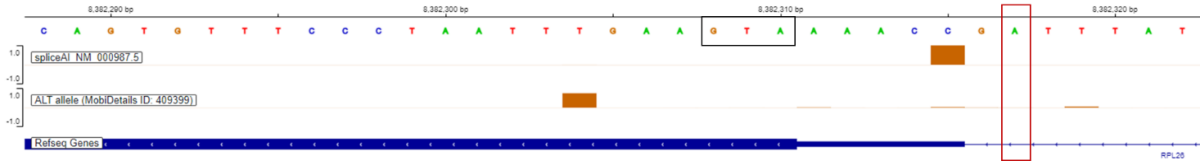

Splice predictions are represented with SpliceAI-visual bioinformatic tool.[1] The red square shows the variation site. Orange bars represent predicted acceptor sites ([0;1]), the spliceAI raw score being the absolute value. The first track is the spliceAI prediction for the wild-type transcript. The second track is the prediction for the variant (ALT allele), +/- 10kb. Predictions for the variant are in favor of the loss of the acceptor splice site of intron 1, and the use of a cryptic acceptor site, 11 bp away in exon 2. This would result in the deletion of the ATG translation initiation codon (black square).

Suppl. Figure 2: Immunoblots on CD34^{+} cells from D7 to D12.

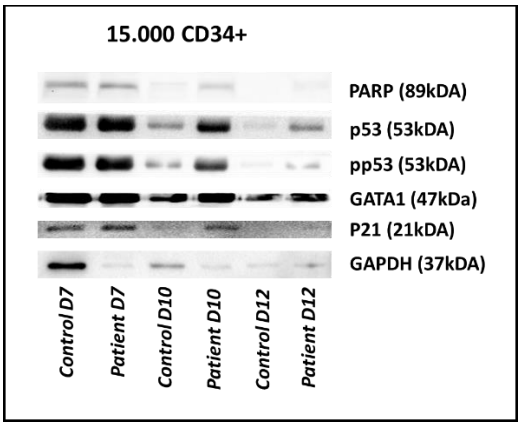

Suppl. Figure 3: *In silico* translation start predictions for abnormal transcripts due to variant NM_000987.5(*RPL26*):c.-6+3_-6+25del.

Abnormal transcript with partial retention of 272 bp from intron 1

CTCTTCCCTTTTGCGGCCATCACCGAAGCGGGAGCGGGTGTAATCAGCAGCCATCCGTTCTTGGGCATGGTGGCTTCCGACCGCGGGGACCCCGAGAGTCTCTTGTCGGCCGAGTAGCA
GCCAGGAAGGAGAGACTGGGATGGTTTTTTATCTGTTGCTTTCTTAAATCAAGGGCCGCCGGGCCGGAGATGGATGGAGGGACCGGGGATTTGGGAACTCGAAAACGAGCTGAGGGA
AGGGAGCCTGTGGAAATAGACTGGAGTCTGGGTAGTGTCGTTTCCTAGAGAATGGTCTCGAAGTAACTTCTCG**CCAAAATGAAGTTTAATCCCTTTGTGACTTCCGACCGAAGCAAGA
ATCGCAAAAGGCATTTCAATGCACCTTCCCACATTCGAAGGAAGATTATGTCTTCCCCTCTTTCCAAAGAGCTGAGACAGAAGTACAACGTGCGATCCATGCCCATCCGAAAGGATGA
TGAAGTTCAGGTTGTACGTGGACACTATAAAGGTCAGCAAATTGGCAAAGTAGTCCAGGTTTACAGGAAGAAATATGTTATCTACATTGAACGGGTGCAGCGGGAAAAGGCTAATG
GCACAACTGTCCACGTAGGCATTCACCCCAGCAAG**

ATG position (relative to natural ATG)	Premature stop codon	NetStart score	ATGpr score
1	No (natural ATG)	0.240	0.22
-721	Yes	0.503	0.04
-672	Yes	0.498	0.10
-573	Yes	0.438	0.04

Abnormal transcript with partial retention of 353 bp from intron 1

CTCTTCCCTTTTGCGGCCATCACCGAAGCGGGAGCGGGTGTAATCAGCAGCCATCCGTTCTTGGGCATGGTGGCTTCCGACCGCGGGGACCCCGAGAGTCTCTTGTCGGCCGAGTAGCA
GCCAGGAAGGAGAGACTGGGATGGTTTTTTATCTGTTGCTTTCTTAAATCAAGGGCCGCCGGGCCGGAGATGGATGGAGGGACCGGGGATTTGGGAACTCGAAAACGAGCTGAGGGA
AGGGAGCCTGTGGAAATAGACTGGAGTCTGGGTAGTGTCGTTTCCTAGAGAATGGTCTCGAAGTAACTTCTCGGTAAAGTCTTCACGGAATTTCCAGACCACACTTGCCCACTGGGAGG
CTTTTAGGACCCGAGACGTGTGCAGGCTTTTCCAG**CCAAAATGAAGTTTAATCCCTTTGTGACTTCCGACCGAAGCAAGAATCGCAAAAGGCATTTCAATGCACCTTCCCACATTCGAA
GGAAGATTATGTCTTCCCCTCTTTCCAAAGAGCTGAGACAGAAGTACAACGTGCGATCCATGCCCATCCGAAAGGATGATGAAGTTCAGGTTGTACGTGGACACTATAAAGGTCAGC
AAATTGGCAAAGTAGTCCAGGTTTACAGGAAGAAATATGTTATCTACATTGAACGGGTGCAGCGGGAAAAGGCTAATGGCACAACTGTCCACGTAGGCATTCACCCCAGCAAG**

ATG position (relative to natural ATG)	Premature stop codon	NetStart score	ATGpr score
1	No (natural ATG)	0.134	0.31
-721	Yes	0.503	0.04
-672	Yes	0.498	0.10
-573	Yes	0.411	0.04

Predictions of translation initiation were performed with NetStart[2] and ATGpr[3] bioinformatics tools (lastly assessed, September 2023) on the abnormal transcripts with partial intron 1 retention (272 or 353 bp). For both transcripts; NetStart suggests the use of a cryptic ATG with higher scores than the natural initiation site. These abnormal uORF would produce a stop codon upstream of the natural initiation site, in which case none of the native protein is synthesized. ATGpr scores are higher for the natural initiation site than alternative ATG sites. Exons are represented in bold. The natural ATG is highlighted in yellow and the alternative ATG are in green, blue or pink.

References

1. De Sainte Agathe JM, Filser M, Isidor B, et al. SpliceAI-visual: a free online tool to improve SpliceAI splicing variant interpretation. *Hum Genomics*. 2023;17(1):7. doi:10.1186/s40246-023-00451-1

2. Pedersen AG, Nielsen H. Neural network prediction of translation initiation sites in eukaryotes: perspectives for EST and genome analysis. *Proc Int Conf Intell Syst Mol Biol*. 1997;5:226-233.

3. Salamov AA, Nishikawa T, Swindells MB. Assessing protein coding region integrity in cDNA sequencing projects. *Bioinformatics*. 1998;14(5):384-390. doi:10.1093/bioinformatics/14.5.384

Dans cette étude, nous avons montré que *RPL26* est principalement associé à des malformations congénitales (en particulier les anomalies du rayon radial) d'expressivité variable. La dysostose mandibulo-faciale et les anomalies du tube neural sont potentiellement associées au DBA11, et viennent s'ajouter à la liste croissante des malformations qui peuvent être rencontrées dans le DBS. Chez un individu, nous avons montré que l'haploinsuffisance de *RPL26* était responsable d'une altération infraclinique de la prolifération érythroïde et de l'énucléation. L'absence d'atteinte hématologique chez quatre adultes de cette série est un argument supplémentaire en faveur du fait que l'insuffisance médullaire n'est pas systématiquement associée à tous les gènes responsables de DBS.

Cette variabilité d'expression et ce chevauchement entre formes syndromiques et non-syndromiques a déjà été décrit dans les champs de la génétique de la déficience intellectuelle ou de la surdité notamment (54,55). Dans le champ des malformations des membres, cette variabilité d'expression est également observée pour les phénotypes en lien avec les variants de *TBX5*, comme décrit en partie II, mais également pour d'autres gènes tels que *TP63* (56).

L'amélioration de l'accès aux analyses pangénomiques pour les patients présentant des atteintes non-syndromiques permettra de mieux repérer les causes génétiques chevauchantes et préciser les corrélations génotype/phénotype.

PARTIE IV. CARACTERISATION DE NOUVEAUX GENES IMPLIQUES DANS LES DYSPLASIES RADIALES

En soutien de ces travaux de thèse, nous avons obtenu un financement du GIRCI Nord-Ouest (Projet HOS-REG) afin de réaliser le séquençage génome entier de 6 cas index atteints d'anomalie du rayon radial d'étiologie indéterminée et 9 apparentés (Familles 1, 2, 3, 4, 6, 7). Le séquençage génome entier a été effectué au Science for Life Laboratory - Genomics (NGI) (Université d'Uppsala, Suède). Par ailleurs, nous avions récupéré les données de séquençage de génome d'une autre famille (Famille 5), comportant un cas index et 5 apparentés, auparavant générées au Center for Mendelian Genomics (Université of Washington, Seattle) (Figure 6).

Figure 7 : Familles sélectionnées pour séquençage de génome

Les individus indiqués en rouge ont fait l'objet d'un séquençage de génome.

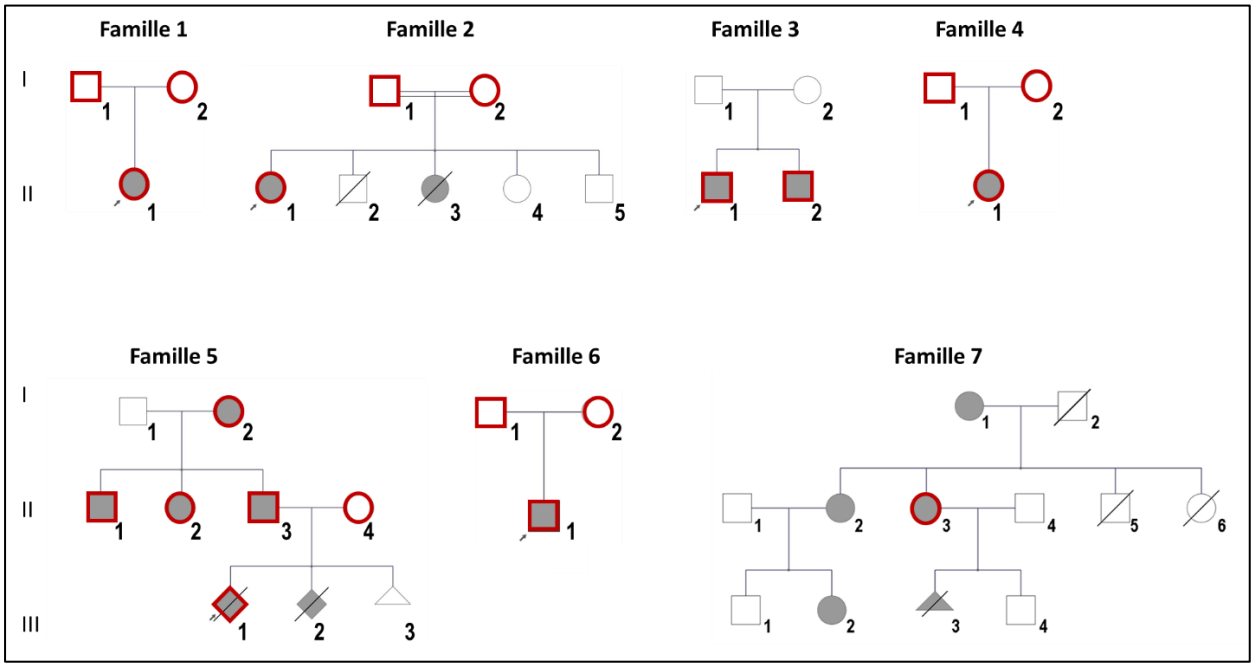

La couverture moyenne est de 39,5X, avec 79% des nucléotides couverts à 30X minimum. Les analyses bioinformatiques ont été réalisées par Emilie Aït Yahya et Fabrice Bonte de l'équipe de bioinformatique du CHU de Lille. Le pipeline DRAGEN V2 a été appliqué aux données pour détecter les Variants Nucléotidiques Simples (SNV) et les Insertions/Délétions (InDels) dans toutes les familles. Le pipeline CNV a été appliqué pour détecter les variants du nombre de copies. Le pipeline DRAGEN Virtual Long-Read Detection (VLRD) a été utilisé pour détecter les variants structurels.

Les SNV et les InDels ont été annotés à l'aide de l'algorithme Ensembl Variant Effect Predictor. Une annotation avec les données de Genehancer, Limb Enhancer Genie, ENCODE et une annotation personnalisée (localisation dans un TAD comprenant un gène impliqué dans le développement du membre) a été effectuée (45,47,57). Les CNV ont été annotés avec AnnotSV. Nous avons ajouté des annotations spécifiques aux gènes et éléments régulateurs impliqués dans le développement des membres.

Concernant les **familles 1, 4 et 6**, comme il s'agit de cas sporadiques, nous avons utilisé la stratégie *de novo*. Aucun variant candidat n'a été identifié. L'interprétation pourrait être poursuivie par l'hypothèse d'autres modes de transmission.

Dans la **famille 3**, nous avons filtré sur les variants communs aux deux frères. Les parents étant asymptomatiques, plusieurs modes de transmission peuvent être suspectés : autosomique récessif, lié à l'X ou autosomique dominant avec un mosaïcisme germinal parental ou un défaut de pénétrance. Nous n'avons pas identifié de variant candidat.

Pour les **familles 5 et 7**, la stratégie d'analyse a permis d'identifier le variant en cause dans la pathologie. Ces résultats ont été présentés dans deux articles de thèse : variant intronique profond du gène *TBX5* identifié dans la famille 5 (article publié en 2024 dans *Genetics in Medicine*, présenté dans la partie II-B) ; variant dans le 5'UTR du gène *RPL26*, identifié dans la famille 7 (article publié en 2024 dans *Genetics in Medicine*, présenté dans la partie III).

Dans la **famille 2**, nous avons identifié un variant candidat. Le cas index est issu de parents apparentés asymptomatiques. Nous avons déterminé les régions d'homozygotie

observées uniquement chez la probante et non chez ses parents, également issus d'unions consanguines.

Par cette stratégie, nous avons identifié 1057 régions supérieures à 1kb, dont 80 de plus de 1Mb et 17 de plus de 3 Mb. Une grande région a été identifiée sur le chromosome 12, mais n'est pas chevauchante avec le TAD comprenant le gène *TBX5*. Aucun variant homozygote pertinent n'a été identifié dans les deux petites régions d'homozygotie du TAD de *TBX5*.

Nous nous sommes concentrés sur les variants SNP homozygotes dans ces régions d'homozygotie. Après avoir filtré les variants rares, avec un bon score de qualité, couverts au minimum 8 fois, nous avons identifié chez le cas index un variant faux-sens homozygote du gène *RPL17* : c.542T>C ; p.(Met181Thr). Il s'agit d'un variant de signification incertaine pour lequel les prédictions sont discordantes.

Le gène *RPL17* code pour la protéine ribosomique L17 et n'avait jusqu'alors pas été décrit en pathologie humaine. En parallèle de nos travaux, en août 2024, Fellmann *et al.* ont publié 2 variants d'intérêt de *RPL17*, chez des patients atteints de DBA (58). Cette équipe a montré que les poissons-zèbre traités par morpholinos contre rpl17 présentent une micrognathie et une anémie, reproduisant une partie du phénotype humain associé à l'anémie de Blackfan-Diamond. Aucune restauration du phénotype n'était observée après complémentation par les transcrits porteurs de deux des variants chez le modèle poisson-zèbre. Le premier variant (NM_000985.5: c.217-3C>G; p.?) a été identifié dans une famille où ségrége une anémie de Blackfan-Diamond sur un mode autosomique dominant. Il s'agit d'un variant d'épissage hétérozygote, entraînant un saut d'exon et un décalage du cadre de lecture avec codon stop prématuré. Le second variant (c.452delC; p.(Thr151Argfs*25)) était rapporté chez un patient présentant un tableau hématologique et son père asymptomatique.

Enfin, 3 patients porteurs de VSI hétérozygotes introniques de *RPL17*, c.217-70A>G et c.-14+1G>T, avec un phénotype d'anémie de Blackfan-Diamond sont rapportés en Supplementary Data, dans une vaste étude récente publiée au New England Journal of Medecine, sans détails cliniques ni études fonctionnelles a priori (59).

Malgré le mode de transmission discordant avec notre observation, ces éléments font du variant identifié un bon candidat. L'étude de sa ségrégation dans la fratrie du cas index est compatible, la sœur atteinte étant également porteuse du variant à l'état homozygote, la sœur saine étant hétérozygote et le frère sain homozygote sauvage.

Bien que le cas index n'ait pas d'anémie, les explorations hématologiques ont apporté des arguments supplémentaires en faveur d'un syndrome de Blackfan-Diamond. La patiente présente une élévation du taux d'adénosine désaminase érythrocytaire, marqueur spécifique de la pathologie. De plus, en collaboration avec l'Équipe d'Accueil 4666, Hématopoïèse et Immunologie (HEMATIM) de l'Université de Picardie Jules Verne (Amiens), les progéniteurs érythroïdes CD34+ de la patiente ont été isolés. Un arrêt précoce de leur pousse à J7 a été observé, témoignant probablement d'un défaut de prolifération cellulaire.

Un appel à collaboration international (GeneMatcher, ERN-ITHACA) n'ayant pas permis d'identifier d'autre observation similaire, plusieurs pistes sont poursuivies pour la caractérisation fonctionnelle du variant (53).

En collaboration avec l'équipe « Dynamique et dysfonctionnements de la synthèse des ribosomes » de PE Gleize (Centre de Biologie Intégrative, Université de Toulouse, CNRS), l'étude de l'intégration de la protéine L17 dans la sous-unité 60S du ribosome va être effectuée à partir de lignées lymphoblastiques.

En collaboration avec l'équipe « Plasticité Cellulaire et Cancer » et la plateforme poisson-zèbre de PO Angrand (Canther, UMR9020, CNRS-U1277 INSERM), une lignée knock-out *rpl17-/-* est en cours de phénotypage. Chez le poisson zèbre, les morphants et les mutants générés pour plusieurs gènes codant des protéines ribosomiques montrent des malformations similaires à celles observées dans les ribosomopathies : défaut du développement de la tête et du corps, diminution des érythrocytes (60–63). Une caractérisation phénotypique fine du modèle *rpl17-/-* sera réalisée (défauts squelettiques, anémie) et permettra ensuite des études de complémentation *in vivo* après transcription *in vitro* de l'ARNm sauvage et porteur du variant faux-sens. Ce projet va être mené dans le cadre d'un Master 2 Recherche au cours de l'année 2025.

Au sein de l’équipe RADEME, la caractérisation fonctionnelle à haut-débit des variants de *RPL17* va être mise en place dans le cadre d’une thèse d’Université au cours de l’année 2025.

DISCUSSION

A l'issue de ce projet, nous avons pu identifier un diagnostic formel pour 2 familles en impasse diagnostique de notre cohorte, en identifiant un variant intronique profond de *TBX5* et un variant dans le 5' UTR de *RPL26*, par l'étude des régions non codantes des gènes impliqués dans le développement des membres. Par ailleurs, nous avons pu confirmer l'implication de *TBX5* pour 9 familles en reclassant les variants de signification incertaine en probablement pathogènes, par la réalisation de tests fonctionnels spécifiques. L'identification d'un variant causal de *RPL26* chez des patients présentant une atteinte radiale isolée a justifié d'un appel à collaboration pour une description phénotypique plus précise du phénotype lié aux altérations de ce gène. Enfin, nous avons identifié un variant homozygote d'intérêt dans un gène candidat (*RPL17*) chez une patiente issue une famille consanguine, pour laquelle des investigations complémentaires sont en cours.

a. Recherche clinique : un socle indispensable

En pratique clinique, ces confirmations diagnostiques ont permis la mise en place d'un suivi adapté, notamment cardiaque pour les patients avec syndrome de Holt-Oram et hématologique pour les patients concernés par le syndrome de Blackfan-Diamond. L'impact du diagnostic moléculaire sur la prise à charge du patient atteint de maladie rare est majeur en période postnatale, notamment du fait des recommandations de bonne pratique établis pour un nombre grandissant de syndromes génétiques. Dans ce cadre, et à partir du travail réalisé pour cette thèse, nous travaillons actuellement, avec un groupe d'experts multidisciplinaires, sur la rédaction du Protocole National de Diagnostic et de Soins du syndrome de Holt-Oram. En période prénatale, l'extension des indications de l'exome/génome prénatal permet parfois un diagnostic moléculaire très précoce, et peut éventuellement influencer l'issue de la grossesse en fonction de la recevabilité ou non d'une interruption médicale de grossesse en cas de forte probabilité d'atteinte associée considérée comme grave et incurable au moment du diagnostic.

Nous avons montré, dans notre article « *Holt-Oram syndrome: clinical and molecular description of 78 patients with TBX5 variants* » que la description détaillée des caractéristiques cliniques et moléculaires des patients atteints d'une maladie rare, permettait d'en améliorer le diagnostic et la prise en charge. Ce travail de cohorte a bâti les fondations des travaux de thèse présentés ici. Dans les pathologies ultra-rares, les collaborations internationales sont indispensables, par le biais d'appels à collaboration ou d'outils de partage de données tels que GeneMatcher ou DECIPHER, comme illustré par notre article « *RPL26 variants: a rare cause of Diamond-Blackfan Anemia Syndrome with multiple congenital anomalies at the forefront* » (27,53). Les efforts de collecte massive de données cliniques et moléculaires des patients permettront de préciser ces données épidémiologiques et l'histoire naturelle de chaque pathologie. La mise en place de la BNDMR (Banque Nationale de Données Maladies Rares) en France ainsi que l'intégration récente du cartouche génomique SDM-G pourrons nourrir cet axe de recherche clinique. Dans cette dynamique, le projet ReUseRare a pour but d'accompagner la construction un recueil de données structurées pour un projet scientifique portant sur maladie rare en réutilisant les données issues des dossiers médicaux au sein de l'application web BaMaRa. A l'échelle européenne, l'ERN (European Reference Network) ITHACA (Intellectual disability, TeleHealth, Autism and Congenital Anomalies) développe actuellement un registre compilant les données cliniques et moléculaires des bases nationales pour les patients porteurs de syndromes malformatifs et/ou de déficience intellectuelle, appelé ILIAD (International Library of Intellectual disability and Anomalies of Development).

b. Caractérisation des variants de signification incertaine : difficultés et perspectives

Avec la production massive de données de séquençage haut-débit en routine diagnostique, l'identification de variants de signification incertaine a explosé et les tests fonctionnels sont désormais indispensables pour aider à leur interprétation. L'implémentation de ces tests dans les laboratoires de diagnostic est l'objectif principal de la FHU G4 Génomique à laquelle l'équipe RADEME est associée.

Une limite majeure à laquelle nous faisons face pour les gènes impliqués dans les malformations des membres est leur territoire d'expression restreint en postnatal, rendant difficile l'accessibilité à des tissus d'intérêt pour l'étude transcriptomique ou protéomique.

Au cours de ce travail de thèse, des tests fonctionnels *in vitro* à faible débit ont été utilisés, dont la mise en place a été longue et coûteuse. Ces tests ne permettant d'étudier qu'un seul variant à la fois, ils sont en général réalisés de manière rétrospective, après l'identification d'un variant de signification incertaine.

Depuis quelques années, des tests fonctionnels *in vitro* à haut-débit ont été développés, permettant l'étude de multiples variants de manière simultanée : les *Multiplexed Assays of Variant Effect* ou MAVE (Test multiplexé d'expression de variants)(64). Parmi ceux-ci, la saturation mutationnelle par édition du génome (*Saturation Genome Editing* ou SGE)(65,66) permet d'étudier simultanément la pathogénicité de la totalité des variants ponctuels théoriques d'une séquence génique cible courte (100-150 pb). Cette technique a été validée pour la première fois en 2019 pour le gène *BRCA1*, et reproduite pour quelques gènes depuis (67,68).

Elle est en cours de mise en place au sein de l'équipe RADEME, dans le cadre d'un projet de thèse d'université. Les variants des régions codantes de *RPL26* et *RPL17*, gènes dont le lien avec la pathologie humaine a été suspecté au cours de notre travail, seront étudiés par cette méthode. Ces gènes répondent au prérequis principal puisqu'ils sont indispensables à la survie en culture des cellules haploïdes. Le principe de la technique est de générer l'ensemble des variants de la séquence d'intérêt au sein d'une lignée cellulaire haploïde en utilisant l'outil CRISPR-Cas9. La survie de chaque clone est étudiée par séquençage haut-débit à différents temps de culture de cette population cellulaire hétérogène, permettant d'observer l'impact de chaque variant sur la survie et donc d'en déduire sa pathogénicité. Cette méthode à haut-débit permet d'anticiper l'interprétation de variants n'ayant encore jamais été identifiés en pathologie humaine, leur conférant une puissance bien supérieure à celle des tests à faible-débit.

Une bonne connaissance de la fonction du gène et du mécanisme moléculaire de la pathologie (perte ou gain de fonction) est un prérequis indispensable à la mise au point de ces tests à haut-débit. Pour les gènes codant des facteurs de transcription, l'étude de

la survie ou de la croissance cellulaire est rarement adaptée. Récemment, les variants de *PAX6* localisés dans le site de fixation à l'ADN ont pu être étudiés en adaptant un test sur les levures mono-hybrides (Y1H). Un site de fixation d'un facteur de transcription est cloné en amont d'un gène rapporteur de résistance à un antibiotique, dont l'expression dépend donc de la fixation d'un facteur de transcription spécifique. Ce système pourrait donc être utilisé pour étudier des librairies de facteurs de transcription sauvages ou mutés, comme TBX5, sur leur capacité à se fixer à leur ADN cible (69). Du fait de leur grande homologie, ces résultats pourraient être applicables pour des variants d'autres gènes de la famille *T-box*. D'autres équipes ont montré l'application de la technique de saturation mutationnelle dans des éléments régulateurs, tels que la ZRS, région régulatrice du gène *SHH* spécifique du membre, responsables de polydactylies pré-axiales (70,71).

La généralisation de l'utilisation des critères ACMG a pour but d'harmoniser la classification des variants. Néanmoins, la conviction clinico-biologique a fait naître la notion de « hot-VUS » ou « classe 3 + » pour des variants candidats, justifiant de la réalisation de tests fonctionnels dont les conclusions permettraient une reclassification en « classe 4 ». Les outils de prédiction sont d'une aide précieuse, comme nous avons pu le montrer dans l'article « *Functional characterization vs in silico prediction for TBX5 missense and splice variants in Holt-Oram syndrome* ». Néanmoins, ces outils ne prennent pas en compte les conclusions publiées des tests fonctionnels déjà réalisés pour un variant donné. Ils peuvent notamment être mis en défaut pour un variant responsable d'un gain de fonction. Enfin, du fait de l'évolution du membre supérieur chez les mammifères et de spécificités propres à l'Homme telles que l'opposition du pouce, la place du niveau de conservation inter-espèces d'un nucléotide dans ces outils de prédiction pourrait être pondérée.

c. *Patients en impasse diagnostique : exploration du génome non codant et autres approches moléculaires*

Alors que la plupart des causes génétiques décrites jusqu'à présent se situent au sein du génome codant, ne représentant qu'environ 2% du génome entier, de récentes publications impliquent des éléments régulateurs ou des ARN non codants (72,73). Très

récemment, l'étude du génome chez plus de 800 familles avec suspicion de maladie monogénique a permis de poser un diagnostic chez 29% des familles. Parmi eux, 8 % n'auraient pas pu être mis en évidence par l'exome, incluant des variants codants dans des régions mal couvertes, des variants introniques, des variants de structure, des inversions, des réarrangements complexes et des expansions de triplets (59). Néanmoins, nous n'avons pas identifié au sein des patients décrits de phénotypes impliquant les membres. Pour les patients avec anomalies radiales isolées restant en impasse diagnostique, plusieurs hypothèses peuvent être explorées, même si, de façon globale, le taux diagnostique par génome pour des malformations isolées est plutôt estimé à 11% (59). L'exploration du génome non codant a permis, dans notre étude, la description d'un variant intronique profond responsable d'une forme familiale de HOS. Nous avons montré la force de l'outil de prédiction SpliceAI notamment pour la priorisation de ces variants. En revanche, la priorisation des variants associés à une malformation isolée pouvant affecter des régions régulatrices de gènes cibles d'intérêt est plus complexe. Plusieurs travaux ont cherché à identifier et caractériser des enhancers spécifiques du membre supérieur, notamment de *Tbx5*. Deux séquences régulatrices ont été décrites dans la littérature. La première, d'une taille de 361 pb, est localisée dans l'intron 2 et a été identifiée à partir de modèles de souris transgéniques, dans lesquels cet élément était cloné en amont du gène Tbx5 et inséré au hasard dans le génome (74). Cet élément est suffisant pour initier l'expression de *Tbx5* au niveau du bourgeon de membre supérieur à partir de E8.5. Les gènes *Hox* (*Hoxa4, Hoxa5, Hoxb4, Hoxb5, Hoxc4, Hoxc5*) interviennent en amont de *Tbx5* en se fixant à cet élément. La seconde séquence régulatrice (cns12sh), localisée en aval de *Tbx5* et conservée du poisson aux mammifères, a été décrite par la même technique chez le poisson zèbre (75). Ces éléments auraient pu être de bons candidats à explorer chez les patients avec dysplasie radiale ou malformation sévère des membres supérieurs isolées. Cependant, leur invalidation chez la souris, par délétion homozygote de l'intron 2 ou de la région cns12sh, montrent une expression normale de *Tbx5* dans le bourgeon de membre supérieur, ainsi qu'une absence de conséquence sur l'initiation du bourgeon de membre supérieur à E9.5 et la formation squelettique à E14. Ainsi, alors que ces 2 éléments peuvent activer l'expression de *Tbx5* quand ils sont clonés à proximité immédiate de leur promoteur cible,

à une position génomique ectopique, ils ne sont pas indispensables au contrôle de l'activation de l'expression de *Tbx5* au membre supérieur à leur position génomique normale (76). La redondance des enhancers, estimée à 8 par gène codant pour un facteur de transcription chez les mammifères, pourrait expliquer ce phénomène (77). Ces données suggèrent que les variants des séquences régulatrices ne seraient responsables que de phénotypes mineurs, notamment lorsque leurs gènes cibles sont indispensables au développement précoce.

De façon récente, des phénotypes ont été mis en lien avec des variants d'ARN non codants, notamment des variants de RNU4-2, un petit ARN nucléaire, qui pourrait figurer parmi les premières causes de déficience intellectuelle d'origine génétique (78). Des phénotypes impliquant les membres ont pu être associés à des altérations de longs ARN non codants ou de micro-ARNs (79). Ces connaissances devront ensuite être implémentées dans les outils d'interprétation du génome pour la priorisation des variants, puis justifieront des tests fonctionnels adaptés (49,59,80).

L'hypothèse polygénique doit également être considérée pour les formes isolées de dysplasies radiales, comme décrit dans les holoprosencéphalies isolées par exemple (81,82). De façon intéressante, les voies de signalisation impliquées dans ce mode d'hérédité rare dans les holoprosencéphalies (SHH, FGF) sont également impliquées dans les dysplasies radiales : *ZIC3* de la voie SHH dans l'association VACTERL, gènes de la voie des FGFs dans le syndrome LADD notamment, comme précisé dans notre revue « *Radial ray : from developmental biology to human disease* ».

Pour les patients restant en impasse diagnostique, d'autres approches moléculaires sont à envisager. Les variants structuraux (SV), comprenant les translocations et les délétions, duplications, insertions ou inversions de plus de 50 pb, peuvent, en modifiant l'architecture du génome, déréguler l'expression de gènes impliqués dans le développement des membres, comme cela a pu être précédemment décrit (83). Les variants structuraux pourraient expliquer jusqu'à 10% des anomalies congénitales rares et des déficiences intellectuelles, actuellement en impasse diagnostique (73). Or, ils sont souvent rendus comme « de signification incertaine », en l'absence d'information sur l'organisation structurale réelle de la séquence génomique du patient. La résolution de

l'ACPA (Analyse Chromosomique sur Puce à ADN) est trop faible pour déterminer les points de cassure, et ne permet pas d'obtenir d'informations sur l'organisation des séquences. Quant au séquençage haut débit de 2e génération, il implique une étape d'assemblage bio-informatique de la séquence du patient à partir de courtes séquences d'ADN, d'environ 300 paires de bases. Cet assemblage *in silico* est mis en défaut dans les régions répétées du génome, les régions de faible complexité, et les régions difficiles à séquencer, qui sont souvent les « hots spots » de points de cassure des SV. Avec l'émergence des technologies de séquençage de 3e génération, permettant de séquencer des fragments en pleine longueur de 10000 à 45000 pb en moyenne, il est dorénavant possible de disposer d'informations structurales génomiques réelles pour un patient, et de lever l'incertitude sur les points de cassure des SV. Un variant structurel candidat peut ensuite être exploré par des techniques de conformation chromatinienne (4C, HiC notamment). Ces techniques sont actuellement utilisées au sein de l'équipe de recherche RADEME, dans le cadre du projet de thèse d'université CAR-SV, pour la caractérisation des variations génomiques de structure.

L'étude du transcriptome est limitée dans le champ des malformations des membres, car l'expression des gènes impliqués est précoce au cours du développement et faible dans le sang. Néanmoins, l'apport du RNA-seq dans le diagnostic des maladies rares génétiques n'est plus à prouver (84). En parallèle de la mise en place du RNA-seq au sein du laboratoire de génétique moléculaire de routine au CHU Lille, nous projetons donc d'établir un atlas de l'expression des gènes impliqués dans le développement des membres à partir de plusieurs tissus chez l'humain (sang, peau, muscle, os, urines) et à différents âges. Cette base de données nous permettrait de proposer une approche transcriptomique aux patients porteurs de malformations des membres en impasse diagnostique, ou pour la validation fonctionnelle des variants génomiques de signification incertaine. Sur le plan transcriptomique, des investigations peuvent également être réalisés sur les voies d'aval dérégulées. Par exemple, nous avons pu montrer précédemment la dérégulation de la voie WNT par RNA-seq sur culture fibroblastique chez un patient porteur d'une anomalie du rayon radial syndromique en lien avec un variant du gène *LEF1* impliqué dans cette voie de signalisation (85).

Enfin, l'étude des marques épigénétiques pourrait apporter des informations supplémentaires pour les patients en impasse diagnostique, présentant une malformation isolée et sporadique. L'étude de l'implication potentielle d'anomalies de la méthylation chez les patients atteints de malformations des membres connues pour être sporadiques, telles que les amélies ou le syndrome Femur-Fibula-Ulna, est actuellement en cours dans l'équipe RADEME, dans le cadre d'une thèse d'université. Ces travaux devraient permettre d'améliorer nos connaissances sur les mécanismes moléculaires impliqués dans la régulation des gènes du développement des membres.

d. Biologie du développement et génétique humaine : apports mutuels

La biologie fondamentale permet la caractérisation de nouveaux acteurs du développement des membres pouvant devenir de nouveaux gènes candidats en pathologie ; la description de la régulation de l'expression des gènes, cruciale à l'interprétation du génome non codant ; et l'identification de voies de signalisation en amont et en aval, base indispensable aux études transcriptomiques.

Certains gènes impliqués dans le développement des membres supérieurs ont été associés, non seulement à l'initiation et à la croissance du bourgeon de membre, mais aussi à la mise en place des muscles et des tendons à un stade plus tardif de développement, par leur expression au sein du tissu conjonctif musculaire (86–88). De plus, une altération de la matrice extracellulaire a été observée sur des cultures de fibroblastes issus de patients atteints de dysplasie radiale. Ces anomalies pourraient expliquer la récurrence de la déviation radiale chez ces patients après correction chirurgicale de la dysplasie radiale (89). Ces données pourront à l'avenir justifier d'études spécifiques de l'organisation des muscles et des tendons chez les patients afin d'améliorer leur prise en charge. La réalisation de prélèvements tissulaires lors d'interventions chirurgicales permettra de préciser à la fois les atteintes anatomiques mineures associées, mais également les éventuelles modifications d'expression des gènes cibles. La caractérisation des gènes cibles de *TBX5* au sein du tissu conjonctif

musculaire dans la mise en place des muscles et des tendons permettrait d'identifier d'éventuels gènes candidats pour expliquer des atteintes mineures du pouce par exemple. La description d'une désorganisation des muscles et des tendons chez le modèle transgénique murin pour lequel *Tbx5* a été inactivé à un stade plus tardif du développement des membres nous incite à explorer les patients concernés par le HOS à ce niveau anatomique, comme cela a été montré pour les patients atteints de syndrome Ulnar-Mammary, lié aux variants de *TBX3* (88).

De nombreuses questions développementales sont encore en suspens, ou partiellement explorées. L'axe radial semble plus « sensible » aux variations génétiques que le rayon ulnaire. D'une part, les atteintes du rayon radial sont plus fréquentes que les atteintes du rayon ulnaire. D'autre part, alors que les gènes impliqués dans les dysplasies radiales sont exprimés de façon homogène dans le bourgeon de membre, ils n'affectent pas le développement de l'axe ulnaire. Dans notre revue « *Radial ray : from developmental biology to human disease* », nous avançons l'hypothèse que la régulation du développement de l'axe radial serait moins robuste, car son apparition et son adaptation chez l'homme (pouce opposable) sont plus récentes dans l'évolution. De plus, l'axe ulnaire est sous la dépendance de *SHH*, gène majeur du développement et donc particulièrement robuste. De façon plus générale, le membre supérieur semble plus « sensible » aux variations génétiques que le membre inférieur. Alors que certains gènes sont exprimés indifféremment au membre supérieur et au membre inférieur, leurs altérations n'impactent pas, ou très faiblement, le développement du membre inférieur (gènes *SALL1/4* par exemple).

CONCLUSION

Le Ministère de l'Enseignement Supérieur de la Recherche et de l'Innovation a avancé dans ses objectifs pour le Plan National Maladies Rares 4, non publié à ce jour, l'amélioration du rendement diagnostique par des liens accrus entre le soin et la recherche, la collecte des données, la constitution de collections biologiques et leur partage à l'échelle européenne.

Cette thèse illustre à plusieurs niveaux le caractère indispensable de l'interdisciplinarité et les collaborations nationales et internationales dans le champ des maladies rares. Dans la caractérisation des bases génétiques des dysplasies radiales, l'interconnexion entre les champs de la biologie du développement et de la génétique humaine permet une évolution constante des connaissances et de leurs applications. La constitution de cohortes de patients présentant une même maladie rare repose sur la collaboration entre cliniciens et biologistes de différentes spécialités et est favorisée par la création d'outils dédiés, tels que GeneMatcher, pour échanger des informations et mener des projets communs à échelle internationale (53). La collecte des données et leur partage avec les différents acteurs du soin et de la recherche, de façon anonyme et sécurisée, dans le respect du consentement du patient, de la législation et du cadre éthique de chaque pays, sont de vrais challenges, à l'échelle européenne et mondiale.

La coopération est à la base du caractère social de l'espèce humaine, par des mécanismes biologiques, environnementaux ou culturaux et est indispensable à sa survie (90). En recherche scientifique, la compétition entre chercheurs ou équipes de recherche peut être une motivation ou être sous-jacente à certains critères de sélection académiques (91). Pourtant, il a pu être montré combien l'esprit collaboratif pouvait améliorer la productivité et faire avancer les connaissances dans l'intérêt du progrès de la science et de la santé du patient (91). La crise liée à la pandémie COVID-19 a illustré le besoin de coopération scientifique pour résoudre les enjeux majeurs de notre époque, tels que le réchauffement climatique. Dans le champ de la recherche en biologie et en santé, cette thèse témoigne, à son niveau, de la nécessité de collaborations

interdisciplinaires et internationales pour réduire l’impasse diagnostique dans les maladies rares et améliorer la prise en charge des patients.

RÉFÉRENCES

1. Hamosh A, Scott AF, Amberger J, Valle D, McKusick VA. Online Mendelian Inheritance in Man (OMIM). Hum Mutat. 2000;15(1):57-61.

2. Enquête de l'Alliance Maladies Rares. L'errance diagnostique dans les maladies rares ERRADIAG [Internet]. 2016 [cité 25 juin 2024]. Disponible sur: https://www.alliance-maladies-rares.org/wp-content/uploads/2020/05/Erradiag-l-errance-diagnostic-dans-les-maladies-rares1.pdf

3. Ministère des Solidarités et de la Santé, Ministère de l'enseignement supérieur, de la recherche et de l'innovation. Plan National Maladies Rares 3 2018-2022 [Internet]. 2018 [cité 25 juin 2024]. Disponible sur: https://sante.gouv.fr/IMG/pdf/plan_national_maladies_rares_2018-2022.pdf

4. Adams DR, Eng CM. Next-Generation Sequencing to Diagnose Suspected Genetic Disorders. N Engl J Med. 4 oct 2018;379(14):1353-62.

5. Chung CCY, Hue SPY, Ng NYT, Doong PHL, Chu ATW, Chung BHY. Meta-analysis of the diagnostic and clinical utility of exome and genome sequencing in pediatric and adult patients with rare diseases across diverse populations. Genet Med. 1 sept 2023;25(9):100896.

6. Burdick KJ, Cogan JD, Rives LC, Robertson AK, Koziura ME, Brokamp E, et al. Limitations of exome sequencing in detecting rare and undiagnosed diseases. Am J Med Genet A. juin 2020;182(6):1400-6.

7. Souche E, Beltran S, Brosens E, Belmont JW, Fossum M, Riess O, et al. Recommendations for whole genome sequencing in diagnostics for rare diseases. Eur J Hum Genet EJHG. sept 2022;30(9):1017-21.

8. HCSP, HCERES. ÉVALUATION DU PLAN NATIONAL MALADIES RARES 3 VOLET SOINS ET VOLET RECHERCHE. 2023.

9. Young NM. Integrating « Evo » and « Devo »: The Limb as Model Structure. Integr Comp Biol. 1 déc 2017;57(6):1293-302.

10. Masson E. EM-Consulte. [cité 1 juill 2024]. Classification des malformations congénitales des membres. Disponible sur: https://www.em-consulte.com/article/1599475/classification-des-malformations-congenitales-des-

11. Al-Qattan MM, Kozin SH. Update on Embryology of the Upper Limb. J Hand Surg. 1 sept 2013;38(9):1835-44.

12. Vasluian E, van der Sluis CK, van Essen AJ, Bergman JEH, Dijkstra PU, Reinders-Messelink HA, et al. Birth prevalence for congenital limb defects in the

northern Netherlands: a 30-year population-based study. BMC Musculoskelet Disord. 2013;14:323.

13. Bedard T, Lowry RB, Sibbald B, Kiefer GN, Metcalfe A. Congenital limb deficiencies in Alberta-a review of 33 years (1980-2012) from the Alberta Congenital Anomalies Surveillance System (ACASS). Am J Med Genet A. nov 2015;167A(11):2599-609.

14. Froster UG, Baird PA. Congenital defects of the limbs in stillbirths: data from a population-based study. Am J Med Genet. 15 juin 1993;46(5):479-82.

15. Goldfarb CA, Ezaki M, Wall LB, Lam WL, Oberg KC. The Oberg-Manske-Tonkin (OMT) Classification of Congenital Upper Extremities: Update for 2020. J Hand Surg. 1 juin 2020;45(6):542-7.

16. Oberg KC. Classification of congenital upper limb anomalies: towards improved communication, diagnosis, and discovery. J Hand Surg Eur Vol. 1 janv 2019;44(1):4-14.

17. Blauth W. [The hypoplastic thumb]. Arch Orthop Unfallchir. 1967;62(3):225-46.

18. Koskimies E, Lindfors N, Gissler M, Peltonen J, Nietosvaara Y. Congenital upper limb deficiencies and associated malformations in Finland: a population-based study. J Hand Surg. juin 2011;36(6):1058-65.

19. Paladini D, Greco E, Sglavo G, D' Armiento MR, Penner I, Nappi C. Congenital anomalies of upper extremities: prenatal ultrasound diagnosis, significance, and outcome. Am J Obstet Gynecol. 1 juin 2010;202(6):596.e1-596.e10.

20. Antoine P, Fantini-Hauwel C, Brugallé É, Geerts L, Petit F, Vanlerberghe C, et al. 4. Vivre avec une maladie génétique rare : analyse interprétative phénoménologique de la construction de soi avec le syndrome de Holt-Oram. In: Maladies rares [Internet]. Toulouse: Érès; 2023 [cité 4 juill 2024]. p. 67-84. (Essais – Sociétés). Disponible sur: https://www.cairn.info/maladies-rares--9782749277707-p-67.htm

21. Jourdain AS, Petit F, Odou MF, Balduyck M, Brunelle P, Dufour W, et al. Multiplex targeted high-throughput sequencing in a series of 352 patients with congenital limb malformations. Hum Mutat. janv 2020;41(1):222-39.

22. Elsner J, Mensah MA, Holtgrewe M, Hertzberg J, Bigoni S, Busche A, et al. Genome sequencing in families with congenital limb malformations. Hum Genet. 1 août 2021;140(8):1229-39.

23. Richards S, Aziz N, Bale S, Bick D, Das S, Gastier-Foster J, et al. Standards and guidelines for the interpretation of sequence variants: a joint consensus recommendation of the American College of Medical Genetics and Genomics and the Association for Molecular Pathology. Genet Med Off J Am Coll Med Genet. mai 2015;17(5):405-24.

24. Vears DF, Sénécal K, Borry P. Reporting practices for variants of uncertain significance from next generation sequencing technologies. Eur J Med Genet. 1 oct 2017;60(10):553-8.

25. Karczewski KJ, Francioli LC, Tiao G, Cummings BB, Alföldi J, Wang Q, et al. The mutational constraint spectrum quantified from variation in 141,456 humans. Nature. mai 2020;581(7809):434-43.

26. Landrum MJ, Lee JM, Riley GR, Jang W, Rubinstein WS, Church DM, et al. ClinVar: public archive of relationships among sequence variation and human phenotype. Nucleic Acids Res. janv 2014;42(Database issue):D980-985.

27. Firth HV, Richards SM, Bevan AP, Clayton S, Corpas M, Rajan D, et al. DECIPHER: Database of Chromosomal Imbalance and Phenotype in Humans Using Ensembl Resources. Am J Hum Genet. avr 2009;84(4):524-33.

28. Fokkema IFAC, Kroon M, López Hernández JA, Asscheman D, Lugtenburg I, Hoogenboom J, et al. The LOVD3 platform: efficient genome-wide sharing of genetic variants. Eur J Hum Genet EJHG. déc 2021;29(12):1796-803.

29. Frazer J, Notin P, Dias M, Gomez A, Min JK, Brock K, et al. Disease variant prediction with deep generative models of evolutionary data. Nature. nov 2021;599(7883):91-5.

30. Wu Y, Li R, Sun S, Weile J, Roth FP. Improved pathogenicity prediction for rare human missense variants. Am J Hum Genet. 7 oct 2021;108(10):1891-906.

31. Rentzsch P, Witten D, Cooper GM, Shendure J, Kircher M. CADD: predicting the deleteriousness of variants throughout the human genome. Nucleic Acids Res. 8 janv 2019;47(Database issue):D886-94.

32. Ioannidis NM, Rothstein JH, Pejaver V, Middha S, McDonnell SK, Baheti S, et al. REVEL: An Ensemble Method for Predicting the Pathogenicity of Rare Missense Variants. Am J Hum Genet. 6 oct 2016;99(4):877-85.

33. Kelley LA, Mezulis S, Yates CM, Wass MN, Sternberg MJE. The Phyre2 web portal for protein modeling, prediction and analysis. Nat Protoc. juin 2015;10(6):845-58.

34. Jumper J, Evans R, Pritzel A, Green T, Figurnov M, Ronneberger O, et al. Highly accurate protein structure prediction with AlphaFold. Nature. août 2021;596(7873):583-9.

35. Pennica C, Hanna G, Islam SA, Sternberg MJE, David A. Missense3D-PPI: A Web Resource to Predict the Impact of Missense Variants at Protein Interfaces Using 3D Structural Data. J Mol Biol. 15 juill 2023;435(14):168060.

36. Ittisoponpisan S, Islam SA, Khanna T, Alhuzimi E, David A, Sternberg MJE. Can Predicted Protein 3D Structures Provide Reliable Insights into whether Missense Variants Are Disease Associated? J Mol Biol. 17 mai 2019;431(11):2197-212.

37. Cheng J, Novati G, Pan J, Bycroft C, Žemgulytė A, Applebaum T, et al. Accurate proteome-wide missense variant effect prediction with AlphaMissense. Science. 22 sept 2023;381(6664):eadg7492.

38. Yeo G, Burge CB. Maximum entropy modeling of short sequence motifs with applications to RNA splicing signals. J Comput Biol J Comput Mol Cell Biol. 2004;11(2-3):377-94.

39. Leman R, Parfait B, Vidaud D, Girodon E, Pacot L, Le Gac G, et al. SPiP: Splicing Prediction Pipeline, a machine learning tool for massive detection of exonic and intronic variant effects on mRNA splicing. Hum Mutat. déc 2022;43(12):2308-23.

40. Jaganathan K, Kyriazopoulou Panagiotopoulou S, McRae JF, Darbandi SF, Knowles D, Li YI, et al. Predicting Splicing from Primary Sequence with Deep Learning. Cell. 24 janv 2019;176(3):535-548.e24.

41. Brnich SE, Abou Tayoun AN, Couch FJ, Cutting GR, Greenblatt MS, Heinen CD, et al. Recommendations for application of the functional evidence PS3/BS3 criterion using the ACMG/AMP sequence variant interpretation framework. Genome Med. 31 déc 2019;12(1):3.

42. Kanavy DM, McNulty SM, Jairath MK, Brnich SE, Bizon C, Powell BC, et al. Comparative analysis of functional assay evidence use by ClinGen Variant Curation Expert Panels. Genome Med. 29 nov 2019;11(1):77.

43. Gaildrat P, Killian A, Martins A, Tournier I, Frébourg T, Tosi M. Use of splicing reporter minigene assay to evaluate the effect on splicing of unclassified genetic variants. Methods Mol Biol Clifton NJ. 2010;653:249-57.

44. Tamayo A, Núñez-Moreno G, Ruiz C, Plaisancie J, Damian A, Moya J, et al. Minigene Splicing Assays and Long-Read Sequencing to Unravel Pathogenic Deep-Intronic Variants in PAX6 in Congenital Aniridia. Int J Mol Sci. 13 janv 2023;24(2):1562.

45. ENCODE Project Consortium. The ENCODE (ENCyclopedia Of DNA Elements) Project. Science. 22 oct 2004;306(5696):636-40.

46. Luo Y, Hitz BC, Gabdank I, Hilton JA, Kagda MS, Lam B, et al. New developments on the Encyclopedia of DNA Elements (ENCODE) data portal. Nucleic Acids Res. 8 janv 2020;48(D1):D882-9.

47. Monti R, Barozzi I, Osterwalder M, Lee E, Kato M, Garvin TH, et al. Limb-Enhancer Genie: An accessible resource of accurate enhancer predictions in the developing limb. PLoS Comput Biol. août 2017;13(8):e1005720.

48. Visel A, Minovitsky S, Dubchak I, Pennacchio LA. VISTA Enhancer Browser--a database of tissue-specific human enhancers. Nucleic Acids Res. janv 2007;35(Database issue):D88-92.

49. Ellingford JM, Ahn JW, Bagnall RD, Baralle D, Barton S, Campbell C, et al. Recommendations for clinical interpretation of variants found in non-coding regions of the genome. Genome Med. 19 juill 2022;14(1):73.

50. Wassel HD. The results of surgery for polydactyly of the thumb. A review. Clin Orthop. 1969;64:175-93.

51. Ulirsch JC, Verboon JM, Kazerounian S, Guo MH, Yuan D, Ludwig LS, et al. The Genetic Landscape of Diamond-Blackfan Anemia. Am J Hum Genet. 6 déc 2018;103(6):930-47.

52. Gazda HT, Preti M, Sheen MR, O'Donohue MF, Vlachos A, Davies SM, et al. Frameshift mutation in p53 regulator RPL26 is associated with multiple physical abnormalities and a specific pre-ribosomal RNA processing defect in diamond–blackfan anemia. Hum Mutat. 2012;33(7):1037-44.

53. Sobreira N, Schiettecatte F, Valle D, Hamosh A. GeneMatcher: a matching tool for connecting investigators with an interest in the same gene. Hum Mutat. oct 2015;36(10):928-30.

54. Lee S, Rudd S, Gratten J, Visscher PM, Prins JB, Dawson PA. Gene networks associated with non-syndromic intellectual disability. J Neurogenet. 2 janv 2018;32(1):6-14.

55. Vona B. Rethinking non-syndromic hearing loss and its mimics in the genomic era. Eur J Hum Genet. 6 mars 2024;1-4.

56. Rinne T, Brunner HG, van Bokhoven H. p63-associated disorders. Cell Cycle Georget Tex. 1 févr 2007;6(3):262-8.

57. Fishilevich S, Nudel R, Rappaport N, Hadar R, Plaschkes I, Iny Stein T, et al. GeneHancer: genome-wide integration of enhancers and target genes in GeneCards. Database J Biol Databases Curation. 1 janv 2017;2017:bax028.

58. Fellmann F, Saunders C, O'Donohue MF, Reid DW, McFadden KA, Montel-Lehry N, et al. An atypical form of 60S ribosomal subunit in Diamond-Blackfan anemia linked to RPL17 variants. JCI Insight. 1 août 2024;9(17):e172475.

59. Wojcik MH, Lemire G, Berger E, Zaki MS, Wissmann M, Win W, et al. Genome Sequencing for Diagnosing Rare Diseases. N Engl J Med. 6 juin 2024;390(21):1985-97.

60. Danilova N, Sakamoto KM, Lin S. Ribosomal protein S19 deficiency in zebrafish leads to developmental abnormalities and defective erythropoiesis through activation of p53 protein family. Blood. 15 déc 2008;112(13):5228-37.

61. Amsterdam A, Sadler KC, Lai K, Farrington S, Bronson RT, Lees JA, et al. Many ribosomal protein genes are cancer genes in zebrafish. PLoS Biol. mai 2004;2(5):E139.

62. Palasin K, Uechi T, Yoshihama M, Srisowanna N, Choijookhuu N, Hishikawa Y, et al. Abnormal development of zebrafish after knockout and knockdown of ribosomal protein L10a. Sci Rep. 2 déc 2019;9(1):18130.

63. Chen C, Huang H, Yan R, Lin S, Qin W. Loss of rps9 in Zebrafish Leads to p53-Dependent Anemia. G3 Bethesda Md. 3 déc 2019;9(12):4149-57.

64. Gasperini M, Starita L, Shendure J. The power of multiplexed functional analysis of genetic variants. Nat Protoc. oct 2016;11(10):1782-7.

65. Findlay GM, Boyle EA, Hause RJ, Klein JC, Shendure J. Saturation editing of genomic regions by multiplex homology-directed repair. Nature. 4 sept 2014;513(7516):120-3.

66. Dace P, Findlay GM. Reducing uncertainty in genetic testing with Saturation Genome Editing. Med Genet. 1 déc 2022;34(4):297-304.

67. Findlay GM, Daza RM, Martin B, Zhang MD, Leith AP, Gasperini M, et al. Accurate classification of BRCA1 variants with saturation genome editing. Nature. oct 2018;562(7726):217-22.

68. Radford EJ, Tan HK, Andersson MHL, Stephenson JD, Gardner EJ, Ironfield H, et al. Saturation genome editing of DDX3X clarifies pathogenicity of germline and somatic variation. Nat Commun. 6 déc 2023;14(1):7702.

69. McDonnell AF, Plech M, Livesey BJ, Gerasimavicius L, Owen LJ, Hall HN, et al. Deep mutational scanning quantifies DNA binding and predicts clinical outcomes of PAX6 variants [Internet]. bioRxiv; 2023 [cité 20 oct 2023]. p. 2023.07.25.550478. Disponible sur: https://www.biorxiv.org/content/10.1101/2023.07.25.550478v1

70. Kircher M, Xiong C, Martin B, Schubach M, Inoue F, Bell RJA, et al. Saturation mutagenesis of twenty disease-associated regulatory elements at single base-pair resolution. Nat Commun. 8 août 2019;10(1):3583.

71. Kvon EZ, Zhu Y, Kelman G, Novak CS, Plajzer-Frick I, Kato M, et al. Comprehensive In Vivo Interrogation Reveals Phenotypic Impact of Human Enhancer Variants. Cell. 19 mars 2020;180(6):1262-1271.e15.

72. The 100,000 Genomes Project Pilot Investigators. 100,000 Genomes Pilot on Rare-Disease Diagnosis in Health Care — Preliminary Report. N Engl J Med. 11 nov 2021;385(20):1868-80.

73. Pagnamenta AT, Camps C, Giacopuzzi E, Taylor JM, Hashim M, Calpena E, et al. Structural and non-coding variants increase the diagnostic yield of clinical whole genome sequencing for rare diseases. Genome Med. 9 nov 2023;15:94.

74. Minguillon C, Nishimoto S, Wood S, Vendrell E, Gibson-Brown JJ, Logan MPO. Hox genes regulate the onset of Tbx5 expression in the forelimb. Dev Camb Engl. sept 2012;139(17):3180-8.

75. Adachi N, Robinson M, Goolsbee A, Shubin NH. Regulatory evolution of Tbx5 and the origin of paired appendages. Proc Natl Acad Sci U S A. 06 2016;113(36):10115-20.

76. Cunningham TJ, Lancman JJ, Berenguer M, Dong PDS, Duester G. Genomic Knockout of Two Presumed Forelimb Tbx5 Enhancers Reveals They Are Nonessential for Limb Development. Cell Rep. 12 2018;23(11):3146-51.

77. Osterwalder M, Barozzi I, Tissières V, Fukuda-Yuzawa Y, Mannion BJ, Afzal SY, et al. Enhancer redundancy provides phenotypic robustness in mammalian development. Nature. 08 2018;554(7691):239-43.

78. Chen Y, Dawes R, Kim HC, Stenton SL, Walker S, Ljungdahl A, et al. *De novo* variants in the non-coding spliceosomal snRNA gene *RNU4-2* are a frequent cause of syndromic neurodevelopmental disorders [Internet]. 2024 [cité 20 juill 2024]. Disponible sur: http://medrxiv.org/lookup/doi/10.1101/2024.04.07.24305438

79. Nowosad K, Hordyjewska-Kowalczyk E, Tylzanowski P. Mutations in gene regulatory elements linked to human limb malformations. J Med Genet. juin 2020;57(6):361-70.

80. Stenton SL, O'Leary MC, Lemire G, VanNoy GE, DiTroia S, Ganesh VS, et al. Critical assessment of variant prioritization methods for rare disease diagnosis within the rare genomes project. Hum Genomics. 29 avr 2024;18:44.

81. Mouden C, Dubourg C, Carré W, Rose S, Quelin C, Akloul L, et al. Complex mode of inheritance in holoprosencephaly revealed by whole exome sequencing. Clin Genet. juin 2016;89(6):659-68.

82. Dubourg C, Carré W, Hamdi-Rozé H, Mouden C, Roume J, Abdelmajid B, et al. Mutational Spectrum in Holoprosencephaly Shows That FGF is a New Major Signaling Pathway. Hum Mutat. déc 2016;37(12):1329-39.

83. Petit F, Sears KE, Ahituv N. Limb development: a paradigm of gene regulation. Nat Rev Genet. 2017;18(4):245-58.

84. Riquin K, Isidor B, Mercier S, Nizon M, Colin E, Bonneau D, et al. Integrating RNA-Seq into genome sequencing workflow enhances the analysis of structural variants causing neurodevelopmental disorders. J Med Genet. 1 janv 2024;61(1):47-56.

85. Dufour W, Alawbathani S, Jourdain AS, Asif M, Baujat G, Becker C, et al. Monoallelic and biallelic variants in LEF1 are associated with a new syndrome combining ectodermal dysplasia and limb malformations caused by altered WNT signaling. Genet Med Off J Am Coll Med Genet. août 2022;24(8):1708-21.

86. Hasson P, DeLaurier A, Bennett M, Grigorieva E, Naiche LA, Papaioannou VE, et al. Tbx4 and Tbx5 Acting in Connective Tissue Are Required for Limb Muscle and Tendon Patterning. Dev Cell. janv 2010;18(1):148-56.

87. Besse L, Sheeba CJ, Holt M, Labuhn M, Wilde S, Feneck E, et al. Individual Limb Muscle Bundles Are Formed through Progressive Steps Orchestrated by Adjacent Connective Tissue Cells during Primary Myogenesis. Cell Rep. 10 mars 2020;30(10):3552-3565.e6.

88. Colasanto MP, Eyal S, Mohassel P, Bamshad M, Bonnemann C, Zelzer E, et al. Development of a subset of forelimb muscles and their attachment sites requires the ulnar-mammary syndrome gene Tbx3. Dis Model Mech. 4 août 2016;

89. Murphy GRF, Feneck E, Paget J, Sivakumar B, Smith G, Logan MPO. Investigating the role connective tissue fibroblasts play in the altered muscle anatomy associated with the limb abnormality, Radial Dysplasia. J Anat. 16 avr 2024;

90. The cooperative human. Nat Hum Behav. juill 2018;2(7):427-8.

91. Ellemers N. Science as collaborative knowledge generation. Br J Soc Psychol. janv 2021;60(1):1-28.